

# **The role of Memo in premature aging and FGFR signaling**

## **Inauguraldissertation**

zur Erlangung der Würde eines Doktors der Philosophie

vorgelegt der

Philosophisch-Naturwissenschaftlichen Fakultät

der Universität Basel

von

**Barbara Hänzi**

aus Meinisberg (BE)

Leiter der Arbeit: Prof. Dr. Nancy E. Hynes

Friedrich Miescher Institute for Biomedical Research, Basel

Basel, 2012

Genehmigt von der Philosophisch-Naturwissenschaftlichen Fakultät auf Antrag von

Prof. Dr. Nancy E. Hynes

Prof. Dr. Lukas Sommer

Prof. Dr. Denis Monard

Basel, den 13. Dezember 2011

Prof. Dr. Martin Spiess

Dekan

# 1 Table of Content

<b>1</b>	<b>Table of Content</b> .....	<b>1</b>
<b>2</b>	<b>Table of Figures</b> .....	<b>5</b>
<b>3</b>	<b>Summary</b> .....	<b>6</b>
<b>4</b>	<b>Introduction</b> .....	<b>8</b>
4.1	Memo (Mediator of ErbB2 driven cell motility).....	8
4.1.1	The ErbB family .....	8
4.1.2	Memo (Mediator of ErbB driven cell motility) .....	9
4.1.3	The structure of Memo .....	9
4.1.4	Memo and migration .....	10
4.2	The Fibroblast Growth Factor (FGF) tyrosine kinase receptor family .....	10
4.2.1	The FGF receptors .....	11
4.2.2	The FGFR ligands .....	13
4.2.3	The FGF coreceptors: Heparin/Heparan sulfate proteoglycans and the Klotho family... 18	
4.2.4	Signaling of the FGFR pathway .....	19
4.2.5	FGFRs and cancer .....	24
4.3	Aging and Premature aging .....	30
4.3.1	Different Models of premature aging .....	32
4.3.2	Aging and Metabolism .....	34
4.4	Phosphate homeostasis .....	36
4.4.1	FGF23, a member of the endocrine FGF family.....	37
4.4.2	Klotho.....	42
4.4.3	FGF receptors .....	48
4.4.4	Vitamin D .....	49
4.4.5	The sodium phosphate co-transporters Na-Pi2a and Na-Pi2c.....	50
4.4.6	The parathyroid hormone (PTH) .....	50
4.4.7	Players in phosphate homeostasis.....	52
<b>5</b>	<b>Material and Methods</b> .....	<b>56</b>

## Table of Content

5.1	Reagents and antibodies.....	56
5.2	Cell Culture.....	56
5.3	Lysates, western blot analyses and immunoprecipitations .....	58
5.4	Electron Microscopy.....	59
5.5	Hypoxia .....	59
5.6	Proliferation assay .....	59
5.7	Apoptosis assay .....	59
5.7.1	YoPro.....	59
5.7.2	MitoProbe™ DilC <sub>1</sub> (5) Assay .....	60
5.8	Migration assay.....	60
5.9	RNA extraction, RT-PCR and real-time PCR.....	61
5.10	Immunohistochemistry.....	62
5.11	Generation of the mouse strains .....	62
5.11.1	Memo cKO and KO mice.....	62
5.11.2	Meox2Cre mice .....	63
5.11.3	Memo cKO Actin Cre mice .....	63
5.11.4	Memo cKO rtTA LC-1 Cre mice .....	64
5.12	Microarray of livers and kidneys (performed by the microarray facility inhouse) .....	66
5.12.1	Sample preparation.....	66
5.12.2	The array .....	66
5.13	Blood- and Urine analysis.....	67
5.13.1	Measurement of bilirubin, cholesterol, Creatine Kinase, insulin, iron, glucose, potassium, triglycerides, total protein .....	67
5.13.2	Blood analysis performed in Dallas.....	67
5.13.3	Measurement of phosphate, calcium, sodium, potassium, BUN, creatinine and Albumin .....	67
5.14	Metabolic cages.....	68
5.15	Isolation of brush border membrane .....	68
5.16	ELISA for VEGF, PTH and FGF23.....	68
5.16.1	VEGF ELISA .....	68

## Table of Content

5.16.2	PTH ELISA .....	69
5.16.3	FGF23 ELISA .....	69
<b>6</b>	<b>Rational of the work .....</b>	<b>70</b>
<b>7</b>	<b>Results.....</b>	<b>71</b>
7.1	Submitted manuscript .....	72
7.2	Analysis of Memo in development .....	105
7.2.1	Analysis of Memo conventional knock-out animals (Memo KO) (R. Masson and P. Kaeser) .....	105
	The main work of this analysis was done by Régis Masson. He did the planning of the experiment and he had the main responsibility. I helped in plugging the animals and isolating the embryos, taking pictures and genotyping them. ....	105
7.2.2	Analysis of Memo conditional knock-out (Memo cKO) mice crossed to Meox2Cre transgene mice (J. Zmajkovic) .....	106
7.2.3	Analysis of the Memo conditional knock-out (Memo cKO) strain crossed to the pCX-CreER <sup>TM</sup> transgene mice.....	107
7.3	Characterisation of the Memo cKO actin Cre ER <sup>TM</sup> Mice .....	107
7.4	Characterization of the inducible kidney-specific Memo knock-out mouse line .....	118
7.5	Characterization of the defect in calcium homeostasis in Memo null and kidney-specific Memo KO animals.....	123
7.6	Memo is a novel downstream effector of the FGFR pathway .....	126
7.6.1	Signaling in the HEK293-kl cells .....	127
7.6.2	Signaling in the HEK293-βkl cells.....	128
7.6.3	Investigation of complex formation of Memo, Klotho and FGFR1 .....	129
7.6.4	Inhibitory effect of secreted Klotho.....	130
7.7	Memo downstream of FGFR signaling in mouse mammary carcinoma cells.....	134
7.7.1	Effect of Memo down regulation on FRS2 phosphorylation in 4T1 cells (F. Maurer)..	135
7.7.2	Apoptosis, proliferation and migration in control and Memo down regulated (KD) cells .....	135
7.7.3	Memo and oxidative stress .....	140
7.7.4	Memo and VEGF secretion .....	143

## Table of Content

<b>8</b>	<b>Outlook and Discussion .....</b>	<b>145</b>
8.1	The premature aging defect .....	146
8.1.1	Analysis of the FGF23-Klotho axis .....	147
8.1.2	Blood- and urine analysis .....	148
8.2	FGFR signaling.....	151
8.3	The role of Memo in FGFR signaling dependent apoptosis and migration.....	153
8.4	The role of Memo in VEGF secretion.....	154
8.5	The role of Memo in oxidative stress.....	155
8.6	The role of Memo in TOR-HIF1 $\alpha$ crosstalk .....	156
8.7	Conclusion .....	157
<b>9</b>	<b>References.....</b>	<b>159</b>
<b>10</b>	<b>Abbreviations .....</b>	<b>185</b>
<b>11</b>	<b>Acknowledgments .....</b>	<b>188</b>
<b>12</b>	<b>Curriculum Vitae .....</b>	<b>189</b>

## Table of Figures

### 2 Table of Figures

Figure 4-1 Structure of the FGF receptors .....	12
Figure 4-2 The evolutionary relationships within the human FGF gene family (Itoh et al. 2004) .....	14
Figure 4-3 FGFR specificity for ligand binding (Turner et al. 2010).....	18
Figure 4-4 The FGFR signalosome.....	21
Figure 4-5 FGFR signaling (Turner et al. 2010) .....	22
Figure 4-6 Regulation of phosphate homeostasis (Bergwitz et al. 2010).....	36
Figure 4-7 Vitamin D metabolism.....	40
Figure 4-8 Regulation in active renal Ca <sup>2+</sup> reabsorption (from de Groot et al. 2008).....	44
Figure 4-9 Activation of the Calcium-sensing receptor and subsequent downstream effects (Kumar et al. 2011).....	51
Figure 4-10 Downregulation of Na-Pi2a (Forster et al. 2006) .....	52
Figure 5-1 The doxycycline inducible kidney specific Memo knock out mouse .....	65
Figure 7-1 Control and Memo KO embryos at E11.5 .....	106
Figure 7-2 Hindlimb reflex and organ weight of Memo null and control animals .....	108
Figure 7-3 Pictures of mitochondria in the heart of control and Memo null mice .....	109
Figure 7-4 Memo staining of the Kidney.....	110
Figure 7-5 RNA levels of vitamin D receptor (VDR) .....	115
Figure 7-6 Level of Na-Pi2a in the renal brush border membrane of WT and Memo null mice.....	118
Figure 7-7 Western analysis of whole kidney lysates from kidney-specific knock-out and control animals.....	119
Figure 7-8 Body weight curve of male animals .....	120
Figure 7-9 Level of Na-Pi2a in the renal brush border membrane of WT and kidney-specific KO mice .....	122
Figure 7-10 Fractional excretion and Excretion rate.....	123
Figure 7-11 Von Kossa staining on the heart of Memo null mice .....	125
Figure 7-12 FGFR pathway stimulation by FGF23, FGF19 and FGF21 .....	128
Figure 7-13 IP of FGFR1 and Klotho in HEK293-kl cells.....	130
Figure 7-14 Stimulation of WT and KO MEFs with insulin and IGF-1 .....	132
Figure 7-15 Inhibitory effect of Klotho on the insulin and IGF-1 pathway in the MEFs.....	133
Figure 7-16 Down regulation of Memo in 4T1 cells by shRNA hairpin against Memo (S. Jacob and I. Samarzija).....	134
Figure 7-17 Phosphorylation status of FRS2 in 4T1 control and Memo down regulated cells (F. Maurer) .....	135
Figure 7-18 Apoptosis of 4T1 .....	137
Figure 7-19 Apoptosis of WT and KO MEFs upon Etoposide treatment.....	138
Figure 7-20 Proliferation assay with 4T1 cells .....	139
Figure 7-21 Boyden Chamber Migration assay with 4T1 cells.....	140
Figure 7-22 Staining of mitochondria in MEFs after CoCl <sub>2</sub> treatment.....	141
Figure 7-23 Cell Signaling downstream of CoCl <sub>2</sub> .....	142
Figure 7-24 CoCl <sub>2</sub> and hypoxia treatment of 4T1 cells.....	143
Figure 7-25 VEGF secretion and expression in 4T1 cells.....	144
Figure 8-1 Effects of CoCl <sub>2</sub> .....	155

### 3 Summary

Memo was recently identified in a screen for proteins required for ErbB receptor induced cell migration. Encoded by a single-copy gene present in all branches of life, it is ubiquitously expressed during all stages of embryogenesis and in adult tissues. This study aimed to investigate the physiological role of Memo. Initially, we generated a conventional knock out of Memo, which was embryonic lethal between E12.5 to E14.5. We subsequently generated a mouse strain to allow temporal control of Memo deletion by crossing a mouse strain harboring a homozygous floxed Memo allele (Memo<sup>fl/fl</sup>) with pCX-CreER<sup>TM</sup> transgenics, where the ubiquitous actin promoter drives the Cre recombinase. Following tamoxifen treatment, Memo was deleted in all organs (Memo null mice). Knock out of Memo in mice at the age of 2 to 14 weeks revealed a severe premature aging phenotype accompanied by alterations in insulin and glucose metabolism. The phenotype of the Memo null mice, especially the metabolic phenotype, revealed an interesting similarity to the Klotho and FGF23 mutant mice. In particular, insulin and glucose metabolism was very similar to the phenotype shown by both Klotho mutant and FGF23 knock-out mice. To investigate this phenotype further, and as Klotho is mainly expressed in the renal tubular cells, we generated a mouse model, which lacked Memo specifically in the kidney. We chose a Pax8 promoter system to delete Memo in the renal tubular cells (1). Kidney specific Memo knock-out mice were generated by crossing Memo floxed (Memo<sup>fl/fl</sup>) mice with a mouse line expressing the tetracycline-sensitive transactivator rtTA under control of the Pax8 promoter, and a mouse line harboring Cre recombinase under a promoter that contains a tetracycline-responsive promoter element. In these mice doxycycline treatment induced loss of Memo in renal tubular epithelial cells.

By investigation of the Memo null and kidney-specific Memo KO mice we found that only the Memo null mice showed premature aging symptoms. However, both KO models showed deregulation of the FGF23-Klotho axis measuring expression of enzymes involved in vitamin D metabolism and phosphate reabsorption. Moreover, blood analysis of both models showed renal insufficiency and hypercalcemia. For the kidney-specific Memo KO animals we also performed analysis of the urine and found hypercaliuria. Surprisingly, for both models there was no difference in serum phosphate levels, which



## Summary

has earlier been shown by others to be causative for the premature aging syndrome.

In conclusion, we found that deletion of Memo in the full body or specifically in the kidney induces renal insufficiency and hypercalcemia. Furthermore, Memo deletion in the full body results in severe premature aging symptoms that cannot be explained by elevated serum phosphate levels. To date, it is not clear how hypercalcemia and hypercalciuria affects Memo mice and what specifically induces the premature aging in Memo null animals.

To investigate the function of Memo *in vitro* we isolated and immortalized mouse embryonic fibroblasts (MEFs) from Memo<sup>fl/fl</sup> embryos. These cells were then infected with a Cre recombinase containing vector, which following 4-hydroxytamoxifen treatment ablated Memo expression (KO MEFs). Our studies showed that signaling downstream of FGF2 was reduced in activity and duration in Memo KO MEFs and furthermore that Memo was associated with the FGFR signaling complex (FGFR-FRS2-GRB2-GAB1). In addition, we tested mammary carcinoma cells (4T1) for sensitivity to FGFR inhibition and revealed lower sensitivity to FGFR inhibition in Memo downregulated cells. To investigate the role of Memo in the metabolic signaling we used HEK293 cells that are stably transfected with Klotho or  $\beta$ Klotho and therefore responsive to FGF19, 21 and 23. We found that in Memo downregulated HEK293-Klotho and  $-\beta$ Klotho cells, FGFR signaling activity after stimulation with FGF23 and FGF19 was affected.

In summary, this study provides evidence for a physiological role of Memo downstream of the FGFR pathway. We show that Memo is part of the FGFR signaling complex. Loss of Memo affects the intensity and duration of the FGFR signaling and modulates sensitivity to FGFR inhibition and to oxidative stress. Furthermore, we uncovered an important role of Memo in renal physiology that contributed to a premature aging phenotype, which is similar to that observed in Klotho mutant or FGF23 knock out animals.

## 4 Introduction

### 4.1 Memo (Mediator of ErbB2 driven cell motility)

#### 4.1.1 The ErbB family

The ErbB2 receptor family has been shown to be very important in a wide range of physiological processes as well as in disease. The family consists of four ErbB receptors, EGFR/ErbB1, ErbB2, ErbB3 and ErbB4. Their extracellular region consists of four domains (I-IV); Domain I and III are important for peptide binding, while domain II is important for receptor-receptor interaction. Upon activation of the receptor homo- and heterodimers are formed. ErbB1, ErbB3 and ErbB4 bind their ligands leading to activation, while ErbB2 does not bind a ligand, but is a preferred binding partner of the other receptors and is activated by crossphosphorylation.

The Erb receptor ligands are expressed by 10 different genes (2) and include EGF, betacellulin (BTC), transforming growth factor- $\alpha$  (TGF- $\alpha$ ), heparin-binding EGF-like growth factor (HB-EGF), epiregulin, amphiregulin (AREG) and four neuregulins (NRG 1-4). The ligand family members are expressed as transmembrane precursor protein molecules, which possess a conserved epidermal growth factor (EGF)-like domain (3), and undergo ectodomain proteolytic cleavage by a procession of different ADAMs to release the mature active growth factors.

Upon activation of the receptors different downstream pathways are activated, including the mitogen-activated protein kinase (MAPK) and the phosphatidylinositol 3-kinase (PI3K)-AKT pathways. Furthermore, activation of signal transducer and activator of transcription proteins (STATs), SRC tyrosine kinase and the mammalian target of rapamycin (mTOR) can be observed. The EGFR pathway is important for a wide range of physiological processes, as such the constitutive knock out of EGFR in mice results in death during the first postnatal week. ErbB2, ErbB3 and ErbB4 have been shown to have an essential role in cardiac development and in disease, such as in breast cancer where it has been found that about 30% human breast cancers show overexpression of ErbB2 (4).

### 4.1.2 Memo (Mediator of ErbB driven cell motility)

Much research has focused on understanding tumor etiology and developing strategies for therapeutic elimination of primary tumors. However, as up to 90% of tumor related mortality is related to metastatic disease rather than a consequence of the primary tumor, research in the field of tumor metastasis has become increasingly important. Metastasis formation is a multi-step process, consisting of extravasation, migration and intravasation. Our group was interested in the process of cancer cell migration and aimed at finding binding partners of ErbB2 which were relevant for migration. They showed that mainly two phosphorylation sites of ErbB2 are relevant for migration; Tyr1201 and 1227. Based on this, the focus was set on proteins that bind to peptides containing Tyr1201 or Tyr1227. Binding proteins were identified by liquid chromatography-tandem mass spectrometry (LC-MS/MS). In this screen several known binding partners were confirmed and in addition a novel 32kDa protein was found and named Memo (Mediator of ErbB driven cell motility). Memo is a 297-amino-acid protein. A single protein is encoded in the human genome, and Memo homologs are found in all branches of life. Boyden chamber migration assays have shown that down-regulation of Memo in human cancer cells interferes with cell migration. In addition, it has been shown that not only migration downstream of the ErbB pathway, but also downstream of the FGFR pathway was affected by Memo down-regulation.

### 4.1.3 The structure of Memo

In collaboration with the group of Daniel J. Leahy we investigated the structure and possible function of Memo (5) and the Leahy group determined the 2.1 Å crystal structure of human Memo. We showed that Memo is structurally homologous to ligB, a member of the class II of bacterial non-heme iron dioxygenase. The active site of ligB family members is formed by two histidines and glutamine. Memo contains the two histidines, but the glutamine is replaced by a cysteine. This exchange does not necessarily imply loss of metal binding, but it was not possible to detect any metal binding in the structure or enzymatic activity of Memo. While we published earlier that in cellular lysates Memo binds Tyr1201 of ErbB2 via Shc (6), it was shown here that Memo can directly bind the phospho-peptide as well, although the dissociation constant for this interaction is relatively high in the range at  $k_D=32 \mu\text{M}$ . Therefore, *in vivo* it is likely that Memo uses other factors which enhance its binding to the receptor, e.g. shc. More recently, it has been shown that Memo binds with its vestigial active site to a 16 amino acid helical structure of the phospho-peptide (7). In addition, there is evidence that

## Introduction

phosphorylation of Tyrosine 8 of the phospho-peptide is important for Memo binding. Furthermore, three asparagine-sites proved to be essential. In Memo the three histidines as well as the cysteine, described earlier (5), are important for the interaction with the phospho-peptide. This data suggest that Memo contains a novel phosphotyrosine motif, different to the known SH2 and PTB domains.

### **4.1.4 Memo and migration**

Memo positively affects migration downstream of heregulin and FGF2 stimulation (6) and affects the formation of short-lived adhesion sites and outgrowth of microtubules, resulting in a defect in migration. Memo-RhoA-mDia1 signaling coordinates the organization of the lamellipodial actin network (8). Memo is also specifically important for directionality (9) and we demonstrated that Memo is important for PLC $\gamma$  activation by showing that in Memo knock-down T47D cells phosphorylation of PLC $\gamma$  is impaired (9). Our data suggest that Memo cooperates with PLC $\gamma$  in the migration process; both Memo knock-down cells and PLC $\gamma$  knock-down cells show impaired directional migration in T47D cells. Furthermore, our data shows that Memo interacts with cofilin, an actin severing and depolarizing protein and that in F-actin polymerizing assays Memo binds F-actin, therefore in cells Memo may enhance PLC $\gamma$  activation via altering the actin cytoskeleton (9).

## **4.2 The Fibroblast Growth Factor (FGF) tyrosine kinase receptor family**

The FGF superfamily has been shown to be important in normal physiology, both during development and in the adult organism, and as well in disease. During embryonic development, FGF receptor (FGFR) signaling orchestrates a multitude of processes. FGFRs are master regulators of mesenchymal-epithelial communication and thus are required for organogenesis and pattern formation (10, 11). They have been shown to be relevant for the formation of the nervous system, the limbs, midbrain, and the lungs (12). Furthermore, FGFR signaling also plays a key role in the induction and development of the embryonic mammary gland (13-16). In the adult, FGFs continue to regulate tissue homeostasis but also play important roles in wound healing, tissue repair, cholesterol metabolism (17, 18) and serum phosphate regulation (19-24). They have also been shown to have a role in angiogenesis and neovascularization, although FGFR signaling is thought to mainly play an indirect role by influencing other growth factors such as the vascular endothelial growth factor (VEGF) and hepatocyte growth factor (HGF) (25). Imbalances in FGF signaling cause a wide spectrum of human pathological

## Introduction

conditions, including skeletal syndromes (26), olfactory syndromes (27), phosphate wasting disorder (28, 29), and cancer (30-32).

### 4.2.1 The FGF receptors

#### 4.2.1.1 *The structure*

The FGF superfamily consists of four different FGF receptors (1-4) of which there exist various splice variants of receptors 1-3. Like all receptor tyrosine kinases, they are composed of an extracellular ligand binding domain, a single transmembrane domain and a cytoplasmic domain containing the catalytic protein tyrosine kinase core as well as additional regulatory sequences (33, 34).

The extracellular ligand-binding domain of FGFR is composed of three immunoglobulin (Ig) like domains, designated D1-D3; the stretch of D1 and D2 contains an “acid box” consisting of 7-8 acidic residues that link D1 and D2 and a conserved positively charged region in D2 that serves as a binding site for heparin (35). The third of the IgG loops can be alternatively spliced resulting in different isoforms of the receptors 1-3. The isoforms arise by two alternative exons, IIIb and IIIc, which are spliced to the common exon IIIa in a mutually exclusive fashion. These isoforms are expressed by different cell types and tissues and are referred to in the literature as ‘c’ for mesenchymal and ‘b’ for epithelial (Figure 4-1).

The cytoplasmic juxtamembrane domain of FGFRs is considerably longer than that of other receptor tyrosine kinases. This region contains a highly conserved sequence that serves as a binding site for the phosphotyrosine binding (PTB) domains of the two members of the FRS2 family of docking proteins, FRS2 $\alpha$  and FRS2 $\beta$  (36, 37). In FGFR1, seven tyrosine residues have been identified as the major autophosphorylation sites: Tyr463, 583, 585, 653, 654, 730, and 766. (38, 39).

## Introduction

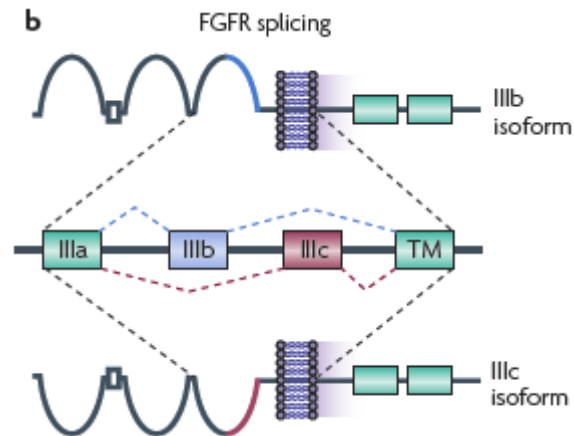


### Figure 4-1 Structure of the FGF receptors

FGFRs 1-3 are alternatively spliced. The first half of the third Ig is encoded by exon IIIa. This exon is spliced to either exon IIIb or IIIc. Epithelial tissues predominantly express the isoform IIIb and mesenchymal tissues express the isoform IIIc. This alternative splicing also influences ligand-binding specificity. Adapted from Turner et al. 2010

#### 4.2.1.2 Mutations of the FGF receptors

The knock-out of *Fgfr1* and 2 are embryonic lethal.

Mutation of *Fgfr1*: leads to growth retardation and defect of mesodermal patterning lethal at E7.5-9.5 (40, 41)

Mutation of *Fgfr2*: is lethal at E4.5-5.5 (42)

Knock-out of *Fgfr3* results in bone over growth and inner ear defect (43, 44).

Mice with a knock-out of *Fgfr4* look morphologically normal, but their liver function is decreased (depleted gallbladders, elevated bile acid pool and excretion of bile acids) and those mice are sensible to xenobiotics (CC14). (45, 46)

Mutations of the FGF receptors cause many different diseases, showing the importance of these receptors in normal physiology. Mutations are known for receptors 1-3, Table 4-1.

## Introduction

Table 1. Birth defects associated with mutations in fibroblast growth factor receptors <sup>a</sup>		
Gene	Syndrome	Typical mutations
FGFR1	Pfeiffer	IgI-IgIII linker
FGFR2	Crouzon	Mainly in third Ig-like domain. Creation or removal of cysteines, leaving an unpaired number of cysteine residues. Highly conserved amino acids
	Pfeiffer	As for Crouzon, sometimes with identical mutations
	Jackson-Weiss	As for Crouzon
	Apert	IgI-IgIII linker
	Beare Stevenson	Missense mutations leading to creation of cysteine residues
FGFR3	Craniosynostosis	IgI-IgIII linker region
	Achondroplasia	Transmembrane Gly380Arg
	Crouzon with acanthosis nigricans	Transmembrane, Ala391Glu
	Hypochondroplasia	Tyrosine kinase domain Asn540Lys
	Thanatophoric dysplasia I	Missense mutations leading to creation of cysteine residues
	Thanatophoric dysplasia II	Tyrosine kinase domain Lys650Glu
	Skeletal-Skin-Brain syndrome (SSB)	Tyrosine kinase domain Lys650Met

<sup>a</sup>Abbreviations: FGFR, fibroblast growth factor receptor; Ig, immunoglobulin.

**Table 4-1 Birth defects associated with mutations in FGF receptors**

Adapted from Burke et al. 1998

### 4.2.2 The FGFR ligands

There are 22 identified FGFs which are widely expressed in embryonic and adult tissues and have various biological activities both *in vivo* and *in vitro*, including roles in angiogenesis, mitogenesis, cellular differentiation, cell migration and tissue-injury repair. The diversity of the FGF gene family was generated both by gene and chromosomal duplication and translocation during evolution.

#### 4.2.2.1 Structure of the FGFs

Although FGFs vary in size from 17 to 34 kDa, all members of the family share a conserved sequence of 120 amino acids that show 16-65% sequence identity (47). They have a homologous core region that consists of 120-130 amino acids ordered into 12 anti-parallel  $\beta$ -strands ( $\beta$ 1- $\beta$ 12), flanked by divergent amino and carboxyl termini. In general, primary sequence variation of the N- and C-terminal tails of FGFs accounts for the different biology of the ligands (48). The heparan sulphate glycosaminoglycan (HSGAG) binding site (HBS) which is composed of the  $\beta$ 1- $\beta$ 2 loop and parts of the region spanning  $\beta$ 10 and  $\beta$ 12 is in the FGF core. For paracrine FGFs, the elements of the HBS form a contiguous, positively charged surface. In contrast, the HBS of the FGF19/endocrine subfamily contains ridges formed by the  $\beta$ 1- $\beta$ 12 loop and the  $\beta$ 10- $\beta$ 12 region, which sterically hinders HSGAG binding to the core backbone of the FGFs thus, leading to the endocrine nature of this subfamily (49). Most of the FGF ligands contain a non-cleavable N-terminal hydrophobic sequence which is required for their

## Introduction

secretion, although there are exceptions as FGF 9, 16 and 20. They lack such a signal sequence but are secreted nevertheless. FGF1 and FGF2 also lack these signal peptides, however, they are not secreted but can be released from damaged cells or by an exocytotic mechanism that is independent of the endoplasmic reticulum-Golgi pathway (47). The 22 known FGF ligands are divided into seven subgroups (Figure 4-2).

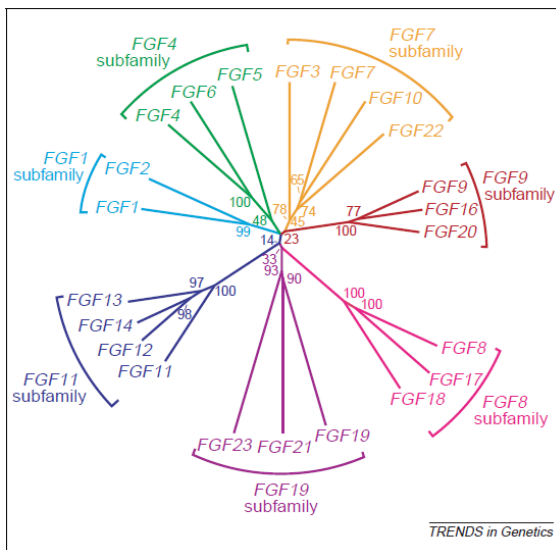


**Figure 4-2 The evolutionary relationships within the human FGF gene family (Itoh et al. 2004)**

22 genes have been identified. Phylogenetic analyses suggest grouping of those genes into seven subfamilies, each containing two to four members. Branch lengths are proportional to the evolutionary distance between each gene. The value at each branch-point indicates the percentage of times that a node was supported in 1000 bootstrap pseudoreplications. *Fgf15* is the mouse gene that is the ortholog to the human *fgf19*.

- FGF1 subfamily (FGF1 and FGF2)

The exact physiological roles of FGF1 and FGF2 are still unclear. However, it is likely that they play a part in the maintenance of vascular tone, as administration of FGF1 and FGF2 lowers blood pressure in rats (50) and can restore nitric oxide synthase activity in spontaneously hypertensive rats (51). The angiogenic properties of FGF2 are well known: exogenous FGF2 stimulates migration and proliferation of endothelial cells *in vivo* (52), it has anti-apoptotic activity (53) and it stimulates mitogenesis of smooth muscle cells in fibroblasts, which induces the development of large collateral vessels with adventitia (54). However, the physiological relevance of these effects is uncertain. Evidently, there is a high level of compensation among the growth factors mediating angiogenesis (55).



## Introduction

- The FGF4 subfamily (FGF4, FGF5, FGF6)

FGF4 has wide-ranging functions in development, including cardiac valve leaflet formation (56) and limb development (57), and it is as well important for trophoblast proliferation (58).

Thus far, roles for FGF5 in the negative regulation of the hair follicle growth cycle (59) and for FGF6 in myogenesis (60) have been elucidated.

- The FGF7 subfamily (FGF3, FGF7, FGF10, FGF22)

FGF7 is also known as keratinocyte growth factor (KGF). It is expressed specifically in the mesenchyme. Its levels are increased by up to 150-fold in the skin after cutaneous injury (61), and are also increased after bladder or kidney injury (62, 63). Homozygous deletion of FGF3 was shown to cause hereditary deafness, leading to total inner ear agenesis in humans (64). While FGF10 knock-out mice lack limbs and the pulmonary structures (65). In addition, they also exhibit defects in all other branching organs. FGF22, along with FGF7 and FGF10, are presynaptic organizers with roles in vesicle clustering and neurite branching (66).

- The FGF8 subfamily (FGF8, FGF17, FGF18)

FGF8 is involved in brain, limb, ear and eye development (67) and, along with FGF17, is crucial for forebrain patterning (68). FGF8 knock-out mice do not undergo gastrulation (69). FGF17 knock-out mice exhibit abnormalities in the development of cerebral and cerebellar structures (70) while FGF18 knock-out mice have decreased expression of osteogenic markers and delayed long-bone ossification (71, 72).

- The FGF9 subfamily (FGF9, FGF16, FGF20)

FGF9 knock-out mice demonstrate male-to-female sex reversal and lung hypoplasia that quickly leads to postnatal death (73). Importantly, the FGF9 subfamily, which signals from the epithelium to the mesenchyme, functions in a reciprocal way to the FGF7 subfamily, which signals from the mesenchyme to the epithelium. FGF9 stimulates mesenchymal proliferation, and the mesenchyme in turn produces ligands of the FGF7 subfamily. Accordingly, knocking out FGF9 disrupts the mesenchymal-epithelial signaling loop that helps to regulate these FGFRb-binding ligands. And the concomitant reduction in production of the FGF7 subfamily ligands is the proximate cause of the

## Introduction

observed lung hypoplasia (74). FGF16 knock-out mice exhibit significant cardiac defects (75).

- The FGF19 subfamily (FGF19/15, FGF21, FGF23)

This family is also called the endocrine family, as this is the way these FGFs function. FGF15 is the mouse ortholog of the human FGF19. The members of the FGF19 subfamily do not bind Heparin/HS, but interact with the Klotho family as coreceptors, which are discussed in more details in chapter 4.4.2 FGFR pathway & Metabolism.

As detailed above, the functions of the various FGF ligands are diverse and very important. Therefore, it is not surprising that null mutations in these genes lead to severe phenotypes, many of which are summarized in Table 4-2.

## Introduction

### FGF knockout mice

Gene	Survival of null mutant*	Phenotype
<i>Fgf1</i>	Viable	None identified
<i>Fgf2</i>	Viable	Mild cardiovascular, skeletal, neuronal
<i>Fgf3</i>	Viable	Mild inner ear, skeletal (tail)
<i>Fgf4</i>	Lethal, E4-5	Inner cell mass proliferation
<i>Fgf5</i>	Viable	Long hair, angora mutation
<i>Fgf6</i>	Viable	Subtle, muscle regeneration
<i>Fgf7</i>	Viable	Hair follicle growth, ureteric bud growth
<i>Fgf8</i>	Lethal, E7	Gastrulation defect, CNS development, limb development
<i>Fgf9</i>	Lethal, P0	Lung mesenchyme, XY sex reversal
<i>Fgf10</i>	Lethal, P0	Development of multiple organs, including limb, lung, thymus, pituitary
<i>Fgf12</i> ( <i>Fhf1</i> )	Viable	Neuromuscular phenotype
<i>Fgf14</i> ( <i>Fhf4</i> )	Viable	Neurological phenotypes
<i>Fgf15</i>	Lethal, E9.5	Not clear
<i>Fgf17</i>	Viable	Cerebellar development
<i>Fgf18</i>	Lethal, P0	Skeletal development

\*E, embryonic day; P, postnatal day.

**Table 4-2 FGF knock-out mice (Ornitz et al. 2001)**

#### 4.2.2.2 FGF-FGFR specificity

FGF signaling is in general important for the reciprocal communication between mesenchymal and epithelial tissue, although ligands, such as FGF1, pose exceptions to this general rule by promiscuously binding to both the b and c isoforms of certain FGFRs. (Figure 4-3). Pathological states can result from a breakdown in binding specificity, as is common in cancers in which FGFs are overexpressed (76). Structural studies of FGF1, 2, 8 and 10 with their cognate FGFRs show that sequence diversity at the FGF N-termini, variation in  $\beta 1$  strand length and the alternatively spliced regions in D3 dictate binding

specificities.

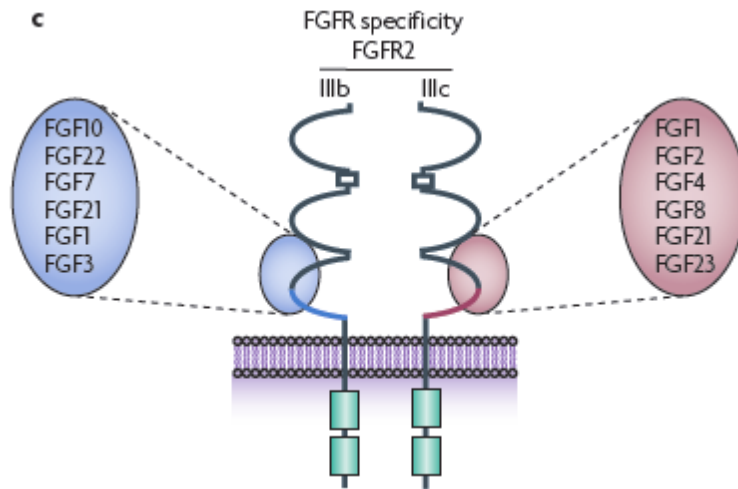


**Figure 4-3 FGFR specificity for ligand binding (Turner et al. 2010)**  
Ligand specificity shown on the example of FGFR IIIb and IIIc.

#### 4.2.2.3 Modulators of FGF signaling

There are two known factors that facilitate specific ligand activity:

- FGF-binding protein (FGFBP): activates FGFs by releasing them from the extracellular matrix, where they are bound by Heparan sulfate glucosaminoglycans (HSGAGs) (77).
- Fibronectin leucine-rich transmembrane protein 3 (FLRT3): facilitates FGF8 activity through the MAPK pathway (78).

### 4.2.3 The FGF coreceptors: Heparin/Heparan sulfate proteoglycans and the Klotho family

FGF ligands show low affinity for their receptors therefore binding of the ligands with their receptors is greatly enhanced by binding to coreceptors. For most of the ligands, with the notable exception of the three metabolic ligands, Heparin/Heparan sulfate proteoglycans (HS) serve as coreceptors and stabilize the FGF ligand/receptor complex. The three metabolic ligands on the other hand interact with members of the Klotho family.

#### 4.2.3.1 Heparin/Heparan sulfate proteoglycans (HS)

Heparin and HS are heterogeneously sulfated linear polymers containing repeating disaccharide subunits of hexuronic acid (iduronic or glucuronic acid) and D-glucosamine (79). It has been shown

## Introduction

that, although there is formation of a minimal FGF/FGFR complex in the absence of heparin/HS (80), Heparin/HS are essential for high affinity binding of the FGFs to their receptors. High affinity binding between the receptors and their ligands is important to induce signaling. Heparin/HS are found in the extracellular matrix adjacent to cell surfaces and as integral components of the plasma membrane (81, 82). Their binding of the FGFs keeps these ligands and their effects close to the secreting cell. Heparin/HS were proposed to: (i) stabilize and protect FGFs from thermal, proteolytic, or pH-dependent degradation (83, 84), (ii) function as storage reservoirs from which FGFs can be liberated for interaction with FGFRs (85-89), or (iii) facilitate FGF-FGFR encounters by limiting the diffusion of the FGF ligands (90). Finally, Heparin/HS also facilitate FGFR clustering, as they are able to simultaneously bind multiple FGF ligands. Moreover, heparin degrading enzymes (heparanases) release soluble FGF/HS complexes and therefore inhibit FGFR signaling. Another function of heparanases is to reduce adherence of cells (91).

### 4.2.3.2 *The Klotho family*

The Klotho family consists of two distinct members, named Klotho and  $\beta$ Klotho, which are encoded by two genes. They are both type I membrane proteins and have a single membrane-spanning region with a short intracellular tail (92, 93). And they both share structural similarity to family 1 glucosidase members (92, 94, 95). In contrast, for Klotho, but not for  $\beta$ Klotho a secreted form has been found (93).

Members of the FGF19 subfamily show very little affinity for their cognate FGFRs in the absence of Klotho, therefore, FGF23 uses Klotho as coreceptor and FGF19 and 21  $\beta$ Klotho. The extracellular domain of Klotho proteins was demonstrated to bind directly to multiple FGFRs (96, 97).

Klotho is discussed in more detail in chapter 4.4.2.

## 4.2.4 Signaling of the FGFR pathway

### 4.2.4.1 *FRS2 dependent signaling*

The FGFR is constitutively associated with FGFR substrate 2 (FRS2), a key adaptor protein that is largely specific to FGFRs although it can also bind other tyrosine kinase receptors, such as neurotrophic tyrosine kinase receptor type 1 (NTRK1) (36, 98), RET (99-101) and anaplastic

## Introduction

lymphoma kinase (ALK) (102). In contrast to FGFRs, RET and the neurotrophin receptors TrkA and TrkB bind only the phosphorylated form of FRS2 (36, 100).

FRS2 proteins contain myristyl anchors and PTB domains in the N-termini and a large region with multiple tyrosine phosphorylation sites at their C-termini (103, 104). They contain four binding sites for the adaptor protein GRB2 and two binding sites for the protein tyrosine phosphatase SHP2. The FRS2 family consists of two members, FRS2 $\alpha$  and FRS2 $\beta$ , which are structurally very similar. Expression of FRS2 $\alpha$  begins in the early stages of development, whereas expression of FRS2 $\beta$  begins at mid-gestation, predominantly in tissues of neuronal origin (98). The different expression patterns of FRS2 $\alpha$  and  $\beta$  suggest specific, nonoverlapping roles for each docking protein.

FRS2 is bound constitutively to the receptor but phosphorylation occurs only upon ligand binding to the receptor, dimerization and autophosphorylation of the receptor at different tyrosines. Subsequent to its phosphorylation it recruits different FRS2-dependent adaptor proteins, such as son of sevenless (SOS) and growth factor receptor-bound 2 (GRB2) to activate RAS and the downstream RAF and MAPK pathways (105). A separate complex involving GRB2-associated binding protein 1 (GAB1) that is recruited to GRB2, stimulates PI3K and the AKT pathway (106). Adaptor proteins or enzymes, which are FRS2-independent, are directly recruited to the receptor tyrosine sites, as for example PLC $\gamma$  is recruited to Tyr766. Figure 4-4

## Introduction

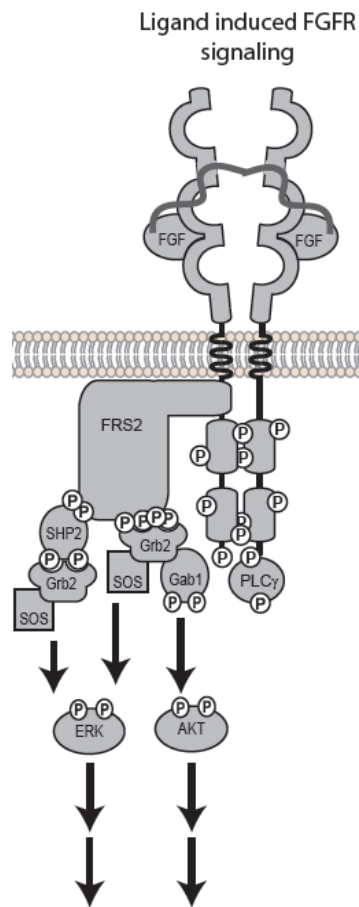


**Figure 4-4 The FGFR signalosome**

FRS2 is responsible for the assembly of both positive (i.e. SOS, PI3K) and negative (i.e. CBL), signaling proteins resulting in a balanced FGF signal transduction (105).

In addition, while tyrosine phosphorylation of FRS2 by the receptor induces positive signaling, threonine phosphorylation of FRS2 by ERK affects signaling negatively. In FGFR signaling this allows a negative feedback loop between activated ERK and FRS2. In contrast, signaling downstream of Insulin, EGF, and PDGF induces only threonine phosphorylation of FRS2 via ERK and always results in a negative outcome of the signaling downstream of FRS2 in response to Insulin, EGF and PDGF (107, 108).

### 4.2.4.2 FRS2 independent signaling

Autophosphorylation on Tyr766 in the C-terminus of FGFR1 creates a specific-binding site for the SH2

## Introduction

domain of phospholipase PLC $\gamma$  (39). Upon complex formation of Tyr766 with PLC $\gamma$ , the phospholipase is activated and phosphatidylinositol-biphosphate (PIP<sub>2</sub>) is hydrolysed leading to the generation of the two second messengers, diacylglycerol (DAG) and phosphatidylinositol-3,4,5-triphosphate (PIP<sub>3</sub>) (109). DAG activates among others, protein kinase C (PKC), which partly reinforces the activation of the MAPK pathway by phosphorylating RAF-1 (c-raf). (Figure 4-5)

Membrane recruitment of PLC $\gamma$  is aided by binding of the pleckstrin homology domain of PLC $\gamma$  to PIP<sub>3</sub> molecules that are generated in response to PI3K stimulation (110).

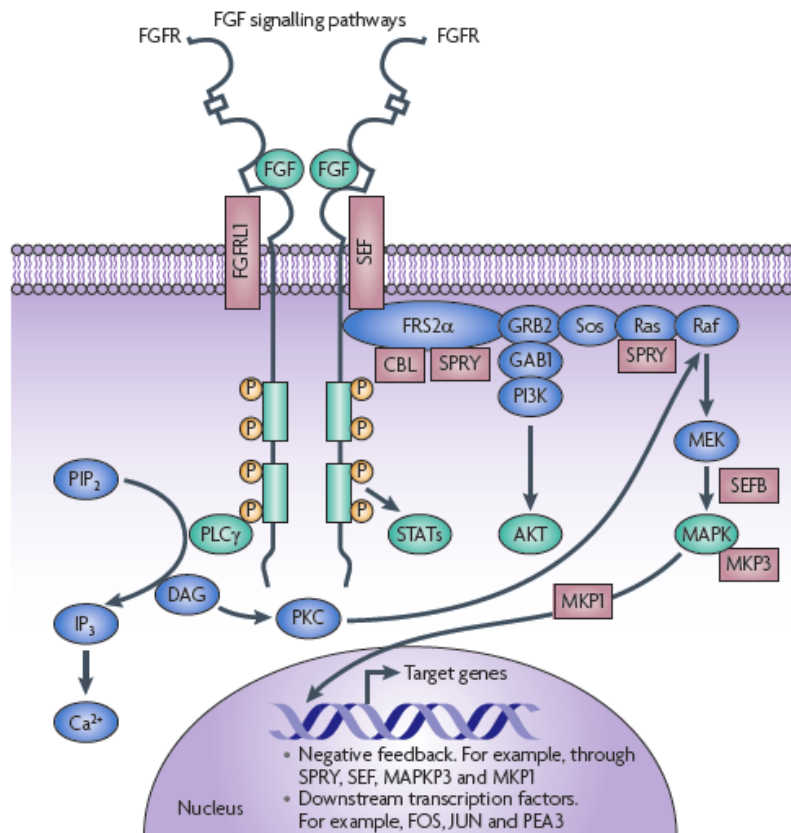


**Figure 4-5 FGFR signaling (Turner et al. 2010)**

Several other pathways are also activated by FGFRs depending on the cellular context, including the p38 MAPK and Jun N-terminal kinase (JNK) pathways, signal transducer and activator of transcription (STAT) signaling (111) and ribosomal protein S6 kinase 2 (112).



## Introduction

### 4.2.4.3 *Negative regulators of FGFR signaling*

The mechanisms of attenuation and negative feedback control of FGFR signaling are only partly understood.

- CBL

Cells that are stimulated by FGF2 induce not only activation of many pathways, but as well FGFR degradation via GRB2 dependent binding of CBL, an ubiquitin ligase, to FRS2 (113, 114). GRB2 and CBL are constitutively associated. Upon stimulation GRB2/CBL and GRB2/SOS compete for binding to FRS2. GRB2/SOS induces positive signaling while GRB2/CBL induces internalization and ubiquitination of the receptor, followed by lysosomal degradation. CBL is responsible for the main bulk of degradation, although there are also other processes that may involve other members of the CBL family that induce degradation (114).

- Negative feedback loop

MAPK signaling, particularly ERK1 and ERK2 signaling, has been shown to phosphorylate FRS2 on multiple threonine residues (canonical ERK phosphorylation sites (PXTP motif)), inhibiting the recruitment of GRB2. This inhibition is induced by a variety of ligands, FGF, insulin, EGF and PDGF (107).

- Phosphatases

Downstream signaling can be attenuated through the induction of MAPK phosphatases such as MAPK phosphatase 3 (MKP3). MKP3 dephosphorylates ERK1 and ERK2 to attenuate MAPK signaling (115).

- Sprouty (SPRY) and SEF

Sprouty proteins (116, 117) and SEF (similar expression to fgf genes) (118, 119) family members modulate receptor signaling at several points in the signal transduction cascade (120). Sprouty proteins are thought to function in either a dominant-negative fashion, by competing for GRB2 binding and thereby preventing SOS-mediated RAS activation, or by directly binding to RAF and blocking subsequent MAPK signaling (116, 117). Similarly, SEF encodes a conserved protein that shares sequence similarities with the intracellular domain of the interleukin 17 receptor. SEF is a member of the FGF synexpression group and its expression is regulated by FGF. It acts similarly to sprouty, it functions at multiple levels and has a transmembrane form that can directly interact with FGFRs; both

## Introduction

the transmembrane form and a splice variant that is confined to the cytoplasm seem to be capable of inhibiting ERK phosphorylation (121).

- Receptor recycling

Receptor recycling is a mechanism to ensure prolonged activation of the receptor and to enable dynamic regulation of signaling. NCAM has been identified as a non-canonical ligand for FGFR1. It induces internalization of the receptor to the endosome, but prevents CBL binding and thus ubiquitination and degradation. Instead the receptor is recycled to the membrane via Rab11-positive vesicles resulting in sustained signaling and cell migration (122). While FGF2 stimulated ERK activation is Ras dependent, stimulation with NCAM probably triggers an integrin-FAK-Src-ERK1/2 pathway.

### 4.2.5 FGFRs and cancer

FGFR signaling has been found to be altered in several cancers. Excessive signaling may cause; increased proliferation, enhanced survival, migration/invasion or angiogenesis.

Excess FGFR signaling can be caused by several mechanisms. Gene amplification, activating mutations, and chromosomal rearrangements in the genes encoding FGFRs can give rise to receptors with altered signaling activities. Other mechanisms involve higher ligand availability, switching of alternatively spliced isoforms, germline single nucleotide polymorphism (SNP) and inability to terminate FGFR signaling.

#### 4.2.5.1 Excessive FGFR signaling

- FGFR gene amplification

Elevated levels of FGFRs have been found in numerous human cancers such as cancer of the brain, head and neck, lung, breast, stomach, and prostate and in sarcomas and multiple myeloma (123-130). However, an elevated level of a protein in cancer cells does not necessarily mean that this protein plays a role in carcinogenesis.

Amplifications of both FGFR1 and FGFR2 have commonly been described, while amplification of FGFR3 has only been rarely described in cancers (131)

Amplification of FGFR1:

## Introduction

Amplification of the chromosomal region 8p11-12, the genomic location of FGFR1, is one of the most common focal amplifications in breast cancer (132-134), and occurs in approximately 10% of breast cancers, predominantly in oestrogen receptor (ER)-positive cancers (132). FGFR1 amplifications have also been reported in oral squamous carcinoma (129) and are found at a low incidence in ovarian cancer (135), bladder cancer (136) and rhabdomyosarcoma (137). Nevertheless, the role of FGFR1 in the amplicon is debated, because the 8p11-12 region contains many genes and FGFR1 is not always overexpressed when it is amplified. Even though Reis-Filho and colleagues showed that the FGFR1-amplified cell line MDA-MB-134 is dependent on FGFR1 for proliferation (134), it is not universally accepted that FGFR1 is a driver of cancer harboring 8p11-12 amplification.

### Amplification of FGFR2:

Approximately 10% of gastric cancers show FGFR2 amplification. There is a correlation of FGFR2 amplification and poor prognosis of diffuse-type gastric cancers (138, 139), which is a cancer type that consists of poorly differentiated tumor cells. The stomach wall is often thick and rigid, caused by diffuse infiltration of tumor cells and extensive fibrosis.

- **Activating mutations**

Mutated forms of FGFRs have been identified in cancer of the brain, head and neck, lung, stomach, prostate, colon uterus, and bladder as well as in cancer of white blood cells (140-154).

Many of the identified mutations give rise to more active forms of the receptors. Some mutations have also been shown to induce dimerization of the receptor and thereby leading to constitutive activation of the receptor kinase domain. Furthermore, mutations of the intracellular domain give rise to constitutively active kinase domains or impaired termination of FGFR signaling.

### Mutated FGFR1:

Mutations of the kinase domain of FGFR1 have been found in glioblastomas (140).

### Mutated FGFR2:

Mutations of FGFR2 are frequently extracellular and identical to the activating germline mutations found in craniosynostosis syndromes (155). Mutations have been described in 12% of endometrial carcinomas (151).

## Introduction

### Mutated FGFR3:

Bladder cancer has the most established link to FGFR mutations. Overall about 50% of bladder cancers have somatic mutation in the FGFR3-coding sequence (156). FGFR3 mutations have also been identified in many other cancer types, including cervical cancers (157), multiple myeloma, prostate cancer (150) and spermatocytic seminomas (158).

In contrast to the EGFR gene, in which activating mutations occur almost exclusively in the kinase domain, more than half of the mutations in FGFR3 occur at a single position in the extracellular domain (S249C). This mutation leads to the formation of an aberrant intermolecular cysteine disulphide bridge, which results in constitutive dimerization and activation of the receptor (159, 160). Mutations are also commonly found in the transmembrane domain, as well as less common kinase domain mutations.

### FGFR4:

Several mutations in FGFR4 were identified in approximately 7% to 8% of rhabdomyosarcoma (RMS) tumors (161).

- FGFR fusion proteins/chromosomal rearrangements

At least 11 fusion partners have been identified for FGFR1 (eg. ZNF198, FOP, and BCR 108). In the fusion proteins, the tyrosine kinase domain of the FGFR is typically juxtaposed to a dimerization domain from the partner gene, inducing constitutive dimerization and activation of the tyrosine kinase (162). Most of the FGFR fusion proteins are identified in patients with the myeloproliferative disorder stem cell leukemia/lymphoma syndrome (SCLL) also known as the 8p11 myeloproliferative syndrome (163).

Some of the strongest evidence linking FGF signaling to oncogenesis has come from the study of haematological malignancies, in which translocations involving the FGFRs have been identified. 15% of multiple myeloma cases harbor a t(4;14) translocation, that links FGFR3 at 4p16.3 to the immunoglobulin heavy chain locus at 14q32. FGFR3 translocation in multiple myeloma is associated with a poor prognosis and is rarely found in a precursor condition of multiple myeloma, which suggests that FGFR3 translocations promote a rapid conversion to full multiple myeloma (164).

## Introduction

- Ligand availability

Increased ligand availability likely leads to increased FGFR signaling. Inappropriate expression or release of FGFs from the extracellular matrix by malignant cells or cells of the tumor environment may lead to increased ligand availability.

Elevated levels of FGF8 have been reported in human breast and prostate cancer (126, 165-167), and elevated levels of FGF8, FGF3, and FGF4 have been identified as mammary proto-oncogenes in mouse mammary tumor virus (MMTV)-infected mice (168-170). In prostate cancer, several FGFs, including FGF2 (171) and FGF6 (172), are upregulated. It has been proposed that these changes in prostate cancer may result in androgen independence (126). As in prostate cancer, the expression of FGF1, FGF2 and FGF7 is higher in breast cancer stroma than in normal breast stroma (173, 174). FGF19 is overexpressed in a subgroup of liver, colonic and lung squamous carcinomas (175), while elevated levels of FGF2 might also play an important role in cancer progression. FGF2 is a potent angiogenic factor, and antisense-mediated inhibition of FGF2 in human melanoma xenografts led to tumor regression and block of intratumoral angiogenesis (176). Six different somatic mutations in FGF9 leading to loss of function have been identified in colorectal and endometrial cancer (177).

It's not only the stromal cells that secrete FGF ligands. The first strong evidence for autocrine FGF signaling driving human tumorigenesis comes from studies of melanoma, which expresses high levels of FGFR1 and FGF2. Frequent amplification of FGF1, resulting in increased FGF1 expression, has also been reported in ovarian cancer and is associated with poor survival (178). An autocrine FGF2-FGFR1-IIIc feedback loop has also been reported in non-small-cell lung cancer cell lines that show resistance to the EGFR antagonist gefitinib (179).

- Switching between alternatively spliced isoforms

Several reports have indicated different oncogenic potential of the various isoforms of the FGFRs (139, 180-183). A shift in splicing generating more oncogenic isoforms during carcinogenesis could thus promote tumor growth, while a switch from one isoform to another can lead to autocrine signaling. Exon switching in epithelial cells from the FGFR2IIIb isoforms to the mesenchymal FGFR2IIIc isoforms by alternative splicing has been described in a rat model of prostate and bladder cancer (184-186). So far it is not clear whether alternative splicing of the third Ig-like domain contributes to carcinogenesis in humans (126).

## Introduction

- Germline single nucleotide polymorphism (SNP)

SNPs are the most common type of genetic variation among humans. There are roughly 10 million SNPs in the human genome. Most of them are silent mutations. But dependent on their location they can lead to disease susceptibility.

FGFR2 has been identified as breast cancer susceptibility gene (187, 188). Interestingly, the SNP seems to appreciably increase the risk of developing ER-positive breast cancer only, with little or no effect on ER-negative breast cancer (189).

A SNP for FGFR4, G388R, has also been found. This SNP does not seem to increase the incidence of cancer, but has been reported to associate with poor prognosis in multiple cancer types, including breast cancer, colon cancer (190) and lung adenocarcinoma (191).

- Prolonged activation of FGFR signaling

There are several possibilities to attenuate FGFR signaling, e.g. the activity of the sprouty (192) and SEF (193) proteins. The protein expression of SEF is decreased in intermediate or high-grade tumors originating from the breast, ovary, thyroid, and prostate (194). Loss of SEF is correlated with increased FGF2, FGF8, and FGFR4 expression in metastatic prostate tumors (167).

### 4.2.5.2 *Oncogenic mechanisms of FGF signaling*

- FGF and proliferation

FGF10 overexpression has been found in the stromal compartment of the murine prostate, resulting in epithelial hyperproliferation, concomitant with the upregulation of the androgen receptor (195). PTEN (phosphatase and tensin homolog) a counterplayer of PI3K, has been found to be deficient in prostate epithelium synergized with autocrine overexpression of FGF8, leading to prostate adenocarcinoma (196).

- FGF and survival

Several studies have suggested that FGF2 mediates a cytoprotective effect by upregulating the expression of the anti-apoptosis proteins BCL-2, BCL-X, X-linked inhibitor of apoptosis (XIAP) and inhibitor of apoptosis 1 (IAP1) through an S6 kinase (S6K2 and RSK2)-mediated pathway, therefore promoting resistance to chemotherapy (197-199).

## Introduction

- FGF and migration/invasion

It has been shown that invasion of pancreatic cancer is FGF10- and FGFR2-IIIb dependent (200). Pancreatic cancer cells express FGF10 which induces migration and invasion by interacting with FGFR2-IIIb expressed by the stromal cells.

One study has shown that constitutive FGFR1 signaling led to the loss of polarity and the gain of a matrix metalloproteinase 3 (MMP3)-dependent invasive phenotype (201). In addition, another study showed that FGFR1 dependent epithelial-mesenchymal-transition (EMT) occurs. The EMT phenotype was accompanied by upregulation of both Sox9, an FGF target gene associated with EMT (202), and the pro-angiogenic factor angiopoietin 2 (ANG2) (203).

- FGF and angiogenesis

Angiogenesis is the process of new blood vessel formation from pre-existing vessels. It plays a key role in various physiological and pathological conditions, including embryonic development, wound repair, inflammation, and tumor growth (204). Numerous inducers of angiogenesis have been identified, including members of the FGF family. They affect angiogenesis via different mechanisms:

- Experimental evidence indicates that different members of the FGF family, but mostly FGF1 and FGF2, can induce *in vitro* a “pro-angiogenic phenotype” in endothelial cells (205).
- Activation of FGFR1 or FGFR2 by angiogenic FGFs (including FGF1, FGF2, and FGF4) leads to endothelial cell proliferation (206).
- FGF/FGFR activity leads to upregulation of VEGF expression in tumors (207). Exogenous FGF2 induces VEGF expression in endothelial cells (208).
- FGF/FGFR signaling results in expression of matrix metalloproteinases (MMPs) that allow mobilization of angiogenic growth factors from the extracellular matrix (ECM) of tumor and stromal cells by degeneration of the ECM (207). The plasmin-plasminogen activator system and MMPs cooperate in this degradation (209).
- FGF1, FGF2 (210, 211), the FGF8b isoforms (212), and FGF10 (213) stimulate chemotaxis and/or chemokinesis in endothelial cells.
- FGFs can promote both endothelial cell scattering, that is required during the first steps of the

## Introduction

angiogenic process, and the formation of the cell-cell interactions required for vessel maturation (214).

### 4.2.5.3 *FGFR signaling and tumor suppression*

FGFRs have also been suggested to have tumor suppressor activity, which is best illustrated by studies of FGFR2. Reduced expression of FGFR2 has been reported in several human cancers, such as bladder, liver, salivary gland, and prostate cancer (215-217). In addition several loss-of-function mutations in FGFR have been identified in melanoma (218).

## 4.3 Aging and Premature aging

Aging is a natural process that is not influenced by selection. Aging is associated with a number of events at the molecular, cellular and physiologic levels that influence carcinogenesis and subsequent cancer growth in both humans and laboratory animals. Therefore the study of cancer and premature aging syndromes has become increasingly important to gain a clearer understanding of these events. It is evident that the mechanisms underlying cancer and premature aging are often similar and affect mainly DNA instability. All of the premature aging diseases found in humans so far are related to DNA instability, the main cause for development of cancer.

Most of the conditions with errors in genome maintenance fall into three classes:

- Many attributes of ageing are accelerated but cancer incidence is reduced
- Specific cancer types are enhanced
- Incidence of both cancer and segmental progeria is increased.



## Introduction

**Table List of syndromes carrying defects in genome maintenance**

Progeria			
Syndrome	Mutated genes	Affected processes	Mouse models
Cockayne syndrome (CS)	CSA, CSB	TC-NER	<i>Csa</i> <sup>-/-</sup>
			<i>Csb</i> <sup>tm</sup>
		TC-NER; GG-NER	<i>Csb</i> <sup>tm</sup> <i>Xpa</i> <sup>+/-</sup> ; <i>Csb</i> <sup>tm</sup> <i>Xpc</i> <sup>+/-</sup>
			<i>Csa</i> <sup>+/-</sup> <i>Xpa</i> <sup>+/-</sup> ; <i>Csa</i> <sup>+/-</sup> <i>Xpc</i> <sup>+/-</sup>
Trichothiodystrophy (TTD)	<i>XPB</i> , <i>XPD</i> , <i>TTDA</i>	Partial GG/TC-NER	<i>Xpd</i> <sup>td</sup>
COFS	<i>CSB</i> , <i>XPD</i> , <i>XPG</i>	GG-NER; TC-NER	<i>Xpg</i> <sup>+/-</sup>
XPE	<i>XPF/ERCC1</i>	GG/TC-NER, ICL repair, HR	<i>Ercc1</i> <sup>+/-</sup>
Rothmund-Thomson (RTS)	<i>RECQL4</i>	Oxidative DNA damage repair	<i>Recq14</i> <sup>+/-</sup>
Dyskeratosis congenita	<i>DKC1</i> , <i>TERC1</i>	Telomere maintenance	<i>Dkc1</i> <sup>m</sup>
			<i>mTR</i> <sup>+/-</sup>
Hutchison-Gilford progeria syndrome (HGFS)	<i>LMNA</i>	Nuclear lamina function	<i>Zmpste24</i> <sup>+/-</sup>
Atypical Werner syndrome			<i>Lmna</i> <sup>L530P/L530P</sup>
Restrictive dermopathy (RD)			
Mandibuloacral dysplasia (MAD)			
Cancer			
Syndrome	Mutated genes	Affected processes	Mouse models
Breast cancer 1, early onset	<i>BRCA1</i>	DSB repair (HR)	<i>Brca1</i> <sup>+/-</sup> ; early lethality
Breast cancer 2, early onset	<i>BRAC2</i>		<i>Brca2</i> <sup>+/-</sup> ; early lethality
Li-Fraumeni	<i>P53</i>	Checkpoint control	<i>p53</i> <sup>+/-</sup>
Chk2	<i>CHK2</i>	G1 checkpoint control	<i>Chk2</i> <sup>+/-</sup>
von Hippel-Lindau syndrome	<i>VHL</i>	Cell-cycle regulation	<i>Vhl</i> <sup>+/-</sup>
Hereditary non-polyposis colorectal cancer	<i>Msh2</i> ; <i>Mlh1</i>	Mismatch repair	<i>Msh2</i> <sup>+/-</sup>
XP	<i>XPC</i>	GG-NER	<i>Xpc</i> <sup>+/-</sup>
Progeria + cancer			
Syndrome	Mutated genes	Affected processes	Mouse models
Fanconi anaemia (FA)	<i>FANC</i> , <i>BRCA2</i>	DNA crosslink repair	<i>Fancc</i> ; <i>Fanca</i> ; <i>Fancg</i> ; <i>Fancd2</i> ; <i>Brca2</i>
Xeroderma pigmentosum (XP) combined with CS (XPCS)	<i>XPB</i> , <i>XPF</i> , <i>XPD</i> , <i>XPG</i>	NER	<i>Xpd</i> <sup>xpcs</sup>
Xeroderma pigmentosum (XP)+DeSanctis-Cacchione syndrome (DSC)	<i>XPA</i> , <i>XPD</i>	NER	<i>Xpg</i> <sup>+/-</sup>
Ataxia telangiectasia (AT)	<i>ATM</i>	DSB repair	<i>Atm</i> <sup>+/-</sup> <i>mTR</i> <sup>+/-</sup>
Ataxia telangiectasia-like disorder (ATLD)	<i>MRE11</i>	DSB repair	<i>Mre11</i> <sup>+/-</sup>
Nijmegen breakage syndrome (NBS)	<i>NBS1</i>	DSB and telomere maintenance	<i>Nbs1</i> <sup>p70</sup>
Bloom syndrome (BLS)	<i>BLM</i>	Mitotic recombination	<i>Blm</i> <sup>+/-</sup>
Werner syndrome (WS)	<i>WRN</i>	Telomere maintenance, DNA recombination and repair	<i>Wrn</i> <sup>+/-</sup> <i>mTR</i> <sup>+/-</sup>

From Garinis et al. 2008. Abbreviations: TC-NER: transcription-coupled nucleotide excision repair, GG-NER: global genomic nucleotide excision repair (repair of damage in transcribed and untranscribed DNA strands in active and inactive genes throughout the genome), COFS: cerebro-oculo-facio-skeletal syndrome, HR: homologous recombination, ICL: interstrand crosslinks, DSB: double-strand break, XFE: Epf-Errcc1 syndrome.

### 4.3.1 Different Models of premature aging

The mutations leading to DNA instability are various. There are mutations in telomerases (eg. Werner Syndrome) or mutations in proteins important for nucleus stability and shape (Laminopathies, eg. Hutchinson-Gilford progeria syndromes). More recently it has been shown that mutations affecting the metabolism (eg. affecting the serum level of phosphate) can also promote aging.

- DNA instability

e.g. Werner Syndrome:

The gene on chromosome 8p12, the Werner gene (*WRN*) was identified in 1996 by positional cloning and encodes a 162 kDa RecQ helicase protein (219). The human RecQ helicase family consists of five proteins, of which only *WRN* possesses 3'→5' exonuclease activity and 3'→5' helicase activity (220, 221). All of the disease-associated *WRN* mutations (222, 223) confer a common biochemical phenotype: they lead to truncation or, in one instance, apparent destabilization and loss of *WRN* protein from patient cells (224, 225). In mammalian cells the function of *WRN* is limiting genetic instability and cell death. It does so by repairing DNA-strand breaks that arise from replication arrest. *WRN* also has an important role in the maintenance of telomere length and the suppression of telomere sister-chromatid exchanges (226-230). In the absence of *WRN* function cells accumulate potentially toxic DNA intermediates or critically short telomeres that can trigger genetic instability, DNA damage and apoptotic response pathways (226, 230, 231). So far, three different Werner-syndrome mouse models have been developed; 1) mouse strain expressing a mutant *WRN* protein that is truncated in the middle of the helicase region, resulting in mice that are functionally null (*WRN*<sup>-/-</sup>) (232). This mutation resembles many of the mutations in WS patients. MEFs showed accelerated replicative senescence, and this was enhanced in cells from mice on a Bloom's syndrome (*BLM*) +/- background. Histopathological studies failed to show any unusual lesions in these mice up to the age of seventeen month. 2) a mouse strain with an in-frame deletion of the helicase domain (which leads to a truncated protein that retains exonuclease activity) (233). MEFs showed a progressively reduced growth rate with increased passage number. The mice itself exhibited a normal phenotype until the age of twelve month. Mice with either a deletion or a truncation in the *WRN* helicase domain showed gross abnormalities when they were crossed to mice on a p53 <sup>-/-</sup> background. *WRN* +/- mice showed increased rates of

## Introduction

mortality, as assessed by both median survival and maximum survival. Interestingly, the mice with the in-frame deletion on a p53  $-/-$  background exhibited increased numbers of tumors, and a larger variety of tumor types at an earlier age, as compared to WRN  $+/+$ ;p53  $-/-$  mice (234). This suggests that WRN and p53 play a synergistic role in the maintenance of genomic stability. 3) transgenic expression of a human Lys577Met WRN variant protein that lacks helicase activity and ATP-ase activity in a background of normal murine WRN protein (235). Tail fibroblasts showed reduced replicative lifespan. The mice did not show any histopathological abnormalities until the age of eighteen month.

To date, there is no animal model of WS that accurately mimics the human disease.

- Nucleus stability and shape

e.g. Laminopathies:

Laminopathies include at least ten distinct diseases, each caused by dominant missense mutations in *LMNA* (236), the single locus that encodes lamin A, B and C through alternative splicing (237). Lamins are intermediate filament proteins and lamin A and C are components of the nuclear lamina. The ability of lamins to multimerize into filaments lends both rigidity and elasticity to the nuclear lamina (238). Lamin A and C have been implicated in the regulation of transcription, DNA replication, cell-cycle control and cellular differentiation (239-242).

The Lamin A protein is synthesized as a 664-amino-acid precursor protein, called prelamin A (243). Prelamin A contains a C-terminal CAAX amino-acid motif that undergoes farnesylation at the cysteine residue. Farnesylated prelamin A undergoes two cleavages; the first takes place C-terminal to the modified Cysteine, whereas the second removes 15 C-terminal residues, including the farnesyl-Cysteine.

The most famous laminopathy is the Hutchinson-Gilford progeria syndrome (HGPS):

HGPS is the most severe of the progeroid syndromes; affected individuals have a mean lifespan of only 13 years (244). The disease was first described in 1886 (245), and is rare: there are currently fewer than 150 documented cases of HGPS worldwide. HGPS patients generally appear normal at birth, but prematurely develop several features that are associated with ageing. Death in patients with HGPS frequently results from stroke or coronary failure.

The genetic basis of HGPS was uncovered in 2003, when it was found that most cases of the disease are associated with a single nucleotide substitution that leads to aberrant splicing of *LMNA*

## Introduction

(246-248). The most common HGPS-associated mutation, Gly608Gly, causes 150 nucleotides encoded in exon 11 to be spliced out of the final mRNA and results in a protein that lacks 50 amino acids. This protein was named progerin and retains its C-terminal CAAX motif but lacks sequences that are required for complete processing and is, therefore, uncleaved (prelamin A) and stably farnesylated.

Deletion of the endopeptidase-encoding gene *Zmpste24* has also been found. It results in a block of both prelamin A cleavage events and the production of mature lamin A. The resulting protein that accumulates is farnesylated, uncleaved prelamin A (249).

- **Metabolism**

Accumulating evidence has demonstrated that inorganic phosphate has a significant impact on glucose metabolism and oxidative stress, which potentially affects aging processes of any organism from yeast to human (250). This is discussed in greater detail in the following chapter.

### **4.3.2 Aging and Metabolism**

It has been shown that the FGF23-Klotho-FGFR1 pathway in the kidney regulates serum levels of vitamin D, phosphate and calcium. Disruption of this pathway leads to hypervitaminosis and hyperphosphatemia and ultimately to a premature aging phenotype (23, 92, 251). Klotho and FGF23 mutant mice that were fed with low-vitamin D or low-phosphate diet, showed rescue of the premature aging phenotype:

- High levels of vitamin D were reduced by placing the animals on a vitamin D deficient diet. This not only restored serum phosphate and calcium levels to normal but also rescued several aging-like phenotypes in both Klotho and FGF23 mutant mice (252, 253).
- Ablation of vitamin D action in Klotho and FGF23 mutant mice via disruption of either the *Cyp27B1* (251, 254) or *vitamin D receptor* gene (255) also rescued the hyperphosphatemia, hypercalcemia, and the premature-aging syndrome.
- Low phosphate diet rescued the premature aging phenotype even though the vitamin D and calcium levels were upregulated (252, 256).
- Double knock-out mice of Klotho and the renal sodium phosphate cotransporter (Na-Pi2a) (*Klotho*<sup>-/-</sup> *Na-Pi2a*<sup>-/-</sup> mice) are rescued from hyperphosphatemia and premature aging signs. Nevertheless, when challenged with a high phosphate diet the premature aging signs observed

## Introduction

in the Klotho mutant mice reappeared (257).

Thus, data provided by the last two points suggest that elevated phosphate, rather than calcium or vitamin D, is primarily responsible for the aging-like phenotypes (250, 257). Nevertheless, it is possible and likely that low vitamin D diet and ablation of vitamin D activity rescues accelerated aging by contributing to the reduction of phosphate levels.

- Phosphate and aging

A major question is how phosphate can cause aging:

There is still little known about the direct effects of phosphate on aging, however, accumulating evidence suggests that inorganic phosphate significantly impacts glucose metabolism and oxidative stress, potentially affecting the aging processes of any organism from yeast to human (250).

- Glucose metabolism

The effect of phosphate on metabolism is apparently conserved from yeast to human. In yeast it has been shown that low phosphate induces similar metabolic changes as caloric restriction, which is also called glucose restriction (258-260). It has been shown in mammals that diet restriction and a low phosphate diet cause similar metabolic changes. Animals under diet restriction reduce blood insulin levels to adapt to the reduced carbohydrate availability. In addition, they alter the expression of insulin-responsive genes, leading to changes in glucose metabolism, including increased gluconeogenesis and decreased glycolysis (261-265). Although reduced blood insulin levels are not a consequence of the low phosphate diet, the diet alters the expression of insulin-responsive genes similar to diet restriction (266, 267), also resulting in increased gluconeogenesis and decreased glycolysis. Adequate suppression of the insulin-like signaling pathway is an evolutionarily conserved mechanism for anti-aging and life span extension in *Caenorhabditis elegans* and *Drosophila* (268-272).

- Oxidative stress

In addition to its involvement in glucose metabolism and insulin sensitivity, inorganic phosphate has been shown to increase oxidative stress both *in vivo* and *in vitro* (273, 274). Inorganic phosphate enters cells and gets transported into mitochondria where it functions as a substrate of ATP synthase and as a key regulator of oxidative phosphorylation. The mitochondrial potential increases proportionally to the extra-mitochondrial phosphate

## Introduction

concentration (275) and is known to correlate with ROS production in the electron transport chain (276). Thus, inorganic phosphate plays multiple roles in the regulation of oxidative stress and mitochondrial function in health and disease, which potentially affect aging processes.

- Hypoglycemia

Most models for premature aging exhibit a diabetes-like phenotype and insulin resistance. The FGF23 and Klotho deficient mouse models are an exception to this, as they both manifest hypoglycemia and increased insulin sensitivity (23, 92, 277). To date these are the only two premature aging models described that present with postprandial hypoglycemia and high insulin sensitivity due to the high phosphate levels.

### 4.4 Phosphate homeostasis

There are several organs and pathways which contribute to phosphate homeostasis. Phosphate is taken up via nutrition and enters the blood stream in the gut. In the kidney excess phosphate gets excreted, while enough is reabsorbed to ensure steady levels of phosphate in the blood. Parathyroid hormone (PTH), secreted by the parathyroid gland, and FGF23 secreted by the bone influence the activity of uptake, excretion and reabsorption of phosphate (Figure 4-6).

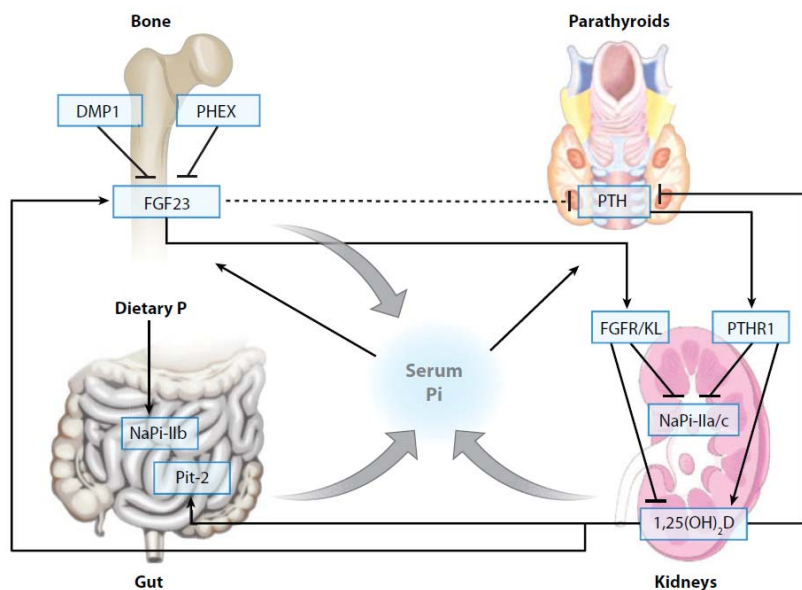


**Figure 4-6 Regulation of phosphate homeostasis (Bergwitz et al. 2010)**

Phosphate (P) is absorbed from the diet in the gut, stored in the skeleton, and excreted by the kidneys. Active vitamin D (1,25(OH)<sub>2</sub>D) stimulates absorption of phosphate from the diet. FGF23 increases renal phosphate clearance, suppresses synthesis of 1,25(OH)<sub>2</sub>D, and may decrease parathyroid hormone (PTH). PTH increases renal phosphate clearance and

## Introduction

stimulates synthesis of 1,25(OH)<sub>2</sub>D. DMP1: Dentin Matrix Protein-1, PHEX: phosphate regulating gene with homologies to endopeptidases on the X chromosome, Na-Pi2: sodium phosphate cotransporter, Pit-2: a type III Na-Pi cotransporter, that belongs to the SLC20 gene family, KL: Klotho, PTHR1: parathyroid hormone receptor 1

Important players of these processes are:

- FGF23, a member of the endocrine FGFs
- Klotho
- The FGF receptors
- Vitamin D (and Cyp27B1/Cyp24A1)
- The sodium phosphate cotransporters Na-Pi2a and Na-Pi2c
- The parathyroid hormone (PTH)

### 4.4.1 FGF23, a member of the endocrine FGF family

The members of the FGF19/endocrine subfamily are also called the metabolic FGFs as they have important functions in metabolism. The family consists of three members FGF15/19, FGF21 and FGF23. These ligands require specific coreceptors, the Klotho family, to bind to their cognate FGFRs. FGF23 binds to Klotho and FGF15/19 and 21 bind to  $\beta$ Klotho. The expression of these receptors is limited, which ensures organ specificity for these ligands.

#### 4.4.1.1 FGF15/19

*FGF19* is the human orthologue of the murine *FGF15* and was cloned by homology to mouse *FGF15* (278). FGF15/19 is produced by the intestine and is involved in bile acid synthesis and gallbladder filling. *FGF15* knock-out mice were reported to display contracted gallbladders (279) and enhanced bile acid synthesis due to high expression levels of *cholesterol 7 $\alpha$ -hydroxylase (CYP7A1)* in the liver (280). *Cyp7A1* encodes for the key rate-limiting enzyme for the bile acid synthesis pathway. There is strong evidence that FGF15/19 signals via FGFR4 and binds  $\beta$ Klotho as a coreceptor, based on the similar phenotype of *FGFR4* (280) or  *$\beta$ Klotho* (281) knock-out models and *FGF15* knock-out mice.

#### 4.4.1.2 FGF21

FGF21 is a 209 amino-acid protein including a 28 amino-acid signal peptide (282). It is mainly

## Introduction

expressed in the liver and was shown to be involved in carbohydrate and fat metabolism (283). Furthermore, it has been reported that FGF21 is involved in the response to fasting (284, 285).  $\beta$ Klotho and FGFR1 have been reported to be essential for these effects of FGF21 (286, 287).

### 4.4.1.3 *FGF23*

FGF23 is the third endocrine FGF ligand. It is secreted primarily from the bone and acts on several organs, including the kidney where it inhibits phosphate reabsorption and vitamin D biosynthesis (288, 289). FGF23 was originally identified as a gene mutated in patients with autosomal dominant hypophosphatemic rickets (ADHR), one of the rare hereditary disorders that exhibit renal phosphate wasting (290). The stimuli for FGF23 synthesis and secretion are phosphate and active vitamin D levels.

- The structure

The *FGF23* gene encodes a 32kDa secreted protein that has N-terminal FGF homology to other FGFs and a unique 71-amino-acid C-terminal domain (291, 292).

- Function

The principal actions of FGF23 are to inhibit sodium-dependent phosphate reabsorption and  $1\alpha$ -hydroxylase activity in the proximal tubule of the kidney, leading to phosphaturia and suppression of circulating active vitamin D ( $1,25(\text{OH})_2\text{D}$ ) levels.

- Production

FGF23 is predominantly produced by osteocytes in bone; however, the exact mechanism controlling its expression is still unclear. Based on studies of mutations leading to diseases in human, it is known which factors play important roles:

**PHEX** (phosphate regulating gene with homologies to endopeptidases on the X chromosome): Inactivating mutations of PHEX (hyp mice) lead to upregulated levels of FGF23. PHEX is mutated in XLH patients, patients with X-linked hypophosphatemic rickets. (See also further down).

**DMP1** (Dentin Matrix Protein-1):

DMP1 is an acidic noncollagenous extracellular matrix protein and belongs to the SIBLING (small integrin binding ligand N-linked glycoprotein) family. Mutations in DMP1 lead to increased production of FGF23 (293, 294). Mutation of DMP1 in humans leads to autosomal recessive hypophosphatemic rickets (ARHR). (See also further down).



## Introduction

The mechanisms how PHEX and DMP1 regulate the level of FGF23 is so far unknown.

GALNT3 (UDP-N-acetyl- $\alpha$ -D-galactosamine/polypeptide N-acetylgalactosaminyl transferase 3):

This enzyme is responsible for the initiation of O-linked glycosylation (295). Loss-of-function mutations in GALNT3 destabilize FGF23 and/or impair its secretion. This results in low levels of intact FGF23 but high levels of biologically inactive C-terminal FGF23 fragments in the serum (296). Mutation of GALNT3 in humans leads to hyperostosis-hyperphosphatemia syndrome (HHS). Patients with HHS are characterized by hyperphosphatemia, inappropriately normal or elevated vitamin D and cortical hyperostosis.

- Knock-out of FGF23

FGF23 knock-out mice showed hypercalcemia, hyperphosphatemia, growth retardation, ectopic calcifications, severe osteoidosis, skin atrophy, and renal dysfunction (23). This phenotype is very similar to the Klotho mutant phenotype (see below). Therefore, it was hypothesized that FGF23 and Klotho may share the same pathway (96). It has since been revealed that both FGF23 and Klotho regulate vitamin D, phosphate and calcium levels by controlling the Klotho-FGFR1 pathway in the kidney. This is also referred to as the FGF23-Klotho axis. Although FGF23 and Klotho cooperate in controlling phosphate and calcium levels, there are also independent activities.

- Signaling in the kidney

FGF23 binds FGFR1 in the renal proximal tubule of the nephron with the help of the coreceptor Klotho. The FGF23-Klotho axis controls the levels of vitamin D, phosphate and calcium.

- Vitamin D

The level of vitamin D is controlled by the vitamin D converting enzyme 1 $\alpha$ -hydroxylase encoded by *Cyp27B1* and the vitamin D catalyzing enzyme 24-hydroxylase encoded by *Cyp24A1*. 1 $\alpha$ -hydroxylase synthesizes the active form of vitamin D (1,25-dihydroxyvitamin D<sub>3</sub>) from its inactive precursor (297). 24-hydroxylase catalyses active vitamin D and 25-dihydroxyvitamin D<sub>3</sub> to 24,25-dihydroxyvitamin D<sub>3</sub> (298). FGF23-Klotho signaling inhibits transcription of *Cyp27B1*, and upregulates transcription of *Cyp24A1*. Klotho mutant mice show decreased levels of *Cyp27B1* and *Cyp24A1* RNA (299).

## Introduction

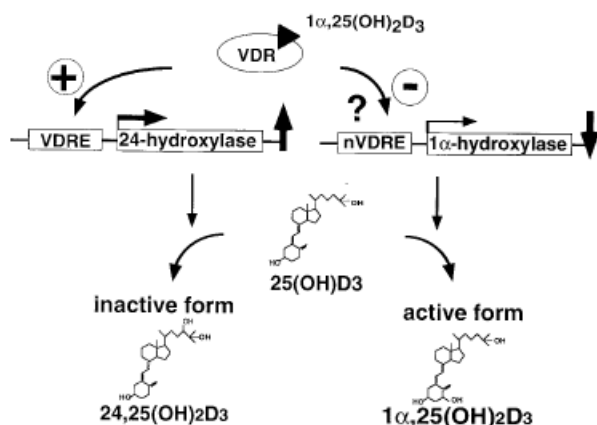


**Figure 4-7 Vitamin D metabolism**

### ○ Phosphate

Sodium phosphate cotransporters Na-Pi2a and 2c are expressed in the brush border membranes (BBMs) of the renal tubular cells. FGF23-Klotho signaling controls the levels of expression of these transporters as well as their internalization. Klotho mutant mice show lower levels of expression of Na-Pi2a and 2c (300) but higher activity and localization to the BBM of the expressed transporters (301). This leads to more reabsorption of phosphate from the urine and results in hyperphosphatemia found in the Klotho mutant mice.

### ○ Calcium

Calcium is reabsorbed from the urine into the blood by Calcium specific transport proteins. These proteins are transcribed by vitamin D mediated gene transcription. Therefore, active FGF23-Klotho signaling regulates Calcium reabsorption indirectly via control of the level of active vitamin D (302-306).

### ● Vitamin D independent functions of FGF23

FGF23 may directly modulate trafficking of the Na-Pi2a transporter from the apical membrane to the intracellular organelles (307, 308).

So far, the role of FGF23 in calcium regulation has not been investigated in great detail as administration of FGF23 did not affect the serum calcium level in normal mice (24).

### ● FGF23 and disease

## Introduction

- Autosomal dominant Hypophosphatemic rickets/osteomalacia (ADHR) (309)

ADHR was first described in 1971 as a phosphate wasting disease with an autosomal dominant inheritance (310). It is characterized by a missense mutation in either the Arg176 or Arg179 site, resulting in a FGF23 protein that is not recognized or cleaved by furin (311). This results in high serum levels of full-length FGF23 protein, causing the phenotype of hypophosphatemia, renal phosphate wasting, inappropriately low or normal levels of 1,25dihydroxyvitamin D3 along with skeletal defects that include rickets/osteomalacia, fractures, and dental abscess.

- Tumor-induced rickets/osteomalacia (TIO) (21)

TIO is an acquired paraneoplastic disorder characterized by tumors that are mainly of mesenchymal origin and which produce excessive amounts of phosphaturic peptides (20, 312-315). It has been shown that they secrete excessive levels of FGF23 (19-21, 313), MEPE (a gene expressed in the bone marrow and tumors causing osteomalacia) (316), FGF7 (317), and sFRP-4 (318). Tumors causing TIO are usually benign and of mesenchymal origin, and the majority can be classified as phosphaturic mesenchymal tumors with a mixed connective tissue variant (319, 320).

- Autosomal recessive hypophosphatemic rickets (ARHR)

ARHR shares a similar phenotype with ADHR (321, 322). Patients with ARHR have hypophosphatemia, phosphaturia, low or inappropriately normal levels of 1,25dihydroxyvitamin D3, high serum alkaline phosphatase, and evidence of skeletal defects (rickets/osteomalacia). The genetic defect for ARHR has been identified and shown to be caused by a homozygous inactivation mutation of the DMP1 (Dentin matrix acidic phosphoprotein 1) (293, 294).

- Fibrous dysplasia (FD)

FD is characterized by fibrous skeletal lesions and mineralization defects of the bone.

- X-linked hypophosphatemic rickets (XLH)

It is the most common form of inherited rickets with an incidence of 1:20,000. Patients with this disorder have severe hypophosphatemia due to renal phosphate wasting that is not caused by hyperparathyroidism, and vitamin D levels are not elevated as predicted, but are abnormally normal or low for their level of hypophosphatemia. These abnormal vitamin D levels are due to both: low 1 $\alpha$ -hydroxylase activity (323-325) and increased 24-hydroxylase activity (326).

- Familial tumoral calcinosis

## Introduction

This is an autosomal recessive condition characterized by painful depositions of calcium and phosphate in the joints and soft tissues (327-329). Mutations in *GALNT3* and in the *fgf23* gene have been identified to cause this disease.

### ○ Chronic kidney disease (CKD)

CKD is very common. 1 out of 10 will develop CKD; in young adults only 1 out of 50 will be affected, in elderly people (over 75 years) 1 out of 2 is affected. But not all of them will ever require dialysis or a kidney transplant. A CKD patient is at higher risk of heart attack or stroke. Patients suffering from CKD have hyperphosphatemia as a result of kidney failure. In early stages of CKD, serum FGF23 is elevated to maintain normal serum phosphate levels by promoting urinary phosphate excretion and decreasing the levels of vitamin D to lower phosphate absorption in the gut. In the beginning of the disease this is a helpful compensation, but in advanced stages overt phosphate loading may overcome such compensation and the elevated FGF23 levels result in decreased renal production of vitamin D, worsening secondary hyperparathyroidism (330). Patients with more advanced CKD exhibit impaired urinary phosphate excretion despite extremely high FGF23 levels. FGF23 is increased about 1000 fold compared to healthy individuals. In late stage CKD the parathyroid gland develops resistance against FGF23 by downregulating the FGFR1c-Klotho complex on the cell surface. While in healthy individuals FGF23 suppresses secretion of PTH (331), in late stage CKD, PTH secretion remains stimulated despite extremely high FGF23 levels as the parathyroid glands becomes FGF23 insensitive (332, 333). Therefore, PTH levels decrease and patients develop secondary hyperparathyroidism. Furthermore, high levels of FGF23 cause cardiovascular disease. Thus, FGF23 is a bad prognosis factor in CKD. A possible approach for therapy could be to apply a low phosphate diet in a stage of the disease before the initial rise of FGF23 levels.

### 4.4.2 Klotho

The Klotho family consists of two members: Klotho and  $\beta$ Klotho, which share a 41% amino acid identity.

- The structure

## Introduction

The mouse *Klotho* gene is composed of 5 exons and 4 introns and resides on chromosome 13q12 with a size over 50kb (92). The transcript of the mouse *Klotho* gene is about 5.2kb. Its promoter lacks a TATA-box and contains four potential binding sites for Sp1 (334). In the third exon, there is an alternative splicing at an internal splice donor site. Therefore, two transcripts arise from the template by alternative RNA splicing: a transmembrane and a secreted form of the Klotho protein (334-336). The transmembrane form of Klotho is produced from the full length transcript and encodes 1014 amino acids. The extracellular domain of Klotho can be shed from the cell surface and is detected in the blood and cerebrospinal fluid in mice and humans (337).

Klotho and  $\beta$ Klotho have two  $\beta$ -glucosidase-like domains in the extracellular regions. However, it has been unclear whether Klotho and  $\beta$ Klotho actually function as  $\beta$ -glucosidases *in vivo*.

- The expression of Klotho and  $\beta$ Klotho

Klotho is expressed in several tissues including kidney, parathyroid gland and choroid plexus (338). Kidney is the organ with the highest expression of Klotho. For several years it is known that Klotho is expressed in the distal convoluted tubules, but more recently, applying more sensitive techniques Klotho has been found also in the proximal tubules. Klotho is transcribed and expressed in those two segments of the nephron (339).  $\beta$ Klotho is expressed in adipose tissue, liver and pancreas (93).

- Function of Klotho

- Coreceptor for endocrine FGFs:

Klotho is an essential coreceptor for FGF23 signaling in the kidney (96) and in the parathyroid gland.  $\beta$ Klotho functions as coreceptor for FGF15/19 in the liver and FGF21 in the adipose tissue (287).

- Klotho as a calcitonin

The regulation of Calcium reabsorption is depicted in Figure 4-8:

## Introduction

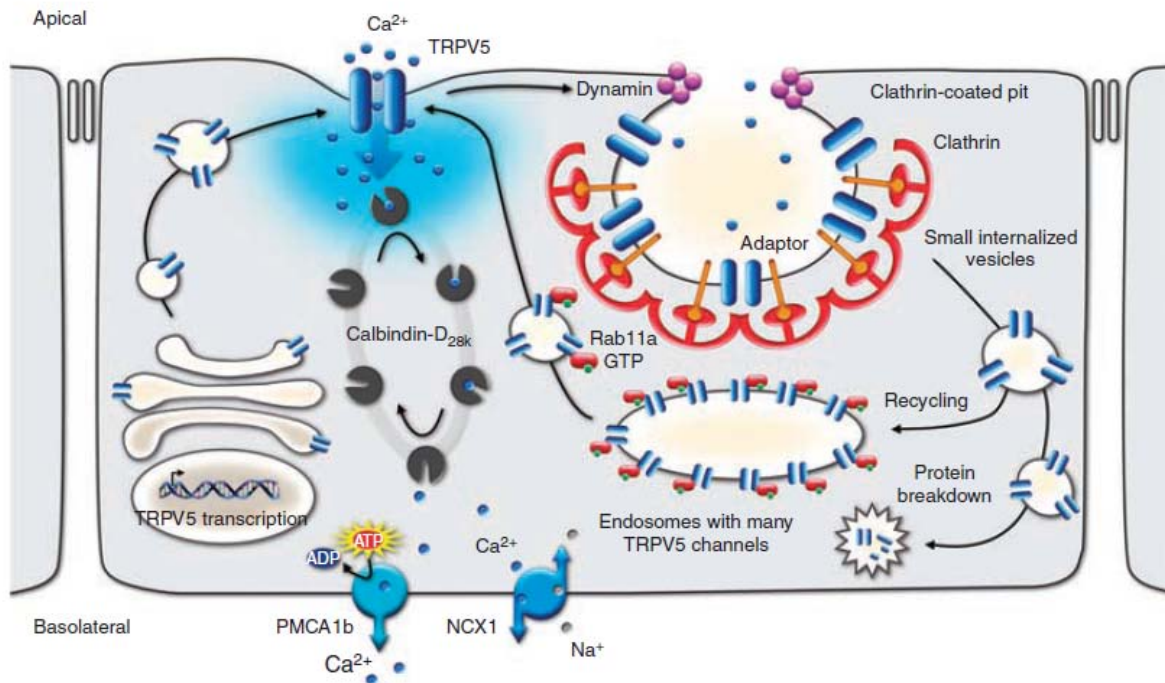


**Figure 4-8 Regulation in active renal  $\text{Ca}^{2+}$  reabsorption (from de Groot et al. 2008)**

TRPV5 is a tetrameric channel. TRPV5 is sorted by the Golgi apparatus and integrated into the plasma membrane of the nephron. The function of TRPV5 is to allow influx of  $\text{Ca}^{2+}$ . Following entry of  $\text{Ca}^{2+}$  into the cell,  $\text{Ca}^{2+}$  binds to calbindin- $\text{D}_{28\text{K}}$  and diffuses to the basolateral side of the cell, where it is transported out of the cell into the blood stream with the help of NCX1, a sodium-calcium transporter, and to a lesser extent PMCA1b. To recycle or degrade TRPV5, the channel is internalized through dynamin- and clathrin-dependent processes shortly after arrival in the plasma membrane. Internalized TRPV5 is either degraded or recycled via endosomes. By interaction with Rab11a proteins in the endosome TRPV5 channels can re-translocate to the plasma membrane and undergo another round of  $\text{Ca}^{2+}$  influx. (340)

It has been shown that Klotho has sialidase activity and that it activates ‘plasma membrane resident transient receptor potential vanilloid 5’ (TRPV5) ion channels by removing the terminal sialic acids from their glycan chains (341). TRPV5 is a calcium channel expressed in epithelial cells of distal convoluted tubules. However, sialidase activity is not the only way Klotho affects calcium levels, as it has been reported that Klotho also interacts with the  $\text{Na}^+$ ,  $\text{K}^+$  ATPase to regulate calcium homeostasis (342).

### - Klotho as phosphatonin:

It has been reported that Klotho has a glycosidase function. The two external domains of Klotho share 20-40% amino acid sequence similarity with members of the glycosidase family, including  $\beta$ -glucosidase,  $\beta$ -glucuronidase, and glycosidase (92, 343). While the sequence of Klotho is missing the critical catalytic glutamic acid residues (92), studies by the Nabeshima group have shown that

## Introduction

Klotho *in vitro* hydrolyzes  $\beta$ -glucosides and  $\beta$ -D-glucuronide, and this effect is inhibited by a  $\beta$ -glucuronidase inhibitor (343).

*In vivo* evidence for  $\beta$ -glucuronic activity has been shown by the group of Orson Moe (301). Na-Pi2a and 2c function as sodium-phosphate cotransporters in the kidney and are essential for reabsorption of phosphate. Na-Pi2 is a highly glycosylated protein (344) with conserved asparagine-linked glycosylation sites (343). Therefore Na-Pi2 could be a substrate of Klotho. Hu et al. showed that injection of recombinant mouse extracellular domain of Klotho into mice and rats induced an inhibition of phosphate uptake from the urine into the blood. This block has shown to be a biphasic process. Thus far regulation of Na-Pi2a activity was believed to occur exclusively via changes in protein trafficking in the first phase (345) and via protein degradation in the second phase (346). Here Hu et al. showed that the first phase is independent of Na-Pi2a internalization. Only during the second phase Na-Pi2a was internalized. While in the first phase there was a shift of full length Na-Pi2a expression to N-terminal fragments. Nevertheless, the presence of a protease inhibitor had no effect of Klotho induced inhibition of Phosphate uptake, whereas the presence of a  $\beta$ -glucuronic inhibitor abolished the block of Klotho. This suggests that the Klotho induced deglycosylation from N-glycan is sufficient to suppress Na-dependent Pi transport and does not require proteolysis (301).

### - Inhibitor of the insulin and IGF-1 pathway

There are data that show the secreted form of Klotho has humoral functions and inhibits the insulin/IGF-1 pathway. The first evidence was given by Kurosu et al. that showed that mice overexpressing the soluble form of Klotho lived longer than wild type mice (347). By showing that those mice are insulin resistant they indicated *in vivo* a link of Klotho to the IGF-1/insulin pathway. Furthermore, they crossed the Klotho knock out mouse line to the IRS-1 loss of function line and found enhanced survival in the double transgenic mice. Studies in *C.elegans* show also that Klotho interacts with the insulin pathway to prolong survival (348). In parallel, they showed *in vitro* in myoblastic cells (L6) that Klotho binds to the surface of target cells and inhibits autophosphorylation of the IGF-1 and insulin receptor (347).

But there is also contradictory *in vitro* data provided by other groups in HEK293, L6 and HepG2

## Introduction

cells (349). Thus, the function of the secreted form of Klotho has not been fully elucidated. However, it has also been shown that soluble Klotho inhibited the insulin and IGF-1 pathway in the MCF-7 and MDA-MB-231 human cancer cells (350). In addition it has been shown in the same publication that Klotho inhibited the activation of the FGF pathway in HEK-293 cells, but enhanced its activation in MCF-7 and MDA-MB-231 cells. Nevertheless, Klotho does not affect the epidermal growth factor pathway and had not been described to influence the activities of hormone receptors (350). In conclusion, role for soluble klotho is cell type and receptor dependent.

### - Klotho and oxidative stress:

It has been discussed (see above) that high phosphate levels induce oxidative stress *in vivo* and *in vitro*. In addition, it has been shown that mice which lack Klotho expression show more activated ASK complex and sustained activated p38 MAPK (351), which indicates high oxidative state of the cell. The mechanism of p38 MAPK activity regulation in response to mitochondrial generated ROS involves activation of the ASK1-signalosome, a ROS-sensitive signaling complex composed of inhibitor and activator proteins (352-354). Reduced thioredoxin Trx(SH)<sub>2</sub> interacts with the N terminal domain of ASK1 and inhibits ASK1 activity and thereby p38 MAPK activation (353, 355). The ROS-mediated oxidation of ASK1-bound Trx(SH)<sub>2</sub> stimulates dissociation of the complex thereby allowing activation of the ASK1 and p38 MAPK (353, 355-357).

### - Klotho and acute kidney injury (AKI)/chronic kidney disease (CKD)

AKI arises from ischemia or nephrotoxins and can lead to CKD. AKI and CKD are a state of drastically reduced Klotho levels in serum, urine and kidney. Reduction of Klotho levels takes place very rapidly, as soon as 3 hours after the injury. Therefore, Klotho is a marker for AKI and CKD. It comes up earlier and more strongly than the commonly used marker: Neutrophil gelatinase-associated lipocalin (NGAL). Klotho is not only a marker for AKI and CKD but also has neuroprotective therapeutic potential. In AKI and CKD patients the values for blood urea nitrogen and creatinine were upregulated. Upon intraperitoneal injection of Klotho (soluble extracellular domain of the protein) in mice and rats suffering from AKI or CKD all the blood and urinary parameters return to nearly basal. Treatment with Klotho is most effective when started less than 60 minutes after the injury, which rarely happens in the clinic.



## Introduction

- **Klotho mutants**

The *Klotho* gene was originally identified as a gene mutated in a transgenic mouse strain (homozygous for the mutated *Klotho*) that developed multiple aging-like phenotypes (92). This mouse strain carries an insertional mutation from a transgene that disrupted the 5'-flanking region of the *Klotho* gene, resulting in a strong hypomorphic allele. Later, a conventional knock-out mouse was generated (358). Mice homozygous for the mutation are defective in *Klotho* gene expression. The hypomorphic model as well as the knock-out model (collectively referred to as 'Klotho mutant models') exhibit a syndrome resembling human aging, including; short life span, hypoactivity, muscle atrophy, skin atrophy, atrophy of outer genital organs, impaired maturation of gonadal cells, sterility of both sexes, arteriosclerosis, impaired glucose metabolism (92), cognition impairment (273), hearing disturbance (359), motoneuron degeneration (360), atrophy of thymus (361), osteopenia (362), vascular calcification, soft tissue calcification and pulmonary emphysema (363-365).

- **Klotho overexpressing mice**

It has been shown that mice overexpressing Klotho lived longer than wild-type mice and had higher blood insulin levels. In addition, Klotho overexpression induces resistance to insulin and IGF-1(347). Presumably, it is the effect of Klotho on the insulin IGF-1 signaling that results in longevity.

- **Klotho and breast cancer**

It has been shown by immunohistochemistry analysis that Klotho is highly expressed in normal breast but very low in breast cancer (detected with antibody directed against the intracellular domain of the transmembrane form of Klotho) (350). The physiological function of Klotho in the normal mammary gland has not yet been elucidated. Wolf and colleagues propose that the soluble form of Klotho acts as a tumor suppressor, by inhibiting insulin and IGF-1 signaling in breast cancer cells and that Klotho binds to the respective receptors. Nonetheless, it has also been shown earlier that binding of Klotho to these receptors is not needed to inhibit their signaling (347). Thus, the mechanism by which Klotho affects insulin and IGF-1 signaling needs to be further explored. Klotho-induced inhibition of IGF-1 signaling might also affect expression of the transcription factors CCAAT/enhancer-binding protein (C/EBP)  $\alpha$  and  $\beta$ . These factors are downregulated by the IGF-1 pathway and have been identified as breast cancer growth suppressors (366-368).

It is very well known that germ-line mutations in *BRCA1* and *BRCA2* genes substantially increase

## Introduction

lifetime risk of breast- and ovarian cancers. *Klotho* and *BRCA2* are located on 13q12. More recently it has been shown that there is a linkage disequilibrium between a functional variant of *Klotho* that shows reduced activity and a *BRCA2* mutation (369). The biological interaction between *Klotho* and *BRCA1* is not known yet. Recent data also indicate an association between mutations in *BRCA1* and *BRCA2* and the IGF-1 pathway in breast cancer. IGF-1 levels are increased in cancers from carriers of *BRCA1* and *BRCA2* mutations, and levels of the IGF-1 receptor are increased in breast cancer from *BRCA1* carriers (369). In addition, intact *BRCA1* protein can lower IGF-1 receptor protein levels in breast cancer cells (370, 371). Thus, a possible explanation of our observation is the combination of increased activation of the IGF-1 pathway because of *BRCA1* mutation and reduced inhibition of *klotho*.

- **Klotho in C.elegans**

*Klotho* has two known functions in *C.elegans*: promotion of longevity and resistance against oxidative stress. There exist two redundant homologues of *Klotho* in *C.elegans*, C50F7.10 and E02H9.5. They encode predicted proteins homologues to the  $\beta$ -glucosidase-like KL1 domain of mammalian *Klotho*.

*C.elegans* *Klotho* has been shown to promote survival in an EGL15(FGFR)/EGL17(FGF ligand) dependent way. In addition, the survival promoting function of *Klotho* is dependent on the *daf2/daf16* pathway (*daf2* – insulin receptor; *daf16* – FOXO) (348).

*Klotho* has been shown to increase resistance against oxidative stress via the EGL15/EGL17 pathway and dependent on *daf16*, but independent of *daf2* (348).

- **Klotho in humans**

- A homozygous missense mutation in the *Klotho* gene causes decreased *Klotho* levels resulting in tumoral calcinosis, analogous to the tumoral calcinosis seen in patients with decreased FGF23 levels (327).

### 4.4.3 FGF receptors

FGFR1 is the predominant receptor for the hypophosphatemic action of FGF23, while FGFR4 may also play a minor role. This has been shown by characterizing phosphate homeostasis in FGFR4 ko and FGFR1 conditional knock-out mice where Cre recombinase was expressed in the metanephric mesenchyme, driven by the Pax3 promoter (372).

## Introduction

Another study showed that phosphate homeostasis controlled by FGF23/Klotho/FGFR1 signaling is mediated by MEK/ERK1/2 signaling. This has been established by characterizing phosphate homeostasis in hyp mice (inactivating mutations of PHEX) that were treated with a MEK inhibitor, PD0325901 (373).

### 4.4.4 Vitamin D

- Vitamin D Metabolism

There are two sources of vitamin D (chalciferol). Either it is taken up by diet (fortified dairy products or fish oils) or it is produced from 7-dihydrocholesterol. 7-dihydrocholesterol resides in the skin where it is modified by UV irradiation. Subsequently, Cholecalciferol (pre-vitamin D) is transported in the blood, where it binds the vitamin D binding protein and reaches the liver. In the liver cholecalciferol gets hydroxylated at C25 by one or more cytochrome P450 vitamin D 25 hydroxylases, e.g. Cyp27A1, resulting in the formation of 25-hydroxyvitamin D<sub>3</sub> (25(OH)D<sub>3</sub>). 25(OH)D<sub>3</sub> is the major circulating form of Vitamin D. It is bound to the vitamin D binding protein and gets transported to the kidney where it gets internalized by megalin, a member of the LDL receptor family. In the kidney 25(OH)D<sub>3</sub> gets hydroxylated by the 1 $\alpha$ -hydroxylase at the position of carbon 1 of the A ring, which results in the hormonally active form of vitamin D, 1,25-dihydroxyvitamin D<sub>3</sub> (1, 25(OH)<sub>2</sub>D<sub>3</sub>). 1 $\alpha$ -hydroxylase is encoded by the gene Cyp27B1. It is a cytochrome P450 monooxygenase found mainly in the kidney, but also present in some extrarenal sites including placenta, monocytes and macrophages (374-377).

Vitamin D exerts its functions by interacting with the high-affinity vitamin D receptor (VDR), which is a ligand-dependent transcription factor (378). VDR is a member of the nuclear receptor superfamily. It forms heterodimers with the retinoid receptor (RXR) to regulate gene transcription by binding to vitamin D responsive elements (VDREs) in the promoter region of target genes.

- Vitamin D and premature-aging

In the premature aging models of FGF23 or Klotho mutant hypervitaminosis is found, because there is no longer inhibition of the renal 1 $\alpha$ -hydroxylase in these animals. High levels of vitamin D affect aging by building up high levels of phosphate. Vitamin D induces uptake of phosphate from

the gut.

- Vitamin D and cancer

Clinical studies have been performed which show that there might be a correlation between levels of vitamin D and cancer risk. It was shown for colorectal- (379), pancreatic- (380), gastrointestinal- (381), and breast-cancer (382) that high levels of vitamin D may be beneficial. Vitamin D is not the only tumor suppressor in this system. Klotho has also been found to have a positive effect in relation with cancer. In addition, there were vitamin D response elements (VREs) identified in the vicinity of mouse and human Klotho (383). Nonetheless, thus far it is not clear if there is a link between the tumor suppressor function of vitamin D and Klotho.

#### **4.4.5 The sodium phosphate co-transporters Na-Pi2a and Na-Pi2c**

Phosphate transport across the apical membrane is mediated by the three members of the SLC34 family (SLC34A1-A3) of solute carriers. Expression of SLC34A1/Na-Pi2a and SLC34A3/Na-Pi2c is restricted to the brush border membrane of renal proximal tubules. In rats and mice, Na-Pi2a has the most important role in renal phosphate reabsorption (70-80%), while Na-Pi2c was thought to have the most important regulatory role around weanling animals. However, in adult animals, maintained on a normal phosphate diet Na-Pi2c mediates only a very small percentage of phosphate reabsorption. SLC34A2/Na-Pi2b expression is restricted to the gut.

Transcription of the Na-Pi2a and 2c is controlled by the FGF23-Klotho axis, but RNA levels do not reflect protein activity as the localization of the cotransporters to the brush border membrane, where these transporters are active, is highly regulated. Na-Pi2a and 2c are expressed in the brush membrane of the renal tubular cells. They are co-transporters that reabsorb phosphate from the urine. The FGF23-Klotho and PTH induce internalization of the co-receptors and therefore, inhibit phosphate reuptake.

#### **4.4.6 The parathyroid hormone (PTH)**

Serum PTH concentrations are dependent upon the release of PTH stored in secretory granules within the parathyroid gland and by the synthesis of new PTH. Calcium, phosphate and vitamin D metabolites play a role in regulating PTH release and synthesis. On the other hand PTH regulates calcium, phosphate and vitamin D levels resulting in a loop of positive and negative feedback (339).

## Introduction

PTH regulation:

The PTH pool in the secretory vesicles is controlled by RNA binding proteins that regulate PTH-mRNA stability by binding to the 3' untranslated region. In addition, vitamin D negatively affects transcription of PTH. PTH is synthesized as prepro-peptide containing a 25-amino-acid presequence and a 6-amino presequence. Both are cleaved off in the endoplasmic reticulum, and mature full-length PTH (1-84aa) is stored in secretory vesicles.

Calcium homeostasis:

Calcium binds to the calcium-sensing receptors (CaRs) on the parathyroid chief cells to decrease secretion of PTH as released PTH increases Calcium uptake and decreases calcium wasting. In detail, PTH inhibits reabsorption of Calcium by the bone and excretion by the kidney by inhibiting the FGF23-Klotho axis in the renal tubules. Inhibition of the FGF23-Klotho axis also increases the production of vitamin D, which enhances absorption of calcium from the intestine (339). Continuous exposure to PTH can result in bone resorption.

CaR is a G protein-coupled receptor that activates phospholipase C (PLC) and mitogen-activated protein kinases (MAPKs) and inhibits adenylate cyclase (AC) (Figure 4-9). This activates calcium-sensitive proteases in the secretory vesicles of the parathyroids, resulting in cleavage and inactivation of PTH.

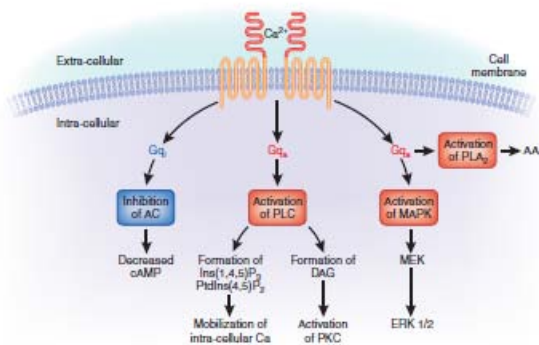


**Figure 4-9 Activation of the Calcium-sensing receptor and subsequent downstream effects (Kumar et al. 2011)**

The calcium-sensing receptor (CaR) is activated by calcium and in turn inhibits adenylate cyclase (AC) and activates phospholipase C (PLC) and mitogen-activated protein kinase (MAPK).

## Introduction

### Phosphate homeostasis:

PTH induces internalization of the sodium-phosphate cotransporters Na-Pi2a and Na-Pi2c, resulting in renal phosphate wasting and hypophosphatemia (384). PTH binds to the PTH/PTHrP-receptor (PTHr1) at the basolateral and apical membrane of the proximal renal tubule. In the basolateral membrane the receptor activates the PKA pathway while in the apical membrane it activates the PLC pathway, both leading to ERK activation. This stimulates internalization of NaPi2a and Na-Pi2c via clathrin-coated pits (384). Figure 4-10

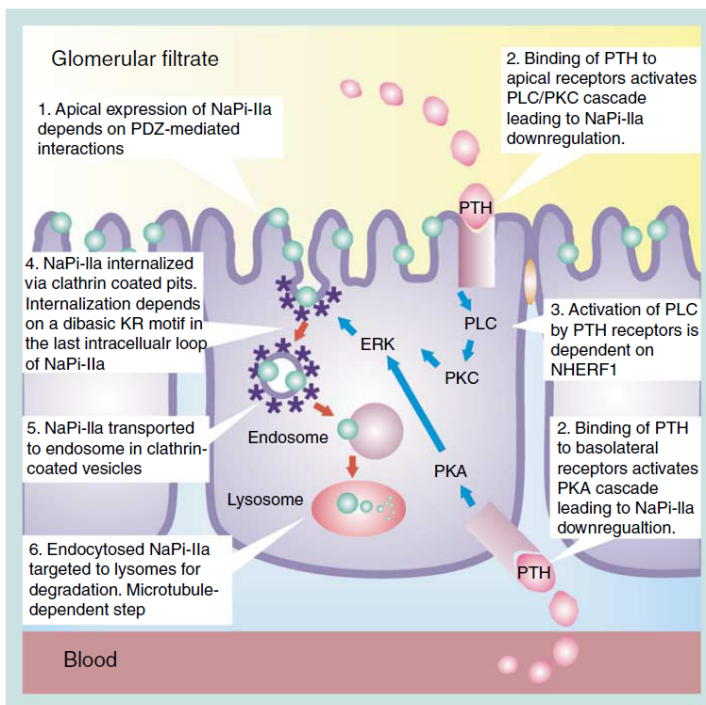


**Figure 4-10 Downregulation of Na-Pi2a (Forster et al. 2006)**

Schematic representation of the sequence of steps involved in PTH-induced down-regulation of Na-Pi2a in an epithelial proximal tubule cell. PDZ: PSD-95, Discs-large and ZO-1, NHERF1: Na/H-exchanger regulatory factors, dibasic KR motif: a motive in the last intracellular loop of the NA-Pi2a protein that is required for PTH sensitivity, light blue spheres: Na-Pi2a, dark blue stars: clathrin.

### 4.4.7 Players in phosphate homeostasis

Many different players of the phosphate homeostasis have been mutated or knocked out in mice. All

## Introduction

these studies contributed to the picture of the actual complexity of phosphate homeostasis.

### KO of 1 $\alpha$ -hydroxylase (385):

Those mice do not produce any vitamin D. Their phenotype consists of retarded growth, secondary hyperparathyroidism, and hypogonadism.

Analysis of the mice showed that they suffer from hypocalcemia and elevated levels of PTH. In addition the levels of 24-hydroxylase were reduced.

### Na-Pi2a/Na-Pi2c double knock out (386):

In contrast to humans, in mice Na-Pi2a and Na-Pi2c are essential for phosphate reuptake. Therefore, it is necessary to study the double knock out.

These mice show growth retardation, hypophosphatemia, hypercalcemia and hyperphosphaturia. In addition, the level of vitamin D is increased and the levels of PTH and FGF23 are decreased.

### Conditional Knock out of *fgfr1* (372):

The renal tubules express FGFR1, 3 and 4. In order to investigate, which receptor is essential for regulation of phosphate levels recombinant FGF23 was injected in a conditional knock out for *fgfr1* and knock out animals for *fgfr3* or *fgfr4*. The resulting measurement of serum phosphate led to the conclusion that FGFR1 plays the principal role in phosphate regulation, while FGFR4 plays a minor role. Interestingly, *fgfr1* conditional knock out animals showed elevated levels of FGF23, probably due to a negative feedback loop, but unchanged phosphate levels. This suggests the presence of compensatory mechanisms against high serum phosphate levels.

### Pan inhibition of FGFRs (387):

In this study a selective pan-FGFR inhibitor, PD173074, was injected into WT animals. This pharmacological inhibition of the FGFRs had similar effects on the Cyp27B1 and Cyp24A1 levels as the Klotho mutation or FGF23 knock out. Injection of PD172074 induced upregulation of 1 $\alpha$ -hydroxylase and parathyroid hormone as well as downregulation of 24-hydroxylase, causing hyperphosphatemia and hypervitaminosis D.

In addition, this study shows that FGFR inhibition blocks FGF23 transcription in the bone and that this is dominant over vitamin D induced FGF23 transcription.

## Introduction

### Vitamin D receptor mutant (388, 389):

The vitamin D receptor mutant mice are short lived and retarded in growth. In addition, their skin is wrinkled, they have alopecia and rickets as well as impaired bone formation. Furthermore, they show hypocalcemia and hypophosphatemia.

### Hyp mice (390):

Mice that have a deletion of the *pheX* gene, that's located on the X chromosome, are named after their most prominent phenotype: hypophosphatemia. It has been confirmed that the phenotype is caused by elevated levels of FGF23 (see below).

In addition to hypophosphatemia, the mice also show rickets in the bone, retarded growth, hyperphosphaturia, hypocalcemia and kyphosis.

This mouse model has proven to be well suited for rescue studies (see below)

### Anti FGF23 antibodies in hyp mice (391):

Hyp mice that were injected with an antibody against FGF23 recovered from hypophosphatemia. In addition, they had elevated levels of Na-Pi2a, 1 $\alpha$ -hydroxylase, and 24-hydroxylase compared to untreated hyp mice. The level of vitamin D was also elevated compared to the hyp mice, while the level of PTH was decreased. There was no change in the calcium levels. This shows that rescue of FGF23 levels is essential for rescue of vitamin D and PTH levels and of Na-Pi2a localization to the brush border membrane. In addition, rescue of FGF23 is important to stabilize serum phosphate levels. In contrast, regulation of FGF23 levels is not enough to rescue Calcium levels.

### Inhibition of the MEK signaling pathway in the hyp mice (373):

In this study it was shown that the FGF23-Klotho axis, that controls phosphate levels, signals through the MEK signaling pathway.

Hyp mice that were treated with a MEK inhibitor, PD0325901, recovered in terms of 1 $\alpha$ -hydroxylase expression, vitamin D levels, phosphate levels, and expression of NaPi2a expression in the brush border membrane.



## Introduction

**Table 4-3 Overview over the changes in the different mouse models**

No diff = no difference; Ab = antibody

Defect	Cyp27B1	Cyp24A1	Vitamin D	PTH	Phosphate Blood	Phosphate Urine	Na-Pi2a	Calcium Blood	Calcium Urine	FGF23 protein
<b>Klotho KO</b>	Up	Down	Up	Down	Up	Down	Down	Up	Up	
<b>FGF23 KO</b>	Up	Down	Up	Down	Up	Down	Down	Up	Down	
<b>Na-Pi2a KO</b>			Up	Down		Up			Up	Down
<b>Na-Pi2c KO</b>					Down				Up	
<b>Na-Pi2a/2c KO</b>			Up	Down	Down	Up			Up	Down
<b>VDR KO</b>	No diff	No diff	Up							
<b>Cyp27B1 KO</b>										
<b>FGFR1 conditional KO</b>					Up		Up			Up
<b>Hyp mice</b>	UP		Down		Down		Down			Up
<b>Ab against FGF23 in hyp mice</b>	No diff	No diff		No diff	No diff	No diff	No diff			
<b>Inhibition of MEK in hyp mice</b>	Up			Up			Up			
<b>Pan FGFR inhibition</b>	Up	Down	Up	Up	Up	No diff		No diff	Up	

## 5 Material and Methods

### 5.1 Reagents and antibodies

FGF2 was from Sigma-Aldrich (St. Louis, MO, USA). The FGFR kinase inhibitor TKI258 [388] was provided by Drs. D. Graus-Porta and C. Garcia-Echeverria (Novartis Institutes for Biomedical Research, Basel, Switzerland). The compound indicated in the thesis as “FGFR inhibitor” is another compound, that more potently the FGFRs. The following antibodies were used: Pser<sup>473</sup>-AKT (9271), AKT (9272), Pser<sup>65</sup>-4E-BP1 (9451), Asp<sup>175</sup>-cleaved caspase 3 (9661), P Tyr<sup>196</sup>-FRS2 (3864), P Tyr<sup>436</sup>-FRS2 (3861), FGFR1 (3472), P Tyr<sup>202</sup>/Tyr<sup>204</sup>-ERK1/2 (9101), ERK1/2 (9102), GAB1 (3232), P Tyr<sup>180</sup>/Tyr<sup>182</sup>-p38 (9215), p38 (9212), Pser<sup>240</sup>/Ser<sup>244</sup>-S6 ribosomal protein (2215) from Cell Signaling (Danvers, MA, USA); FRS2 (sc-8318), SHP2/SH-PTP2(c-18) (sc-280) from Santa-cruz Biotechnology Inc. (Santa Cruz, CA, USA); actin (MAB1501) from Chemicon (Billerica, MA, USA); GRB2 (G16720) from Transduction Laboratories (BD Biosciences, Mississauga, ON, CDN); Flag (F7425) from Sigma-Aldrich (St. Louis, MO, USA); CD31 (550274) from BD Bioscience (San Jose, CA, USA); HIF1 $\alpha$  (NB100-449) Novus Biological; Na-Pi2a rabbit polyclonal antibody was a courtesy of Jörg Biber in Zurich (Switzerland); Polyclonal antibodies to a 19 amino acid peptide of human Memo, which shows high similarity to the mouse Memo, were produced in rabbits (aa 25-43 human Memo NM\_015955: NAQLEGWLSQVQSTKRPAR), the same peptide was used for mAB production in mice. Monoclonal antibody of Klotho was produced in mice by immunizing them against a synthesized amino peptide (DDAKYMYYLKKFIMETLKAIKLDGV), which is a part of the human Klotho protein.

### 5.2 Cell Culture

Mouse embryonic fibroblasts (MEFs):

Immortalized mouse embryonic fibroblasts (MEF) were grown in Dulbecco's modified Eagle's medium (DMEM) supplemented with 10% Fetal Calf Serum (GIBCO Invitrogen AG, Basel, Switzerland) and Penicillin and Streptomycin (growth medium).

## Material and Methods

MEFs were generated by digestion of the torso and lower part of the head from Memo conditional knock-out mice. Digestion was performed by addition of fresh trypsin-EDTA in PBS every 30 minutes; the samples were incubated on 37°C on an Eppendorf shaker until digestion was complete. The cell suspension was decanted in a fresh tube containing FBS. After centrifugation at 1000rpm for 5 minutes the pellet was resuspended in DMEM containing 10% FBS. Next day, the medium was exchanged and thereby most non-fibroblastic cells were removed.

Immortalization was achieved by growing the MEFs until they entered crisis at about passage 3. Then we waited for spontaneous immortalization.

To obtain inducible Memo knock-out MEFs, the spontaneously immortalized cells were transfected with a tamoxifen inducible Cre recombinase. Virus production: Ecophoenix cells were transfected with 24µg of pMSCV-CreER<sup>T2</sup>-puro<sup>r</sup> plasmid with lipofectamin 2000 (from invitrogen). After 3.5 days of growing at 37°C the supernatant was collected, filtrated on 0.45µm filter and 5µg/ml polybrene was added. 5ml of this supernatant was used to infect one 10cm dish of MEFs. After 6 hours of incubation at 37°C the supernatant was removed and fresh DMEM-10%FBS was added. After 48 hours of expression the selection with puromycin was started.

Knock-out MEFs were generated by incubation of the cells in 0.5 µg/ml 4-hydroxytamoxifen in DMEM-10%FBS for 3 days. Control cells were incubated in DMEM-10%FBS with ETOH.

HEK293-kl and HEK293-βkl:

HEK293 cells were stably transfected with full length Klotho (HEK293-kl) [98] or βKlotho (HEK293-βkl) [290] to achieve FGF23 (HEK293-kl) and FGF19 and 21 (HEK293-βkl) responsive HEK293 cells [290].

Memo was downregulated with siRNA. HEK293-kl cells were seeded in 6 well plates. Next morning siRNA treatment was performed: Mix1: 2.5ul Optimem, 4ul Lipofectamin, Mix2: 2.5ul Optimem, 4ul siRNA for Memo or LacZ as control. Mix1 and 2 were combined, mixed and incubated at room temperature for 15 minutes before adding to the plate. After 4 to 6 hours fresh DMEM-10%FCS was added. 24 hours later the cells were starved before they were stimulated. Lysates were prepared as described before (392).

4T1 mouse mammary carcinoma cells:

## Material and Methods

The mouse mammary tumor cell line 4T1 (obtained from Dr. R. Weinberg, Whitehead Institute for Biomedical Research, USA) was grown in DMEM-10%FBS and Penicillin and Streptomycin.

Short hairpin (sh) RNAs for targeting Memo in 4T1 cells were designed using algorithms available from Invitrogen and the corresponding sense and antisense oligonucleotides were obtained from Microsynth AG (Switzerland). The two Memo sequences targeted NM\_015955 nucleotides 1002 to 1022 (sh7) and 1213 to 1231 (sh10). The annealed shRNA oligos were cloned into BglII/HindIII digested pSUPERretro-Neo-GFP. A double stranded LacZ shRNA oligo was cloned into the same vector to use as a control.

4T1 mammary tumor cells were transfected with the two independent Memo shRNA specific vectors (sh10 and sh7) and with the control lacZ vector using lipofectamine (Invitrogen, Carlsbad, CA, USA). Resistant cells were selected in 0.5 mg/ml G418 (11811031) from Invitrogen (Carlsbad, CA, USA) and individual clones expressing sh10 and sh7 and the control LacZ were selected.

### **5.3 Lysates, western blot analyses and immunoprecipitations**

Over-night serum starved cultures (DMEM-0.1%BSA (Sigma)) were stimulated with 50ng/ml FGF2 or treated with 500 $\mu$ M CoCl<sub>2</sub>, 50nM FGFR inhibitor, or 30 $\mu$ M LY294002 for the indicated time.

Whole cell lysates for western blot analyses were prepared in NP-40 buffer (50mM Hepes (pH 7.4), 150mM NaCl, 25mM beta-glycerophosphate, 25mM NaF, 5mM EGTA, 1mM EDTA, 15mM PPI and 1% NP-40) supplemented with leupeptin (10 ug/ml), aprotinin (10 ug/ml), vanadate (2mM), DTT (1mM) and PMSF (1mM). The lysates were boiled in sample buffer, separated by SDS-PAGE, blotted onto polyvinylidene difluoride membranes (Millipore Corporation) and probed with the specific antibodies. Whole cell lysates for co-immunoprecipitations (Co-IP) were prepared in 2 times Co-IP buffer (50mM Tris (pH 7.5), 5mM EGTA, 150mM NaCl, 25mM beta-glycerophosphat, 25mM NaF) supplemented with 10% Triton X-100, 10% Glycerol, vanadate (2mM), PMSF (1mM), aprotinin (10 ug/ml), leupeptin (10 ug/ml) and MgCl<sub>2</sub> (10mM). The IPs were collected with protein-A or G sepharose beads (Sigma) and centrifuged. The pellets were washed three times with Co-IP buffer.

## Material and Methods

Proteins were released by boiling in sample buffer SDS-PAGE and immunoblotting was performed as described for whole cell lysates.

### 5.4 Electron Microscopy

For electron microscopy, pieces of hearts were fixed in Karnovsky's fixative (3% paraformaldehyde, 0.5% glutaraldehyde in 10 mM PBS pH 7.4), washed, and post-fixed in 1% OsO<sub>4</sub>. After dehydration with graded series of ethanol, samples were embedded in Epon and sections of 60 to 70 nm thickness were cut [389]. Sections were double stained with uranyl acetate and lead acetate [390] and viewed in a FEI Morgangi 268D transmission electron microscope.

### 5.5 Hypoxia

Control and Memo KD 4T1 cells were put in hypoxic chambers that were filled with hypoxic gas (1% O<sub>2</sub>, 5% CO<sub>2</sub>, 94% N<sub>2</sub>) for 20 minutes. Afterwards, the chambers were disconnected and cells were incubated in the chambers filled with the hypoxic gas in the cell incubator for the indicated times. Lysates were prepared immediately after opening the chambers. As mimetic for hypoxic conditions lysates were prepared from cells that were incubated in 500µM CoCl<sub>2</sub> for the indicated times.

### 5.6 Proliferation assay

Proliferation was measured by seeding cells at a density of 8000 per well in a 96 well plate and growing to 80% confluency. After addition of 10µM 5bromo-2'-deoxyuridine (BrdU), the cells were incubated for 2 hours at 37°C. BrdU incorporation was measured using the Biotrack<sup>TM</sup> cell proliferation ELISA system (GE-healthcare, Little Chalfont, UK).

### 5.7 Apoptosis assay

#### 5.7.1 YoPro

Cytotoxic effect of CoCl<sub>2</sub> treatment, FGFR inhibition, and AKT inhibition was evaluated by YoPro assays (Invitrogen, Carlsbad, CA, USA) [391]. Control and KD 4T1 cells were seeded on 96 well plates (in quadruplets) and were either treated with CoCl<sub>2</sub> or with inhibitors blocking specific signaling molecules (a specific FGFR inhibitor, or the commercially available FGFR inhibitor TKI258 or the

## Material and Methods

PI3K-inhibitor LY204002) for the indicated times. The first measurement with the YoPro assay measures apoptosis or cytotoxicity: 25 $\mu$ l of YoPro-Mix (3ml 5 \* YoPro buffer (100mM pH4 Na-citrate, 134mM NaCl) and 37.5 $\mu$ l 1mM YoPro (Invitrogen, Carlsbad, CA, USA)) is freshly prepared in the dark and added to the 96 wells; cells are incubated 10 minutes in the YoPro-Mix before the plate is read in a Cytofluor II, filter 485/529nm. The second measurement allows a determination of cell growth and total cell number: 25 $\mu$ l of lysis buffer (3ml per plate: 0.18ml 500mM EDTA, 0.18ml 500mM EGTA, 0.18ml 10% NP-40, 2.46ml 1 \* YoPro buffer) is added into the wells, plates are incubated for 30 minutes in the dark and then read in a Cytofluor II, filter 485/529nm.

### 5.7.2 MitoProbe™ DilC<sub>1</sub>(5) Assay

DilC<sub>1</sub>(5) stains cells that have an active mitochondrial potential. Loss of mitochondrial potential correlates proportionally with loss of DilC<sub>1</sub>(5) staining and indicates cellular death.

The analysis of stress response to CoCl<sub>2</sub> and Etoposide was performed by measuring the mitochondrial membrane potential via staining with Dilc<sub>1</sub>(5) (M34151, Invitrogen, Carlsbad, CA, USA) according to the manufacturer's protocol. Cells were treated with CoCl<sub>2</sub> or Etoposide for the indicated times, before they were collected for FACS analysis: Supernatant and trypsinised cells were combined, centrifuged and resuspended in PBS. 5 $\mu$ l of Dilc<sub>1</sub>(5) was added to 10<sup>6</sup> cells in 1ml PBS. Cells were incubated for 20 minutes at 37°C, centrifuged and resuspended in 500 $\mu$ l of PBS. A FACScalibur Flow Cytometer (Becton Dickinson, Franklin Lakes, NJ, USA) was used for analysis.

### 5.8 Migration assay

Control and Memo KD 4T1 were preincubated for 1 hour in DMEM-10% FCS supplemented with DMSO or FGFR inhibitor. Cells were counted and 100'000 cells per well were seeded on collagen (11179179001, Roche, IN, USA) coated transwell cell culture chambers (8.0 $\mu$ m polycarbonate Membrane, 6.5 mm Insert, 24 well plate, Costar, Corning Incorporated, NY, USA). After the indicated time the migrated cells were stained with cristal violet (101408, Merck KGaA, Darmstadt, Germany) and counted.

## 5.9 RNA extraction, RT-PCR and real-time PCR

RNA from growing 4T1 cells was extracted using the Qiashtredder and RNeasy Mini Kit coupled with RNase-free DNase set (Qiagen, Venlo, The Netherlands Qiagen) following the manufacturer's instructions. RNA from tissues and tumors were obtained from snap frozen tumor pieces, following extraction with TRIzol reagent (Invitrogen, Carlsbad, CA, USA) according to the manufacturer's protocol. RNAs were washed using the RNeasy Mini Kit (Qiagen) and treated with RNase-free DNase set (Qiagen). cDNA was obtained from 1µg of total RNA, using the Ready-to-go You-Prime First-Strand Beads kit (GE-healthcare, Little Chalfont, UK) with oligos-dT primers (Promega). Semi-quantitative PCR was performed as follow: 2ml of 10X Buffer (Roche), 0.2ml of Taq polymerase (5U/ml Roche), 0.4ml of 10mM dNTP mix (Roche), 0.1ml of each primer (100mM), 1ml of cDNA, filled to a final volume of 20ml with sterile H<sub>2</sub>O. Thermal cycling reaction using an Icycler device (Bio-Rad, Reinach, Switzerland) was: 94°C for 2 min; followed by 25 to 35 cycles of 95°C for 30 sec, 60°C for 30 sec, 72°C for 45 sec. The amplified products were further extended by additional incubation at 72°C for 10 min. PCR products were then loaded on a 1% agarose gel containing ethidium bromide. QRT-PCR was performed with ABI prism 7000 (Applied Biosystems, Austin, TX, USA) using Absolute QPCR SYBR Green ROX Mix (THERMO Scientific, Waltham, MA, USA) following the manufacturer's guidelines. All quantitations were normalized to GAPDH. GAPDH primers for semi-quantitative PCR and real-time PCR are described in Chapter 0.

Primers used for detection of

VEGF-A: 5'-ACCCTGGCTTTACTGCTGTACC-3'

5'-TGCATTCACATCTGCTGTGCTG-3'

TRPV5: 5'- TTGGTGCCTCTCGCTACTTT-3'

5'- AGCGCAGTAGGTCTCCAAAA-3'

NCX1: 5'- CGAGACTGTGTGCGAACCTGA-3'

5'- TCAGGGACCACGTAAACACA-3'

PMCA: 5'- GATCCTCTTGTCGGTGGTGT-3'

5'- CCGTACTTCACTTGGGCAAT-3'

## Material and Methods

CB28: 5' - GACGGAAGTGGTTACCTGGA-3'

5' - TTCCTCGCAGGACTTCAGTT-3'

### 5.10 Immunohistochemistry

Kidneys were fixed 24 hours in PBS containing 4% paraformaldehyde then incubated 24 hours in 70% ethanol. Fixed tissues were embedded in paraffin. Immunohistochemistry was performed on 4µm thick sections using the monoclonal Memo antibody. The staining was carried out with the Discovery XT Staining Module (Ventana Medica Systems S.A.).

### 5.11 Generation of the mouse strains

Animal experiments were done according to the Swiss guideline governing animal experimentation and approved by the Swiss veterinary authorities.

#### 5.11.1 Memo cKO and KO mice

A mouse strain with a loxP-flanked (floxed) *Memo* gene was generated by targeting the second exon of *Memo*. PCR synthesis of homology arms and loxP-exon 2 were performed on 15ng/µl gDNA extracted from ES cells (129/OLA), 1.5mM MgCl<sub>2</sub>, 0.2mM dNTP mixture, 0.03 U/µl Red Hot DNA polymerase (Abgene, ref. AB-0406/A9), 0.005 U/µl Pwo polymerase (Roche diagnostics, ref. 1 644 947), respective primer pair (200nM each) in the following cycling conditions:

Pre-denaturation step 2 min. at 94°C, 14 cycles [15 s at 94°C – 3 min. at 70°C (-0.5°C per cycle)], 20 cycles [15 s at 94°C – 3 min. (+ 10 s per cycle) at 63°C], post elongation step 7 min. at 63°C, storage at 4°C.

Each PCR product was purified, SfiI digested and ligated in a vector containing a pgk-neomycine cassette flanked with 2 loxP sites and 2 Frt sites. Sequencing of the exonic regions, loxP and FRT sites was performed to avoid any risk of PCR-induced mutations.

The targeting construct was linearized by SallI restriction and overhanging ends were filled by the Klenow fragment. Purification was carried out by two successive rounds of phenol/chloroform extractions followed by an ethanol precipitation and two washes with 70% ethanol. Pure DNA was air dried and resuspended in sterile deionized water. Embryonic cells (ES) were electroporated with the



## Material and Methods

targeting construct and selected for resistance to G418. ES clones that underwent recombination and were hence resistant were initially screened for homologous recombination at the *Memo* locus by PCR using 5' external forward combined with a neo cassette specific reverse primer, as well as with a neo cassette forward primer 5' combined with a 3' external reverse primer using the Expand-Long-Template-PCR system (Roche # 11 681 834 001), according to manufacturer's instructions. Single integration was confirmed by Southern blotting using a neo specific radiolabeled probe. Two ES clones showed specific homologous recombination at the *Memo* locus (3 lox allele) and were used for aggregation experiments and chimera production. Only one clone (109) gave a chimera with germline transmission. Those mice were crossed to a FLP deleter transgenic mouse to remove the Neo cassette and generate the **Memo cKO mice**. By crossing those mice with a Cre deleter transgenic mouse strain exon number 2 of *Memo* was removed and the **Memo KO mice** were generated.

### 5.11.2 Meox2Cre mice

Meox2Cre mice express the Cre recombinase under the control of the mesenchyme homeobox 2 promoter starting at day E5. The Cre recombinase is active in the embryo and in extra-embryonic mesoderm derivatives, including the chorionic plate and yolk sac mesoderm. All other regions of placenta are Cre negative [393].

### 5.11.3 Memo cKO Actin Cre mice

To achieve a mouse strain which can be temporally controlled for memo excision, the Memo cKO strain ( $Memo^{fl/fl}$ ) was crossed to a mouse strain harboring the Cre recombinase under a tamoxifen inducible actin promoter, the pCX-CreER<sup>TM</sup> transgenic.  $Memo^{fl/fl}$  mice were crossed with pCX-CreER<sup>TM</sup> transgenics to generate heterozygous offspring for the floxed *Memo* allele and the Cre. Homozygous founders for the floxed *Memo* allele were generated by mating these heterozygous mice. Loss of Memo was induced by intraperitoneal (IP) injections of Tamoxifen (Sigma) in corn oil (Sigma) on 4 to 5 consecutive days. The age of the mice at the time of injection varied between 2 to 14 weeks. Homozygous negative Cre mice were control treated with tamoxifen. Injected mice were controlled by weight.

## Material and Methods

### 5.11.4 Memo cKO rtTA LC-1 Cre mice

In order to generate a kidney-specific, temporally controlled Memo knock out strain we used a kidney specific tet-ON system. The Memo cKO strain (Memo<sup>fl/fl</sup>) was crossed to a mouse strain harboring the doxycycline rtTA under the Pax8 promoter (B6.Cg-Tg(Pax8 rtTA2S\*M2)1Koes/J) and to a mouse strain harboring the LC-1 Cre recombinase under a P<sub>tet</sub> bi-1 promoter that is expressed in all cells of the mouse.

B6.Cg-Tg(Pax8 rtTA2S\*M2)1Koes/J mouse line:

Transgenic Pax8-rtTA mice are viable and fertile. These mice express an optimized reverse tetracycline-sensitive transactivator (rtTA2<sup>S</sup>-M2) protein under the control of the murine Pax8 promoter. The Pax8 promoter directs expression to proximal and distal tubules and the collecting duct system of both embryonic and adult kidney. The rtTA2<sup>S</sup>-M2 variant of rtTA contains five amino acid changes in the TetR moiety (S12G, E19G, A56P, D148E, and H179R) and a synthetic optimized transactivating domain, resulting in reduced basal activity and enhanced doxycycline sensitivity compared to wild-type rtTA. When mated to a second strain carrying a gene of interest under the regulatory control of a tetracycline-responsive promoter element (TRE or tetO), expression of the target gene in kidney cells is induced with administration of the tetracycline analog, doxycycline (dox). These Pax8-rtTA mice provide a Tet-On tool that allows the inducible expression of genes in renal tubular epithelial cells.

Development of this strain: The Pax8-rtTA construct was designed to contain an optimized rtTA variant (rtTA2s-M2) cDNA and SV40 polyA sequence replaced at the endogenous ATG translational start site of a murine Pax8 sequence. This 6.6 kb transgene was microinjected into the pronucleus of one-cell fertilized mouse embryos obtained from superovulated F2 (C57BL/6 \* DBA) females, which were then implanted into pseudopregnant foster mice. Founder mice were bred to C57BL/6 mice, and the resulting transgenic offspring were bred together for many generations. The mice were backcrossed to C57BL/6J for at least five generations to generate the congenic strain that was used in this study (Jackson Laboratory Stock nr. 007176). The Pax8-rtTA construct integrated approximately five copies in a head-to-tail orientation within a mouse L1 line repetitive element (which are located throughout the genome).

LC-1 Cre mice line:

## Material and Methods

This mouse line contains the Cre recombinase and the luciferase gene under the control of a bidirectional  $P_{tet}bi-1$  promoter, that contains the tetracycline responsive promoter element [394, 395].

The resulting Memo cKO-rtTA-LC-1 mouse line is a tet-On tool that allows the inducible excision of Memo in renal tubular epithelial cells. Simultaneously to the induction of Cre transcription the enzyme luciferase is transcribed. Therefore, the activity of  $P_{tet}bi-1$  transcription can be controlled by luciferin injection and transillumintor imaging.

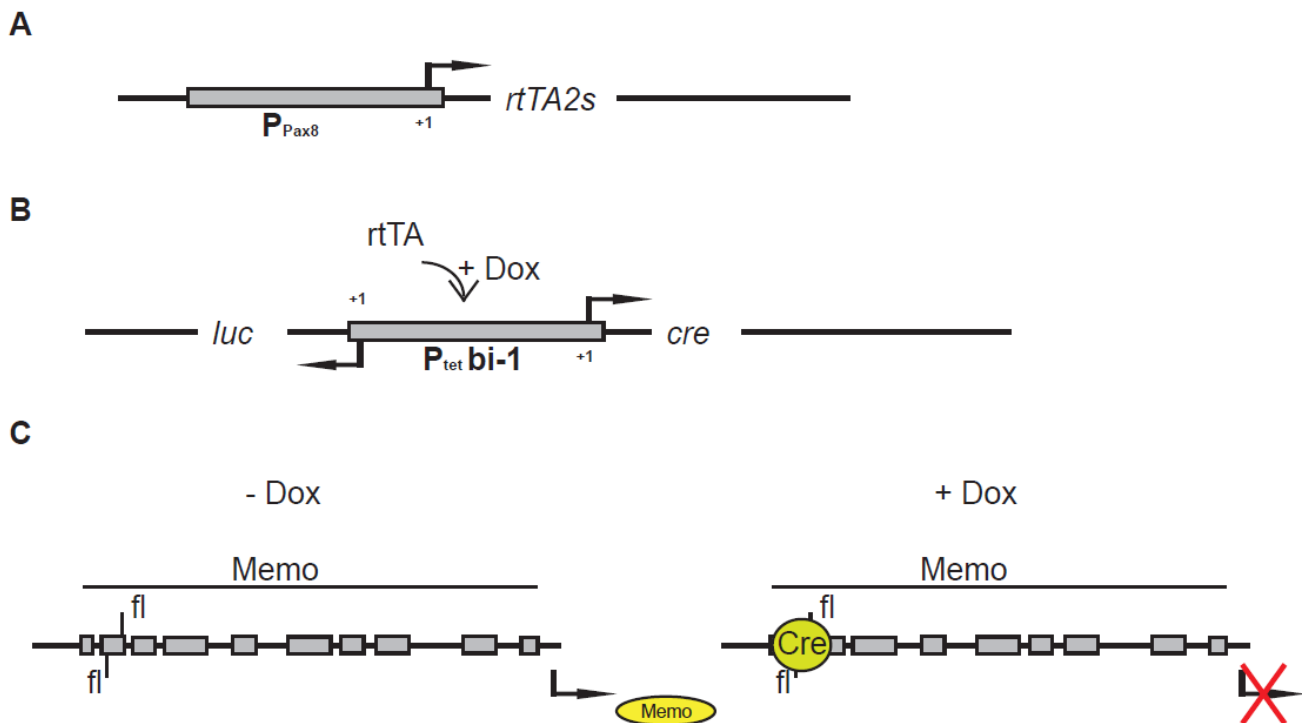


**Figure 5-1 The doxycycline inducible kidney specific Memo knock out mouse line**

A) Transgenic Pax8-rtTA mice express the rtTA2S-M2 transactivator protein under the control of the murine Pax8 promoter, which directs expression to proximal and distal tubules and the collecting duct system of the kidney.

B) In the presence of doxycycline rtTA activates the bidirectional tet-promoter. Subsequently the Cre recombinase is expressed specifically in the cells that express rtTA.

C) In the cells that are expressing the PAX8 promoter and therefore, are expressing the Cre recombinase exon number 2 of Memo gets excised and no Memo protein is transcribed.

Female Memo<sup>fl/fl</sup> mice that were not positive for rtTA and Cre recombinase expression at the same time were bred with males in order to give rise to offsprings that harbored two floxed Memo alleles and were positive for rtTA and Cre recombinase expression at the same time. Pregnant females of such breedings were doxycycline induced at E0.5. As doxycycline transgresses the uterus the embryos

## Material and Methods

positive for rtTA and Cre expression where induced for Memo loss. Doxycycline treatment was continued until the pups were born and reached the age of about 3 weeks.

### **5.12 Microarray of livers and kidneys (performed by the microarray facility inhouse)**

#### **5.12.1 Sample preparation**

##### *5.12.1.1 Microarray of livers*

200ng of total RNA per sample were processed. cDNA was made with the WT cDNA Synthesis and Amplification kit and labeling was performed with the WT Terminal Labeling kit from Affymetrix (Affymetrix, Santa Clara, CA) according to the manufacturer's instructions.

##### *5.12.1.2 Microarray of kidneys*

100ng of total RNA per sample was amplified with the Ambion WT expression Kit (Ambion) according to the manufacturer's instructions. The resulting cDNA was fragmented and labeled with the Affymetrix GeneChip WT Terminal Labeling and Controls Kit according to the manufacturer's instructions.

#### **5.12.2 The array**

GeneChip Mouse Gene 1.0 ST arrays were hybridized following the "GeneChip Whole Transcript (WT) Sense Target Labeling Assay Manual" (Affymetrix, Santa Clara, CA) with a hybridization time of 16 hours. The Affymetrix Fluidics protocol FS450\_0007 was used for washing. Scanning was performed with Affymetrix GCC Scan Control v. 3.0.1 on a GeneChip® Scanner 3000 with autoloader (Affymetrix).

Probesets were summarized and probeset-level values normalized with justRMA() function from R (version 2.9.0) / Bioconductor (version 2.5) package affy using the CDF environment MoGene-1\_0-st-v1.r3.cdf (as provided by Bioconductor) and annotation from Netaffx ([www.netaffx.com](http://www.netaffx.com)).

Differentially expressed genes were identified using the empirical Bayes method (F test) implemented in the LIMMA package. Adjusted p-values were calculated with the false discovery rate method (Wettenhall JM Smyth GK. limmaGUI: a graphical user interface for linear modeling of microarray

## Material and Methods

data. Bioinformatics (Oxford, England) 2004).

Probesets with a p-value of < 0.01, and an absolute log 2 fold-change of more than 2-fold (in linear space) were selected.

### 5.13 Blood- and Urine analysis

#### 5.13.1 Measurement of bilirubin, cholesterol, Creatine Kinase, insulin, iron, glucose, potassium, triglycerides, total protein

Blood was collected from males (wt n=5, ko n=5) via orbital sinus bleeding after anesthesia with Isoflurane, Forene<sup>R</sup> (ABBOTT, ZG, Switzerland). At the time of Memo loss mice were 14 weeks of age, the first blood collection was performed 3 weeks later and the second measurement 14 weeks after Memo loss. The analysis of the blood parameters was performed by ICS, Strasbourg, France.

#### 5.13.2 Blood analysis performed in Dallas

Blood was collected from males (wt n=16, ko n=19) that were induced for loss of Memo at the age of 2 to 3 weeks. About 8 weeks later these mice were fasted overnight and blood collection was performed from the vena cava after the mice have been anaesthetized with a mixture of 1.2ml of narketan 10 (Vétoquinol), 0.8 ml of Rompun 2% (Bayer), 8 ml of PBS-Ca<sup>2+</sup>/Mg<sup>2+</sup>. Analysis was performed on the Vitros 250 in Dallas, Tx, USA at the UTSouthwestern University of Medical Center.

#### 5.13.3 Measurement of phosphate, calcium, sodium, potassium, BUN, creatinine and Albumin

Blood was measured at the Zentrallabor of the University of Basel and Urine was analysed by the hospital in Lausanne (CHUV).

##### 5.13.3.1 Calculations

The fractional excretion was calculated as:

Fractional excretion of x =  $(U_x * U_{Cr} * 100) / (P_x * U_{Cr})$ ; U = concentration in urine, P = concentration in plasma, Cr = creatinine, if x= calcium, then  $P_x = P_{Ca} / 2$  as only half of the calcium is free in the blood

Excretion rate was calculated as:

## Material and Methods

Excretion rate of x =  $U_x/\text{Volume of urine}$

### **5.14 Metabolic cages**

Kidney-specific Memo KO (n=3) and control animals (n=10) were placed in metabolic cages and acclimatized for three days during which body weight was measured. Following the three acclimatization days three days of measurement followed. We performed three measurements, each 24 hours. We measured body weight, food- and water intake, amount of feces and urine. At the end of the experiment all animals were sacrificed. In addition to the urine we collected blood, kidney, liver, thyroid gland, and bone for analysis.

### **5.15 Isolation of brush border membrane**

Adapted from Biber et al. 2007 (393). The left kidney of KO and control animals were isolated from the animals and each cut into pieces. These pieces were kept on ice and ice cold buffer was added. Buffer: 300mM D-mannitol, 5mM EGTA, 12mM Tris-base (pH 7.1), freshly added PMSF (0.5mM). The samples were homogenized with a Polytron (PT 1600 E) until all big pieces were processed. 1.12ml of H<sub>2</sub>O and MgCl<sub>2</sub> up to 12mM were added. Incubation on ice for 15 minutes before the samples were centrifuged for 15 minutes at 4500rpm (1500g) at 4°C. The supernatant was decanted into new Eppendorf tubes and were centrifuged at 18500rpm (25000g) for 30 minutes. The pellet was re-suspended in 500µl of the same buffer than before. For complete re-suspension we homogenized with a 25G needle. The solution was processed 10 times. Concentration was measured by NanoDrop (witec AG, 6014 Littau, Switzerland) and sample buffer was added. The samples were boiled, separated by SDS-PAGE, blotted onto polyvinylidene difluoride membranes (Millipore Corporation) and probed with specific antibodies.

### **5.16 ELISA for VEGF, PTH and FGF23**

#### **5.16.1 VEGF ELISA**

Control and KD 4T1 cells were plated at a density of 8000 cells per 96-well and allowed to grow for 24 hours in DMEM supplemented with 10% FCS. Treatment with CoCl<sub>2</sub>, FGFR or PI3K inhibitor was for 24 hours. Control cells were treated with DMSO, the vehicle of FGFR and PI3K inhibitors.

## Material and Methods

Supernatants from 3 wells were pooled and divided into 3 wells for the ELISA. The levels of VEGF-A were quantified using the Quantikine ELISA kit (R&D Systems, Minneapolis, USA). The number of viable cells was determined using CellTiter 96<sup>®</sup> AQueous One Solution Cell Proliferation Assay (Promega, WI, USA)

### **5.16.2 PTH ELISA**

Blood was collected from Memo KO and control animals, centrifuged for 15 minutes, 6000rpm at 4°C. Serum was collected and snap frozen. Thawed samples were of used for the ELISAs.

The concentration of PTH was measured in the serum of 9 Memo null and 6 control mice and of 6 kidney-specific Memo KO and 12 control animals. We performed the measurement with the ELISA kit from Immutopics (60-2305, Immutopic International, San Clemente, CA) according to the manufacturers protocol.

### **5.16.3 FGF23 ELISA**

Blood was collected from Memo KO and control animals, centrifuged for 15 minutes, 6000rpm at 4°C. Serum was collected and snap frozen. Thawed samples were of used for the ELISAs.

The concentration of FGF23 was measured in the serum of 11 Memo null and 4 control mice as well as of 6 kidney-specific Memo KO and 12 control animals. We performed the measurement with the ELISA kit from Kainos Laboratories (Kainos Laboratories, Inc, Japan) according to the manufacturers protocol.

## 6 Rational of the work

Memo (Mediator of ErbB2 driven cell motility) was identified in a screen for binding partners of ErbB2. ErbB2 has five major phosphorylation sites, two of which (Y1201=YC and Y1227=YD) are required for cellular migration and therefore might play an important role in breast cancer metastasis. To identify binding partners of these two sites, a screen using YC- and YD-phospho-peptides was performed and interacting partners were ascertained by a massspec approach. One of the unannotated proteins found to associate with the phospho-YD site was subsequently given the name Memo, due to its important function in mediating heregulin-induced migration. It was later revealed that the importance of Memo for migration is not confined to mediating signaling downstream of ErbB2, but that it also functions downstream of other receptor tyrosine kinases.

As we were interested in continuing to explore the role of Memo in mouse mammary carcinoma cells, we used shRNA-based approaches to focus in on the functions of Memo in migration, cellular sensitivity to FGFR inhibition and resistance to stress conditions.

Another part of this study aimed at shedding light on the role of Memo in normal physiology. Conventional Memo knock-out led to embryonic lethality. Therefore, we generated an inducible, full-body Memo knock-out model (Memo null animals). We found that embryos that lost Memo after E13.5 survived until birth, but died rapidly thereafter. Studies in pups and young adults showed that Memo null animals suffered from severe premature aging symptoms. In addition, these mice showed postprandial hypoglycemia and increased sensitivity to insulin.

Although this is a rare metabolic phenotype for mouse models of premature aging, which mainly arise from DNA repair defect or nuclear structural alterations, it has been reported for two, namely the Klotho mutant and FGF23 knock-out models. The Klotho and FGF23 mutant mice illustrated for the first time that a defect in the kidney, not directly related to DNA damage, can result in a severe systemic phenotype such as premature aging. These two strains were shown to have defects in the regulation of physiological levels of phosphate, calcium and vitamin D. Since the characterization of these two mouse models, much research has been performed to understand the process of aging and the roles that vitamin D and phosphate play. Given that Memo null animals share this rare metabolic phenotype, we believed that it could be a novel protein player in the Klotho-FGF23 system.



## Rational of the work

To investigate this we took two approaches:

- 1) First, we generated a second mouse model that allowed us to temporally induce Memo loss specifically in the kidney, in the same cells that express Klotho, since only cells that express the co-receptor Klotho are sensitive to FGF23. We subsequently examined the kidney metabolism in both the Memo null and kidney-specific Memo KO models; and
- 2) Second, we investigated the general role of Memo in *in vitro* FGFR signaling, specifically looking at its function in FGF23-mediated FGFR activation.

The goal of this thesis was to further understand the process of aging, the effects of which affect our quality of life and put a strain on our limited healthcare resource.

## 7 Results

### 7.1 Submitted manuscript

#### **Memo is a regulator of FGFR signaling and Memo loss induces premature aging in mice**

Barbara Haenzi<sup>1</sup>, Régis Masson<sup>1,4</sup>, Susanne Lienhard<sup>1</sup>, Julien H. Dey<sup>1,5</sup>, Olivier Bonny<sup>2</sup>, Makoto Kuro-  
o<sup>3</sup>, Nancy E. Hynes<sup>1</sup>

<sup>1</sup>Friedrich Miescher Institute for Biomedical Research, Maulbeerstrasse 66, CH-4058 Basel, Switzerland

<sup>2</sup>Departement of Pharmacology and Toxicology, University of Lausanne, Rue du Bugnon 27, CH-1005 Lausanne, Switzerland

<sup>3</sup>Departement of Pathology, University of Texas Southwestern Medical Center, 5323 Harry Hines Blvd, Dallas, Texas, 75390-9072, USA

Current addresses:

<sup>4</sup>TaconicArtemis, Neurather Ring 1, 51063 Köln, Germany

<sup>5</sup>Nestlé Nutrition, Avenue Nestlé 55, 1800 Vevey, Switzerland

Corresponding author:

Nancy E. Hynes, Growth Control Department, Friedrich Miescher Institute for Biomedical Research, Maulbeerstrasse 66, CH-4058 Basel, Switzerland. Phone: 41 61 6978107; FAX: 41 61 6973976; E-mail: [nancy.hynes@fmi.ch](mailto:nancy.hynes@fmi.ch)

## Results

The contributing authors declare no conflict of interest.

Running title: Memo regulates FGFR signaling

### Abstract

Memo is encoded by a single-copy gene present in all branches of life and is ubiquitously expressed in adult organs and during embryogenesis. To study Memo's role in physiology, we generated a conditional strain, Memo<sup>f/f</sup>. These mice were crossed with the pCX-CreER<sup>TM</sup> strain, in which expression of the inducible Cre transgene is driven by the actin promoter. Tamoxifen treatment of Memo<sup>f/f</sup> / pCX-CreER<sup>TM</sup> mice resulted in deletion of Memo in all organs. Loss of Memo led to the rapid onset of a premature aging phenotype accompanied by alterations in insulin and glucose metabolism. Memo null mice share many features of Klotho and FGF23 mutant strains. Therefore, we investigated Memo's role in FGFR signaling *in vivo* and *in vitro*. Memo null kidneys have altered expression of Cyp27B1, Cyp24A1 and the sodium phosphate (Na-Pi) cotransporter, important regulators of vitamin D production and phosphate reabsorption. Using an inducible system to ablate Memo in mouse embryonic fibroblasts (MEFs) isolated from Memo<sup>f/f</sup> embryos, we show that FGFR signaling activity and duration is lower in knock-out, compared to wild-type MEFs. The results obtained both *in vivo* and *in vitro* support the hypothesis that Memo is a novel regulator of FGFR signaling.

## Results

### Introduction

Memo was discovered during a screen for proteins essential for ErbB2 induced tumor cell motility (Memo; mediator of ErbB2-driven cell motility) (1). We have shown that the 33kDa Memo is complexed with heregulin (HRG)-activated ErbB2 and is essential for maintaining directionality during HRG-induced migration (2). In addition, we observed that migration induced by epidermal growth factor (EGF) or fibroblast growth factor (FGF) also requires Memo (1), suggesting that it might have a broad function in signaling downstream of receptor tyrosine kinases. In this study we present evidence that Memo is a novel downstream regulator of the FGFR pathway.

To study the role of Memo in normal physiology, we generated a mouse strain harboring a conditional allele of the *Memo* gene. In order to control temporal *Memo* deletion, Memo floxed ( $Memo^{fl/fl}$ ) mice were crossed with pCX-CreER<sup>TM</sup> transgenics which allows Memo deletion following tamoxifen treatment. Surprisingly, loss of Memo led to the rapid onset of a premature aging phenotype accompanied by alterations in insulin and glucose metabolism. Memo null mice share many features of *Klotho* and FGF23 mutant strains (3-5).

Unlike the majority of the FGF ligands, the three endocrine ligands, FGF15, FGF21 and FGF23, have low affinity for heparin/heparan sulfate proteoglycans (6) and use *Klotho* family proteins as coreceptors. Thus, for binding to their cognate FGFRs, FGF15 and FGF21 require  $\beta$ Klotho (7), while FGF23 requires *Klotho* (8, 9). *Klotho*, which encodes a single-pass transmembrane protein of 130 kDa, is mainly expressed in renal tubular cells, parathyroid chief cells, and epithelial cells of the choroid plexus (5). FGF23 is secreted from bone and signals in the renal tubules and other organs, where its coreceptor *Klotho* is expressed. Upon binding to the FGFR1-Klotho complex in the nephron, FGF23 controls production of active vitamin D, 1,25-dihydroxyvitamin D<sub>3</sub>, and phosphate reabsorption.

## Results

Defects in FGF23 or Klotho expression in mice lead to a severe premature aging phenotype (3-5), caused by elevated levels of phosphate (10, 11). Moreover, in FGF23 and Klotho mutant strains, low glycemia and increased insulin sensitivity have been observed (12); (13).

In this study we present data supporting the hypothesis that Memo is a novel downstream regulator of the FGFR pathway. The FGFR is constitutively bound to FRS2, an adaptor protein that is phosphorylated upon ligand activation of the receptor (14). FRS2 forms complexes with GRB2/SOS as well as GAB1, leading to activation of the ERK and PI3K pathways. The enzyme PLC $\gamma$  is also recruited to FGFR where it is activated by phosphorylation. We show that Memo binds to the FGF-activated complex of FGFR-pFRS2-GRB2/GAB1. Moreover, loss of Memo in mouse embryonic fibroblasts (MEFs) has a negative effect on FGFR signaling since strength and duration of FRS2 phosphorylation is decreased, and strength and duration of PLC $\gamma$ , AKT, ribosomal protein S6 kinase, and ERK activity is reduced. Taken together, our data suggest that similar to Klotho or FGF23 mutation, deletion of Memo leads to premature aging due to attenuation of FGFR signaling.

## Results

### Material and Methods

#### *Reagents and antibodies*

FGF2 was from Sigma-Aldrich (St. Louis, MO, USA). The following antibodies were used: Pser<sup>473</sup>-AKT (9271), AKT (9272), P Tyr<sup>196</sup>-FRS2 (3864), P Tyr<sup>436</sup>-FRS2 (3861), P Thr<sup>202</sup> / Tyr<sup>204</sup> -ERK1/2 (9101), ERK1/2 (9102), GAB1 (3232), Pser<sup>240</sup> / ser<sup>244</sup>-S6 ribosomal protein (2215), all from Cell Signaling (Danvers, MA, USA); FRS2 (sc-8318), SHP2/SH-PTP2(c-18) (sc-280), HA-probe (sc-7392 and sc-805) from Santa-cruz Biotechnology Inc. (Santa Cruz, CA, USA); actin (MAB1501) and P Tyr<sup>783</sup>-PLC $\gamma$  (07-509) from Millipore (Billerica, MA, USA); GRB2 (G16720) from Transduction Laboratories (BD Biosciences, Mississauga, ON, CDN); Polyclonal antibodies to a 19 amino acid Memo peptide were produced in rabbits (aa 25-43 human Memo NAQLEGWLSQVQSTKRPAR) and monoclonal antibodies to a 18 amino acid Memo peptide were produced in mice (aa 279-294 human Memo RNWQDSSVSYAAGALTVH). Both antisera recognize human and mouse Memo.

#### *Cell Culture and generation of conditional Memo KO MEFs*

Mouse embryonic fibroblasts (MEFs) were generated by standard procedures from Memo<sup>fl/fl</sup> embryos and were spontaneously immortalized by passaging in Dulbecco's modified Eagle's medium (DMEM) supplemented with 10% Fetal Calf Serum (GIBCO Invitrogen AG, Basel, Switzerland) and Penicillin and Streptomycin (growth medium). To obtain inducible Memo knock-out MEFs, cultures were infected with a pMSCV-CreER<sup>T2</sup>-puro<sup>r</sup> retrovirus expressing a tamoxifen inducible Cre recombinase. Virus was produced as follows: Ecophoenix cells were transfected with pMSCV-CreER<sup>T2</sup>-puro<sup>r</sup> plasmid together with lipofectamin 2000 (Invitrogen). After 3.5 days at 37°C the supernatant was collected, filtered through 0.45  $\mu$ m filters and 5  $\mu$ g/ml polybrene was added; 5 ml was used to infect one 10 cm dish of MEFs. After 6 hours of incubation at 37°C the supernatant was removed and fresh

## Results

DMEM-10% FBS was added. After 48 hours, selection with puromycin ((P7255) Sigma-Aldrich (St. Louis, MO, USA)) -containing medium was started. Knock-out of Memo was achieved by incubation of the MEFs in 0.5 µg/ml 4-hydroxytamoxifen ((T5648) Sigma) in DMEM-10% FBS for 3 days. Control cells were incubated in DMEM-10% FBS plus ETOH.

67NR mammary tumor cells (15) were engineered to express Myc-tagged FGFR1. Transfection was performed with 8 µg of pMIRB control vector or Myc-FGFR-pMIRB in 800 µl of Optimem using 16 µl of lipofectamine. One day after transfection, selection was started by addition of 1 mg/ml G418 (11811031 from Invitrogen, Carlsbad, CA, USA) to the medium.

### *Lysates, western blot analyses and immunoprecipitations*

Over-night serum-starved MEF cultures (DMEM-0.1% BSA (Sigma)) were stimulated with 50 ng/ml FGF2 for the indicated time. Whole cell lysates for western blot analyses were prepared in NP-40 buffer (50mM Hepes (pH 7.4), 150mM NaCl, 25mM beta-glycerophosphate, 25mM NaF, 5mM EGTA, 1mM EDTA, 15mM PPI and 1% NP-40) supplemented with leupeptin (10 ug/ml), aprotinin (10 ug/ml), vanadate (2mM), DTT (1mM) and PMSF (1mM). The lysates were boiled in sample buffer, separated by SDS-PAGE, blotted onto polyvinylidene difluoride membranes (Millipore Corporation) and probed with the specific antibodies. Whole cell lysates for co-immunoprecipitations (Co-IP) were prepared in 2 times concentrated Co-IP buffer (50mM Tris (pH 7.5), 5mM EGTA, 150mM NaCl, 25mM beta-glycerophosphat, 25mM NaF) supplemented with 10% Triton X-100, 10% Glycerol, vanadate (2mM), PMSF (1mM), aprotinin (10 ug/ml), leupeptin (10 ug/ml) and MgCl<sub>2</sub> (10mM). The IPs were collected with protein-A or G sepharose beads (Sigma) and centrifuged. The pellets were washed three times with 10% Triton X-100 in PBS. Proteins were released by boiling in sample buffer SDS-PAGE and immunoblotting was performed as described for whole cell lysates.

## Results

### *Generation of the conditional Memo KO and the pCX-CreER<sup>TM</sup> / Memo<sup>fl/fl</sup> mouse strains*

Animal experiments were done according to the Swiss guidelines governing animal experimentation and approved by the Swiss veterinary authorities. Conditional Memo knock-out (Memo<sup>fl/fl</sup>) mice were generated by gene targeting. Briefly, a targeting vector containing a 5' homology arm, two loxP recombination sites flanking exon 2, an FRT-flanked P<sub>gk</sub>-Neomycin resistance cassette, and a 3' homology arm was constructed. The targeting vector was introduced in Sv129/Ola embryonic stem (ES) cells by electroporation. ES clones that had undergone homologous recombination were confirmed by PCR and Southern blot analysis; positive ES clones were used for aggregation, chimera production, and were analyzed for germline transmission. The positive mice were crossed with a FLP deleter transgenic mouse, to remove the neomycin-resistance cassette. These mice referred to as Memo<sup>fl/fl</sup> mice were crossed with pCX-CreER<sup>TM</sup> transgenics (16), in which expression of the tamoxifen-inducible Cre is driven by the ubiquitous actin promoter, in order to generate heterozygous pCX-CreER<sup>TM</sup> /Memo<sup>fl/+</sup> offspring that were mated to generate pCX-CreER<sup>TM</sup> / Memo<sup>fl/fl</sup> mice. Constitutive Memo loss was induced by intraperitoneal (IP) injection of 0.5 – 1 mg of Tamoxifen (Sigma) in corn oil (Sigma) over 4 or 5 consecutive days. The age of the mice at the time of injection varied between 2 to 14 weeks. As controls, Memo<sup>fl/fl</sup> matched littermates that were negative for the Cre recombinase transgene were treated with tamoxifen. The health status of the tamoxifen- injected mice was evaluated by weighing.

### *Analysis of the Memo null mice*

Glucose- and Insulin Tolerance Tests: 14 week-old pCX-CreER<sup>TM</sup> / Memo<sup>fl/fl</sup> males were treated with tamoxifen to induce ubiquitous Memo loss. Glucose- (GTTs) (control n=5; KO n=5) and Insulin



## Results

tolerance tests (ITTs) (control n=2; KO n=3) were performed 6 weeks and 21 weeks, respectively, after tamoxifen injection. For GTTs, glucose (2 g/kg of body weight) (D-(+)-glucose anhydrous; Fluka) was given orally via gauge needle; for ITTs, insulin (1 U/kg) (human recombinant insulin; Sigma) was administered by intraperitoneal injection. Blood samples were collected at the indicated times from tail veins, and glucose levels were determined using a Glucometer (Free Style mini form ABBOTT).

Measurements of blood insulin levels: Memo null and control mice were fasted over-night. Blood was collected and serum was prepared. Measurements for insulin were performed at ICS in Strasbourg, France.

### *RNA extraction, qPCR and isolation of specific nephron segments*

Pieces of kidney or liver were snap frozen and RNA extraction was performed with TRIzol reagent (Invitrogen, Carlsbad, CA, USA), according to the manufacturer's protocol. RNA was washed using the RNeasy Mini Kit (Qiagen) and treated with RNase-free DNase (Qiagen). cDNA was obtained from 1 µg of total RNA using the Ready-to-go You-Prime First-Strand Beads kit (GE-healthcare, Little Chalfont, UK) with oligos-dT primers (Promega). Fold-changes are expressed as expression values of Memo null mice divided by expression values of control littermates. Standard deviation was calculated by using the following formula:

$$STD_{\text{Fold-change}} = ((STD_{\text{Memo-null}}/\text{Fold change}_{\text{Memo-null}})^2 + (STD_{\text{Control}}/\text{Fold change}_{\text{Control}})^2)^{0.5} * \text{Fold change}$$

Isolation of nephron segments was performed as follows. After anesthesia (sodium pentobarbital, 5 mg/100 g mouse body weight) the left kidney was perfused with microdissection medium containing 0.24% collagenase (Type A, Boehringer Mannheim). The microdissection medium was prepared from Hanks sterile solution containing 1 g/liter glucose supplemented with 1mM lactic acid, 1mM glutamine, 1mM sodium pyruvate, 0.5mM MgCl<sub>2</sub>, 1mM CH<sub>3</sub>COONa, 0.1% protease-free serum

## Results

albumin, 20mM Hepes and was adjusted to pH 7.4. Thin pyramids were cut from the kidney and incubated 25 min at 30°C (60 min at 37°C for the inner medulla) in 0.15% collagenase solution and then thoroughly rinsed in microdissection solution. Glomeruli and different nephron segments were microdissected at 4°C according to anatomical and morphological criteria (17). Dissected tubules were analysed by western blot analysis for Memo levels. Alternatively, RNA was extracted and analysed by qPCR.

## Results

### Results

#### *Memo ablation leads to premature aging.*

Memo is a 33 kDa protein that is expressed in all organs from adult mice (Figure 1A and 1B). To gain insight into the physiological role of Memo, a conditional strain with exon two of the *Memo* gene flanked by loxP sites ( $Memo^{fl/fl}$ ) was generated. In order to temporally control the onset of Cre recombinase activity, a strain harboring the pCX-CreER<sup>TM</sup> transgene was used (16). The transgene is under the control of the ubiquitously expressed CAGGS promoter consisting of the CMV early enhancer and the chicken beta-actin promoter. Cre activity is induced by tamoxifen, which results in Memo deletion in all organs; these animals will be referred to as Memo null mice.  $Memo^{fl/fl}$  mice that are negative for the Cre recombinase were control-treated with tamoxifen and are referred to as control mice. Tamoxifen treatment had no detectable effect on these mice.

To test for Cre functionality, 12 week old male mice were treated on 5 consecutive days with tamoxifen; eight weeks later lysates were prepared from various organs and a western analysis was performed for Memo. There was a strong decrease in Memo levels in each of the examined organs. In the liver, duodenum and kidney there is little or no detectable Memo; while in the testis and spleen there is still some protein detectable (Figure 1C).

Next, Memo loss was induced at different ages between 2 and 14 weeks and the phenotypic consequences on the mice were monitored. Remarkably, we observed that the Memo null animals exhibited a small stature and showed multiple signs of premature aging (Figure 2A), including hair graying, alopecia, kyphosis (Figure 2A), hypogonadism, weight loss (data not shown), loss of the subcutaneous adipose layer (Figure 2B top), and loss of spermatozoa in the epididymis (Figure 2B bottom). The earlier Memo loss was induced by tamoxifen injection the more rapid the onset of these

## Results

phenotypes and the shorter the time of survival (Figure 2C). In summary, Memo loss has a dramatic effect on the overall physiology of the mice.

### *Memo null mice have altered insulin and glucose sensitivity*

Prompted by the observation that many mouse models of premature aging show altered insulin sensitivity (18-20), we measured blood glucose and insulin levels in Memo null mice. The mice had normal fasting blood glucose levels, but showed a tendency to lower blood insulin levels than control littermates (Supplemental Figure 1), suggesting that Memo loss increased insulin sensitivity. Next, we performed glucose (GTT) and insulin (ITT) tolerance tests and observed that in the Memo null mice there was an increased capacity for glucose disposal (Figure 2D top) and an increased hypoglycemic response to exogenous insulin (Figure 2D bottom), which is consistent with increased insulin sensitivity in these animals. In Figure 2D one representative experiment of the three that were performed is shown.

### *Investigation of Memo expression and key proteins of the FGF23-Klotho axis in the kidney*

Based on the observation that aging-like phenotypes associated with increased insulin sensitivity were also observed in Klotho and FGF23 mutant strains, we hypothesized that Memo might function as a regulator of the FGF23-Klotho signaling pathway in the kidney. First, we examined Memo RNA and protein levels in different nephron segments that were separated by microdissection. Quantitative PCR (qPCR) carried out on RNA from dissected nephrons showed that Memo is highly expressed in the thick ascending limb (TAL) and to a lesser extent in other nephron segments including the connecting

## Results

tubule (CNT) and distal convoluted tubules (DCT) (Figure 3A), the location of Klotho expression (21). The western analysis showed that Memo protein is present in all the segments, except for the cortical collecting duct (CCD) and the Glomerulus (Glom) (Figure 3B). Thus, Memo is widely expressed throughout the nephron and overlaps with Klotho. The inducible system is efficient since Memo was not detected in kidney lysates prepared from tamoxifen treated Memo<sup>fl/fl</sup>/pCX-CreER<sup>TM</sup> mice (Figure 3C). Finally, we examined whether Memo loss had an impact on FGFR1 or Klotho levels in kidneys by performing qPCR; there were no significant differences in control compared to Memo null mice for FGFR1 levels, while some litters showed a slight downregulation for Klotho (Supplementary Table 1).

In the next set of experiments, we determined whether loss of Memo perturbed expression of genes known to be regulated by FGF23-Klotho signaling. For this, we examined 1 $\alpha$ -hydroxylase, which is encoded by *Cyp27B1*, and synthesizes the active form of vitamin D (1,25-dihydroxyvitamin D3) from its inactive precursor (22); as well as 24-hydroxylase, which is encoded by *Cyp24A1*, and catabolises active vitamin D and 25-dihydroxyvitamin D3 to 24,25-dihydroxyvitamin D3 (23). FGF23-Klotho signaling inhibits transcription of *Cyp27B1*, and upregulates transcription of *Cyp24A1*. Klotho mutant mice show increased levels of *Cyp27B1* and *Cyp24A1* RNA (24). We also examined the type-IIa and -IIc sodium-phosphate cotransporters (Na-Pi2a/Na-Pi2c), which mediate phosphate reabsorption in the kidney and are also controlled by FGF23. Klotho mutant mice have lower levels of Na-Pi mRNA (25).

QPCR was carried out on RNA isolated from kidneys collected from four litters of control and Memo null mice and the levels of *Cyp27B1*, *Cyp24A1* and the Na-Pi2a/2c transcripts were investigated. Na-Pi2a/2c levels are downregulated 1.5 to 3.7 times in Memo null mice in the four litters (Table 1), a phenotype that is comparable to that described in Klotho mutant mice. Moreover Memo null mice all showed abnormal expression of *Cyp27B1* and *Cyp24A1*, however, individual litters showed either up

## Results

(1.5 to 9.3) or down-regulation (1.6 to 2.4) of these transcripts (Table 1).

In summary, the results suggest that Memo deficiency affects activity of the FGF23-Klotho-FGFR1 pathway in the kidney. Since the phenotype observed in Memo null mice shares many similarities with Klotho and FGF23 mutant mice, in particular postprandial low glycemia and increased insulin sensitivity, we consider it likely that aberrant FGFR signaling in Memo null kidneys contributes to the observed premature aging syndrome.

### *Memo regulates FGFR signaling*

Based on our previous publication showing that Memo is required for optimal FGFR-mediated migration in T47D breast cancer cells (1) and the results presented above, we propose that Memo is a novel regulator of FGFR signaling. In order to examine the role of Memo in FGF-induced signaling more closely, we developed a model of immortalized mouse embryonic fibroblasts (MEFs) from Memo<sup>fl/fl</sup> embryos. These were infected with a retrovirus harboring an inducible Cre recombinase (pMSCV-CreER<sup>T2</sup>), allowing us to tightly regulate Memo deletion. Following 3 days of 4-hydroxytamoxifen treatment there was essentially no Memo protein detectable in lysates from these cells compared to matched control Memo<sup>fl/fl</sup> MEFs that were treated with ethanol (referred to as Memo KO MEFs and WT MEFs, respectively) (Supplemental Figure 2A).

QPCR was used to determine FGFR expression in the MEFs, revealing that FGFR2 and FGFR4 are more highly expressed than FGFR1 and FGFR3 and that the Memo KO MEFs have similar levels (Supplemental Figure 3). To measure total FGFR activity, phosphorylation of FRS2, the adaptor protein that links the receptors to intracellular signaling pathways, was used as a read-out. FRS2 is constitutively associated with FGFRs and becomes heavily phosphorylated on Tyr and Thr residues

## Results

following ligand binding to the receptor (14). WT and Memo KO MEFs were stimulated with FGF2, which activates all FGFRs, for various times, lysates were prepared and a western analysis was carried out using site-specific phospho-FRS2 antibodies recognizing Tyr436 and Tyr196 residues. Both residues were rapidly phosphorylated following FGF2 treatment. However, the overall level of phosphorylation on both Tyr residues was significantly reduced and the duration of phosphorylation on both sites was shorter in Memo KO MEFs compared to WT MEFs (Figure 4A upper and lower panels). FRS2 protein levels are equivalent in WT and Memo KO MEFs (Figure 4A and Supplemental Figure 2A). These results suggest that Memo is needed for optimal stimulation of FGFR signaling.

The activity of the downstream PLC $\gamma$ , ERK and PI3K/AKT/S6K pathways was also measured using phospho-specific antibodies. In comparison to the WT MEFs, there was a consistent decrease in pERK 1/2 levels in Memo KO MEFs (Figure 4B). ERK phosphorylates FRS2 on multiple Thr residues (26), which is reflected in a mobility shift in the protein. The upward-shift in FRS2 mobility is not as pronounced in Memo KO MEFs compared to WT MEFs, which is particularly evident in the lower panel of Figure 4A, providing additional evidence for impaired ERK activation in the Memo KO MEFs. The levels of PLC $\gamma$  phosphorylation on Tyr783, AKT phosphorylation on Ser473 and ribosomal S6 phosphorylation on Ser240/244 were also lower in Memo KO MEFs compared to WT cells (Figure 4C). Taken together, the results suggest that in the absence of Memo, FGFR signaling is dampened as evidenced by decreased phosphorylation on FRS2 and decreased activation of PLC $\gamma$ , ERK and PI3K/AKT signaling.

*Memo associates with FGFR-activated signaling proteins*

## Results

Memo loss does not lead to a complete block in FGFR signaling, but lowers the overall level of activation and downstream signaling. To provide mechanistic insight into these results, we first asked whether Memo is associated with FGFR-activated complexes. Since the MEFs express the 4 FGFRs, but at low levels, we used 67NR mammary cancer cells, which were engineered to overexpress a Myc-tagged FGFR1 to probe for FGFR-Memo complexes. FGFR was detected in Memo IPs from lysates of 67NR Myc-FGFR1 transfected cells; no receptor was complexed with Memo in IPs from 67NR control lysates (Figure 5A). The Memo-FGFR complex is constitutive since the level of receptor was the same in IPs from lysates of unstimulated and FGF-stimulated cultures (Figure 5A). Since 67NR tumor cells show constitutive activation of FGFRs and addition of FGF has minimal effects on downstream signaling (27), to examine the effects of FGF on signaling complexes, the remaining experiments were carried out with the MEFs.

Memo was detected in IPs of FRS2 made with lysates of WT MEFs, both from control and FGF stimulated cultures (Figure 5B), suggesting that it is constitutively complexed with the adaptor protein. No Memo was detected in FRS2 IPs made with lysates from Memo KO MEFs (Figure 5B) or in IPs made with a non-specific antibody (Supplemental Figure 2B). Moreover, in lysates from WT MEFs, Memo was detected in GAB1 IPs and in GRB2 IPs, and there was an increase in Memo in IPs from lysates of FGF-treated cultures (Figure 5C upper and lower panels, resp). Taken together the results suggest that Memo constitutively associates with FGFR and FRS2 and can be found in complexes with other FRS2 associated proteins after ligand addition.

Finally, we examined whether Memo influences ligand-activated FGFR-complex formation. FRS2 IPs from lysates of control and FGF-stimulated WT and Memo KO MEFs were probed for complexed SHP2, GAB1 and GRB2 (Figure 5E). In lysates from FGF-treated WT MEFs, there was a strong



## Results

increase in the level of FRS2-complexed SHP2 and GRB2; GAB1 was detected in complexes from unstimulated cells and was moderately increased after FGF treatment (Figure 5D). Importantly, FRS2 IPs from lysates of FGF-treated Memo KO MEFs, had slightly less complexed SHP2 and GRB2; GAB1 levels were not altered (Figure 5D). As shown in Figure 4A, the levels of FRS2 P-Tyr436 and P-Tyr196, sites that recruit SHP2 and GRB2, respectively were significantly reduced in Memo KO MEFs compared to WT MEFs. Thus, the decreased FRS2 binding of SHP2 and GRB2 likely reflects the alterations in FRS2 P<sub>tyr</sub> levels in the Memo KO MEFs (Figure 4A). Taken together, the results show that Memo is constitutively associated with FRS2 and upon ligand stimulation shows increased association with the FRS2-recruited SHP2 and GRB2 (Figure 5E).

## Discussion

Memo has an established role in ErbB2 receptor induced motility, controlling microtubules and adhesion site formation, as well as cell directionality (1, 2, 28). To gain insight into the physiological role of Memo, we generated tamoxifen inducible Memo<sup>fl/fl</sup> / pCX-CreER<sup>TM</sup> mice. Surprisingly, Memo deletion led to a premature aging phenotype and to alterations in insulin and glucose metabolism. We show that Memo binds to the complex of FGFR-FRS2-GRB2/GAB1 and regulates the strength and duration of FGFR signaling. Based on the *in vivo* characteristics of the Memo null animals, and the data generated using cellular models, our results suggest that Memo deletion causes premature aging due to a role for Memo in maintaining physiological FGFR signaling in the kidney. We propose that Memo is a novel regulator of FGFR signaling.

There are multiple mouse models of premature aging. However, after determining that Memo null mice were postprandial hypoglycemic and showed increased insulin sensitivity, we focused on the kidney since FGFR signaling has an essential role in regulation of vitamin D and phosphate homeostasis in this

## Results

organ. FGF23 and Klotho mutant mice show characteristic alterations in this pathway. Klotho mutants have elevated levels of Cyp27B1 and Cyp24A1 (24). Memo null mice also show abnormal expression profiles of Cyp27B1 and Cyp24A1, however, there was not a consistent up- or down-regulation. In the normal kidney, the vitamin D/ Vitamin D receptor (VDR) complex feeds-back to control Cyp27B1 and Cyp24A1 expression (29). In Klotho mutant kidneys VDR is down-regulated, which has been proposed to contribute to alterations in feedback loop control and altered expression of these enzymes (24). In contrast to Klotho mutants, there was no reduction in VDR levels in the kidneys of Memo null mice (data not shown), which could explain why Klotho mutants show consistent up-regulation of Cyp27B1 and Cyp24A1 and Memo null mice show inconsistent alterations.

FGF23 also regulates the Na-Pi2a and Na-Pi2c cotransporters that mediate phosphate reabsorption. We found that the RNA levels of both were downregulated in Memo null kidneys, a phenotype that has also been observed in Klotho mutant mice (25). Since it has been shown that alterations in serum phosphate levels lead to increased Glucose-6-Phosphatase (G6Pase) RNA and activity in the liver (30), we examined RNA from Memo null livers for the level of the catalytic subunit of this enzyme (G6Pc1). Phosphoenolpyruvat-Carboxykinase (PEPCK), another regulator of glucose homeostasis was also examined in liver RNA. Both G6Pc1 and PEPCK levels were increased in Memo null livers compared to control, 1.5 to 3.6 times and 2 to 2.9 times, respectively (Table 2). In summary the specific metabolic phenotype of the Memo null mice, postprandial hypoglycemia and increased insulin sensitivity, that they share with the Klotho and FGF23 mutant animals is a strong indicator that these three proteins are in the same pathway.

We used *in vitro* cellular models to gain insight into Memo's role in regulation of FGFR signaling. Upon FGFR activation the constitutively bound adaptor protein FRS2 is phosphorylated and forms

## Results

complexes with SHP2, GRB2/SOS as well as GAB1, leading to activation of ERK and PI3K pathways (Figure 5E). In the 67NR mammary cells we found association of Memo with Myc-tagged FGFR and in the MEFs, Memo was detected in complexes with FRS2 and other associated signaling partners. Indeed, our results suggest that Memo, like FRS2, is constitutively associated with FGFR. Whether this association is via a direct interaction with FRS2, remains to be explored. Although FGF-induced complexes form in the Memo KO MEFs, ligand-induced activation of the ERK and the PI3K/AKT/S6K pathways is dampened in both strength and in duration. Moreover, FRS2 and PLC $\gamma$ , the latter recruited directly to the active FGFR, both showed decreased Tyr-P levels. Lower FRS2 Tyr-P might in turn contribute to the decreased signaling activity of the ERK and the AKT/S6K pathways observed in the Memo KO MEFs.

A number of proteins modulate FGFR signaling including CBL, Sprouty and SEF. While screening for their expression, we found that SEF is more highly expressed in Memo null kidneys and in Memo KO MEFs compared to controls (Table 2). SEF is a transmembrane protein that has been shown to inhibit FGFR and FRS2 phosphorylation, as well as ERK activation (31). Elevated levels of SEF might contribute to lower FGFR signaling activity in Memo's absence, something that will be explored in the future. FGFR localization to specific compartments of the membrane has been shown to affect signaling (32). Following ErbB receptor activation Memo associates with the RhoA-GTP/ mDia complex to control actin dynamics (28). Thus, it is possible that Memo is required to localize FGFRs to specific compartments of the membrane to ensure proper signaling.

Since Cre recombinase expression is under the control of an actin promoter, Memo is lost in many organs following tamoxifen addition to the Memo<sup>fl/fl</sup>/pCX-CreER<sup>TM</sup> mice. Thus, there might be multiple physiological effects contributing to the premature aging phenotype, something that we have

## Results

not addressed in this study. However, it is worth mentioning that phenotypes reflecting alterations in other FGFRs were not observed in the Memo null mice. FGFR1 and FGFR2 mutant embryos die between E7.5-9.5 and E4.5-5.5, respectively (33-35). Memo null embryos die starting at E13.5 (R.M. unpublished), suggesting that Memo does not have an early role downstream of these receptors. FGFR3 is not essential for embryogenesis, but in its absence adult mice show bone malformation (36, 37), a phenotype that was not observed in the Memo null mice. FGF15 signals via FGFR4/ $\beta$ klotho in the liver (7). FGFR4 and  $\beta$ klotho null strains both show elevated bile acid levels due to upregulation of Cyp7A1 RNA (38, 39). There was no change in Cyp7A1 expression in Memo null livers (not shown). Thus, it is possible that Memo has a specific role in the kidney or that Memo loss in this organ has such a dramatic effect that other phenotypes do not have time to develop. This will be examined in the future once mice with a conditional kidney specific Memo mutation are available. In conclusion, Memo null mice share many features of Klotho and FGF23 mutant strains; the results we present support the hypothesis that Memo is a novel regulator of FGFR signaling.

## Acknowledgements

We would like to thank Debby Hynx and Dmitri Firsov for technical advice, Fawaz G. Haj for the sequences of the G6P1c and PEPCCK primers, and Simon Woehrle, Gwen MacDonald and other Hynes lab members for inspiring discussions. The work of B.H. was partially supported by the Swiss National Fond (SNF 31003A-121574) and a EMBO short term fellowship (ASTF 332-2208). The work of R.M. was partially supported by Transfog FP6 IP (LSHC-CT-2004-503438). The laboratory of N.E.H. is supported by the Friedrich Miescher Institute for Biochemical Research

## Results

### References

1. Marone, R., Hess, D., Dankort, D., Muller, W.J., Hynes, N.E., and Badache, A. 2004. Memo mediates ErbB2-driven cell motility. *Nat Cell Biol* 6:515-522.
2. Meira, M., Masson, R., Stagljar, I., Lienhard, S., Maurer, F., Boulay, A., and Hynes, N.E. 2009. Memo is a cofilin-interacting protein that influences PLCgamma1 and cofilin activities, and is essential for maintaining directionality during ErbB2-induced tumor-cell migration. *J Cell Sci* 122:787-797.
3. Sitara, D., Razzaque, M.S., Hesse, M., Yoganathan, S., Taguchi, T., Erben, R.G., Juppner, H., and Lanske, B. 2004. Homozygous ablation of fibroblast growth factor-23 results in hyperphosphatemia and impaired skeletogenesis, and reverses hypophosphatemia in PheX-deficient mice. *Matrix Biol* 23:421-432.
4. Shimada, T., Kakitani, M., Yamazaki, Y., Hasegawa, H., Takeuchi, Y., Fujita, T., Fukumoto, S., Tomizuka, K., and Yamashita, T. 2004. Targeted ablation of Fgf23 demonstrates an essential physiological role of FGF23 in phosphate and vitamin D metabolism. *J Clin Invest* 113:561-568.
5. Kuro-o, M., Matsumura, Y., Aizawa, H., Kawaguchi, H., Suga, T., Utsugi, T., Ohyama, Y., Kurabayashi, M., Kaname, T., Kume, E., et al. 1997. Mutation of the mouse klotho gene leads to a syndrome resembling ageing. *Nature* 390:45-51.
6. Mohammadi, M., Olsen, S.K., and Ibrahimi, O.A. 2005. Structural basis for fibroblast growth factor receptor activation. *Cytokine Growth Factor Rev* 16:107-137.
7. Ogawa, Y., Kurosu, H., Yamamoto, M., Nandi, A., Rosenblatt, K.P., Goetz, R., Eliseenkova, A.V., Mohammadi, M., and Kuro-o, M. 2007. BetaKlotho is required for metabolic activity of fibroblast growth factor 21. *Proc Natl Acad Sci U S A* 104:7432-7437.
8. Kurosu, H., Ogawa, Y., Miyoshi, M., Yamamoto, M., Nandi, A., Rosenblatt, K.P., Baum, M.G., Schiavi, S., Hu, M.C., Moe, O.W., et al. 2006. Regulation of fibroblast growth factor-23 signaling by klotho. *J Biol Chem* 281:6120-6123.
9. Urakawa, I., Yamazaki, Y., Shimada, T., Iijima, K., Hasegawa, H., Okawa, K., Fujita, T., Fukumoto, S., and Yamashita, T. 2006. Klotho converts canonical FGF receptor into a specific receptor for FGF23. *Nature* 444:770-774.
10. Kuro-o, M. 2010. A potential link between phosphate and aging--lessons from Klotho-deficient mice. *Mech Ageing Dev* 131:270-275.
11. Ohnishi, M., and Razzaque, M.S. 2010. Dietary and genetic evidence for phosphate toxicity accelerating mammalian aging. *FASEB J* 24:3562-3571.
12. Hesse, M., Frohlich, L.F., Zeitz, U., Lanske, B., and Erben, R.G. 2007. Ablation of vitamin D signaling rescues bone, mineral, and glucose homeostasis in Fgf-23 deficient mice. *Matrix Biol* 26:75-84.
13. Utsugi, T., Ohno, T., Ohyama, Y., Uchiyama, T., Saito, Y., Matsumura, Y., Aizawa, H., Itoh, H., Kurabayashi, M., Kawazu, S., et al. 2000. Decreased insulin production and increased insulin sensitivity in the klotho mutant mouse, a novel animal model for human aging. *Metabolism* 49:1118-1123.
14. Eswarakumar, V.P., Lax, I., and Schlessinger, J. 2005. Cellular signaling by fibroblast growth factor receptors. *Cytokine Growth Factor Rev* 16:139-149.

## Results

15. Aslakson, C.J., and Miller, F.R. 1992. Selective events in the metastatic process defined by analysis of the sequential dissemination of subpopulations of a mouse mammary tumor. *Cancer Res* 52:1399-1405.
16. Guo, C., Yang, W., and Lobe, C.G. 2002. A Cre recombinase transgene with mosaic, widespread tamoxifen-inducible action. *Genesis* 32:8-18.
17. Bibert, S., Hess, S.K., Firsov, D., Thorens, B., Geering, K., Horisberger, J.D., and Bonny, O. 2009. Mouse GLUT9: evidences for a urate uniporter. *Am J Physiol Renal Physiol* 297:F612-619.
18. Turek, F.W., Joshu, C., Kohsaka, A., Lin, E., Ivanova, G., McDearmon, E., Laposky, A., Losee-Olson, S., Easton, A., Jensen, D.R., et al. 2005. Obesity and metabolic syndrome in circadian Clock mutant mice. *Science* 308:1043-1045.
19. Knebel, B., Avci, H., Bullmann, C., Kotzka, J., and Muller-Wieland, D. 2005. Reduced phosphorylation of transcription factor Elk-1 in cultured fibroblasts of a patient with premature aging syndrome and insulin resistance. *Exp Clin Endocrinol Diabetes* 113:94-101.
20. Chang, S., Multani, A.S., Cabrera, N.G., Naylor, M.L., Laud, P., Lombard, D., Pathak, S., Guarente, L., and DePinho, R.A. 2004. Essential role of limiting telomeres in the pathogenesis of Werner syndrome. *Nat Genet* 36:877-882.
21. Bergwitz, C., and Juppner, H. 2010. Regulation of phosphate homeostasis by PTH, vitamin D, and FGF23. *Annu Rev Med* 61:91-104.
22. Miller, W.L., and Portale, A.A. 2000. Vitamin D 1 alpha-hydroxylase. *Trends Endocrinol Metab* 11:315-319.
23. Henry, H.L. 2001. The 25(OH)D(3)/1alpha,25(OH)(2)D(3)-24R-hydroxylase: a catabolic or biosynthetic enzyme? *Steroids* 66:391-398.
24. Yoshida, T., Fujimori, T., and Nabeshima, Y. 2002. Mediation of unusually high concentrations of 1,25-dihydroxyvitamin D in homozygous klotho mutant mice by increased expression of renal 1alpha-hydroxylase gene. *Endocrinology* 143:683-689.
25. Segawa, H., Yamanaka, S., Ohno, Y., Onitsuka, A., Shiozawa, K., Aranami, F., Furutani, J., Tomoe, Y., Ito, M., Kuwahata, M., et al. 2007. Correlation between hyperphosphatemia and type II Na-Pi cotransporter activity in klotho mice. *Am J Physiol Renal Physiol* 292:F769-779.
26. Lax, I., Wong, A., Lamothe, B., Lee, A., Frost, A., Hawes, J., and Schlessinger, J. 2002. The docking protein FRS2alpha controls a MAP kinase-mediated negative feedback mechanism for signaling by FGF receptors. *Mol Cell* 10:709-719.
27. Dey, J.H., Bianchi, F., Voshol, J., Bonenfant, D., Oakeley, E.J., and Hynes, N.E. 2010. Targeting fibroblast growth factor receptors blocks PI3K/AKT signaling, induces apoptosis, and impairs mammary tumor outgrowth and metastasis. *Cancer Res* 70:4151-4162.
28. Zaoui, K., Honore, S., Isnardon, D., Braguer, D., and Badache, A. 2008. Memo-RhoA-mDia1 signaling controls microtubules, the actin network, and adhesion site formation in migrating cells. *J Cell Biol* 183:401-408.
29. Takeyama, K., Kitanaka, S., Sato, T., Kobori, M., Yanagisawa, J., and Kato, S. 1997. 25-Hydroxyvitamin D3 1alpha-hydroxylase and vitamin D synthesis. *Science* 277:1827-1830.
30. Xie, W., Li, Y., Mechin, M.C., and Van De Werve, G. 1999. Up-regulation of liver glucose-6-phosphatase in rats fed with a P(i)-deficient diet. *Biochem J* 343 Pt 2:393-396.
31. Kovalenko, D., Yang, X., Chen, P.Y., Nadeau, R.J., Zubanova, O., Pigeon, K., and Friesel, R. 2006. A role for extracellular and transmembrane domains of Sef in Sef-mediated inhibition of FGF signaling. *Cell Signal* 18:1958-1966.

## Results

32. Bryant, M.R., Marta, C.B., Kim, F.S., and Bansal, R. 2009. Phosphorylation and lipid raft association of fibroblast growth factor receptor-2 in oligodendrocytes. *Glia* 57:935-946.
33. Deng, C.X., Wynshaw-Boris, A., Shen, M.M., Daugherty, C., Ornitz, D.M., and Leder, P. 1994. Murine FGFR-1 is required for early postimplantation growth and axial organization. *Genes Dev* 8:3045-3057.
34. Yamaguchi, T.P., Harpal, K., Henkemeyer, M., and Rossant, J. 1994. fgfr-1 is required for embryonic growth and mesodermal patterning during mouse gastrulation. *Genes Dev* 8:3032-3044.
35. Arman, E., Haffner-Krausz, R., Chen, Y., Heath, J.K., and Lonai, P. 1998. Targeted disruption of fibroblast growth factor (FGF) receptor 2 suggests a role for FGF signaling in pregastrulation mammalian development. *Proc Natl Acad Sci U S A* 95:5082-5087.
36. Colvin, J.S., Bohne, B.A., Harding, G.W., McEwen, D.G., and Ornitz, D.M. 1996. Skeletal overgrowth and deafness in mice lacking fibroblast growth factor receptor 3. *Nat Genet* 12:390-397.
37. Deng, C., Wynshaw-Boris, A., Zhou, F., Kuo, A., and Leder, P. 1996. Fibroblast growth factor receptor 3 is a negative regulator of bone growth. *Cell* 84:911-921.
38. Yu, C., Wang, F., Kan, M., Jin, C., Jones, R.B., Weinstein, M., Deng, C.X., and McKeehan, W.L. 2000. Elevated cholesterol metabolism and bile acid synthesis in mice lacking membrane tyrosine kinase receptor FGFR4. *J Biol Chem* 275:15482-15489.
39. Ito, S., Fujimori, T., Furuya, A., Satoh, J., and Nabeshima, Y. 2005. Impaired negative feedback suppression of bile acid synthesis in mice lacking betaKlotho. *J Clin Invest* 115:2202-2208.

## Results

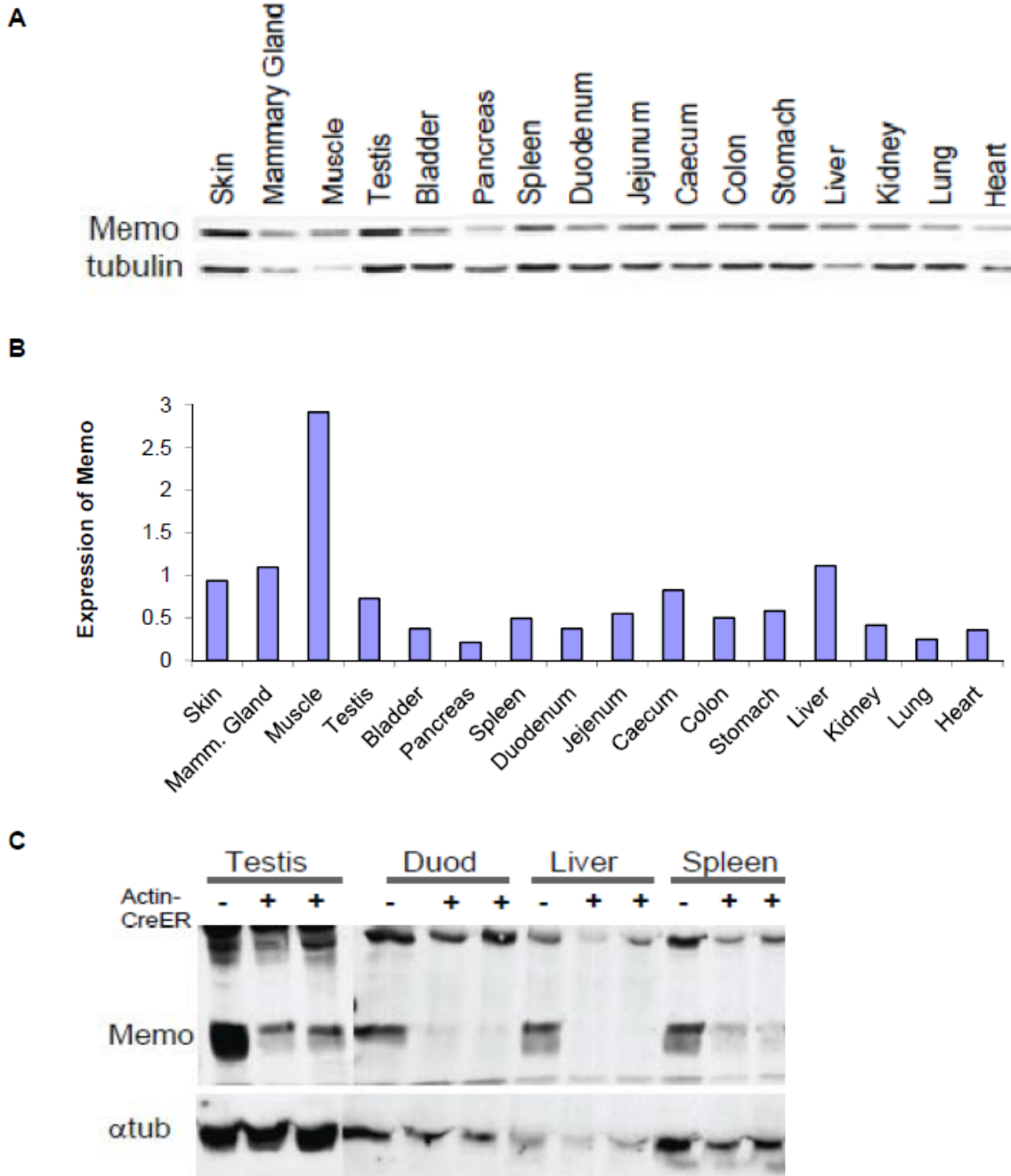


**Figure 1 Memo expression in mouse organs**

(A) Western blot analysis of Memo levels in lysates from the indicated organs of a control mouse.

(B) Quantification of Memo levels in the western analysis of panel A, normalized to tubulin levels (ImageJ).



## Results

(C) 12 week old  $Memo^{fl/fl}$  mice that were pCX-CreER<sup>TM</sup> positive (+) or negative (-) were injected with tamoxifen and sacrificed 8 weeks later. The indicated organs were analyzed by Western for their level of Memo protein.

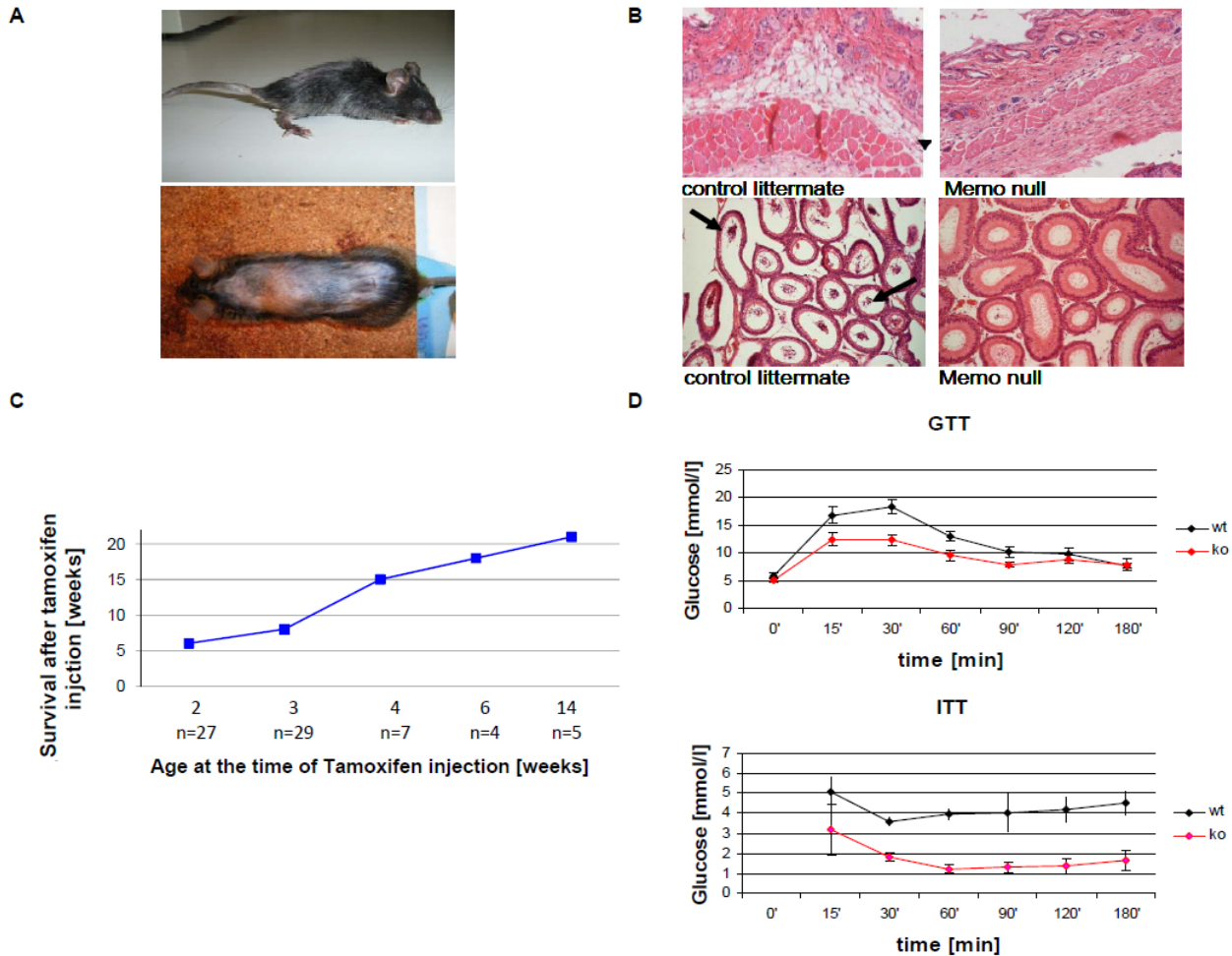


**Figure 2 Premature aging and metabolic phenotype of the Memo null mice**

(A) Memo null mice. The mice were tamoxifen-injected at 2 (upper) and 6 (lower) weeks of age with tamoxifen and pictures were taken 6 and 18 weeks later, respectively.

(B) Hematoxylin and Eosin (H&E) paraffin sections of skin (top) and epididymis (bottom). Memo null mice show loss of subcutaneous fat (arrowhead). The epididymis of the control littermates contain spermatozoa (arrows) that are missing in the Memo null animal.

(C) Mice at the indicated ages (x-axis: 2, 3, 4, 6, or 14 weeks) were injected with tamoxifen and monitored for signs of premature aging (n-number in each group). The experiment was terminated and the animals sacrificed according to the severity of the phenotype; the number of weeks of survival after tamoxifen injection is indicated on the y-axis.

(D) Glucose Tolerance Tests (top) and Insulin Tolerance Tests (bottom) were performed with male mice that were treated with tamoxifen at 14 weeks of age. Mice were fasted overnight and sucrose was administered orally with a gauge needle for the GTTs; insulin was intraperitoneally injected for the

## Results

ITTs. Blood glucose levels were measured at the indicated times. See also Figure S1

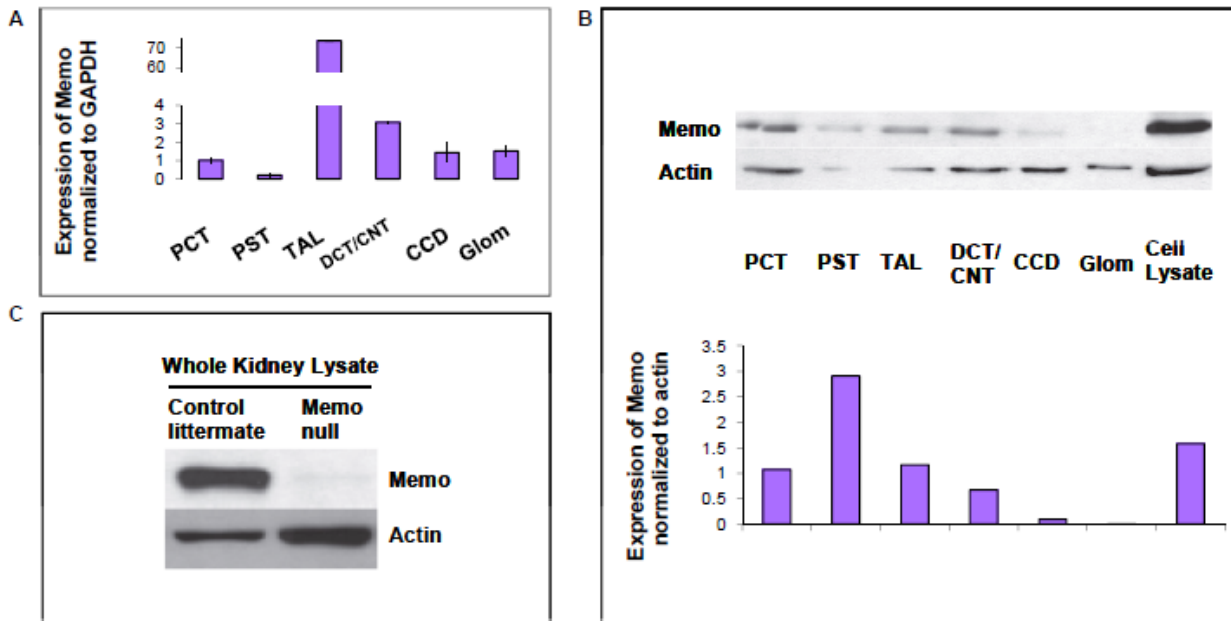


### Figure 3 Expression of Memo in the kidney

The kidney of a WT mouse was microdissected and RNA and protein were isolated from different segments of the nephron. (A) Memo RNA levels were determined by qPCR and normalized to GAPDH levels. (B) A western analysis for Memo protein was performed (upper panel) and quantified with ImageJ normalizing to actin levels (lower panel). Lysates from MEFs served as a positive control. PCT=Proximal Convolved Tubule; PST= Proximal Straight Tubule; TAL=Thick Ascending Limb of Henle's loop; DCT/CNT=Distal Convolved Tubule/Connecting Tubule; CCD=Cortical Collecting Duct; GLM=Glomerulus.

C) Lysates from Memo null mice or control littermates were prepared 4 weeks after tamoxifen injection and a western analysis for Memo was performed.

## Results

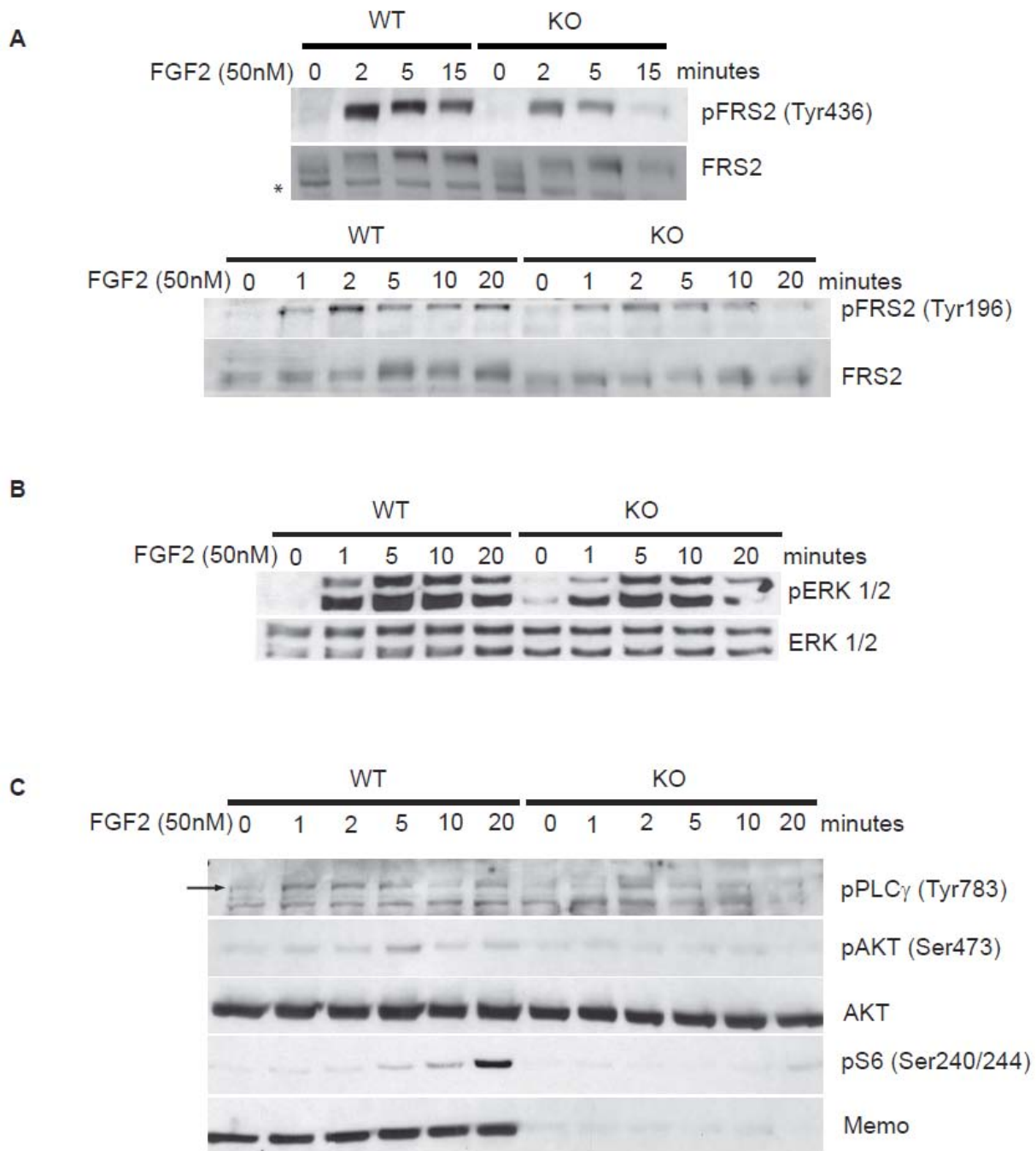


**Figure 4 Analysis of FGFR signaling in WT and Memo KO MEFs**

Cell lysates prepared from serum-starved control and Memo KO MEFs that were treated for the indicated times with FGF2 were analyzed by western for the indicated proteins and P-proteins. (A) FRS2; upper panel pFRS2 (Tyr436); lower panel pFRS2 (Tyr196); \* non-specific band that is not visible on the lower panel due to different running times. (B) ERK 1/2 and pERK1/2. (C) pPLC $\gamma$  (Tyr783); pAKT (Ser473) and AKT; pS6 (Ser240/244) and Memo. The results are

## Results

representative of at least three experiments. See also Figure S2 and S3

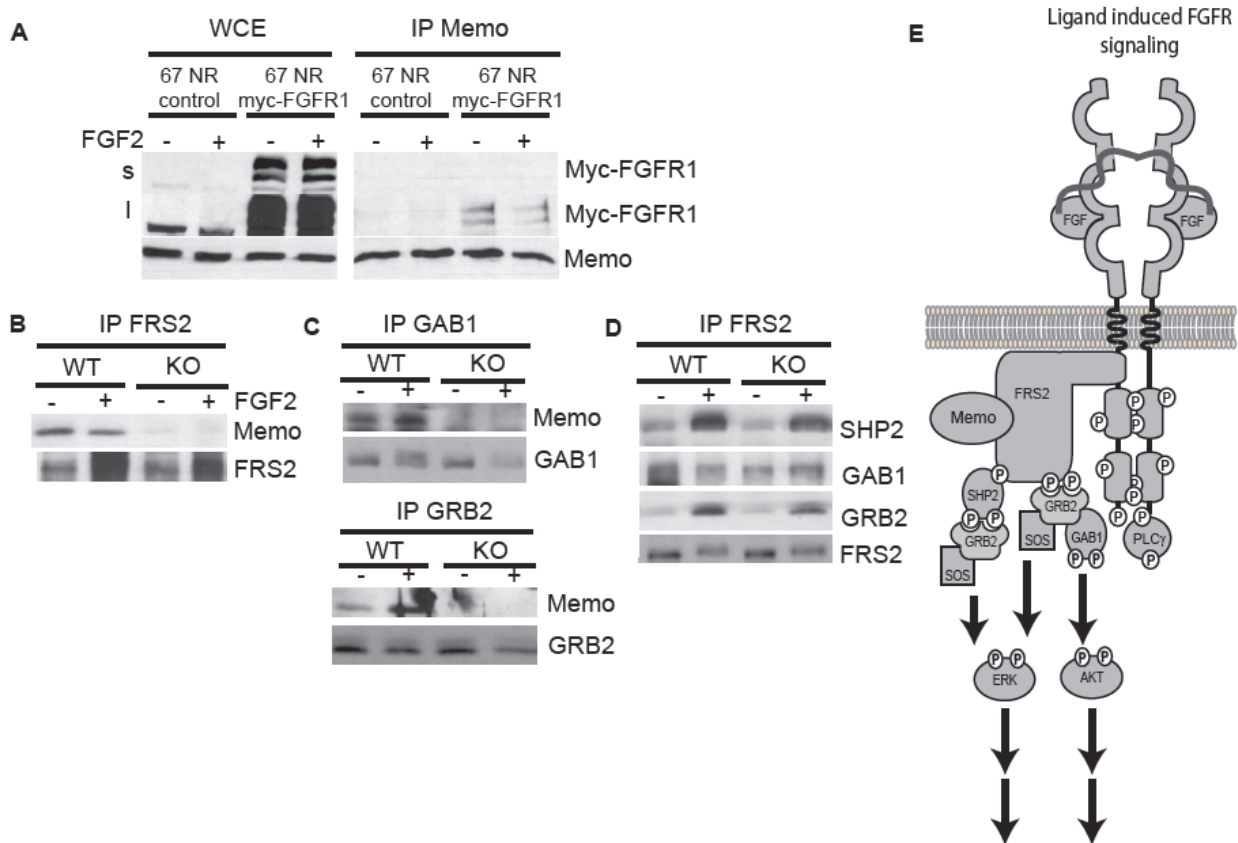


### Figure 5 Identification of Memo containing complexes

(A) Cell extracts were made from 67NR cells, expressing Myc-tagged FGFR1 or a control vector treated for 6 minutes with FGF2 (+) or not treated (-), then subjected to immunoprecipitation with a Memo antiserum. A western analysis was performed with Myc serum to detect complexed Myc-tagged FGFR1 and, as a control, Memo. A western performed with whole cell extracts (WCE) is shown in the left panel. s= short exposure, l= long exposure.

(B-D) Cell lysates were prepared from WT and Memo KO MEFs treated for 6 minutes with FGF2 (+) or not treated (-). (B) Lysates were subjected to immunoprecipitation with an FRS2 antiserum and probed for complexed Memo, and probed with FRS2, as a control. (C) Lysates were subjected to immunoprecipitation with a GAB1 (upper panel) or a GRB2 antiserum (lower panel) and probed for complexed Memo, and probed with GAB1 or GRB2 as controls. (D) Lysates were to immunoprecipitation with an FRS2 antiserum and probed for SHP2, GAB1 and GRB2, and probed with FRS2, as a control.

(E) Scheme of FGF-induced signaling. Upon ligand binding, FGFR and the FRS2 adaptor protein are

## Results

phosphorylated on multiple Tyr residues. PLC $\gamma$ 1 is recruited to the active FGFR. SHP2 and GRB2 are recruited to FRS2 P-Tyr436 and P-Tyr196 residues, respectively, which promotes activation of the ERK and AKT signaling pathways. Memo was found constitutively associated with FRS2 (Panel B). See also Figure S2

**Table 1** Analysis of renal enzymes and cotransporter expression

Litter number	1 <sup>a</sup>	2 <sup>b</sup>	3 <sup>b</sup>	4 <sup>c</sup>
number of control mice	1	1	5	1
number of Memo null mice	4	3	4	2
Cyp27B1	0.44+/-0.2	0.27+/-0.1	1.48+/-0.3	0.53+/-0.3
Cyp24A1	0.62+/-0.1	2.28+/-1.7	0.42+/-0.5	9.3+/-3.2
Na-Pi2a	0.27+/-0.1	0.61+/-0.2	0.67+/-0.2	0.57+/-0.3
Na-Pi2c	0.33+/-0.1	0.64+/-0.2	0.41+/-0.3	0.49+/-0.3

Kidneys were collected and snap frozen from Memo null mice and matched WT control littermates. RNA was prepared and analyzed by quantitative PCR for the level of Cyp27B1, Cyp24A1, Na-Pi2a and Na-Pi2c. Results are relative expression of RNA in kidneys of Memo null mice compared to control littermates. Age when mice were treated with tamoxifen. a-4 weeks; b-2.5 to 3 weeks; c-2 weeks. See also Table S1 and S2

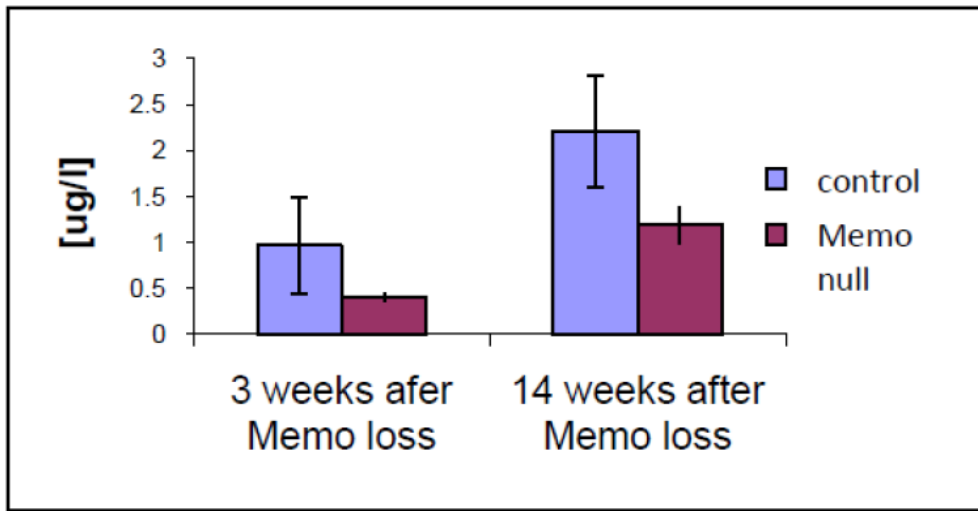
## Results

**Table 2** Analysis of SEF, G6Pc1, and PEPCK in the indicated organs or cells.

Litter/cell line	1 <sup>a</sup>	2 <sup>b</sup>	3 <sup>b</sup>	4 <sup>c</sup>	MEF
nr of control mice	1	1	5	1	
nr of Memo null mice	4	3	4	2	
<b><u>Kidney</u></b>					
SEF	2.74+/-1.7	1.66+/-0.4	1.97+/-1.2	2.07+/-0.7	5.3+/-0.1
<b><u>Liver</u></b>					
G6Pc1	2.86+/-1.5	1.47+/-0.5	3.56+/-1.4	-	-
PEPCK	2.56+/-1.2	2.90+/-1.8	2.04+/-1.4	-	-

Organs were collected and snap frozen from Memo null mice and matched WT control littermates. RNA was prepared from organs or MEFs and analyzed by quantitative PCR for the level of SEF, G6Pase and PEPCK. Results are relative expression of RNA in kidneys or livers of Memo null mice compared to control littermates or of KO MEFs compared to WT MEFs. Age when mice were treated with tamoxifen. a-4 weeks; b-2.5 to 3 weeks; c-2 weeks

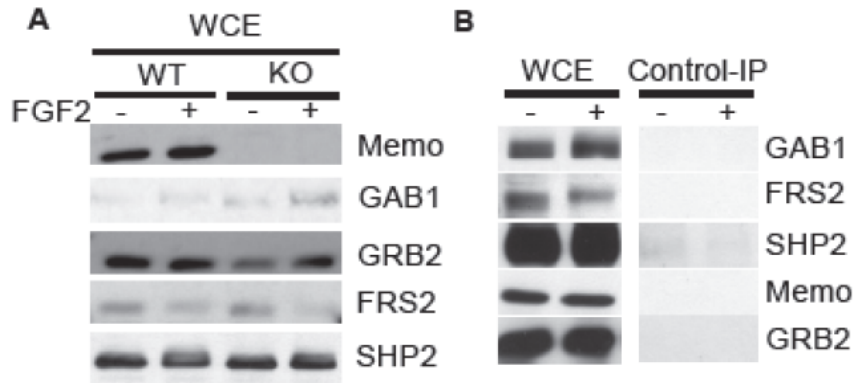
## Results



**Supplementary Figure 1 Measurement of blood insulin levels**

Memo null and control mice were fasted over night and on the following day blood was collected and insulin levels were measured.

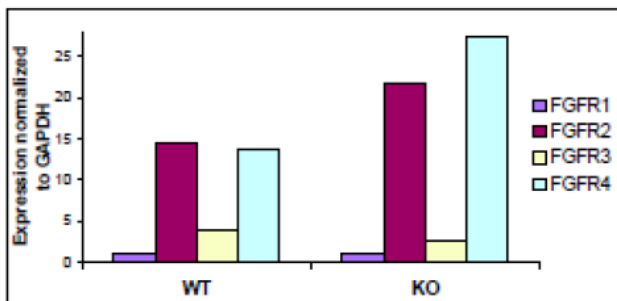
## Results



**Supplementary Figure 2**

(A) WT and KO MEFs were starved for 16 hours then stimulated with 50nM FGF2 for 6 minutes. Lysates were prepared and analyzed for the indicated protein by a western analysis.

(B) To control for specificity of each of the antibodies used for IPs in figure 5, lysates were immunoprecipitated with a control antibody and probed for the indicated proteins by a western analysis.



**Supplementary Figure 3, Expression of FGFRs in WT and KO MEFs**

WT and KO MEFs were grown in DMEM-10% FBS. RNA was extracted from the cells and expression levels of the four FGFRs were measured by quantitative PCR. The expression levels were normalized against GAPDH. Expression of FGFR1 in WT cells was set at 1.



## Results

**Supplementary Table 1**, Expression of FGFR1 and Klotho in the kidney

	<b>Fold increase in Memo null kidneys</b>	<b>Statistical relevance</b>
<b>FGFR1</b>	0.88+/-0.4	ns
<b>Klotho</b>	0.88+/-1.6	ns

Kidneys were collected and snap frozen from Memo null mice (n=10) and matched control littermates (n=6). RNA was prepared and analyzed by quantitative PCR for the level of FGFR1 and Klotho. Results are relative expression of RNA from Memo null mice compared to control littermates. ns = not significant.

## Results

**Supplementary Table 2, Primers and quantitative PCR protocol**

<b>Cyp27B1</b>	5'-GAGGCAGTGAGTCGGTTCTC-3'	5'-ACAAGTGTAGGGTCGGCAAC-3'
<b>Cyp24A1</b>	5'-CCCTTCTGCAAGAAAACCTGC-3'	5'-CTCTTGAGGGCTCTGATTGG-3'
<b>Na-Pi2a</b>	5'-AGTCTCATTTCGGATTTGGTGTCA-3'	5'-GCCGATGGCCTCTACCCT-3'
<b>Na-Pi2c</b>	5'-TAATCTTCGCAGTTCAGGTTGCT-3'	5'-CAGTGGAATTGGCAGTCTCAAG-3'
<b>FGFR1</b>	5'-TTCTGGGCTGTGCTGGTCAC-3'	5'-GCGAACCTTGTAGCCTCCAA-3'
<b>Klotho</b>	5'-ACTCGGCCTCAGATAACCTT-3'	5'-CACCACTGGAGTGATGTTGG-3'
<b>G6Pc1</b>	5'-CTAACTTGGCCATGATGAACC-3'	5'-CTTCACTGAGGTGCCAGGAG-3'
<b>PEPCK</b>	5'-CTAACTTGGCCATGATGAACC-3'	5'-CTTCACTGAGGTGCCAGGAG-3'
<b>SEF</b>	5'-GCCTGACTGGTTTGAGAAGC-3'	5'-CCTCGACTTCCGACAGAAG-3'
<b>GAPDH</b>	5'-TTCATTGACCTCAACTACATG-3'	5'-GTGGCAGTGATGGCATGGAC-3'
<b>MEMO</b>	5'-CTTAGAATTATTCTGCTTCCTG-3'	5'-TTTGAGTGGTAGGTGGAGTCTG-3'
<b>Cre recomb.</b>	5'-TGCACGTTACCGGCATCAACG-3'	5'-TGCACGTTACCGGCATCAACG-3'

All qPCR reactions were performed in duplicates with the following cycling parameters:

50°C 2 min, 95°C 15 min, 40 cycles of 95°C 15 sec, 60°C 20 min, 72°C 1 min.

Genotyping of the Actin CreER<sup>TM</sup> Memo<sup>fl/fl</sup> mice: genomic DNA was extracted by incubation in Chelex 100 Molecular Biology Grade Resin (Bio Rad).

## **7.2 Analysis of Memo in development**

### **7.2.1 Analysis of Memo conventional knock-out animals (Memo KO) (R. Masson and P. Kaeser)**

The main work of this analysis was done by Régis Masson. He did the planning of the experiment and he had the main responsibility. I helped in plugging the animals and isolating the embryos, taking pictures and genotyping them.

A Memo conventional knockout mouse strain was generated to investigate the function of Memo throughout development. Heterozygous knockout animals were viable and fertile, however, following interbreeding no homozygous Memo knockout animals were born. Thus, Memo knockout is embryonic lethal, demonstrating that Memo has an essential but undefined function in mouse embryonic development.

To gain insight into the stage and possible etiology of embryonic lethality, the genotype of embryos derived from heterozygous intercrossing was investigated at various days post coitum. Viable KO embryos on a mixed background were found until E13.5 but showed abdominal bleeding from E11.5. In addition, blood vessels of the yolk sac and placenta were less perfused with blood in the KO animals (unpublished data of Régis Masson and Patrick Kaeser) (Figure 7-1). While more recent data shows that at least some Memo KO embryos on a C57Bl/6 background are viable up to day E17.5 (unpublished data of Shunya Kondo), experiments detailed in my thesis were performed with mice on a mixed background.

## Results

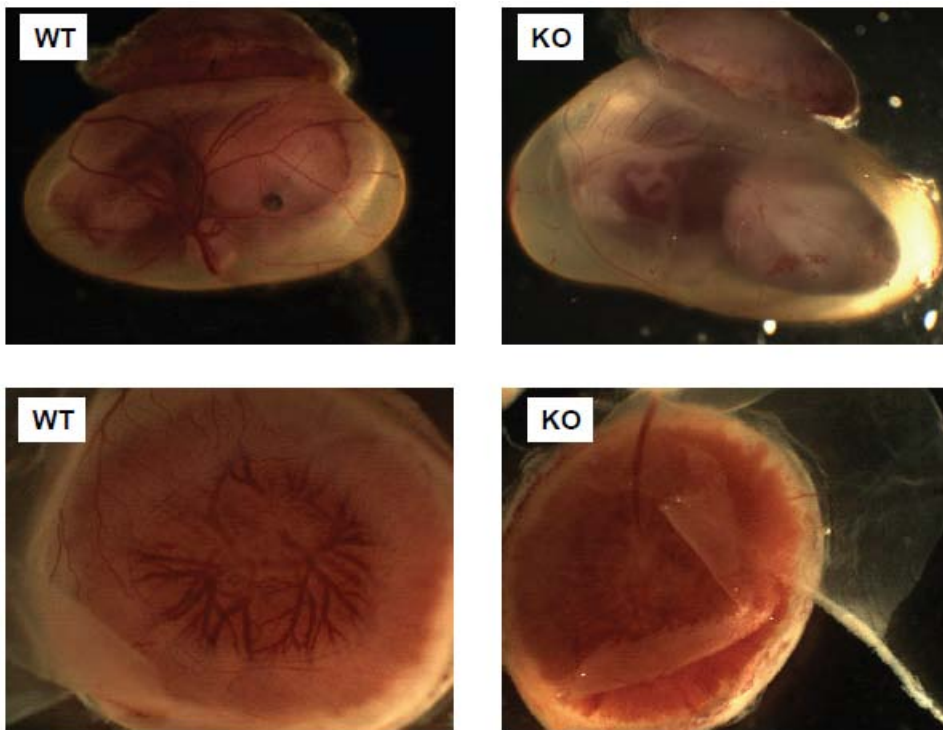


**Figure 7-1 Control and Memo KO embryos at E11.5**

The gross phenotype of resultant embryos from heterozygous Memo KO interbreeding was investigated. Homozygous embryo in the yolk sac (upper) and the separated placenta (lower) are depicted, WT (left) and Memo KO (right). Note poorly perfused yolk sac and placental vasculature and pale appearance of KO embryo.

### **7.2.2 Analysis of Memo conditional knock-out (Memo cKO) mice crossed to Meox2Cre transgene mice (J. Zmajkovic)**

This work was performed by Jakub Zmajkovic under my supervision throughout the study. I taught him how to handle, breed, label and genotype mice. We developed the breeding strategy together and I worked with him throughout his work with mice.

The observed differences in gross vascular appearance in the Memo KO placenta, suggested a role for Memo in placental function. To investigate if this was the origin of the defect in blood supply to the embryo, we tested if expression of Memo in the placenta would rescue the embryonic lethality of Memo KO embryos. Memo conditional knockout animals (Memo cKO) were crossed to Meox2Cre mice, which express Cre recombinase under the control of the mesenchyme homeobox 2 promoter. The promoter activates Cre recombinase specifically in the embryo and in extra-embryonic mesoderm

## Results

derivatives, including the chorionic plate and yolk sac mesoderm, starting at day E5.0 (394), all other regions of the placenta are Cre recombinase negative. Thus in Memo cKO Meox2Cre animals Memo is expressed in the placenta of the embryos, while the embryo does not express the protein. Genotyping the offspring of Memo cKO Meox2Cre interbreeding showed that no Memo cKO Cre positive animals were born, indicating that expression of Memo in the placenta does not rescue the embryonic lethality caused by loss of Memo (unpublished data of Jakub Zmajkovic). Further analysis is needed to investigate if these embryos survive longer than the Memo KO embryos.

### **7.2.3 Analysis of the Memo conditional knock-out (Memo cKO) strain crossed to the pCX-CreER<sup>TM</sup> transgene mice**

Those experiments were done initially together with Régis Masson, but in my second year, I performed and planned all experiments myself.

Next, we asked in which stage of embryonic development Memo function is essential, we designed a mouse model in which deletion of Memo could be temporally controlled. For these experiments the Memo conditional knock-out strain was crossed to a mouse strain harboring the pCX-CreER<sup>TM</sup> transgene (395). This transgene is under the control of the ubiquitously expressed CAGGS promoter, consisting of the CMV early enhancer and the chicken beta-actin promoter. Cre recombinase activity is induced in all cells following tamoxifen injections. To investigate if Memo expression up to E13.5 rescued the observed embryonic lethality, Cre negative Memo cKO females were crossed to Cre positive Memo cKO males and resultant pregnant mice injected with tamoxifen for three consecutive days from E13.5. In treated mice, tamoxifen freely crossed the placenta resulting in loss of Memo in Cre positive embryos. When compared to non-injected mice, tamoxifen treatment resulted in a prolonged gestation of two days. Genotyping of newborn pups revealed that Memo<sup>f/f</sup> (Memo cKO) and Memo null animals were born at the predicted mendelian rate. Nevertheless, the animals that were knock-out for Memo were pale at the time of birth and survived up to one month after birth. The cause of death is thus far unknown and awaits further investigation.

### **7.3 Characterisation of the Memo cKO actin Cre ER<sup>TM</sup> Mice**

The tamoxifen inducible Memo knock-out strain allowed us to induce the deletion of Memo at any given developmental stage. To evaluate the consequence of Memo knock-out in later developmental

## Results

stages, Memo cKO Cre ER<sup>TM</sup> mice at various postnatal ages were treated with tamoxifen for 4 to 5 consecutive days, resulting in knock-out of Memo in all organs (Memo null mice). To control for potential non-specific effects of tamoxifen in these studies, Memo cKO mice that did not express the Cre recombinase (control animals) were treated with tamoxifen. No effect of tamoxifen was observed in these mice. In contrast, following Memo deletion mice developed a severe premature aging phenotype, including well-known aging signs (see chapter 0) and an unusual metabolic phenotype. The time of appearance of the first signs of aging correlated with the age of mice at the time of Memo loss (see also chapter 7.1).

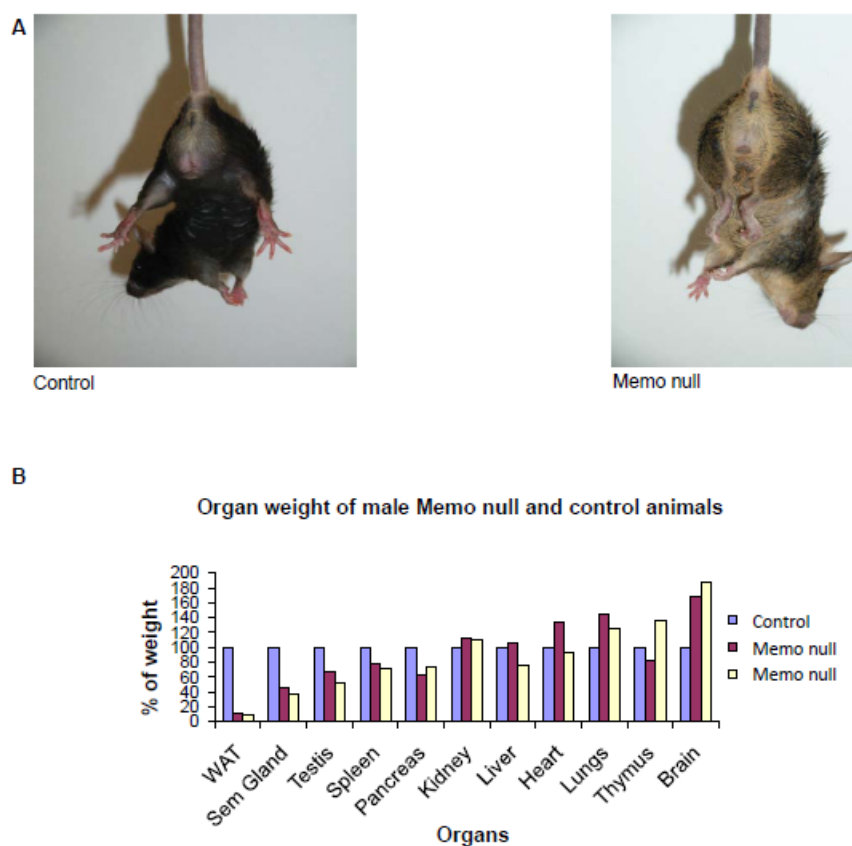


**Figure 7-2 Hindlimb reflex and organ weight of Memo null and control animals**

(A) Pictures of control and Memo null animals held by the tail. On the left the control animal shows a normal hindlimb reflex. On the right the Memo null animal shows an unusual hindlimb reflex. The mice shown on the left and right are littermates.

(B) Organ weights (relative to bodyweight) of one control and two Memo null male animals are depicted. Strong reduction of WAT, seminal glands and testis can be found in the Memo null animals. In contrast, Memo null animals show increased weight of lungs and brains compared to control animals. This is one representative result of many.

## Results

The first signs of premature aging were defects in the hindlimb reflex (Figure 7-2A) and graying of the hair. Later in the course of the study, Memo null mice lost their hair and exhibited severe weight loss and progressively suffered from stiff joints, kyphosis and showed problems with their eyes (see chapter 0). Post mortem weight analysis of different organs demonstrated smaller gonads and severe reduction of the white adipose tissue (WAT) in the Memo null animals compared to control animals, while the lungs and brains were heavier in the Memo null mice (Figure 7-2B). Histological analysis revealed that the skin showed a loss of subcutaneous fat and the epididymis contained no spermatozoa (see Chapter 0), both phenotypes characteristic of aging.

It is known that mouse models that show reduced size of the gonads often display an associated defect in the function of mitochondria (personal communication with A. Trifunovic). Therefore, we investigated the mitochondrial shape, which is predictive for mitochondrial function. We isolated the hearts, an organ with high number of mitochondria, of control and Memo null animals and studied mitochondrial shape by electron microscopy. Organs were fixed, sectioned and investigated with a transmission electron microscopy. Figure 7-3 shows that there is no difference in size or shape of mitochondria in control and Memo null mice.

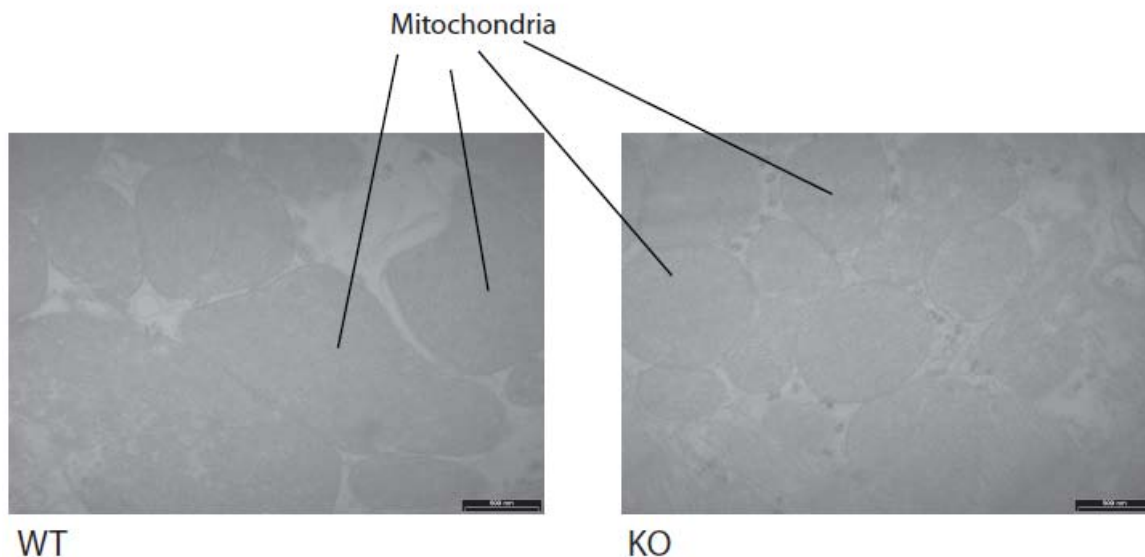


**Figure 7-3 Pictures of mitochondria in the heart of control and Memo null mice**

Representative pictures of mitochondria (from the heart) of control (left) and Memo null (right) mice. Scale bar, 500 nm.

## Results

Since we concentrated in the further experiments on the kidney we performed a Memo staining of the kidney in control and Memo null mice to ensure that there that Memo null mice are knock out for Memo in the kidney. Figure 7-4 (upper panels) shows that Memo is expressed in the kidney. Furthermore, it shows that Memo is more highly expressed in the cortex as compared to the medulla. In the right upper panel we observed that Memo is not highly expressed in the glomeruli as compared to the rest of the cortex. Some cells show a pronounced nuclear staining while other show a more uniform staining of the nucleus and cytoplasm. The lower panel of Figure 7-4 shows a good knock out of Memo in the kidney.

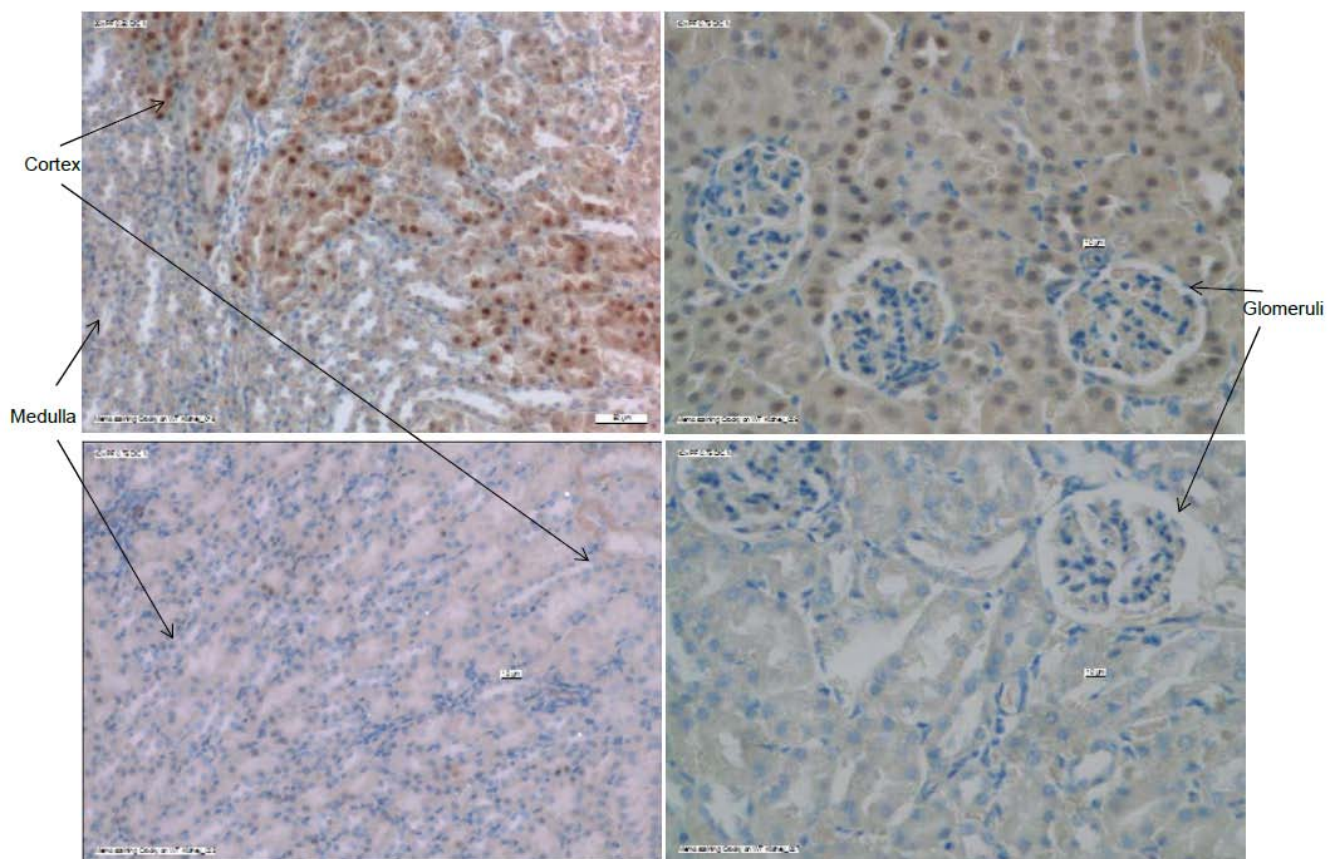


**Figure 7-4 Memo staining of the Kidney**

Staining of formalin fixed and paraffin embedded kidney sections of control (upper panels) and Memo null (lower panels) animals. Scale bar<sub>left panels</sub> 50 $\mu$ M, scale bar<sub>right panels</sub> 10 $\mu$ M

To get an overview over the defects in the Memo null mice we performed microarray on livers and kidneys of Memo null and control cells. For the liver microarray 3 control and 3 Memo null animals



## Results

were included, for the kidney array 4 control and 3 Memo null animals. Organs were collected from the mice, snap frozen and RNA was isolated. Table 7-1 and Table 7-2 show list of genes that are up- or downregulated in the livers or kidneys, respectively, of Memo null mice as compared to control animals. Listed are genes that are changed at least two fold and have a p-value of at least 0.01.

**Table 7-1 List of Genes that are up- or downregulated in the livers of Memo null animals as compared to control animals**

Minimum of two fold change and p-value of 0.01. logFC = logarhythmic fold change; AveExpr = average expression

logFC	AveExpr	P.Value	Accession	Gene_symbol	Description
1.301	4.357	0.00255	---		
1.177	5.862	0.00129	---		
1.055	8.508	0.00379	---		
1.206	5.375	0.00449	---		
1.307	4.357	0.00004	---		
1.062	5.247	0.00279	---		
1.438	5.890	0.00002	---		
1.187	5.873	0.00742	---		
1.146	4.172	0.00007	---		
1.097	4.232	0.00039	---		
1.542	4.678	0.00068	---		
2.914	5.805	0.00429	---		
1.891	4.015	0.00551	---		
1.482	8.224	0.00119	---		
1.410	4.131	0.00279	---		
1.497	5.139	0.00190	---		
1.136	4.483	0.00044	---		
1.045	4.794	0.00215	---		
1.267	4.226	0.00381	---		
1.017	4.333	0.00006	NM_009509	Vil1	villin 1
1.118	6.745	0.00013	NM_145128	Mgat5	mannoside acetylglucosaminyltransferase 5
1.301	7.076	0.00174	NM_145977	Slc45a3	solute carrier family 45, member 3
1.093	4.623	0.00383	NM_001081027	Kcnc2	potassium channel, subfamily T, member 2
1.417	5.072	0.00631	ENSMUST00000111149	EG545391	predicted gene, EG545391
1.277	4.955	0.00929	NM_009061	Rgs2	regulator of G-protein signaling 2
1.362	8.046	0.00003	NM_018881	Fmo2	flavin containing monooxygenase 2
2.546	5.324	0.00008	NM_008030	Fmo3	flavin containing monooxygenase 3
2.391	6.534	0.00003	NM_025557	Pcp4l1	Purkinje cell protein 4-like 1
1.781	7.646	0.00103	NM_013888	Dnajc12	DnaJ (Hsp40) homolog, subfamily C, member 12
1.005	8.594	0.00018	NM_145424	BC089597	cDNA sequence BC089597
2.147	4.537	0.00005	NM_001042580	Cd63	CD63 antigen
1.301	6.088	0.00456	NM_013875	Pde7b	phosphodiesterase 7B
1.053	8.668	0.00831	NM_177388	Slc41a2	solute carrier family 41, member 2
1.448	8.138	0.00108	NM_017372	Lyz2	lysozyme 2
1.040	6.068	0.00036	NM_177708	Rtn4r1	reticulon 4 receptor-like 1
1.098	8.021	0.00013	NM_009657	Aldoc	aldolase C, fructose-bisphosphate
1.015	4.395	0.00906	BC139224	Gm885	gene model 885, (NCBI)
1.124	6.586	0.00559	NM_011943	Map2k6	mitogen-activated protein kinase kinase 6
1.214	9.203	0.00037	NM_009831	Ccng1	cyclin G1
1.367	5.518	0.00512	NM_011579	Tgtp	T-cell specific GTPase
1.165	7.084	0.00591	NM_009853	Cd68	CD68 antigen
1.535	5.618	0.00099	NM_001004148	Slc13a5	solute carrier family 13 (sodium-dependent citrate transporter), member 5
1.128	4.624	0.00033	ENSMUST00000033420	Stxbp4	syntaxin binding protein 4
1.010	5.043	0.00587	NM_008152	Gpr65	G-protein coupled receptor 65
1.714	6.479	0.00493	NR_003633	Meg3	maternally expressed 3
1.581	7.981	0.00035	NM_013562	Iffd1	interferon-related developmental regulator 1
1.094	9.195	0.00143	NM_011175	Lgmn	legumain
1.124	4.588	0.00132	NM_029803	Iff127	interferon, alpha-inducible protein 27
1.180	5.069	0.00116	ENSMUST00000103510	IghmAC38.205.12	Ig mu chain V region AC38 205.12
1.441	4.266	0.00010	BC092065	Igh	immunoglobulin heavy chain complex
1.063	4.918	0.00102	ENSMUST00000103552	LOC435333	similar to monoclonal antibody heavy chain
1.226	5.707	0.00756	NM_178210	Hist1h4j	histone cluster 1, H4j
1.585	4.305	0.00003	NM_145713	Hist1h1d	histone cluster 1, H1d
1.919	7.447	0.00035	NM_015786	Hist1h1c	histone cluster 1, H1c
1.310	6.719	0.00715	NM_010745	Ly86	lymphocyte antigen 86
1.957	6.710	0.00152	NM_152804	Plk2	polo-like kinase 2 (Drosophila)
1.569	5.839	0.00588	NM_020034	Hist1h1b	histone cluster 1, H1b
2.447	8.045	0.00001	NM_175657	Hist1h4m	histone cluster 1, H4m
1.078	6.055	0.00009	NM_175656	Hist1h4i	histone cluster 1, H4i
1.248	5.355	0.00028	NM_175655	Hist1h4f	histone cluster 1, H4f
1.622	8.426	0.00018	NM_178193	Hist1h4b	histone cluster 1, H4b

## Results

1.017	6.756	0.00061	NM_009254	Serpib6a	serine (or cysteine) peptidase inhibitor, clade B, member 6a
2.315	6.202	0.00819	NM_019568	Cxcl14	chemokine (C-X-C motif) ligand 14
1.371	5.779	0.00733	NM_023134	Sftpa1	surfactant associated protein A1
1.274	4.828	0.00059	ENSMUST00000071522	ENSMUSG00000057913	predicted gene, ENSMUSG00000057913
1.186	4.552	0.00008	NM_020275	Tnfrsf10b	tumor necrosis factor receptor superfamily, member 10b
1.028	5.911	0.00001	NM_007904	Ednrb	endothelin receptor type B
1.287	10.676	0.00015	NM_008529	Ly6e	lymphocyte antigen 6 complex, locus E
1.256	6.539	0.00924	NM_153505	Nckap1l	NCK associated protein 1 like
1.257	5.626	0.00225	NM_172514	Tmem71	transmembrane protein 71
1.401	7.569	0.00380	NM_010738	Ly6a	lymphocyte antigen 6 complex, locus A
3.091	7.236	0.00001	NM_007669	Cdkn1a	cyclin-dependent kinase inhibitor 1A (P21)
1.307	7.061	0.00057	NM_013737	Pla2g7	phospholipase A2, group VII (platelet-activating factor acetylhydrolase, plasma)
1.427	6.955	0.00321	NM_018887	Cyp39a1	cytochrome P450, family 39, subfamily a, polypeptide 1
1.013	4.859	0.00153	NM_011560	Tcte3	t-complex-associated testis expressed 3
1.695	5.760	0.00660	L78788	D17H6S56E-5	DNA segment, Chr 17, human D6S56E 5
1.712	6.906	0.00122	NM_181680	Dsg1c	desmoglein 1 gamma
1.726	7.654	0.00025	NM_010079	Dsg1a	desmoglein 1 alpha
1.152	8.053	0.00713	NM_001037859	Csflr	colony stimulating factor 1 receptor
1.298	5.978	0.00080	NM_001048207	Gypc	glycophorin C
1.286	4.416	0.00989	NM_027209	Ms4a6b	membrane-spanning 4-domains, subfamily A, member 6B
1.793	6.193	0.00007	NM_007811	Cyp26a1	cytochrome P450, family 26, subfamily a, polypeptide 1
1.368	4.451	0.00158	BC014805	BC014805	cDNA sequence BC014805
1.526	8.655	0.00100	NM_020283	B3galt1	UDP-Gal:betaGlcNAc beta 1,3-galactosyltransferase, polypeptide 1
1.526	4.908	0.00029	NM_146578	Olfir1033	olfactory receptor 1033
1.959	6.431	0.00177	NM_001011872	Olfir1034	olfactory receptor 1034
1.014	6.108	0.00245	NM_001033293	Uap1l1	UDP-N-acetylglucosamine pyrophosphorylase 1-like 1
1.096	6.222	0.00767	NM_015753	Zeb2	zinc finger E-box binding homeobox 2
1.023	5.993	0.00608	ENSMUST00000049544	2610301F02Rik	RIKEN cDNA 2610301F02 gene
1.098	5.390	0.00787	NM_009851	Cd44	CD44 antigen
1.775	6.969	0.00020	NM_054055	Slc13a3	solute carrier family 13 (sodium-dependent dicarboxylate transporter), member 3
1.054	5.159	0.00064	NM_174995	Mgst2	microsomal glutathione S-transferase 2
1.371	6.147	0.00011	NM_019971	Pdgfc	platelet-derived growth factor, C polypeptide
1.084	8.503	0.00096	NM_011281	Rorc	RAR-related orphan receptor gamma
1.370	8.406	0.00200	NM_021281	Ctss	cathepsin S
1.710	5.126	0.00080	NM_181409	Mtmt11	myotubularin related protein 11
1.038	8.956	0.00072	NM_013549	Hist2h2aa1	histone cluster 2, H2aa1
1.173	6.644	0.00001	NM_178216	Hist2h3c1	histone cluster 2, H3c1
1.584	5.271	0.00004	NM_019976	Psrc1	proline
1.701	4.214	0.00001	ENSMUST00000029642	1700061117Rik	RIKEN cDNA 1700061117 gene
1.048	5.576	0.00366	ENSMUST00000029662	Alpk1	alpha-kinase 1
1.368	5.159	0.00036	NM_009899	Clca1	chloride channel calcium activated 1
1.290	10.066	0.00114	NM_021897	Trp53inp1	transformation related protein 53 inducible nuclear protein 1
1.019	5.764	0.00712	AK006581	4930578G10Rik	RIKEN cDNA 4930578G10 gene
2.519	8.991	0.00180	NM_011016	Orm2	orosomucoid 2
1.046	6.900	0.00069	NM_172520	Arhgef19	Rho guanine nucleotide exchange factor (GEF) 19
1.361	5.571	0.00297	NM_175406	Atp6v0d2	ATPase, H+ transporting, lysosomal V0 subunit D2
1.607	5.749	0.00002	NM_007671	Cdkn2c	cyclin-dependent kinase inhibitor 2C (p18, inhibits CDK4)
1.134	7.919	0.00845	NM_009777	C1qb	complement component 1, q subcomponent, beta polypeptide
1.302	7.866	0.00232	NM_007574	C1qc	complement component 1, q subcomponent, C chain
1.069	8.026	0.00494	NM_007572	C1qa	complement component 1, q subcomponent, alpha polypeptide
1.260	4.745	0.00138	NM_019810	Slc5a1	solute carrier family 5 (sodium)
1.488	4.262	0.00614	NM_152839	Igj	immunoglobulin joining chain
1.001	5.689	0.00845	NM_029509	5830443L24Rik	RIKEN cDNA 5830443L24 gene
1.383	5.100	0.00451	NM_007616	Cav1	caveolin 1, caveolae protein
1.552	4.211	0.00516	ENSMUST00000103302	Igk-V28	immunoglobulin kappa chain variable 28 (V28)
1.175	4.534	0.00817	ENSMUST00000103316	EG434025	predicted gene, EG434025
1.064	6.842	0.00002	NM_028766	Tmem43	transmembrane protein 43
1.935	6.016	0.00011	NM_017379	Tuba8	tubulin, alpha 8
1.337	6.482	0.00371	NM_011909	Usp18	ubiquitin specific peptidase 18
1.648	4.950	0.00325	NM_020001	Clec4n	C-type lectin domain family 4, member n
1.200	4.540	0.00097	ENSMUST00000103328	LOC672291	similar to Ig kappa chain V-V region MOPC 173
1.700	5.101	0.00369	M17720	EG667683	predicted gene, EG667683

## Results

1.069	4.991	0.00464	ENSMUST00000103393	LOC100047162	similar to immunoglobulin kappa-chain
1.181	5.777	0.00013	NM_144943	Cd207	CD207 antigen
1.266	5.770	0.00040	NM_009779	C3ar1	complement component 3a receptor 1
1.018	5.450	0.00723	NM_009201	Slc1a5	solute carrier family 1 (neutral amino acid transporter), member 5
4.597	6.136	0.00000	NM_010000	Cyp2b9	cytochrome P450, family 2, subfamily b, polypeptide 9
1.220	5.381	0.00034	NM_007489	Arntl	aryl hydrocarbon receptor nuclear translocator-like
1.092	6.319	0.00297	NM_008400	Itgal	integrin alpha L
1.570	8.081	0.00076	NM_183257	Hamp2	hepcidin antimicrobial peptide 2
1.004	6.406	0.00077	NM_008594	Mfge8	milk fat globule-EGF factor 8 protein
1.681	4.200	0.00059	ENSMUST0000032877	4632434i11Rik	RIKEN cDNA 4632434i11 gene
1.103	6.145	0.00077	NM_008035	Folr2	folate receptor 2 (fetal)
1.099	7.880	0.00915	NM_007631	Ccnd1	cyclin D1
2.255	6.590	0.00002	NM_008509	Lpl	lipoprotein lipase
1.527	7.517	0.00026	NM_019521	Gas6	growth arrest specific 6
1.189	5.904	0.00504	---	---	---
1.009	6.687	0.00091	NM_031195	Msr1	macrophage scavenger receptor 1
1.040	11.285	0.00115	NM_145594	Fgl1	fibrinogen-like protein 1
1.121	5.916	0.00093	NM_007450	Slc25a4	solute carrier family 25 (mitochondrial carrier, adenine nucleotide translocator), member 4
1.107	4.810	0.00052	NM_144731	Galnt7	UDP-N-acetyl-alpha-D-galactose 4-epimerase
2.661	5.622	0.00128	ENSMUST0000084046	4930467E23Rik	RIKEN cDNA 4930467E23 gene
2.559	4.803	0.00015	ENSMUST0000084046	4930467E23Rik	RIKEN cDNA 4930467E23 gene
1.318	5.500	0.00017	NM_011819	Gdf15	growth differentiation factor 15
1.031	7.917	0.00853	NM_023065	Irf3	interferon gamma inducible protein 30
1.945	6.012	0.00004	BC120812	Cib3	calcium and integrin binding family member 3
1.024	5.146	0.00668	NM_030113	Arhgap10	Rho GTPase activating protein 10
1.127	4.396	0.00526	NM_177350	Gldn	gliomedin
1.308	7.883	0.00046	NM_011254	Rbp1	retinol binding protein 1, cellular
1.205	5.345	0.00053	BC113767	C730027P07Rik	RIKEN cDNA C730027P07 gene
1.416	5.592	0.00030	NM_009917	Ccr5	chemokine (C-C motif) receptor 5
2.670	4.724	0.00000	NM_016886	Gria3	glutamate receptor, ionotropic, AMPA3 (alpha 3)
1.567	5.825	0.00057	XR_031413	EG668271	predicted gene, EG668271
1.603	7.725	0.00386	NM_007807	Cybb	cytochrome b-245, beta polypeptide
1.002	7.584	0.00907	NM_008823	Cfp	complement factor properdin
1.374	5.164	0.00008	NM_023132	Renbp	renin binding protein
1.282	8.482	0.00185	NM_177789	Vsig4	V-set and immunoglobulin domain containing 4
2.392	4.520	0.00021	NM_175540	Eda2r	ectodysplasin A2 isoform receptor
1.178	5.694	0.00086	ENSMUST00000116167	Gm379	gene model 379, (NCBI)
-1.671	4.406	0.00842	---	---	---
-1.029	5.267	0.00544	---	---	---
-1.023	5.211	0.00018	---	---	---
-1.187	4.099	0.00317	---	---	---
-1.521	4.414	0.00025	---	---	---
-1.011	4.294	0.00334	---	---	---
-1.261	4.059	0.00211	---	---	---
-1.085	4.750	0.00037	---	---	---
-1.040	5.607	0.00003	NM_010154	ErbB4	v-erb-b erythroblastic leukemia viral oncogene homolog 4 (avian)
-1.389	6.407	0.00699	NM_009255	Serpine2	serpine (or cysteine) peptidase inhibitor, clade E, member 2
-1.442	4.808	0.00003	NM_053264	4930444G20Rik	RIKEN cDNA 4930444G20 gene
-1.062	4.785	0.00534	NM_146241	Trhde	TRH-degrading enzyme
-2.700	5.136	0.00185	BC086792	Cox7c	cytochrome c oxidase, subunit VIIc
-1.012	7.911	0.00057	NM_145434	Nr1d1	nuclear receptor subfamily 1, group D, member 1
-2.776	8.415	0.00736	NR_002861	Serpina4-ps1	serpine (or cysteine) peptidase inhibitor, clade A, member 4, pseudogene 1
-1.070	7.645	0.00059	ENSMUST0000099550	ENSMUSG0000074917	predicted gene, ENSMUSG0000074917
-1.160	4.398	0.00136	NM_177135	D830030K20Rik	RIKEN cDNA D830030K20 gene
-1.561	7.843	0.00123	NM_026808	1110028A07Rik	RIKEN cDNA 1110028A07 gene
-1.068	7.649	0.00298	NM_007703	Elovl3	elongation of very long chain fatty acids (FEN1)
-1.018	6.493	0.00013	BC034269	BC021614	cDNA sequence BC021614
-1.029	7.289	0.00265	NM_013731	Sgk2	serum
-1.427	6.520	0.00044	NM_027290	Mcm10	minichromosome maintenance deficient 10 (S. cerevisiae)
-1.625	6.763	0.00103	NM_007980	Fabp2	fatty acid binding protein 2, intestinal
-1.048	7.121	0.00111	NM_011797	Car14	carbonic anhydrase 14
-2.120	7.602	0.00731	NM_008295	Hsd3b5	hydroxy-delta-5-steroid dehydrogenase, 3 beta- and steroid delta-isomerase 5
-1.330	7.329	0.00527	NM_027816	Cyp2u1	cytochrome P450, family 2, subfamily u, polypeptide 1
-1.708	9.015	0.00616	NM_001009550	OTTMUSG00000000231	predicted gene, OTTMUSG00000000231
-1.088	7.188	0.00253	NM_019770	Tmed2	transmembrane emp24 domain trafficking protein 2
-1.466	5.745	0.00019	NM_178373	Cidec	cell death-inducing DFFA-like effector c
-1.208	4.230	0.00006	NM_024469	Bhlhb3	basic helix-loop-helix domain containing, class B3
-1.281	7.320	0.00796	XM_001480612	OTTMUSG00000023442	predicted gene, OTTMUSG00000023442
-2.705	6.855	0.00000	NM_178704	Dpy19l3	dpy-19-like 3 (C. elegans)
-1.466	9.892	0.00027	NM_133660	Es22	esterase 22
-1.107	6.344	0.00249	NM_020564	Sult5a1	sulfotransferase family 5A, member 1
-1.247	9.714	0.00004	NM_007468	Apoa4	apolipoprotein A-IV
-1.088	5.891	0.00208	---	---	---
-1.233	6.612	0.00420	NM_001113354	Phf8	PHD finger protein 8

## Results

**Table 7-2 List of Genes that are up- or downregulated in the kidneys of Memo null animals as compared to control animals**

Minimum of two fold change and p-value of 0.01. logFC = logarithmic fold change; AveExpr = average expression

logFC	AveExpr	P.Value	Accession	Gene_symbol	Description
1.01	7.67	2.52E-06	---		
1.25	8.04	1.69E-05	---		
2.36	6.69	1.21E-06	NM_001081456	Plcd4	phospholipase C, delta 4
2.04	7.74	1.57E-05	NM_009255	Serpine2	serine (or cysteine) peptidase inhibitor, clade E, member 2
1.93	10.49	1.25E-06	NM_010145	Ephx1	epoxide hydrolase 1, microsomal
1.23	8.91	7.01E-06	NM_008080	B4galnt1	beta-1,4-N-acetyl-galactosaminyl transferase 1
1.41	7.53	1.14E-05	BC089587	Slc26a10	solute carrier family 26, member 10
1.12	10.81	4.94E-06	---		
1.71	7.47	4.25E-06	NM_008521	Ltc4s	leukotriene C4 synthase
1.06	9.64	1.47E-05	BC025823	Spns2	spinster homolog 2 (Drosophila)
2.74	7.86	1.32E-06	NM_011648	Tshr	thyroid stimulating hormone receptor
2.28	8.65	7.29E-06	---		
1.89	8.07	1.11E-05	ENS MUST00000064162	1700024B05Rik	RIKEN cDNA 1700024B05 gene
1.25	7.67	2.78E-08	NM_020275	Tnfrsf10b	tumor necrosis factor receptor superfamily, member 10b
1.22	6.13	9.10E-06	NM_008555	Masp1	mannan-binding lectin serine peptidase 1
1.53	9.97	6.65E-06	NM_016674	Cldn1	claudin 1
1.19	7.45	1.18E-06	NM_023057	B230120H23Rik	RIKEN cDNA B230120H23 gene
1.95	5.01	7.49E-06	NM_146450	Olf1314	olfactory receptor 1314
2.78	5.23	2.31E-07	NM_146742	Olf1316	olfactory receptor 1316
1.29	9.11	1.21E-05	NM_028072	Sulf2	sulfatase 2
3.36	6.54	3.09E-07	NM_025416	Them5	thioesterase superfamily member 5
2.48	7.50	4.19E-08	NM_019976	Psrc1	proline
1.20	8.54	2.99E-06	NM_009517	Zmat3	zinc finger matrin type 3
1.44	6.43	8.99E-07	NM_198306	Galnt9	UDP-N-acetyl-alpha-D-galactosamine:polypeptide N-acetylgalactosaminyltransferase 9
1.10	9.12	1.29E-06	NM_028766	Tmem43	transmembrane protein 43
1.15	6.84	6.34E-06	NM_198612	Glt8d4	glycosyltransferase 8 domain containing 4
1.42	7.22	6.88E-06	NM_008598	Mgmt	O-6-methylguanine-DNA methyltransferase
1.84	5.16	1.28E-06	ENS MUST00000032877	4632434I11Rik	RIKEN cDNA 4632434I11 gene
1.94	7.84	1.36E-05	ENS MUST00000084046	4930467E23Rik	RIKEN cDNA 4930467E23 gene
1.29	6.77	1.56E-07	XR_031413	EG668271	predicted gene, EG668271
2.52	5.88	8.34E-08	NM_175540	Eda2r	ectodysplasin A2 isoform receptor
-1.51	8.121	1.17E-05	NM_028924	Tc2n	tandem C2 domains, nuclear
-1.44	6.4284	4.96E-08	NM_177016	Slc17a4	solute carrier family 17 (sodium phosphate), member 4
-1.77	6.8074	8.53E-06	NM_146086	Pde6a	phosphodiesterase 6A, cGMP-specific, rod, alpha
-1.59	9.8364	1.40E-05	NM_177450	Cndp1	carnosine dipeptidase 1 (metallopeptidase M20 family)
-1.16	11.428	9.21E-06	NM_053262	Hsd17b11	hydroxysteroid (17-beta) dehydrogenase 11
-2.81	9.3571	1.02E-05	NM_013797	Slco1a1	solute carrier organic anion transporter family, member 1a1

It was not in the scope of this study to follow up on these microarrays and to validate any genes. However, we hope that this data will be useful to us and potentially to others in the future.

Chapter 7.1 demonstrated that the transcriptional levels of enzymes of the FGF23-Klotho axis are affected on loss of Memo. For the Klotho mutant mice it has been shown that not only these enzymes, but also the level of the vitamin D receptor (VDR) were affected (299). Therefore, we investigated the levels of VDR in Memo null mice. Kidneys and livers were collected and snap frozen from Memo null mice and matched control littermates. RNA was prepared and analyzed by quantitative PCR for the level of VDR. Figure 7-5 shows that the level of the VDR is not significantly affected by the postnatal loss of Memo.

## Results

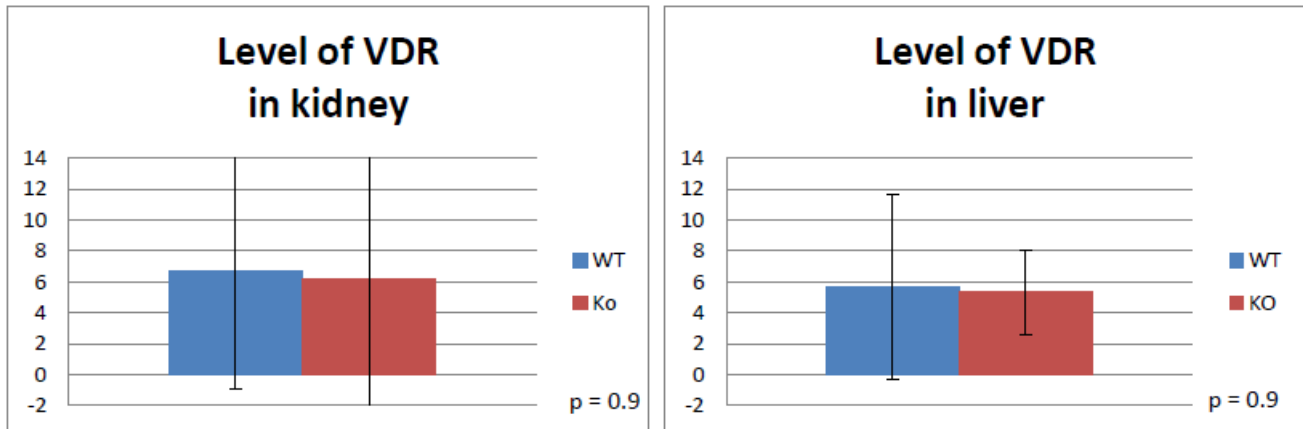


**Figure 7-5 RNA levels of vitamin D receptor (VDR)**  
The values are normalized to GAPDH

To gain further insight into the observed phenotype, blood analysis was performed on Memo null and control male mice that were induced for Memo deletion at the age of 14 weeks. Blood analysis was performed 3 and 14 weeks following tamoxifen treatment weeks (Table 7-3). To investigate the general health of the mice and the function of major organs, we measured total protein level in the serum. In Memo null animals total protein levels were lower, an indication of possible liver or kidney disease. In case of liver or renal insufficiency elevated levels of bilirubin (liver disease) or potassium (kidney disease) would be expected, however the levels of bilirubin and potassium were slightly reduced in Memo null animals. The levels of creatine kinase were also tested, as an indicator of skeletal- and cardio-muscle damage. Memo null mice show decreased levels of creatine kinase, therefore no indication for muscle damage was observed. Increased iron levels were found, which could be indicative of blood haemolysis, however if this were the case a high bilirubin level would also be expected. As the Memo null mice show low bilirubin levels haemolysis can be excluded. To complete the blood analysis glucose, insulin, cholesterol, and triglyceride levels were tested. Levels for glucose and insulin were decreased and levels of cholesterol and triglycerides were increased in Memo null animals when compared to control animals. Interestingly, glucose levels were increased shortly after Memo loss (3 weeks) and subsequently (14 weeks after Memo loss) decreased, while the cholesterol levels were the inverse of this (Table 7-3).

**Table 7-3 Overall blood analysis of Memo null and control animals**

Blood analysis of Glucose, Potassium, Cholesterol, Triglycerides, Iron, Bilirubin, total protein and Creatine Kinase was

## Results

performed with mice that were induced for Memo loss at the age of 14 weeks. The first measurement of blood parameters was performed 3 weeks after Memo loss and the second 14 weeks thereafter. Creatine Kinase was measured only once, 3 weeks after Memo loss. ( $n_{\text{control}}=4$ ,  $n_{\text{Memo null}}=3$ )

	First Measurement		Second Measurement	
	WT	KO	WT	KO
Bilirubin ( $\mu\text{mol/l}$ )	2+/-0.74	1+/-0.06	3.1+/-0.13	2.03+/-0.2
Cholesterol (mmol/l)	3+/-0.35	2+/-0.19	1.89+/-0.03	2.6+/-0.17
Creatine Kinase (U/l)	498+/-95	300+/-48	-	-
Glucose (mmol/l)	11+/-0.44	13+/-0.7	13+/-0.08	9+/-0.8
Insulin ( $\mu\text{g/l}$ )	1.0+/-0.5	0.4+/-0.05	2.2+/-0.61	1.2+/-0.2
Iron ( $\mu\text{g/l}$ )	11+/-1.3	15+/-1	17+/-0.3	19+/-0.81
Triglycerides (mmol/l)	1.77+/-0.24	2.2+/-0.2	1.05+/-0.14	1.46+/-0.09
Potassium (mmol/l)	5.5+/-0.26	5.6+/-0.18	6.7+/-0.45	4.9+/-0.10
Total protein (g/l)	52+/-0.81	49+/-0.51	57+/-0.63	55+/-0.52

We also performed blood analysis to specifically investigate renal function, comparable to how it has been done in the Klotho and FGF23 mutant mice. Blood was collected from Memo null and control animals. This experiment was first done in Dallas, Tx with mice that were induced for Memo loss at about 2.5 weeks of age and blood was collected 8 weeks later. There were 16 WT and 19 Memo null animals analyzed (Table 7-4). Another experiment was performed in Switzerland: loss of Memo was induced at the age of 11 days and blood was collected 20 days later. One WT animal and 5 Memo null animals were analyzed. These samples were measured by the University Hospital in Basel (Table 7-5).

**Table 7-4 Blood analysis of Memo null and control animals performed in Dallas (Memo loss at about 2.5 weeks, sampling 8 weeks later)**

These measurements were performed in Dallas, TX. Therefore, the parameters were measured in mg/dl. The conversion of mg/dl to mmol/l is:  $\text{mmol/l}=(\text{mg/dl})/\sim 3$

## Results

N(WT)=16 N(KO)=19	P (mg/dl)	Ca (mg/dl)	Na (mg/dl)	BUN (mg/dl)
WT	10.56+/-2.1	9.2+/-1	147.25+/-4.1	18.56+/-4.4
KO	10.57+/-2.7	10.19+/-0.82	147.89+/-3.7	27.16+/-10
Fold change	1+/-0.3	1.11+/-0.1	1+/-0.04	1.46+/-0.43
p-value	1	0.003	0.63	0.003

**Table 7-5 Blood analysis of Memo null and control animals (Memo loss at 11 days, sampling 20 days later)**

N(WT)=1 N(KO)=5	P (mmol/l)	Ca (mmol/l)	Na (mmol/l)	Creat ( $\mu$ mol/l)	BUN (mmol/l)
WT	4.01	2.13	139	9	10.4
KO	6.12+/-5.06	2.47+/-0.16	146.40+/- 2.7	11.60+/-3.29	11.40+/-2.48
Fold change	1.53+/-1.26	1.16+/-0.08	1.05+/- 0.02	1.29+/-0.37	1.1+/-0.24

In the Dallas analysis a 1.46+/-0.43 (p-value 0.003) fold increase in blood urea nitrogen (BUN) levels was observed in Memo null animals. BUN is an indicator for renal function and upregulated levels of BUN indicate renal insufficiency. In addition, we also found slight but significant upregulation of Calcium, with a fold increase of 1.11+/-0.1 (p-value 0.003). There was no detectable difference in the serum phosphate levels. In the study performed in Switzerland we measured not only BUN, but also Creatinine, another indicator for renal function. In those mice we observed no change in the levels of both indicators 20 days after induction of Memo loss. Consistent with the Dallas data there was an increase in calcium levels in the KO animals, with a comparable fold increase of 1.16+/-0.1, while phosphate levels were not altered.

In conclusion, blood analysis shows that Memo null mice suffer from renal insufficiency and from a slight hypercalcemia. Surprisingly, we did not find elevated serum phosphate levels. This is in contrast to the findings in Klotho and FGF23 mutant animals.

In addition to the serum phosphate levels, we investigated the expression of the sodium phosphate cotransporters in the brush border membrane of the kidney. Na-Pi2a and Na-Pi2c are cotransporters

## Results

required to reabsorb phosphate from the urine. We isolated the brush border membrane, in which Na-Pi2a is localized, and performed western blot analysis of Na-Pi2a expression (Figure 7-6). We found lower expression of the N-terminal fragment of Na-Pi2a (band at approximately 40kDa in panel A, qualified in B). This indicates that in the absence of Memo enzymatic cleavage of Na-Pi2a is reduced. In one out of 5 KO mice the expression of the full length Na-Pi2a is elevated (Figure 7-6). This is likely related to animal variability and currently we have not considered this in our analysis.

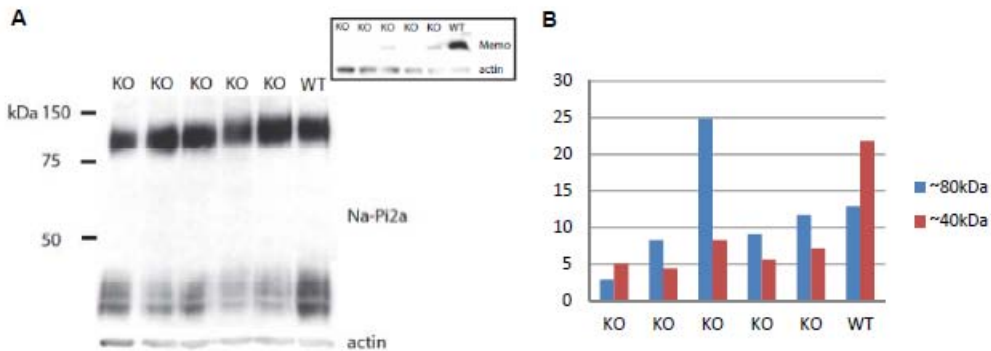


**Figure 7-6 Level of Na-Pi2a in the renal brush border membrane of WT and Memo null mice**

A) Brush border membrane vesicles were isolated from kidneys of WT and Memo null animals and western analysis was performed. The blot was probed with anti Na-Pi2a and actin antibodies. The band at 80-100 kDa in the Na-Pi2a blot represents full length Na-Pi2a and the band at 40 kDa represents the N-terminal fragment of Na-Pi2a. Inset: Whole kidney lysates were prepared from the same WT and Memo null animals and western analysis performed. The blot was probed with anti Memo and anti actin antibodies. B) Quantification of the western blot shown in (A). In blue is the upper (80-100 kDa) and in brown the lower (40 kDa) band of Na-Pi2a, both normalized to actin levels.

In the future, mice will be housed in metabolic cages, to further investigate the renal phenotype. Using these cages we can collect urine samples over a period of 24 hours, allowing us to calculate creatinine excretion rates in order to estimate the volume of serum that is processed by the kidney per minute. This will give us a more detailed picture of kidney function in Memo null and control animals.

### 7.4 Characterization of the inducible kidney-specific Memo knock-out mouse line

Based on the hypothesis that the premature aging phenotype is caused by loss of Memo in the kidney and subsequent dampening of the FGF23-Klotho axis, we generated an inducible, kidney specific, Memo knock-out mouse line.

We crossed the Memo floxed ( $Memo^{fl/fl}$ ) mice with two mouse lines: one expressing the tetracycline-



## Results

sensitive transactivator rtTA, under the control of the Pax8 promoter (the B6.Cg-Tg(Pax8 rtTA2S\*M2)1Koes/J mouse line) (396); and one harboring Cre recombinase under the control of a ubiquitous promoter containing a tetracycline-responsive promoter element (the LC-1 Cre mouse line) (397). Pax8 is only expressed in renal tubular epithelial cells, the same cells that express Klotho. Thus, upon doxycycline treatment the mice specifically lose Memo expression in these cells. Memo floxed animals not simultaneously expressing both the rtTA and the Cre recombinase were used as controls; administration of doxycycline had no detectable effect on these mice.

Pups were exposed to doxycycline starting at E0.5. Only those pups positive for rtTA and Cre recombinase expression lost Memo expression in the kidney upon this treatment. Figure 7-7 shows whole kidney lysates from kidney-specific knock-out (KO) and control (WT) animals. Knock-out animals show no expression of Memo in the kidney.

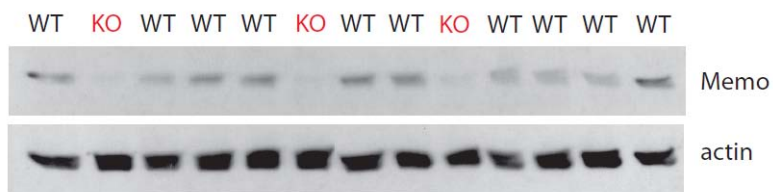


**Figure 7-7 Western analysis of whole kidney lysates from kidney-specific knock-out and control animals**

All doxycycline treated animals were weighed regularly. Although the Memo knock-out animals had lower body weights as compared to the control animals (Figure 7-8), they did not display any overt premature aging symptoms.

## Results

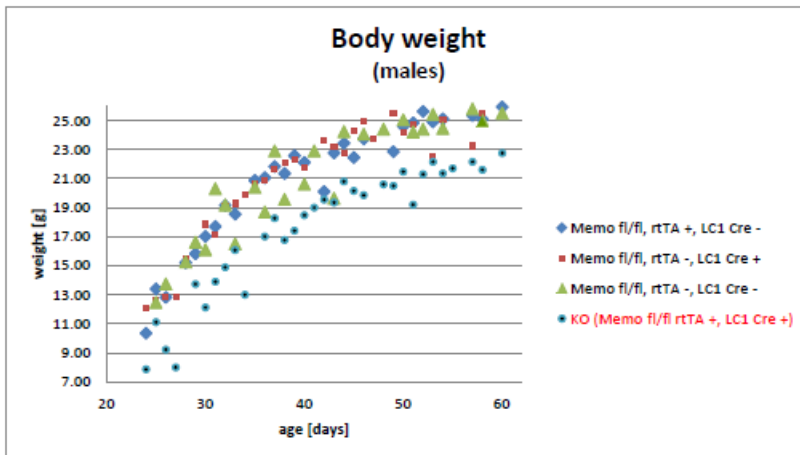


**Figure 7-8 Body weight curve of male animals**

To investigate if the observed lower body weight was due to renal insufficiency, we made use of metabolic cages. Ten control and three knock-out mice were included in this study. All animals were given a three day acclimatization period in the metabolic cages, prior to the onset of sample collections. Measurements were performed over three consecutive days (24 hours each). We measured body weight, food and water intake and fecal and urinary output (Table 7-6). In general, the animals appeared to be in good health over the course of the experimental period, as indicated by the relatively static body weight measurements (WT:  $+0.25\pm 0.35$ ; KO:  $-0.16\pm 0.45$ ). Nevertheless, a tendency of the KO animals to lose some weight can be seen. In addition, the food intake of the KO animals was slightly less when compared to that of the control animals (KO/WT=0.84 $\pm$ 0.1, p-value 0.03). However, as this difference is not significant, we do not believe that food intake alone could be responsible for the body weight differences observed. Furthermore, we measured slightly higher water intake (KO/WT=1.42 $\pm$ 0.6) and larger urinary volumes (KO/WT=1.97 $\pm$ 1.12) from the KO animals. Although the difference in water intake is not statistically significant (p-value 0.14), the larger urinary volume is (p-value 0.01). Therefore, KO animals have a higher urinary output as compared to the control animals.

**Table 7-6 Investigation of the metabolism of kidney-specific KO and control animals in metabolic cages**

Fold change = value (KO) / value (WT)

## Results

N(WT)=10 N(KO)=3	Δ Body weight (g/24h)	Food intake (g/24h)	Feces (g/24h)	Water intake (g/24h)	Urine (g/24h)
WT	0.25+/-0.35	3.64+/-0.34	1.6+/-0.2	7.06+/-3.06	1.75+/-0.67
KO	-0.16+/-0.45	3.1+/-0.19	1.35+/-0.07	10+/-0.78	3.45+/-1.47
Fold change	-0.63+/-2	0.84+/-0.1	0.84+/-0.11	1.42+/-0.6	1.97+/-1.12
p-value	0.12	0.03	0.06	0.14	0.01

At the end of the experiment all animals were sacrificed and the blood, urine and kidneys were collected for analysis. Blood analysis was performed by the University hospital in Basel and urine analysis by the University hospital in Lausanne (CHUV). Blood analysis showed upregulation of BUN (1.6+/-0.6, p-value 0.004) and creatinine (1.8+/-0.8; p-value 0.07) in the KO animals (Table 7-7). In addition we examined the creatinine excretion rate, which gives an indication of proper kidney functioning as it represents how much serum is processed by the kidney per minute. KO mice showed a reduced clearance of creatinine (0.55+/-0.2; p-value 0.01).

**Table 7-7 Blood analysis of kidney-specific Memo knock-out and control animals**

Blood was collected and analyzed for the different parameters. Fold change = value (KO) / value (WT)

N(WT)=10 N(KO)=3	P (mmol/l)	Ca (mmol/l)	Na (mmol/l)	Albumin (g/l)	BUN (mmol/l)	Creatinine (mmol/l)	Creatinine Clearance
WT	3.08+/-0.4	2.2+/-0.07	146+/- 1.34	14.46+/- 0.93	9.24+/-0.9	0.013+/- 0.003	182.06+/- 42.48
KO	3.29+/-0.28	2.36+/-0.09	145.67+/- 3.51	14.5+/- 0.52	15+/-4.94	0.022+/- 0.008	101+/-32
Fold change	1.07+/-0.8	1.11+/-0.05	1+/-0.03	1+/-0.07	1.62+/-0.6	1.78+/-0.78	0.55+/-0.2
p-value	0.42	0.007	0.43	0.94	0.004	0.07	0.012

Furthermore, we investigated phosphate and calcium levels in the serum and urine. In contrast to the Klotho and FGF23 mutant mice, but consistent with the Memo null mice, the kidney-specific Memo knock-out mice did not show altered phosphate levels (1.07+/-0.8) (Table 7-7). The slight increase in calcium levels in the kidney-specific Memo KO animals as compared to controls (1.11+/-0.05, p-value 0.007) is also in agreement with the results obtained with the Memo null mice. The levels of sodium (Na) and albumin remained unchanged (1+/-0.03 and 1+/-0.07).

In summary, these data show that knock-out of Memo in the kidney is enough to induce severe kidney insufficiency. We did not find elevated serum phosphate levels. This is surprising since this is believed to be the main cause for the aging phenotype in Klotho and FGF23 mutant animals. In line with the

## Results

data from the Memo null animals, we found slight hypercalcemia in the kidney-specific Memo KO animals.

In addition to the serum levels of phosphate we also investigated the localization of Na-Pi2a in the brush border membrane (Figure 7-9). Comparable with the results obtained from the Memo null animals, we observed a decrease in the expression of the N-terminal fragment of Na-Pi2a (represented by the band around 40kDa) in two out of three kidney-specific Memo KO animals. This suggests that deletion of Memo in the kidney prevents enzymatic cleavage of Na-Pi2a.

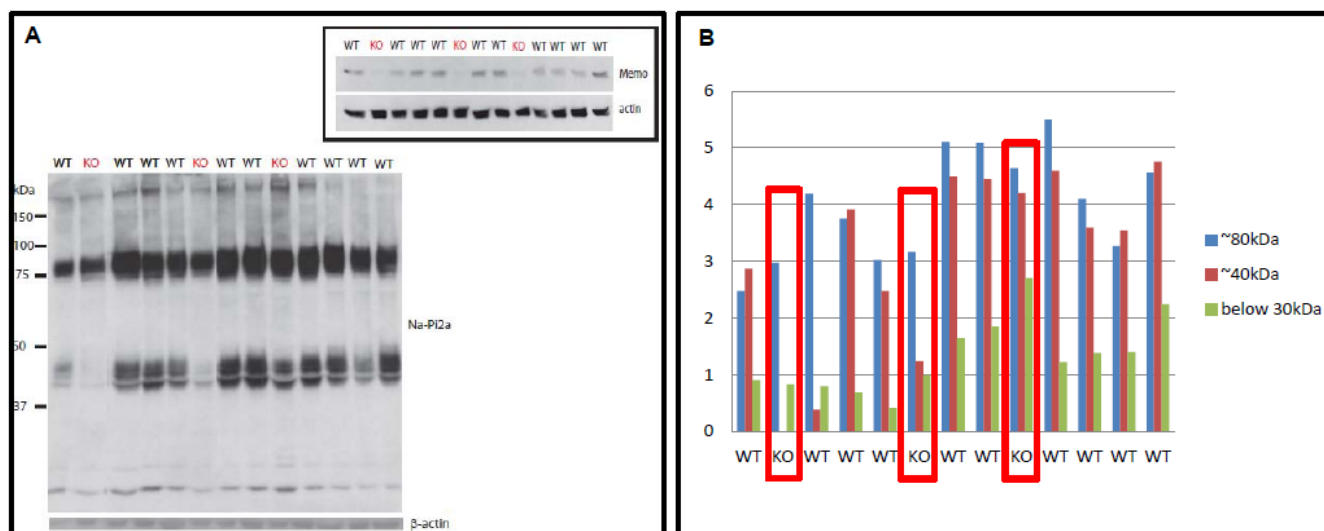


**Figure 7-9 Level of Na-Pi2a in the renal brush border membrane of WT and kidney-specific KO mice**

A) Brush border membrane vesicles were isolated from kidneys of WT and KO animals and western analysis performed. The blot was probed with anti Na-Pi2a and actin antibodies. The band at 80kDa in the Na-Pi2a blot represents full length Na-Pi2a, while the bands between 25 and 40kDa represent N-terminal fragments of Na-Pi2a. Inset: Whole kidney lysates were prepared from the same WT and KO animals and western analysis performed. The blot was probed with anti Memo and anti actin antibodies. B) Quantification of the western blot shown in (A). The values are normalized to actin levels.

Despite the lack of change in the serum phosphate levels, these data further suggested that a defect in phosphate reabsorption exists. We then analyzed the urine and blood samples collected from the animals that were housed in the metabolic cages and calculated the fractional excretion and excretion rates. Figure 7-10 shows that neither the fractional excretion ( $1.5 \pm 1$ , p-value 0.24) nor the excretion rate ( $0.91 \pm 0.28$ , p-value 0.63) of phosphate are different between KO and control animals. We do see slight differences in the fractional excretion rates of sodium ( $1.86 \pm 1.05$ , p-value 0.02) and potassium ( $1.45 \pm 0.58$ , p-value 0.04) which are approaching significance, but more importantly, we observe a highly significant increase in both the fractional excretion and excretion rate of Calcium ( $7.37 \pm 6.16$ ,

## Results

p-value 0.001 and  $4 \pm 2.9$  p-value 0.001, respectively). This indicates that the kidney-specific Memo KO mice are hypercalciuric.

### A Fractional excretion

N(WT)=10 N(KO)=3	P	Ca	Na	K
WT	5.27 $\pm$ 3.2	0.39 $\pm$ 0.16	0.25 $\pm$ 0.06	11.43 $\pm$ 2.54
KO	7.99 $\pm$ 3.5	2.88 $\pm$ 2.1	0.47 $\pm$ 0.24	16.57 $\pm$ 5.46
Fold change	1.5 $\pm$ 1	7.37 $\pm$ 6.16	1.86 $\pm$ 1.05	1.45 $\pm$ 0.58
p-value	0.24	0.001	0.02	0.04

### B Excretion rate

N(WT)=10 N(KO)=3	P	Ca	Na	K
WT	25.97 $\pm$ 7.1	3 $\pm$ 1.7	61.13 $\pm$ 19	123.6 $\pm$ 24
KO	23.82 $\pm$ 3.4	0.75 $\pm$ 0.3	67.43 $\pm$ 20	143.7 $\pm$ 31
Fold change	0.91 $\pm$ 0.28	4 $\pm$ 2.9	0.9 $\pm$ 0.4	0.9 $\pm$ 0.2
p-value	0.63	0.001	0.64	0.3

**Figure 7-10 Fractional excretion and Excretion rate**

A) Fractional excretion in percentage. B) Excretion rate in  $\mu\text{mol}/24\text{h}$

Fractional excretion of x =  $(U_x \cdot U_{Cr} \cdot 100) / (P_x \cdot U_{Cr})$ ; U = concentration in urine, P = concentration in plasma, Cr = creatinine, if x= calcium, then  $P_x = P_{Ca} / 2$  as only half of the calcium is free in the blood.

Excretion rate of x =  $U_x / \text{Volume of urine}$

## 7.5 Characterization of the defect in calcium homeostasis in Memo null and kidney-specific Memo KO animals

To further investigate calcium homeostasis we evaluated the mRNA levels of important calcium regulators in the kidney. QPCR was carried out on RNA isolated from kidneys. We investigated the levels of 'plasma membrane resident transient receptor potential vanilloid 5' (TRPV5), sodium calcium exchanger (NCX1), plasma membrane  $\text{Ca}^{2+}$  ATPase (PMCA) and calbindin (CB28) transcripts. QPCR analysis revealed that none of those targets are significantly altered in Memo null mice (Table 7-8). Thus far, we investigated only three KO animals and 10 control animals. By increasing the number of animals the

## Results

upregulation for TRPV5, NCX1 and CB28 might become significant, while TMCA is definitely not different in Memo null mice as compared to control animals.

**Table 7-8 mRNA levels of TRPV5, NCX1, PMCA and CB28 in Memo null and control mice**

Fold change = expression of KO / expression of control

N(control)=2 N(KO)=5	TRPV5	NCX1	PMCA	CB28
control	1.31+/-0.17	0.59+/-0.26	1.09+/-0.29	0.64+/-0.09
KO	2.59+/-0.87	1.01+/-0.36	1.09+/-0.12	1.61+/-0.71
Fold change	2+/-0.71	1.71+/-0.96	1+/-0.29	2.5+/-0.12
p-value	0.12	0.2	1	0.13

Analysis of RNA isolated from kidney-specific Memo KO animals revealed higher expression of TRPV5, NCX1 and CB28 (Table 7-9). NCX1 (1.96+/-0.97, p-value 0.02) and CB28 (2.24+/-1.07, p-value 0.006) are approximately two fold increased while TRPV5 is three fold increased (3.42+/-2.02, p-value 0.003). This indicates that alterations in expression of calcium regulators in the kidney induce the observed hypercalciuria in kidney-specific Memo KO animals.

**Table 7-9 mRNA levels TRPV5, NCX1, PMCA and CB28 in kidney-specific Memo KO and control cells**

Fold change = expression of KO / expression of control

N(control)=6 N(KO)=3	TRPV5	NCX1	PMCA	CB28
control	1.35+/-0.65	0.98+/-0.41	1.09+/-0.27	1.04+/-0.43
KO	4.63+/-1.62	1.91+/-0.49	1.28+/-0.09	2.32+/-0.55
Fold change	3.42+/-2.02	1.96+/-0.97	1.17+/-0.31	2.24+/-1.07
p-value	0.003	0.02	0.3	0.006

It has been reported that Klotho and FGF23 mutant mice have hypercalcemia and show ectopic calcification in the lungs (bronchi) and heart (255). Therefore, we investigated whether calcification of soft tissues was present in the Memo null mice. We treated paraffin sections of heart isolated from Memo null mice with von Kossa stain for calcium, and found restricted calcium deposition in the heart of Memo null mice (Figure 7-11). Although promising, this initial finding requires further investigation.

## Results

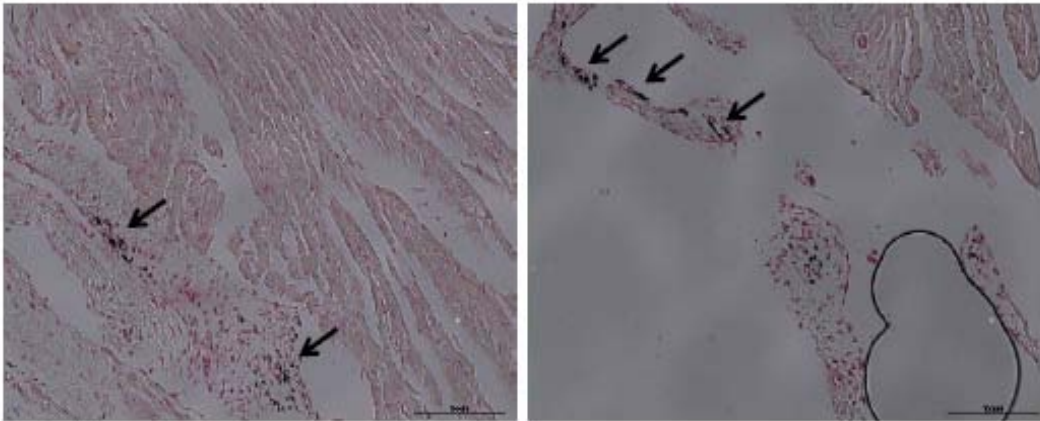


### Figure 7-11 Von Kossa staining on the heart of Memo null mice

Von Kossa staining has been performed on sections of the heart of Memo null mice. These are representative pictures of two different knock out males. Positive von Kossa staining is indicated by arrows. Scale bar 100  $\mu$ m.

Taking all the data into consideration, our results suggest that deletion of Memo, from the whole body or from the kidney alone, induces renal insufficiency and a defect in the cleavage of Na-Pi2a in the brush border membrane. Despite this, KO animals from both models exhibit normal serum phosphate levels. Surprisingly, we found slight but significant hypercalcemia and robust hypercalciuria in the kidney-specific KO animals as compared to the control animals. Supporting these data is the fact that we found upregulated levels of important calcium regulating proteins in the kidney of kidney-specific Memo KO animals.

Thus far, we didn't detect a major changed that occurred only in Memo null animals and not in kidney-specific Memo KO mice and therefore, could be a possible inducer of the premature aging phenotype that we observe exclusively in Memo null mice. Next, we investigated the serum level of parathyroid hormone (PTH) and FGF23. We performed ELISA with serum collected from Memo KO mice and control animals.

### PTH ELISA:

We measured serum of 9 Memo null and 6 control mice as well as of 6 kidney-specific Memo KO and 12 control animals. This revealed a significant downregulation of PTH in Memo null mice ( $0.09 \pm 2.2$ , p-value 0.01) (Table 7-10 on the left). We detected a tendency but no significant decrease of PTH in kidney-specific Memo KO animals ( $0.13 \pm 0.35$ , p-value 0.29) as compared to control animals (Table 7-10 on the right).

## Results

**Table 7-10 Levels of PTH in Memo null (left) and kidney-specific Memo KO animals (right) compared to control mice**

Fold change = Level(KO)/Level(control)

N(control)=6 N(KO)=9	PTH (pg/ml)	N(control)=12 N(KO)=6	PTH (pg/ml)
control	129.9+/-121	control	320+/-611
KO	12+/-26	KO	41+/-81
Fold change	0.09+/-2.2	Fold change	0.13+/-0.35
p-value	0.01	p-value	0.29

### FGF23 ELISA:

We measured serum of 11 Memo null and 4 control mice as well as of 6 kidney-specific Memo KO and 12 control animals. There was no difference in Memo null (5.95+/-12.6, p-value 0.35) or in kidney-specific Memo KO animals (2.71+/-6.6, p-value 0.18) as compared to control animals (Table 7-11 left respectively right).

**Table 7-11 Levels of FGF23 in Memo null (left) and kidney-specific Memo KO animals (right) compared to control mice**

Fold change = Level(KO)/Level(control)

N(control)=4 N(KO)=11	FGF23 (pg/ml)	N(control)=12 N(KO)=6	FGF23 (pg/ml)
control	681.9+/-863.4	control	475+/-1029
KO	4056.9+/-6912	KO	1288+/-1401
Fold change	5.95+/-12.6	Fold change	2.71+/-6.6
p-value	0.35	p-value	0.18

This data shows the first difference between the two Memo KO models; only Memo null animals show a significant decrease in PTH levels.

## 7.6 Memo is a novel downstream effector of the FGFR pathway

Our *in vivo* data indicated that Memo could have a function in the kidney downstream of the FGF23-Klotho pathway. We were interested if there was also evidence for a role of Memo downstream of FGFR signaling *in vitro*. Thus, we investigated the role of Memo downstream of general FGF signaling in mouse embryonic fibroblasts (MEFs) and in the 67NR mouse mammary carcinoma cells (chapter 7.1). We were also interested in the role of Memo downstream of FGFR signaling stimulated by endocrine FGFs. Klotho expression is spatially restricted and expression is required for cells to be



## Results

responsive to FGF23. Therefore, we investigated signaling stimulated by either FGF23 or FGF19 and 21 in HEK293 cells, which were stably transfected with flag-Klotho (HEK293-kl) and flag- $\beta$ Klotho (HEK293- $\beta$ kl) respectively.

### 7.6.1 Signaling in the HEK293-kl cells

Work of chapter 5.4.1 to 5.4.4 was performed in the laboratory of Dr. Makoto Kuro-o at the University of Southwestern Medical School, Dallas, Texas.

Memo was down regulated by siRNA in HEK293-kl cells that were starved overnight and stimulated with FGF23. Control transfection was performed with a scrambled siRNA. Lysates were prepared from cells that were stimulated with FGF23 for the indicated times and analyzed by western. As a readout for the FGF23-Klotho-FGFR1 pathway activity, phosphorylation levels of ERK1/2 and FRS2 were analyzed. As a control for transfection efficiency, levels of flag-Klotho were analysed with an anti Flag-antibody. Flag-Klotho expression was high and equal in control and Memo down regulated cells. As HEK293 cells expressed low levels of the FRS2 protein, the detection of its phosphorylation was challenging, nonetheless the signal detected with the anti-phospho FRS2 antibody suggested that there is less active FRS2 in Memo down regulated HEK293-kl cells stimulated with FGF23 compared to control transfected cells (Figure 7-12A). Because of the poor quality of the FRS2 western blots we concentrated on the activation levels of ERK, which is downstream of FRS2. Western blot analyzes showed that ERK is activated earlier in the Memo down regulated HEK293-kl cells compared to control cells.

## Results

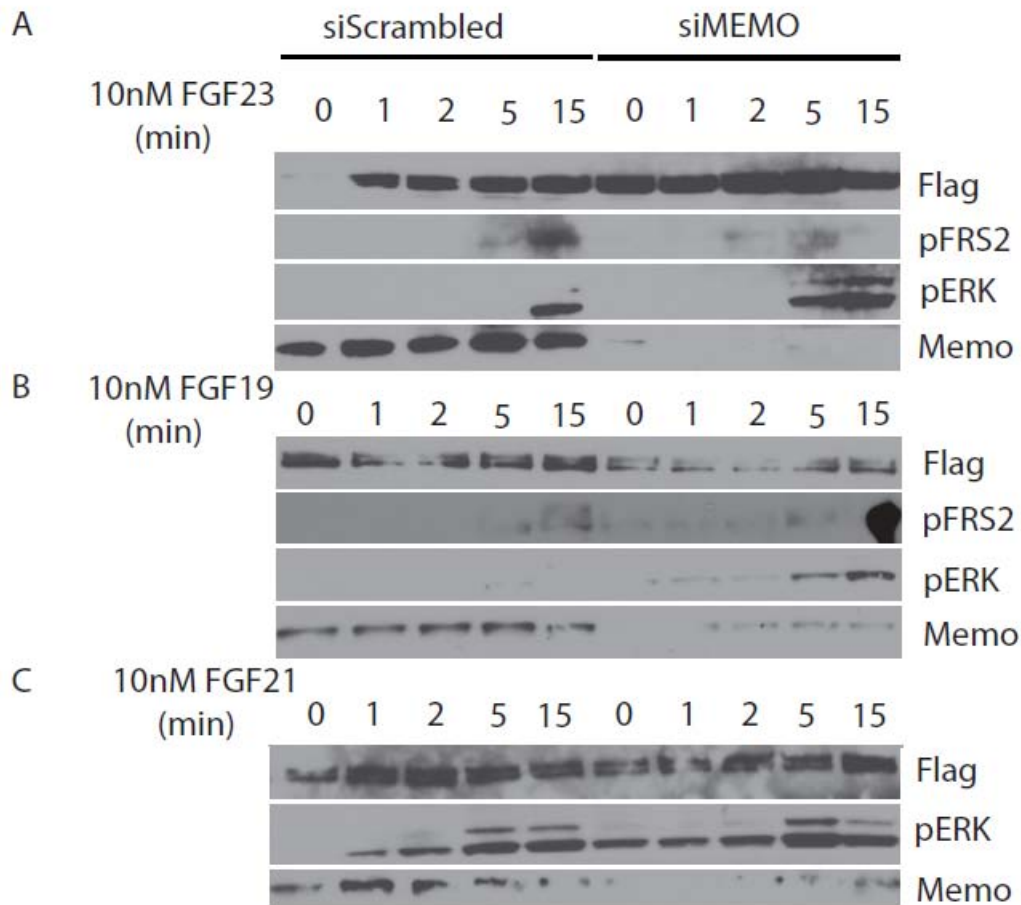


**Figure 7-12 FGFR pathway stimulation by FGF23, FGF19 and FGF21**

Cell lysates were prepared from HEK293 cells that were stably transfected with flagged-Klotho (A) or flagged-βKlotho (B and C), down regulated for Memo (control siRNA treatment with scrambled siRNA), starved over night and stimulated with FGF23 (A), FGF19 (B) or FGF21 (C). The lysates were analysed by western and probed for Flag protein as Klotho/βKlotho transfection control, Memo as siRNA down regulation control and FRS2 (only in A) and ERK as readout for FGFR pathway activity.

### 7.6.2 Signaling in the HEK293-βkl cells

Next we investigated the signaling downstream of the other two endocrine FGFs. For those experiments we used HEK293 cells that were stably transfected with flagged-βKlotho and therefore responsive to FGF19 and FGF21 (HEK293-βkl). Memo was down regulated by siRNA before the cells were starved overnight and stimulated with FGF19 or FGF21. Control transfection was performed with a scrambled siRNA. Lysates were prepared from cells that had been stimulated with FGF19 or FGF21

## Results

for the indicated times and analyzed by western. As a readout for activity of the FGF19 or 21 stimulated  $\beta$ Klotho-FGFR1-pathway the phosphorylation level of ERK1/2 was analyzed. As a control for transfection efficiency the membranes were blotted with an anti-Flag antibody. Flag expression was high and equal in control and Memo down regulated cells. Comparable to FGF23 stimulated cells there was earlier activation of ERK in the Memo down regulated cells stimulated with FGF19 (Figure 7-12B). In contrast, when the cells were stimulated with FGF21 there was no difference in ERK activation between control and down regulated cells (Figure 7-12C).

Collectively, these data suggest that Memo plays a role downstream of FGF23 and FGF19 signaling.

### **7.6.3 Investigation of complex formation of Memo, Klotho and FGFR1**

As there were changes in signaling downstream of FGF23 and FGF19 upon Memo down regulation we investigated if Memo co-precipitates with Klotho and/or FGFR1 in HEK293-kl cells. HEK293-kl cells were down regulated for Memo by siRNA or control transfected with a scrambled siRNA, cells were starved overnight and subsequently stimulated with FGF23. Lysates were prepared and subjected to immunoprecipitation (IP) with FGFR1 and probed for Memo and Klotho (Figure 7-13A), whole cell extract (WCE) is displayed as input-control of the IPs. Klotho could be detected in the precipitates of FGFR1 in control and Memo down regulated cells, irrespective of stimulation with FGF23. In contrast, detection of Memo in the FGFR1 precipitates was not possible. Next, we investigated lysates that were subjected to IP with Klotho and probed with an anti-Memo and anti-FRS2 antibody. While it was possible to detect FRS2 in the precipitates of Klotho, we were unable to detect Memo (Figure 7-13B).

## Results

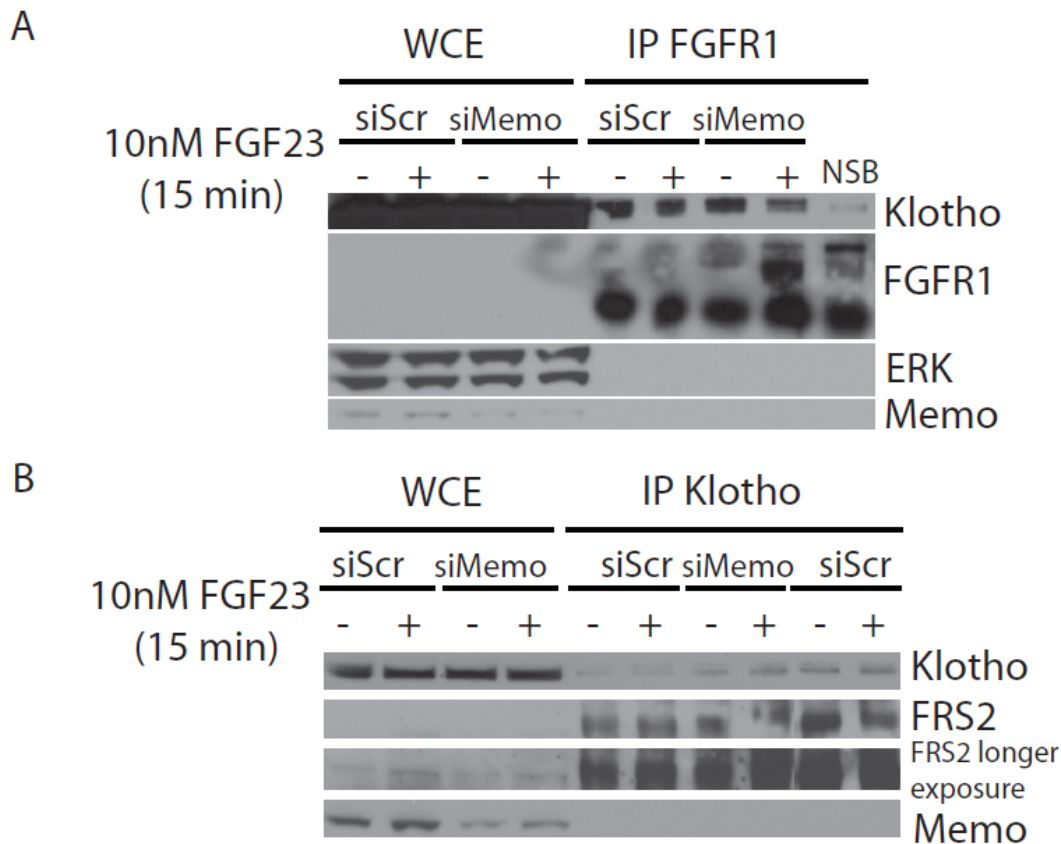


**Figure 7-13 IP of FGFR1 and Klotho in HEK293-kl cells**

HEK293-kl cells were treated with siMemo or siScrambled, starved over night and stimulated with FGF23. Whole cell extract (WCE) or immunoprecipitations of FGFR1 (A) or Klotho (B) were run on a SDS page and immunoblotted. The protein levels of Klotho, FGFR1 and FRS2 were analysed. ERK and Memo protein levels were analysed as loading- and down regulation-controls respectively.

In summary, these data suggest that FGFR1 and Klotho co-precipitate irrespective of Memo expression and FGF23 stimulation. So far it was not possible to show that Memo co-precipitates with FGFR1 or Klotho in these cells.

### 7.6.4 Inhibitory effect of secreted Klotho

It has been published that Klotho has an inhibitory effect on insulin and IGF-1 signaling in cancer cells (347, 350). We were interested if Klotho also has an inhibitory effect on insulin/IGF-1 signaling in mouse embryonic fibroblasts (MEFs) and if so, whether this effect is dependent on Memo expression.

Firstly, we investigated if the MEFs were responsive to insulin and IGF-1. MEFs were isolated from

## Results

Memo cKO embryos and immortalized. Under cell culture conditions Memo expression was lost spontaneously from MEFs. As a control we used unrelated WT MEFs. Memo WT and KO cells were starved over night and stimulated with insulin or IGF-1 for the indicated times. Lysates were prepared and analyzed by western blot analysis. Activation of AKT and ERK downstream of both ligands showed that the MEFs are responsive to insulin and IGF-1 irrespective of Memo expression (Figure 7-14). Due to the fact that there was a difference in the level of total protein content of ERK and AKT between WT and KO cells, quantification by ImageJ was performed. When normalized to total protein levels, the phosphorylation levels show that there is a difference in ERK and AKT activation in WT and KO MEFs stimulated by insulin and IGF-1 (Figure 7-14B). Insulin stimulation induced earlier activation of ERK and AKT in Memo KO cells (activation after 1 minute of stimulation) compared to WT cells (activation after 5 minutes) (lanes 8 and 14). The same was true for IGF-1 stimulation. IGF-1 induced earlier activation of ERK and AKT in the Memo KO cells (activation after 5 minutes) compared to WT cells (activation after 10 minutes) (lanes 4 and 11). The earlier activation of ERK is consistent with the findings in the HEK293-kl cells stimulated with FGF23. In contrast, the earlier activation of AKT is only seen in the MEFs upon insulin and IGF-1 stimulation.

## Results

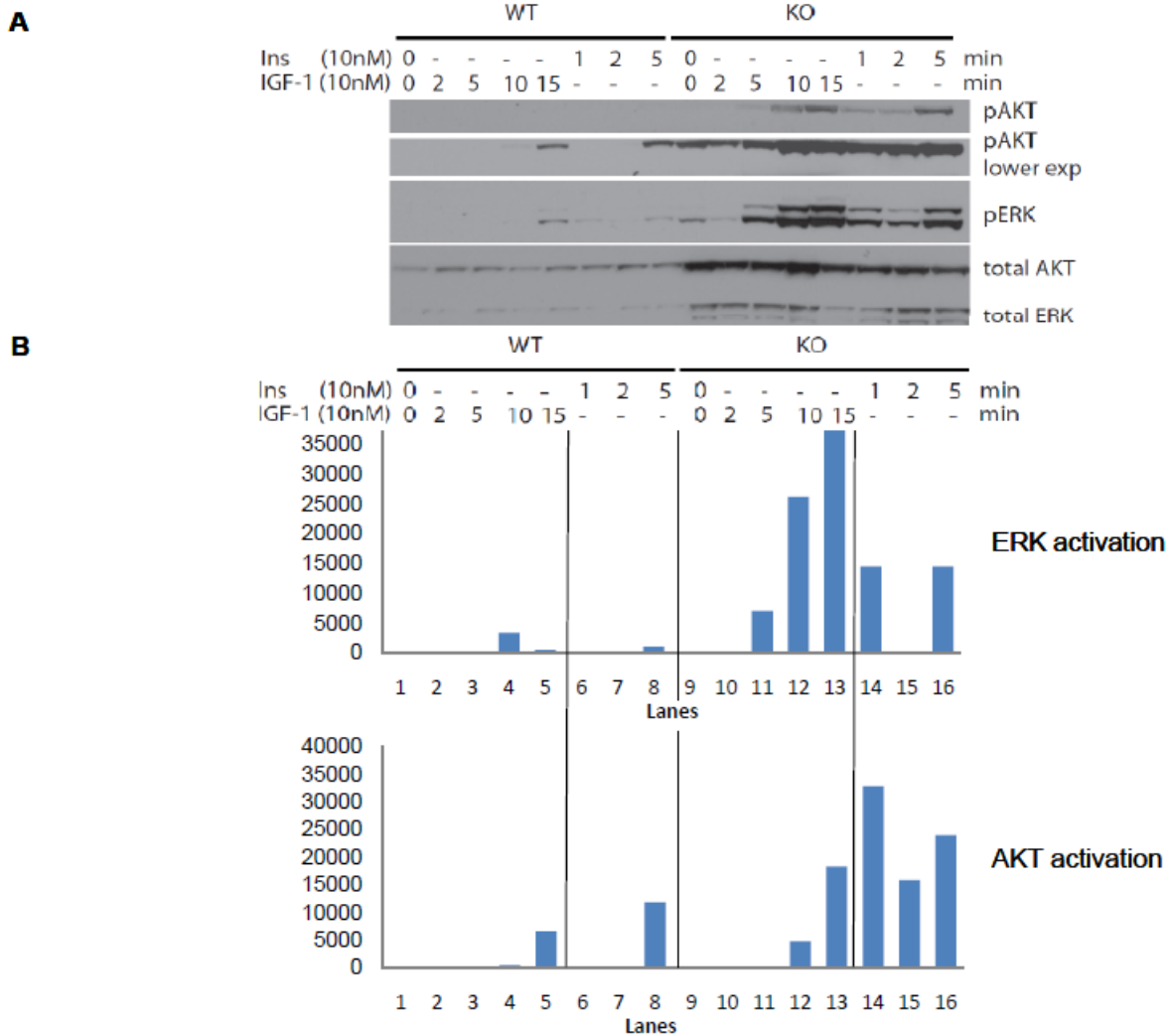


**Figure 7-14 Stimulation of WT and KO MEFs with insulin and IGF-1**

(A) Cell lysates prepared from WT and Memo KO MEFs starved over night and stimulated with insulin and IGF-1 for the indicated times were analysed by western for AKT and ERK as well as their phospho-proteins.

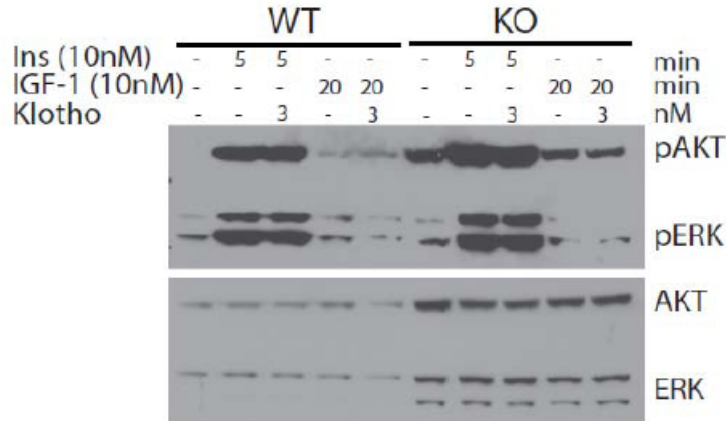
(B) Quantification of the blot shown in (A). The phosphorylation levels of the proteins were normalized to the total protein levels. Depicted is the level of phosphorylation of ERK (top) and AKT (bottom).

To test a possible inhibitory effect of soluble Klotho on insulin and IGF-1 signaling, lysates were prepared from cells starved over night, inhibited with soluble Klotho and stimulated with insulin or IGF-1. For this experiment we also performed quantification of the western analysis by ImageJ as the total amount of protein was not the same in WT and KO cells. We show that Klotho is able to inhibit ERK signaling but not AKT signaling in IGF-1 stimulated WT cells (Figure 7-15, lane 5). This finding

## Results

is not in accordance with prior publications and the current concept of how Klotho would inhibit the pathway. Inhibition of IGF-1 induced ERK activation in KO cells cannot be judged from this western analysis, as we could not detect ERK activation upon IGF-1 stimulation. Nevertheless, there is inhibition of AKT signaling by soluble Klotho in the KO cells (lane 10). Insulin induced signaling could not be inhibited by Klotho in this experiment.

**A**



**B**

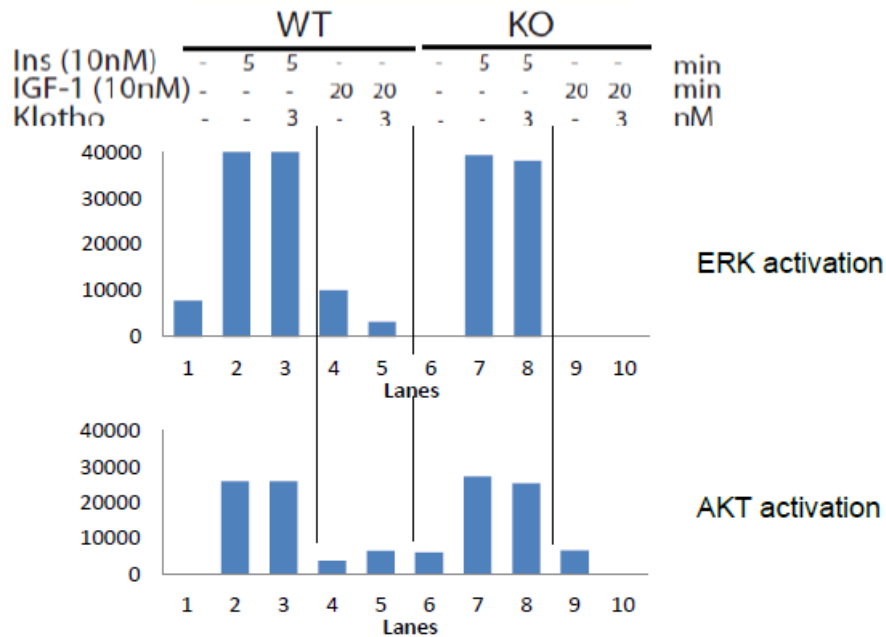


**Figure 7-15 Inhibitory effect of Klotho on the insulin and IGF-1 pathway in the MEFs**

(A) Cell lysates prepared from WT and Memo KO MEFs starved over night, treated with soluble Klotho and stimulated with insulin and IGF-1 for the indicated times were analysed by western for AKT and ERK and their phospho-proteins.

(B) Quantification of the blot shown in (A). The phospho levels of the proteins were normalized to the total levels. Depicted is the level of phosphorylation of ERK (top) and AKT (bottom).

## Results

These results show that the MEFs are responsive to insulin and IGF-1 and that Memo plays a role in their downstream signaling, as shown by earlier activation of the downstream proteins ERK and AKT. Pre-incubation of the cells in soluble Klotho prior to stimulation with IGF-1 and insulin showed that Klotho was able to inhibit IGF-1 signaling in WT and KO cells, but not insulin signaling.

### 7.7 Memo downstream of FGFR signaling in mouse mammary carcinoma cells

When I joined the lab Régis Masson and Susan Jacobs were working with the 4T1 cell line. Susan down regulated Memo in the 4T1 cells by shRNA. This was supervised by Régis Masson. I did not contribute to the generation of the KD cells. I was given the cells by Régis when I started in the group. The aim was that I perform *in vitro* experiments supporting their *in vivo* studies. I worked with the 4T1 cells until the MEFs that I was generating at that time were ready for experiments.

It has been shown that Memo is important for migration downstream of both heregulin and FGF2 (6). Therefore, we studied Memo and its role in FGFR signaling in cancer cells. We used 4T1 mouse mammary carcinoma cells previously described by Aslakson and Miller (398). 4T1 cells have constitutively active FGFR signaling due to autocrine production of the ligands (399).

For the following experiments Memo was stably down regulated by shRNA hairpins in the 4T1 cells (S. Jacob). Memo down regulation was achieved with two different shRNAs against Memo, sh10 and sh7. As control, the non-transfected parental cell line and control transfected cells with shRNA against LacZ were used. These experiments were performed with single clones. For the respective level of Memo in the different clones, please refer to Figure 7-16.

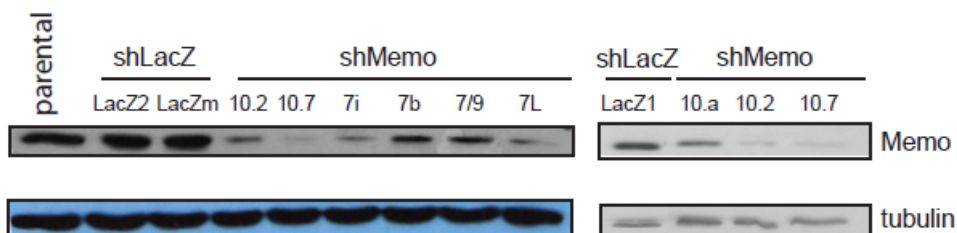


**Figure 7-16 Down regulation of Memo in 4T1 cells by shRNA hairpin against Memo (S. Jacob and I. Samarzija)**

Cell lysates prepared from 4T1 parental cells, 4T1 cells treated with two different shRNA against Memo, (shRNA 10 and 7), or shRNA against LacZ (as control) were analysed by western for the level of Memo and tubulin.



## Results

### 7.7.1 Effect of Memo down regulation on FRS2 phosphorylation in 4T1 cells (F. Maurer)

This experiment was performed by a technician in our lab, Francisca Maurer. She got cells that I cultured and performed the IP and western analysis by herself.

Control and Memo knock-down (KD) 4T1 cells were tested for FRS2 activation. Due to the autocrine FGF loop the cells could not be further stimulated by addition of FGF ligands. Therefore, lysates of growing cells were subjected to immunoprecipitation with FRS2 and total phospho-tyrosine was analysed by western (F. Maurer). Whole cell extract (WCE) is shown as input control. The blot incubated with the pTyr antibody shows that FRS2 was less phosphorylated in the KD cells compared to control cells (Figure 7-17). This data indicates that Memo plays also a role in the FGFR pathway of mouse mammary carcinoma cells.

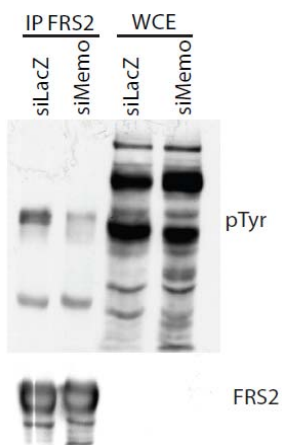


**Figure 7-17 Phosphorylation status of FRS2 in 4T1 control and Memo down regulated cells (F. Maurer)**

Lysates of growing control and Memo KD 4T1 cells were immunoprecipitated by FRS2 and analysed by western. Whole cell extract (WCE) and IP of FRS2 were probed with anti-pTyr and anti-FRS2 antibodies.

### 7.7.2 Apoptosis, proliferation and migration in control and Memo down regulated (KD) cells

Hypothesizing that Memo plays a role in cancer we performed assays to investigate apoptosis, proliferation and migration in control and Memo KD 4T1 cells.

#### 7.7.2.1 Apoptosis

## Results

- YoPro assay of 4T1 cells upon stress induction

Control and Memo KD cells were seeded in 96 well plates and treated with a selective FGFR inhibitor, a PI3K inhibitor LY294002 and CoCl<sub>2</sub>, an oxidative stress inducer. As control the cells were treated with DMSO, the vehicle control for the FGFR1 and PI3K inhibitor. After 32 or 48 hours of treatment the amount of apoptotic cells was assessed by YoPro assay (Figure 7-18A). After 32 or 48 hours almost no basal apoptosis (1-2%) was detectable. FGFR inhibition induced apoptosis in control cells (17% after 32 hours and 24% after 48 hours respectively) but not in the KD cells (3%). Blocking of the PI3K pathway with the LY inhibitor in addition to FGFR inhibition induced even higher apoptosis rates. But the difference between control (59% and 63%) and KD cells (12%) remained about the same. In contrast, treatment with CoCl<sub>2</sub> induced more apoptosis in the KD cells (34% and 59%) compared to control cells (6% and 12%). The experiment was repeated with a different FGFR inhibitor, TKI258, and another control clone as well as an additional Memo KD clone. The results of the first and second experiments were comparable. After 48 hours of treatment with the FGFR inhibitor 26% of the control cells died compared to 2% and 3% of the Memo KD cells.

This suggests that Memo KD cells are more sensitive to oxidative stress, but more resistant to FGFR inhibition.

## Results

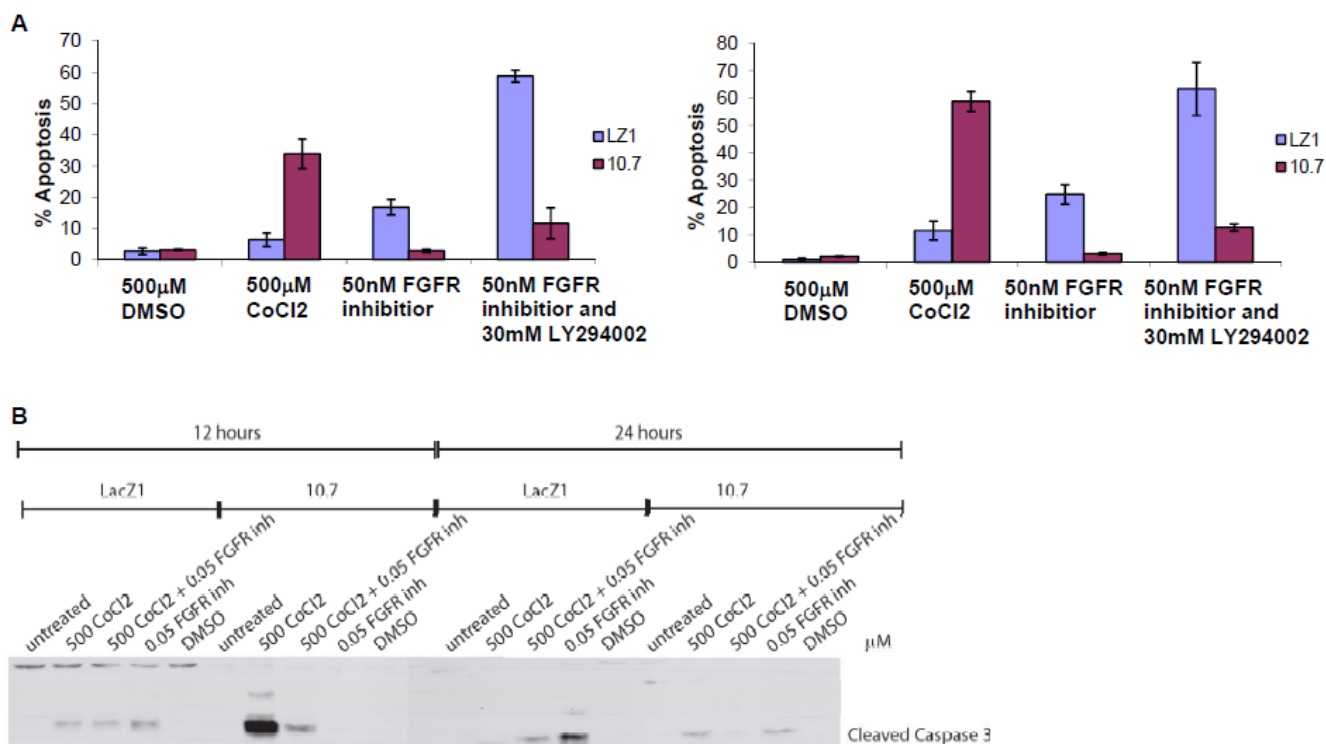


### Figure 7-18 Apoptosis of 4T1

(A) 4T1 cells were treated with CoCl<sub>2</sub>, a FGFR inhibitor or a combination of the FGFR inhibitor and LY294002, a PI3K inhibitor. Cells were treated with the vehicle DMSO of the inhibitors as control. Apoptosis was measured after 32 (left) or 48 hours (right) by YoPro assay.

(B) Cell lysates of 4T1 cells were prepared from cells treated with 500 $\mu$ M CoCl<sub>2</sub>, 500 $\mu$ M CoCl<sub>2</sub> in combination with 50nM of a FGFR inhibitor, or 50nM FGFR inhibitor alone (control of the experiment was untreated cells or treatment with DMSO, the vehicle of the FGFR inhibitor). The lysates were analysed by western and probed for cleaved caspase 3.

- Western analysis for cleaved caspase 3 upon stress induction in 4T1 cells

In addition, we performed western blot analysis on lysates of control and KD 4T1 cells that were treated with CoCl<sub>2</sub>, an FGFR inhibitor or a combination of the two. Treatment with DMSO, the vehicle of the inhibitor, and untreated cells served as controls. To assess the level of apoptosis we used cleaved caspase 3 as readout. There was a clear signal for cleaved Caspase 3 after 12 hours in the KD cells treated with CoCl<sub>2</sub> while the control cells show only a moderate signal (Figure 7-18B). Surprisingly, the combination treatment of CoCl<sub>2</sub> and FGFR inhibitor caused only a moderate level of cleaved caspase 3 in both control and KD cells. The results of the YoPro assay concerning sensitivity to the FGFR inhibitor was confirmed by western analysis of the cleaved caspase 3. There is a moderate level of cleaved caspase 3 in the control cells upon FGFR inhibitor treatment, but no signal in the KD cells

## Results

indicating that the Memo KD cells are more resistant to FGFR inhibition when not challenged with oxidative stress (Figure 7-18B).

- Sensitivity to  $\text{CoCl}_2$  of Memo KO MEFs

Furthermore, we tested sensitivity to  $\text{CoCl}_2$  in the MEFs that were either WT or Memo KO. In this case we stressed WT and KO MEFs by addition of  $\text{CoCl}_2$  and stained with Dilc<sub>1</sub>(5) to measure the mitochondrial membrane potential by FACS. Dilc<sub>1</sub>(5) stains cells with intact mitochondrial membrane potential. Upon cell death the mitochondrial potential is lost. Staining with Dilc<sub>1</sub>(5) is lost proportionally to the loss of mitochondrial membrane potential. Figure 7-19A shows that after 24 hours 15% of the Memo KO cells compared to 3% of the WT cells lost Dilc<sub>1</sub>(5) staining. Those data are in line with the results from the YoPro assay that show that Memo KD cells are more sensitive to  $\text{CoCl}_2$

- Investigation of Memo's effect downstream of DNA damage

To investigate if cells that have no Memo are generally more sensitive to stress, we induced DNA damage by treatment with etoposide. Cells were stained with Dilc<sub>1</sub>(5) and analysed by FACS. After 48 hours of etoposide treatment 33% of the Memo KO cells were apoptotic and only 13% of the WT cells (Figure 7-19B).

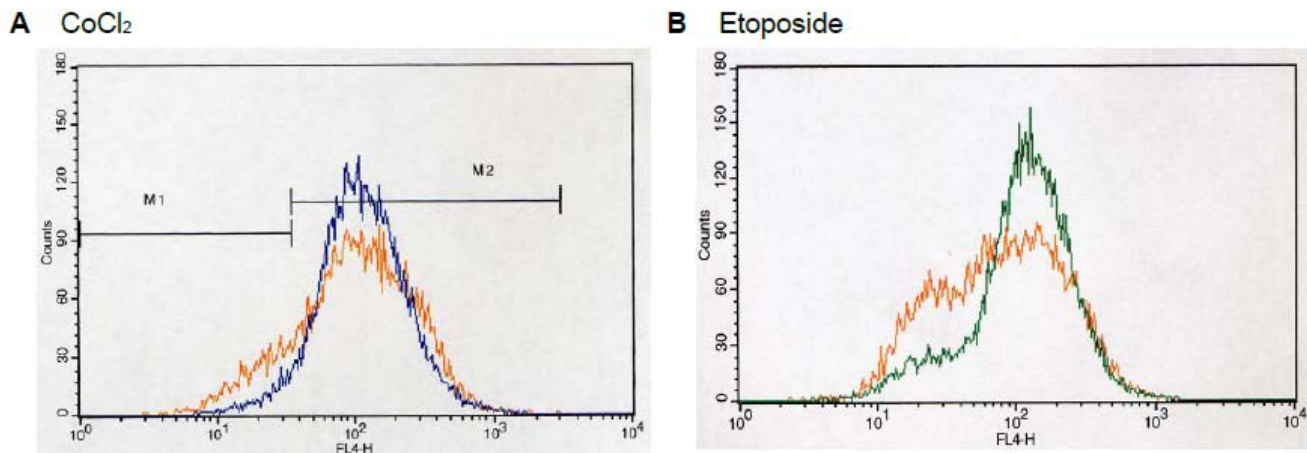


**Figure 7-19 Apoptosis of WT and KO MEFs upon Etoposide treatment**

(A) MEFs were treated with 500 $\mu\text{M}$   $\text{CoCl}_2$  for 24 hours, stained with Dilc<sub>1</sub>(5) and sorted by FACS. Positive staining with Dilc<sub>1</sub>(5) indicates loss of the membrane potential and therefore apoptosis. Orange = membrane potential of Memo KO MEFs, Blue = membrane potential of WT MEFs. M1 is the gate for apoptotic cells, M2 is the gate for living cells. M1<sub>orange</sub>=15%, M1<sub>blue</sub>=3%.

## Results

(B) MEFs were treated with etoposide for 48 hours, stained with Dilc<sub>1</sub>(5) and FACS sorted. Positive staining with Dilc<sub>1</sub>(5) indicates loss of the membrane potential and therefore apoptosis. Orange = membrane potential of Memo KO MEFs, Green = membrane potential of WT MEFs.

These data indicate that Memo KO MEFs are more sensitive to DNA damage and oxidative stress and that loss of Memo renders the cells in general more sensitive to stress.

### 7.7.2.2 Proliferation

Next, proliferation was investigated by quantifying BrdU incorporation. Cells were seeded in 96-well plates and at 80% confluency exposed to BrdU for two hours. There was no difference between the proliferation rates of control and KD clones as measured by BrdU incorporation (Figure 7-20).

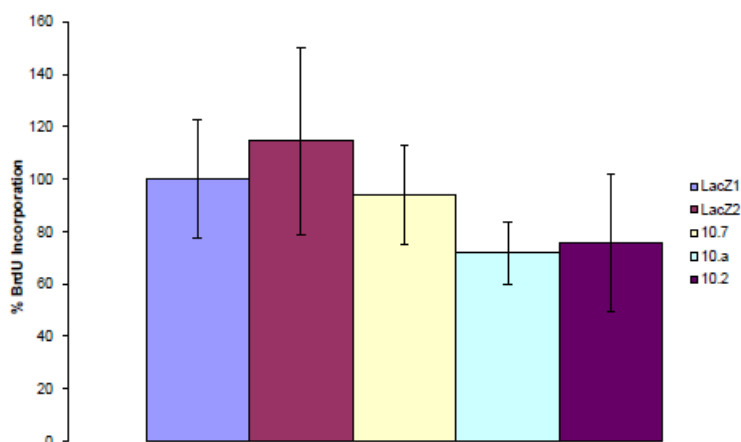


**Figure 7-20 Proliferation assay with 4T1 cells**

Control (LacZ1 and 2) and Memo KD (10.7, 10.a, and 10.2) cells were treated with BrdU for 2 hours. Incorporation of BrdU was evaluated and plotted. Incorporation into LacZ1 cells was set at 100%.

### 7.7.2.3 Migration

As mentioned above our group has reported that Memo down regulation in human cancer cells caused a FGF2-stimulated migration defect (6). Hence, we investigated migration in 4T1 control and Memo KD cells by boyden chamber assays.

Equal numbers of control and KD cells were seeded on top of the membrane. Migrated cells were counted after 6 or 12 hours. During migration the cells were either treated with a selective FGFR inhibitor or DMSO as vehicle control (Figure 7-21). The basal migration was lower in the KD clones (1200 and 3500 migrated cells respectively) than control cells (8000 cells) after 6 hours of migration.

## Results

Nevertheless, after 12 hours the KD cells caught up (17 000 and 16 000 cells compared to 18 000 control cells).

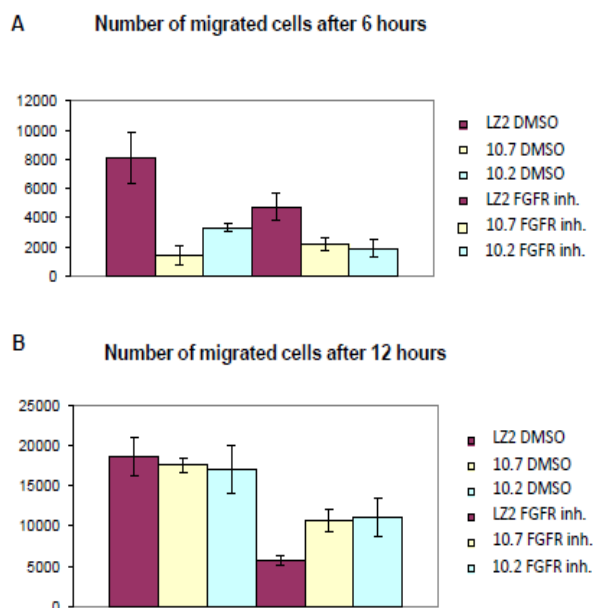


**Figure 7-21 Boyden Chamber Migration assay with 4T1 cells**

4T1 control and Memo KD cells were seeded in Boyden Chambers and treated with a FGFR inhibitor or DMSO as control. Migration was stopped after 6 hours (A) or 12 hours (B) and the cells were counted.

In addition, this experiment showed that blocking FGFR signaling with a FGFR inhibitor was more efficient in control cells (70% of inhibition) than in the KD clones (40% respectively 35% of inhibition).

These data suggest that Memo inhibits FGF2 stimulated migration initially (during the first 6 hours of migration), but that Memo KD cells are able to catch up after 12 hours of migration. Furthermore, these data support the hypothesis that Memo KD clones are more resistant to FGFR signaling inhibition.

### 7.7.3 Memo and oxidative stress

As discussed above (section 7.7.2.1) Memo KD 4T1 clones and Memo KO MEFs are more sensitive to oxidative stress induced by  $\text{CoCl}_2$ .

$\text{CoCl}_2$  induces apoptosis via two different pathways: 1) It blocks the electron chain reaction in the mitochondrial membrane or 2) it activates the ASK-p38 pathway (400).

## Results

Therefore, we investigated if there is a difference in the shape and size of mitochondria in the KO compared to WT MEFs, as this can be a read-out for functionality of mitochondria. We stained WT and KO MEFs that were isolated from different animals with mitotracker that stains the mitochondria. Figure 7-22 shows that there is no obvious difference between the mitochondria of the WT and KO cells.

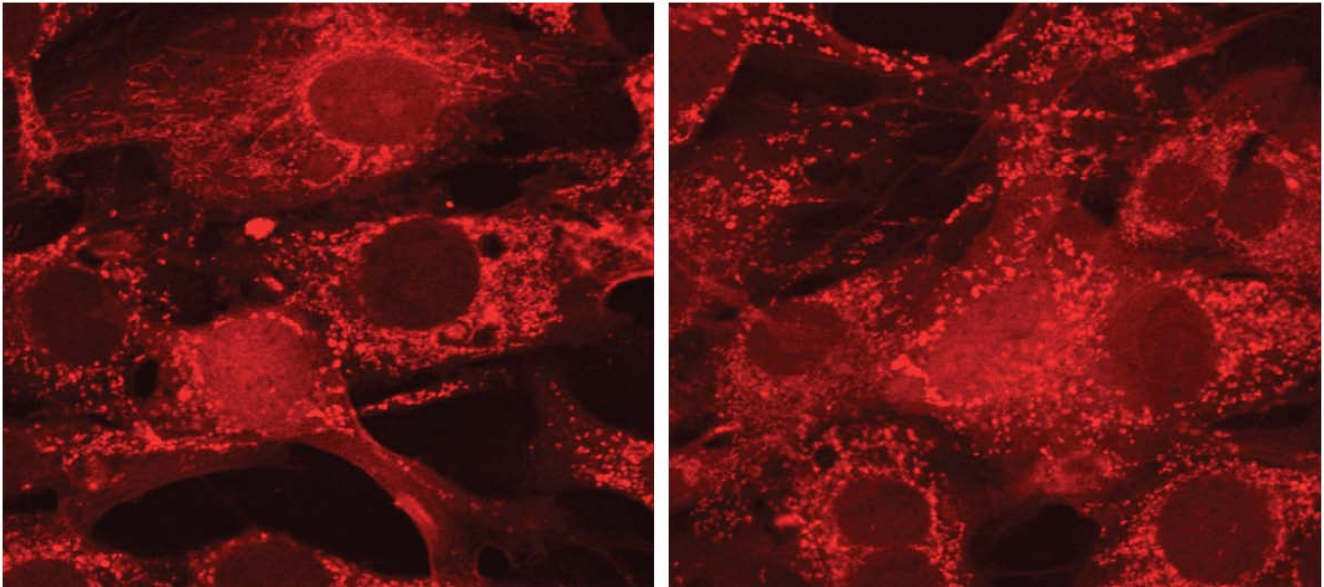


**Figure 7-22 Staining of mitochondria in MEFs after CoCl<sub>2</sub> treatment**

WT (left) and KO (right) MEFs were treated with 500 $\mu$ M CoCl<sub>2</sub> and stained with mitotracker to visualize the mitochondria.

Thus, we investigated p38 signaling downstream of CoCl<sub>2</sub> treatment in 4T1 cells. Lysates were prepared from control and KD cells that were treated with CoCl<sub>2</sub> for the indicated time. Memo KD cells show a stronger induction of p38 after 8 hours of CoCl<sub>2</sub> treatment (Figure 7-23A), which indicates that they are more stressed. The Memo KD clone 10.a has the highest level of Memo and also shows the least amount of p38 induction (see insert Figure 7-23A).

In addition, the KD cells show inactivation of S6 ribosomal protein at all time-points investigated (Figure 7-23B). In parallel, we find dephosphorylation of 4E-BP1 upon CoCl<sub>2</sub> treatment (Figure 7-23C). This suggests an implication of Memo in the TOR-HIF1 $\alpha$  crosstalk that has been earlier described (401).

## Results

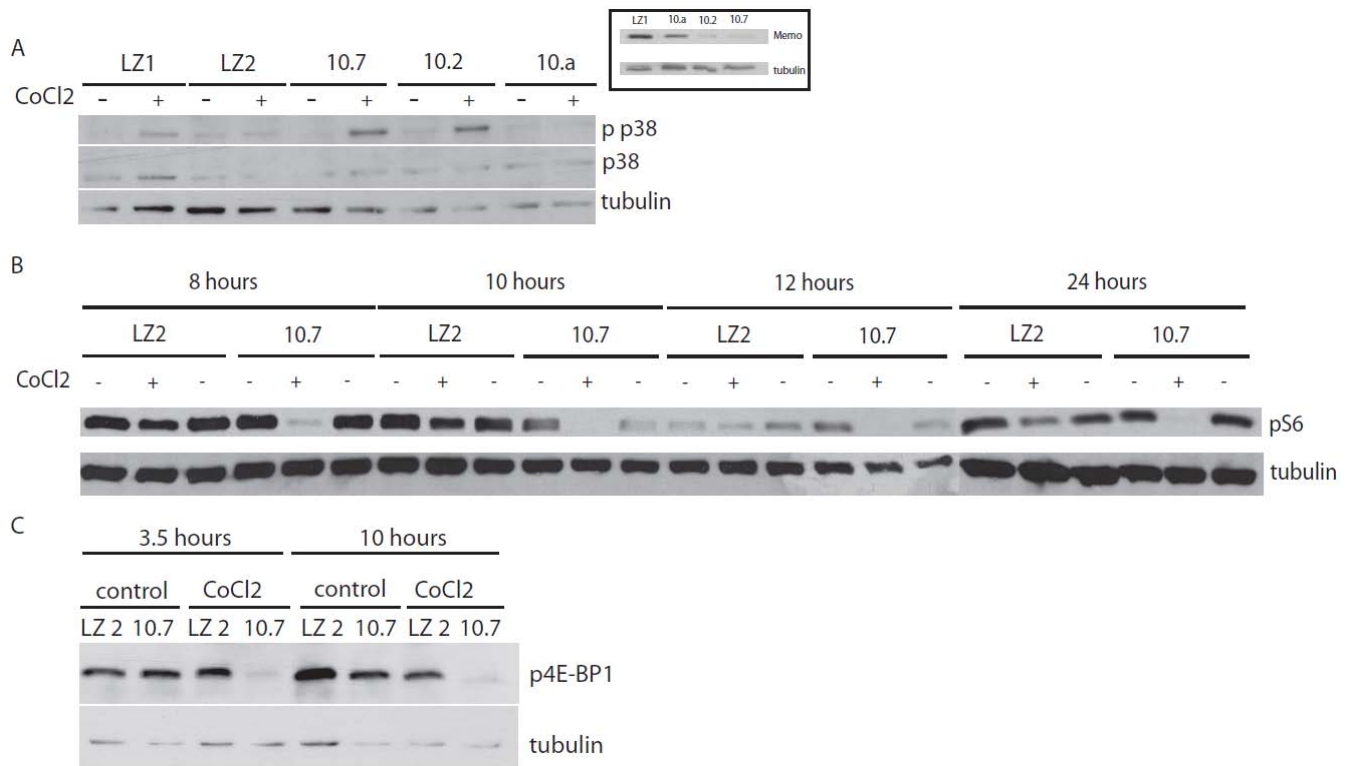


### Figure 7-23 Cell Signaling downstream of CoCl<sub>2</sub>

Cell lysates were prepared from control and Memo KD 4T1 cells that were treated with 500 $\mu$ M CoCl<sub>2</sub> for the indicated times. Protein levels of Memo are shown in the insert of (A). The lysates were analysed by western blot and probed for p38 (A), pS6 (B) and 4E-PB1 (C). Tubulin was used as loading control.

CoCl<sub>2</sub> is not only an oxidative stress inducer, but also a hypoxia-mimicking agent. Therefore, we wanted to exclude that the effects we observed downstream of CoCl<sub>2</sub> are due to its hypoxia mimicking properties. Initially we investigated if the cells show a defect in stabilizing the Hypoxia Induced Factor 1 $\alpha$  (HIF1 $\alpha$ ) (Figure 7-24). In addition, we investigated if the cells show a difference in signaling downstream of real hypoxic conditions. Cell lysates were prepared of control and Memo KD 4T1 cells that were either treated with CoCl<sub>2</sub> or exposed to floating hypoxic gas (1% O<sub>2</sub>, 5% CO<sub>2</sub>, 94% N<sub>2</sub>) for 20 minutes and then incubated in this gas for the indicated time. Figure 7-24 shows that HIF1 $\alpha$  is stabilized upon CoCl<sub>2</sub> and to a lesser extent also by hypoxic conditions in control cells. In the KD cells HIF1 $\alpha$  is stabilized upon CoCl<sub>2</sub> treatment, although to a lesser extent then in the control cells. 4T1 cells show basal stabilization of HIF1 $\alpha$  in normal growing conditions, a feature common to many cancer cells. The same applies for HIF1 $\alpha$  stabilization upon hypoxic conditions. This indicates that stabilization may be slightly affected in 4T1 cells down regulated for Memo. Nevertheless, the



## Results

inactivation of S6 is unique to  $\text{CoCl}_2$  treatment. Thus, this effect seems to correlate with oxidative stress.

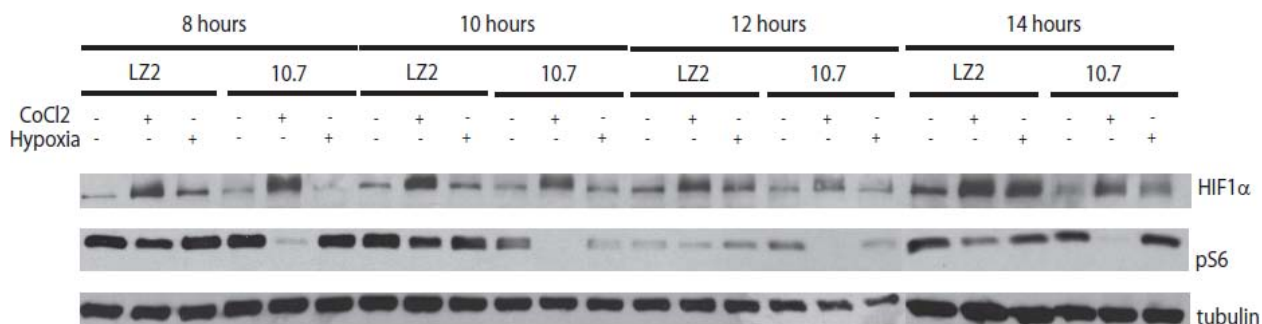


**Figure 7-24  $\text{CoCl}_2$  and hypoxia treatment of 4T1 cells**

Cell lysates were prepared of control and Memo KD 4T1 cells that were incubated in  $500\mu\text{M}$   $\text{CoCl}_2$  or hypoxic gas for the indicated times and analyzed by western. The membrane was blotted for HIF1 $\alpha$ , pS6 and tubulin.

### 7.7.4 Memo and VEGF secretion

Another line of investigation in the lab followed the question of the role of Memo in cancer. Therefore, colleagues in the lab (R. Masson, S. Jacub, I. Samarzija) investigated the effect of down regulation of Memo in an FGF driven cancer model. They injected control and Memo down regulated (KD) cells in the mammary fat pad and measured primary tumor growth. They found that primary tumor growth was initially slower in the tumors formed by KD cells but caught up after 20 days. In addition, they found by histological analyses of the tumors that tumors grown from Memo KD cells are more slowly vascularised, but that vascularisation caught up after several days.

The vascular endothelial growth factor (VEGF) is an essential factor for the in growth of blood vessels into the tumor (402). Endothelial cells of the surrounding blood vessels need to be stimulated by VEGF to grow into the tumor area. VEGF can be secreted by the tumor cells themselves or by cells of the tumor stroma. Interestingly, the FGFR pathway has already been described to induce VEGF release (207). Therefore, we investigated if Memo KD reduced the secretion levels of VEGF-A.

We tested VEGF secretion by performing an ELISA assay on the control and Memo KD clones. Equal numbers of cells were seeded on 96-well plates and the supernatant of triplicates pooled to perform the ELISA assay. The basal level of VEGV-A secretion is higher in the control cells compared to the Memo KD cells (Figure 7-25A). The level of secreted VEGF-A was increased upon addition of  $\text{CoCl}_2$  in

## Results

control and KD cells, although the amount of the increase seemed to correlate with the basal secretion level. Addition of PI3K inhibitor (LY294002) or FGFR inhibitor reduced the secretion level significantly in control and KD cells. Nevertheless, in control cells the FGFR inhibitor was slightly more efficient than LY294002, while in the KD cells the efficiency of the two inhibitors was equivalent.

This data shows that Memo KD induces lower basal VEGF and CoCl<sub>2</sub> stimulated release and additionally supports the preceding data demonstrating that Memo KD cells are less sensitive to FGFR inhibition.

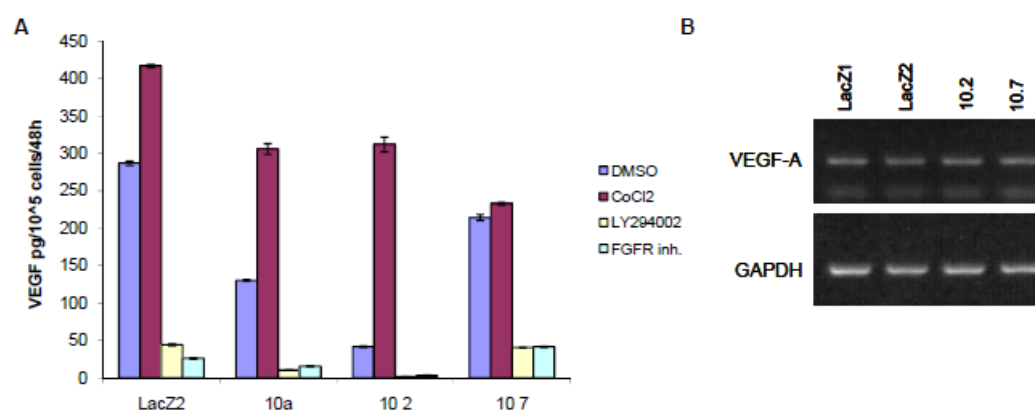


**Figure 7-25 VEGF secretion and expression in 4T1 cells**

(A) ELISA assay for VEGF-A with control and Memo KD cells. Cells were plated and treated with DMSO, CoCl<sub>2</sub>, LY294002 or FGFR inhibitor for 48 hours. The pooled supernatant of triplicates was used to perform the ELISA assay.

(B) RNA was collected of control and Memo KD cells and the level of VEGF-1 and GAPDH were evaluated by semi-quantitative PCR

Furthermore, we investigated if translation of the VEGF is affected. A semi-quantitative PCR for VEGF-A on the cDNA of control and KD Memo clones was performed. There was no difference in the RNA level of VEGF-A in Memo KD clones compared to control clones (Figure 7-25B).

These data suggest that the Memo KD clones translate equal levels of VEGF-A, but secrete or release less into the medium compared to control clones. Overall, this data supports the hypothesis that Memo KD clones show a delay in primary tumor outgrowth, due to slower vascularisation of the tumor, caused by the reduced levels of secreted VEGF-A.

## 8 Outlook and Discussion

The goal of this thesis was to further understand the mechanisms of aging, a fundamental process that is becoming more critical to study as average age of our population increases.

Knock out of Memo in mice is embryonic lethal at E13.5, demonstrating that Memo is an essential protein. Memo knockout embryos at E11.5 show abdominal bleeding and low perfusion of the blood vessels. Nevertheless, the etiology of death is still unclear and needs further investigation. Here we show that conditional knock-out mice induced for loss of Memo in the whole body after E13.5 are viable, but have severe defects that lead to rapid death after birth. Memo null animals developed premature aging symptoms including weight loss, graying hair and hair loss, stiff joints, kyphosis, loss of subcutaneous fat and white adipose tissue, nonfunctional and hypotrophic gonads as well as a defect in the hindlimb reflex. In addition, Memo null mice displayed a severe metabolic phenotype, including postprandial hypoglycemia and higher sensitivity to insulin. This is an unusual phenotype for premature aging models and similar metabolic phenotypes have only ever been reported for two other mouse models, namely the FGF23 and Klotho mutant strains.

Data provided by this study suggest that Memo null mice suffer from renal insufficiency and have a defect in the renal FGF23-Klotho axis that regulates the levels of vitamin D production, phosphate reabsorption and calcium uptake. We show that regulators of the FGF23-Klotho axis are affected upon Memo loss. The current study includes data suggesting that expression of vitamin D metabolizing enzymes and expression of Na-Pi cotransporters, important for phosphate reabsorption, are deregulated. Furthermore, we show evidence that cleavage of Na-Pi2a is inhibited in the Memo KO animals, although we do not find differences in serum phosphate levels. Blood analysis showed possible renal insufficiency and a slight hypercalcemia in Memo null animals. Staining of the hearts of Memo null animals with von Kossa, a stain for calcium deposits, supports the findings of the blood analysis. We found small regions of calcifications of soft tissue in hearts of Memo null mice.

In addition to the full body conditional knock-out, we also generated an inducible, kidney-specific Memo knock-out strain. These mice do not suffer from premature aging, but they show a decrease in body weight compared to control animals and renal insufficiency. In line with the data from Memo null

## Outlook and Discussion

mice, we show that kidney-specific Memo KO animals have a defect in the FGF23-Klotho axis and in the cleavage of Na-Pi2a. In addition, we provide data showing that they have less efficient creatinine clearance. Nevertheless, these animals also have normal serum phosphate levels. Interestingly, our investigations into the renal functioning of these animals, using metabolic cages, revealed that the kidney-specific KO animals are hypercalciuric.

*In vitro* we investigated metabolic FGF signaling in HEK293 cells that were stably transfected with Klotho or  $\beta$ Klotho (HEK293-kl and HEK293- $\beta$ kl) and that were transiently downregulated for Memo. We could show that activation of ERK takes place more rapidly in Memo downregulated cells stimulated with FGF23 and FGF19 as compared to control cells. In addition, we showed that FGF23 stimulation of HEK293-kl cells induces less FRS2 phosphorylation in Memo knock-down cells compared to control cells. Limited by the expression levels of the protein, we could not show activation of AKT.

This study also provides data suggesting that Memo is generally downstream of the FGFR pathway and that Memo binds to the FGFR-signalosome. These experiments were performed in mouse embryonic fibroblasts that were stimulated with FGF2. Knock-out of Memo in these cells dampens FGFR signaling with respect to intensity and duration. We provide evidence that Memo co-immunoprecipitates with all the members of the FGFR-signalosome. In addition, we show that Memo is downstream of the FGFR pathway in 4T1 cells, a mouse mammary carcinoma cell line that has an autocrine FGF loop. We demonstrate that stable downregulation of Memo by shRNA results in lower activation of FRS2.

Another line of investigation showed that Memo KD 4T1 cells are less sensitive to FGFR inhibition, as assessed by apoptosis and migration assays, and more sensitive to CoCl<sub>2</sub> treatment. Treatment with CoCl<sub>2</sub> induced stronger phosphorylation of p38 in the Memo KD cells indicating higher stress levels. Furthermore, inactivation of S6 ribosomal protein as well as dephosphorylation of 4E-BP1 could be detected in Memo KD cells treated with CoCl<sub>2</sub>.

### **8.1 The premature aging defect**

Memo null mice showed a severe premature aging phenotype. In addition to the well known premature aging symptoms they also showed a particular metabolic phenotype: postprandial hypoglycemia and

## Outlook and Discussion

increased sensitivity to insulin. Although atypical for premature aging models, they shared this particular metabolic phenotype with two other aging models: the Klotho- and FGF23-mutant mice. Thus, we investigated if there are other similarities between the Memo and the Klotho/FGF23 mutant models. To accomplish this, we analyzed two different mouse models; knock-out of Memo in the whole body (Memo null mice) and kidney-specific knockout of Memo.

### 8.1.1 Analysis of the FGF23-Klotho axis

The current study provides data supporting the hypothesis that loss of Memo in the kidney deregulates the renal FGF23-Klotho axis. Such a deregulation has been shown for the FGF23 and Klotho mutant mice. Memo null and kidney-specific Memo KO mice (collectively referred to as Memo mice) show similar changes to the FGF23/Klotho mutant mice with respect to the Klotho-FGF23 axis. We provide evidence that the levels of Cyp27B1, the vitamin D converting enzyme, and Cyp24A1, the vitamin D catabolizing enzyme, are deregulated in Memo mice. These deregulations did not yet reach statistical significance. We believe that this is due to high variations of transcription-levels depending on the age of the mice. So far, we were not able to investigate a sufficient number of animals at the same age. Therefore, to date, we don't know if these are significant changes.

However, the observed expression levels of Cyp27B1 and Cyp24A1 are deregulated as compared to control animals. In contrast, Klotho mutant mice show a consistent upregulation of Cyp27B1 and Cyp24A1 [303]. A possible explanation for this discrepancy may be revealed by the fact that Klotho mutant animals show a downregulation of vitamin D receptor (VDR) levels. The vitamin D receptor forms a negative feedback loop by downregulating the expression of  $1\alpha$ -hydroxylase. Conversely, no downregulation of VDR expression was observed in the Memo null animals. Inactivation of the feedback loop probably results in the consistent upregulation of the Cyp27B1 and Cyp24A1 observed in the Klotho mutant mice, whereas in Memo null animals the intact feedback loop would modulate expression of these enzymes to varying degrees. Alternatively, as Memo mice are expected to be normal with respect to Klotho levels, the function of the soluble form of Klotho should be maintained in Memo mice. This is important to consider with regard to the phenotype as it has been published that the soluble form of Klotho has essential functions in regulation of serum phosphate and FGF23 levels (301). It was beyond the scope of this study to investigate the function of soluble Klotho in Memo

## Outlook and Discussion

mice.

One limitation of this study is that due to the limited number of animals available, the level of the Cyps and Na-Pis could in some cases only be analyzed for one control animal. Nevertheless, when more control animals were included, which are not littermates but treated simultaneously and had the same age at the time of treatment (matched breeding), the outcome of the experiments was the same.

We show here that the expression level of the sodium-phosphate cotransporters IIa and IIc (Na-Pi2a/2c) are downregulated in the kidneys of Memo null mice. This is in line with data reporting that the mRNA levels of these transporters are downregulated in Klotho mutant mice [305]. In addition, it has been shown that in the Klotho mutant strain the content of Na-Pi2a in the brush border membrane is increased (301). We show here that cleavage of Na-Pi2a in the brush border membrane, which leads to receptor internalization and degradation (403), is blocked in Memo mice, however, we do not see an accumulation of the full length receptor in the brush border membrane of Memo mice.

Another regulator of Na-Pi2 expression in the brush border membrane is the parathyroid hormone (PTH), which is secreted by the parathyroid gland. PTH is the principal regulator of calcium homeostasis and also inhibits phosphate reabsorption by regulation of  $1\alpha$ -hydroxylase levels. Although, we observed lower PTH levels in Memo null animals there is no difference in NaPi2a expression in the brush border membrane. This could indicate that in this situation the effect of PTH is overruled.

### 8.1.2 Blood- and urine analysis

Different blood analyses of Memo mice compared to control animals have been performed. We provide data showing that both Memo null and kidney-specific Memo KO animals suffer from renal insufficiency. We investigated the levels of two different indicators for renal insufficiency, BUN (in both models) and creatinine (in the kidney-specific KO animals only). Both indicators were deregulated in the Memo mice. Interestingly, we observed upregulated BUN levels in Memo null animals that were induced for Memo loss at the age of 2.5 weeks and for which blood sampling was performed 8 weeks later, but observed no differences in Memo null animals induced for Memo loss at 11 days of age and for which blood sampling was performed 20 days later. It is possible that 20 days is not enough time for these specific changes to be detected, however, both Memo null animal groups showed premature aging symptoms, suggesting that other changes do occur at this time point.

## Outlook and Discussion

In contrast to the published data that suggests that elevated phosphate levels are the cause of premature aging symptoms in Klotho and FGF23 mutant animals (250, 257), both Memo models displayed normal serum phosphate levels. In addition, we tested phosphate excretion of the kidney-specific Memo KO mice and found that to also be normal. These results are surprising, as Memo null mice present with a specific and severe premature aging phenotype which in the literature has been attributed to increased serum phosphate levels.

In addition to phosphate, we also investigated calcium levels. Deregulation of calcium metabolism has been described for the Klotho and FGF23 mutant mice, although it has never been considered to be causative for premature aging. Blood and urine analyses revealed a slight hypercalcemia in both animal models and a robust hypercalciuria in kidney-specific Memo KO animals (analysis of the status of the Memo null animals is ongoing). It is interesting that the major defect that we observe is an abnormal calcium metabolism, something which has not previously been linked to premature aging as causing factor. To date we have not observed any differences in the metabolism between the Memo null and the kidney-specific Memo KO mice.

To elucidate the cause of aging in Memo null mice it was important to find specific differences between Memo null and kidney-specific Memo KO animals. To date it is unclear if the premature aging symptoms of the Memo null animals arise simply by the accumulation of the multiple defects expected from Memo knock-out in the whole body, or if there is a specific difference in the metabolism controlled by the FGF23-Klotho axis. To investigate the possibility of such a specific difference further, we investigated the levels of PTH and FGF23 in the serum of Memo and control animals. Only the Memo null mice showed a significant decrease in PTH levels. Even though the kidney-specific animals have a tendency for reduced PTH levels, the difference is not significant. Therefore, this reduced PTH levels specifically in the Memo null animals could be the trigger of the premature aging symptoms observed in the Memo null animals.

Furthermore, PTH is known to be one of the major regulators of calcium homeostasis. In addition, PTH inhibits vitamin D, directly and indirectly via  $1\alpha$ -hydroxylase (339). To date, we don't know the level of vitamin D in the Memo mice. This will be measured in the future and could further elucidate the role of Memo in aging.

As mentioned above, PTH is an important calcium regulator. PTH is secreted by the parathyroid gland

## Outlook and Discussion

upon a drop of serum calcium concentration. Therefore, low levels of PTH in Memo null mice that show slight hypercalcemia are in line with the published regulation of PTH secretion upon serum calcium levels. We found further evidence for deregulated calcium homeostasis beyond the function of PTH. Our data suggest increased expression of TRPV5, NCX1 and CB28 in kidneys of kidney-specific Memo KO mice. All three proteins are implicated in the active reabsorption of calcium from the urine into the blood stream. Upregulation of these proteins could be a rescue attempt of the organism against the observed hypercalciuria in kidney-specific Memo KO mice.

For Klotho and FGF23 mutant mice defects in calcium homeostasis have been shown (92, 255). Klotho has been shown to be regulator of calcium homeostasis in an FGF23 independent manner. It stabilizes TRPV5 in the kidney membrane by cleaving off sugar residues of the transporter (341, 404) and  $\text{Na}^+\text{K}^+$  ATPase by binding to the ATPase in the membrane of the parathyroid gland in order to induce PTH secretion upon low serum calcium levels (342). In addition, soft tissue calcification has been found in the heart, lungs and kidneys of Klotho and FGF23 mutant mice (92, 255) as a consequence of hypercalcemia. Supported by our findings of only slight hypercalcemia in the serum, we have observed only a very restricted area of the heart to be calcified in Memo null animals and have no evidence of calcification in the lungs. High calcium levels can also cause bone malformation however, other than the kyphosis described earlier, we did not find any obvious bone malformations. This should be investigated more deeply however, for instance with the use of x-ray technologies.

In the general blood analysis we also measured the levels of glucose and insulin. Both were found to be downregulated. In addition, by performing Glucose- and Insulin Tolerance Tests we observed postprandial hypoglycemia and higher insulin sensitivity in Memo null animals. Due to the higher insulin sensitivity we expected to find lower circulating insulin levels in the Memo null animals. This was confirmed by the first blood analysis performed. Surprisingly, we found altered glucose levels in the blood analysis performed by the “Institut Clinique de la Souris (ICS)” (Table 7-3) but we did not detect any difference in glucose levels of the starved animals during the Glucose- and Insulin Tolerance Test (Glucometer (Free Style mini form ABBOTT)) (Chapter 7.1). This might be due to the different sensitivities of the two methods.



## 8.2 FGFR signaling

We have evidence that Memo loss results in a shorter and less intense activation of proteins downstream of the FGFR pathway in mouse embryonic fibroblasts. In addition, we showed supporting data that Memo binds to the FGFR-FRS2-GRB2/GAB1 complex, the FGFR-signalosome. In order to elucidate to which component of the signalosome Memo directly binds, Memo pull-downs with purified proteins should be performed. To date the mechanism by which Memo affects FGFR signaling is unknown. There are a few possibilities: 1) We published earlier that purified Memo binds to actin filaments *in vitro* [8] therefore, we hypothesize that Memo may affect the localization of the FGF receptor. Due to the fact that signaling and signalosome formation is possible in the absence of Memo, a role for Memo in localizing the receptor to the cell membrane can be excluded. Nevertheless, Memo may have a role in localizing the FGFR within the cell membrane. It has been published that localization of FGFR into lipid rafts affects signaling by directing it more towards AKT signaling [402]. To examine this, tagged versions of the receptor should be expressed and colocalisation of the receptor and lipid rafts should be studied. 2) Another hypothesis is that loss of Memo interferes with FRS2-binding partners, thus inhibiting recycling of the receptor, which has been shown to be essential for persistent FGFR signaling [124]. This could be tested by staining for Rab11, an important protein for receptor recycling. 3) My own results and those of other members of the group, show that Memo is localized in the cytoplasm and in the nucleus. In addition, I and others in the lab have shown that Memo localizes to the nucleus upon mild stress induction, such as starvation. Therefore, Memo could be acting as a shuttling protein to bring receptors to the nucleus. It has been shown previously that a nuclear FGFR subpopulation exists (405), although thus far the function of these receptors in the nucleus has not been elucidated. In general, it would be interesting to investigate under which conditions different pools of Memo are delocalized. 4) An additional hypothesis is that the complex of receptor and adaptor proteins forms in the absence of Memo, but the receptor fails to become fully activated. Data has been presented that illustrates that the different phosphorylation sites on the FGF receptor are activated in a kinetic and ordered manner [403]. Thus, it is possible that the receptor only gets partially phosphorylated and not fully activated in Memo KO cells. A massspectrometry approach could shed light on this particular theory. 5) Finally, another possibility to investigate is the potential upregulation of known negative regulators of FGFR signaling, such as sprouty and SEF (similar expression to *fgf* genes), upon loss of Memo.

## Outlook and Discussion

Our group published earlier that Memo binds only the phosphorylated form of ErbB2 [5, 6]. Data from this study shows that Memo binds to FGFR irrespective of stimulation. This is not necessarily contradictory to what we published earlier. FRS2, for instance, has also been found to bind the phosphorylated and non-phosphorylated forms of FGFR, but only the phosphorylated form of Ret [102]. Therefore, it has been established that the binding properties of adapter proteins can vary between different receptors.

Another major interest of this study was cell signaling downstream of FGF23 stimulation. As Klotho expression is spatially restricted, HEK293 cells were engineered to stably express Klotho or  $\beta$ Klotho in order to make these cells responsive to FGF23 and FGF19/FGF21 respectively. In addition, Memo was downregulated in these transfected cells using a siRNA-mediated approach. Consistent with the data obtained from the FGF2 stimulation of MEFs, we found less intense phosphorylation of FRS2 downstream of FGF23 stimulation in Memo knock down (KD) cells. Furthermore, we detected a more rapid activation of ERK downstream of FGF23 and FGF19 in Memo KD cells as compared to control cells. This is initially counterintuitive, as ERK is downstream of FRS2. However, a negative feedback loop from ERK to FRS2 exists (406) and thus one possible explanation for the more rapid activation of ERK observed in Memo KD cells could be the disruption of this negative regulatory mechanism. Another explanation could be the emergence of a compensatory mechanism to activate ERK in these cells.

It is surprising that we found differences between Memo KD and control cells downstream of FGF23 and 19 and but not downstream of FGF21. The mechanism of activation in endocrine signaling is believed to be the same for all three ligands. One could expect that Memo may only influence signaling downstream of  $\alpha$ Klotho and not  $\beta$ Klotho, but here we found that Memo is downstream of both Klotho family members. This could reflect organ-dependent differences in  $\beta$ Klotho signaling as FGF19 activates signaling in the liver while FGF21 does so in adipose tissue. This difference has not been investigated any further in this study.

We also investigated FGFR1 complex formation with Klotho upon stimulation of HEK293 cells with FGF23. Our data shows that FGFR1 and Klotho are found in a complex irrespective of stimulation with FGF23, a point that has been debated in the literature. This study shows that FGFR1 and Klotho can be found in a complex in unstimulated cells.

## Outlook and Discussion

Finally, we investigated the role of Memo downstream of insulin and IGF-1 stimulation in MEFs. It has been shown that the soluble form of Klotho inhibits insulin and IGF-1 signaling in breast cancer cells (350). We tested if treatment of MEFs with Klotho inhibits Insulin and IGF-1 signaling in a comparable way. First, we showed that MEFs were responsive to insulin and IGF-1. In addition, our data gives evidence that Memo KO MEFs activate ERK and AKT faster as compared to control cells. These results confirm our data downstream of FGF23 signaling in the HEK293-kl cells which also showed an earlier induction of ERK phosphorylation. Nevertheless, these results are in contrast to data in the MEFs that were stimulated with FGF2. In this case we observed delayed activation of ERK downstream of FGF2. These opposing results could be due to cell specificity. It would be interesting to investigate the duration of phosphorylation in HEK293 cells and MEFs downstream of IGF-1 signaling. Together this data suggests that Memo has different functions downstream of individual receptors and in different cell types. It has already been shown for FRS2 that it has different functions downstream of specific receptors. It has an activating function downstream of FGFRs, but an inhibiting function downstream of the insulin-, EGF-, and PDGF receptors [110]. We next tested if treatment of MEFs with exogenous Klotho prior to stimulation with insulin or IGF-1 results in an inhibitory effect of Klotho and if so, if loss of Memo affects this function. We found that pretreatment with soluble Klotho had an inhibitory effect on IGF-1 but not on insulin signaling. To date we don't have an explanation for the diverse effect of Klotho on insulin and IGF-1 signaling. Nevertheless, we could not detect any differences in the Memo KO compared to WT cells. It would be interesting to knock down Memo in the published breast cancer cell lines and test the inhibitory function of Klotho in those cells.

### **8.3 The role of Memo in FGFR signaling dependent apoptosis and migration**

We show here that downregulation of Memo dampens FGFR signaling in 4T1 cells. In addition, there is evidence that Memo KD 4T1 cells are more resistant to FGFR inhibition. We provide data indicating that FGFR inhibition induces less apoptosis and blocks migration to a lesser extent in Memo KD cells when compared to control cells. We hypothesize that the Memo KD cells have adapted to promote survival, despite their reduced FGFR activity. This could be tested by transiently downregulating Memo and investigating if the resistance to FGFR inhibition persists.

In addition, we show that inhibition of PI3K in combination with FGFR inhibition has a synergistic effect on apoptosis in Memo KD and control cells. More importantly, our data suggests that control

## Outlook and Discussion

cells are more affected by concurrent pathway inhibition than the Memo KD cells. Given this, it is not surprising that we find that AKT activation is strongly delayed downstream of FGFR stimulation in Memo KO and KD cells. To test if this is due to adaptation of the cells to low FGFR signaling, Memo WT and KO cells could be transfected with constitutively active AKT (myristoylated AKT) to see if this rescues the phenotype.

Our group has previously published that upon downregulation of Memo, human carcinoma cells display a defect in migration downstream of FGF stimulation [6]. We also see a difference in the basal migration of Memo KD 4T1 mouse mammary carcinoma cells, which have autocrine FGF signaling, 6 hours after plating. However, when we look at the number of cells that have migrated after 12 hours, we see that the Memo KD cells catch up to the control cells. It is possible therefore, that the initial migration defect could actually be a reflection of changes that occur in cell adhesion properties upon Memo loss, rather than be the result of a true migration defect. It has recently been shown that loss of Memo results in defective localization of lamellipodial markers and in a reduced number of short-lived adhesion sites (8). Further investigations need to be performed to answer this question.

In addition, we observed that upon FGFR inhibition Memo KD cells not only migrate to the same extent as the control cells, but performed even better, when we look 12 hours after plating. This supports the hypothesis that Memo KD cells are adapted to survive with low FGFR signaling. To further investigate the migration phenotype, scratch assays and migration towards a gradient in Dunn chamber assays could be performed [8].

### **8.4 The role of Memo in VEGF secretion**

By ELISA we show that Memo KD cells secrete or release less VEGF into the medium. VEGF secretion is essential for vascularization *in vivo* and it is well established that impaired FGFR signaling has an effect on vascularization (407). Some studies show that FGFR signaling upregulates VEGF expression, while others show that FGFR signaling mediates the upregulation of metalloproteinases needed for VEGF release from the cellular matrix [209]. The current study indicates that there are no differences in VEGF mRNA levels between control and Memo KD cells, which implies a post-translational defect, although this was tested by semi-quantitative PCR and not by qPCR. Our group published earlier that FGFR signaling is essential for matrix metalloproteinase (mmp) expression,

especially mmp-9, in 4T1 cells [398]. Therefore, we hypothesize that impaired FGFR signaling due to loss of Memo causes reduced expression of metalloproteinases, leading to impaired VEGF release. This hypothesis could be tested by transfection of a constitutively active AKT (myristoylated AKT) construct or by addition of mmp-9 conditioned medium to control and Memo KD cells.

### 8.5 The role of Memo in oxidative stress

This study provides evidence that Memo KD and KO cells are more sensitive to oxidative stress.  $\text{CoCl}_2$  is a hypoxia mimicking agent and an oxidative stress inducer (Figure 8-1b). We provide evidence that the observed effects of  $\text{CoCl}_2$  are not due to its hypoxic mimicking properties as there is HIF1 $\alpha$  activation in control and Memo KD cells.

Nevertheless, we observed that Memo KD and KO cells apoptose more strongly upon  $\text{CoCl}_2$  treatment as compared to control cells. In addition, we found that there is stronger activation of p38 in the Memo KD and KO cells. Therefore, we hypothesize that the increase of apoptosis is due to increased MAPK signaling. Oxidative stress is known to induce phosphorylation and potential kinase activation within four of the five main MAPK pathways [405-407]. Which one of the MAPK pathways is activated is largely dependent upon the origin of the cells and the level of oxidative stress applied. FGFR signaling has been shown to be important for survival of stressed cells by activating the AKT pathway. We have already shown in this study that Memo downregulation results in delayed AKT activation. This delayed activation of AKT could be a reason for the higher sensitivity of Memo KD cells upon stress induction.

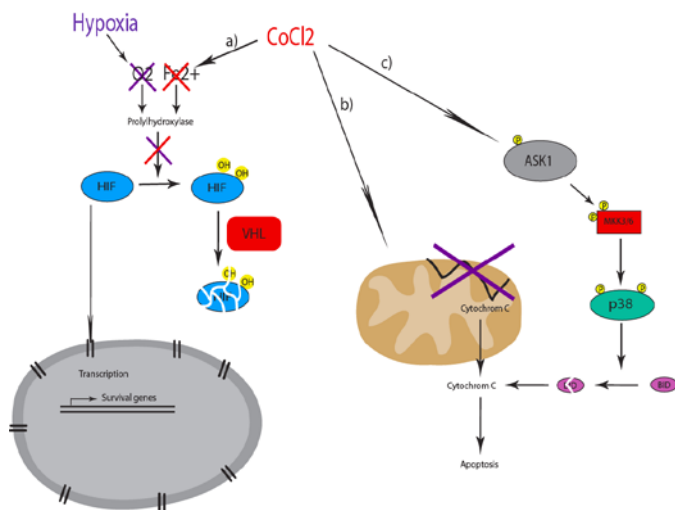


Figure 8-1 Effects of  $\text{CoCl}_2$

## Outlook and Discussion

- a)  $\text{CoCl}_2$  is a known hypoxia mimicking agent as it inhibits the prolylhydroxylase.
- b)  $\text{CoCl}_2$  induces apoptosis by inhibiting the respiratory chain and inducing oxygen reactive species (ROS) or by activating ASK-p38 signaling (c).

### 8.6 The role of Memo in TOR-HIF1 $\alpha$ crosstalk

In addition to looking at apoptosis, we also investigated cell signaling downstream of  $\text{CoCl}_2$ . Our data reveals that under strong hypoxic conditions (treatment of cells with  $500\mu\text{M}$   $\text{CoCl}_2$ ) the ribosomal protein S6 and 4E-BP1, both downstream targets of TOR, are hypophosphorylated. This suggests that Memo plays a role in the crosstalk between TOR and HIF1 $\alpha$ . It has been shown that TOR translationally attenuates HIF1 $\alpha$  (401). On the other hand, a negative feedback loop exists which shuts down TOR signaling under hypoxic conditions to ensure conservation of energy. In addition, it has been shown that constant transcriptional activity is required for S6 hypophosphorylation and that HIF1 $\alpha$  itself is involved in this transcription (401). Furthermore, it has also been shown that some translational activity has to take place under hypoxia. The mRNAs encoding these proteins are believed to have 5' terminal oligopyrimidine tract (TOP) sequences in their 5' untranslated regions, enabling Cap-independent translation. There is an ongoing discussion in the literature about the involvement of ribosomal protein S6 in the translation of mRNAs that harbor such 5' TOP sequences (408-410). Our data predicts that Memo plays a role in these crosstalks. To date it is not clear by which mechanism Memo would accomplish this. The observation that S6 and 4E-BP1 are hypophosphorylated in the Memo KD but not in the control cells further complicates the interpretation of these data as it is not clear what advantage the control cells would gain by inhibiting this hypophosphorylation. Nevertheless, these data suggest that Memo plays a role in this inhibition.

It has also been published that Klotho mutant mice show higher activity of p38 MAPK due to activation of the ASK1 complex [352]. They hypothesized that this is an indication for higher stress levels induced by higher levels of oxidative stress in those mice, caused by hyperphosphatemia. We didn't test the phosphorylation status of p38 in Memo mice yet, but higher basal level of oxidative stress in Memo KD cells could be another explanation for the higher sensitivity of those cells to (additional) stress upon  $\text{CoCl}_2$ . In addition, the observed higher phosphorylation status of p38 is another link between Memo and Klotho.

## 8.7 Conclusion

We have found that Memo null mice develop a severe premature aging phenotype, accompanied by an atypical metabolic phenotype which is shared by the Klotho and FGF23 mutant strains. We therefore investigated the similarities between our models and the Klotho and FGF23 mutant mice and conclude that as with these models: 1) Memo is downstream of FGFR signaling and specifically downstream of FGF23 signaling *in vitro*; 2) the FGF23-Klotho axis in the kidney is affected upon Memo deletion; 3) deletion of Memo either in the whole body or specifically in the kidney results in renal insufficiency as determined by blood and urine analyses; 4) Memo mice suffer from hypercalcemia and hypercalciuria; 5) there is an upregulation of TRPV5, NCX1 and CB28 in kidneys of the kidney-specific Memo KO mice; and finally, 6) Memo null mice exhibit lower PTH levels.

Despite of the many similarities found between our models and the Klotho and FGF23 mutant strains, we did not see the expected elevation in serum phosphate levels and there was no difference in the phosphate excretion. This is intriguing, as elevated serum phosphate levels have been shown to be the cause for this premature aging phenotype in the Klotho and FGF23 mutant animals (250, 257). To date we still do not have a definitive cause for the premature aging phenotype in Memo null animals. Our data suggest that the lower PTH levels in Memo null mice may promote the aging phenotype as it is thus far the only metabolic difference that we observe between the two Memo KO models.

Alternatively, vitamin D levels are known to induce premature aging symptoms when elevated (411) and we have yet to measure the serum levels in our Memo KO mice.

With these two mouse models we have the ideal tools at hand to investigate these differences in the future. Thus far, the question remains if those differences are nonspecific and simply due to the cumulative effect of Memo loss in multiple organs or if there is a specific twist in the FGF23-Klotho axis, e.g. due to Memo knock out in the parathyroid gland, that finally leads to the destructive phenotype of premature aging.

This study furthers our understanding of some of the mechanisms and key players in the processes of aging. As the average age of our population is constantly increasing due to better hygienic conditions, advances in disease treatment and prevention, as well as other factors, the symptoms of aging are

## Outlook and Discussion

becoming most influential on our quality of life. Deciphering the manner in which we age at a molecular level will hopefully lead to new developments for treatments of age related diseases, providing us all with better quality of life in our later years.



## 9 References

1. Plachov, D., Chowdhury, K., Walther, C., Simon, D., Guenet, J.L., and Gruss, P. 1990. Pax8, a murine paired box gene expressed in the developing excretory system and thyroid gland. *Development* 110:643-651.
2. Olayioye, M.A., Neve, R.M., Lane, H.A., and Hynes, N.E. 2000. The ErbB signaling network: receptor heterodimerization in development and cancer. *EMBO J* 19:3159-3167.
3. Heldin, C.H. 1996. Protein tyrosine kinase receptors. *Cancer Surv* 27:7-24.
4. Slamon, D.J., Clark, G.M., Wong, S.G., Levin, W.J., Ullrich, A., and McGuire, W.L. 1987. Human breast cancer: correlation of relapse and survival with amplification of the HER-2/neu oncogene. *Science* 235:177-182.
5. Qiu, C., Lienhard, S., Hynes, N.E., Badache, A., and Leahy, D.J. 2008. Memo is homologous to nonheme iron dioxygenases and binds an ErbB2-derived phosphopeptide in its vestigial active site. *J Biol Chem* 283:2734-2740.
6. Marone, R., Hess, D., Dankort, D., Muller, W.J., Hynes, N.E., and Badache, A. 2004. Memo mediates ErbB2-driven cell motility. *Nat Cell Biol* 6:515-522.
7. Feracci, M., Pimentel, C., Bornet, O., Roche, P., Salaun, D., Badache, A., and Guerlesquin, F. 2011. MEMO associated with an ErbB2 receptor phosphopeptide reveals a new phosphotyrosine motif. *FEBS Lett* 585:2688-2692.
8. Zaoui, K., Honore, S., Isnardon, D., Braguer, D., and Badache, A. 2008. Memo-RhoA-mDia1 signaling controls microtubules, the actin network, and adhesion site formation in migrating cells. *J Cell Biol* 183:401-408.
9. Meira, M., Masson, R., Stajljar, I., Lienhard, S., Maurer, F., Boulay, A., and Hynes, N.E. 2009. Memo is a cofilin-interacting protein that influences PLCgamma1 and cofilin activities, and is essential for maintaining directionality during ErbB2-induced tumor-cell migration. *J Cell Sci* 122:787-797.
10. Martin, G.R. 1998. The roles of FGFs in the early development of vertebrate limbs. *Genes Dev* 12:1571-1586.
11. Kato, S., and Sekine, K. 1999. FGF-FGFR signaling in vertebrate organogenesis. *Cell Mol Biol (Noisy-le-grand)* 45:631-638.
12. Powers, C.J., McLeskey, S.W., and Wellstein, A. 2000. Fibroblast growth factors, their receptors and signaling. *Endocr Relat Cancer* 7:165-197.
13. Dillon, C., Spencer-Dene, B., and Dickson, C. 2004. A crucial role for fibroblast growth factor signaling in embryonic mammary gland development. *J Mammary Gland Biol Neoplasia* 9:207-215.
14. Mailleux, A.A., Spencer-Dene, B., Dillon, C., Ndiaye, D., Savona-Baron, C., Itoh, N., Kato, S., Dickson, C., Thierry, J.P., and Bellusci, S. 2002. Role of FGF10/FGFR2b signaling during mammary gland development in the mouse embryo. *Development* 129:53-60.
15. Lu, P., Ewald, A.J., Martin, G.R., and Werb, Z. 2008. Genetic mosaic analysis reveals FGF receptor 2 function in terminal end buds during mammary gland branching morphogenesis. *Dev Biol* 321:77-87.
16. Parsa, S., Ramasamy, S.K., De Langhe, S., Gupte, V.V., Haigh, J.J., Medina, D., and Bellusci, S. 2008. Terminal end bud maintenance in mammary gland is dependent upon FGFR2b signaling. *Dev Biol* 317:121-131.

## References

17. Yu, C., Wang, F., Kan, M., Jin, C., Jones, R.B., Weinstein, M., Deng, C.X., and McKeehan, W.L. 2000. Elevated cholesterol metabolism and bile acid synthesis in mice lacking membrane tyrosine kinase receptor FGFR4. *J Biol Chem* 275:15482-15489.
18. Holt, J.A., Luo, G., Billin, A.N., Bisi, J., McNeill, Y.Y., Kozarsky, K.F., Donahee, M., Wang, D.Y., Mansfield, T.A., Kliewer, S.A., et al. 2003. Definition of a novel growth factor-dependent signal cascade for the suppression of bile acid biosynthesis. *Genes Dev* 17:1581-1591.
19. White, K.E., Jonsson, K.B., Carn, G., Hampson, G., Spector, T.D., Mannstadt, M., Lorenz-Depiereux, B., Miyauchi, A., Yang, I.M., Ljunggren, O., et al. 2001. The autosomal dominant hypophosphatemic rickets (ADHR) gene is a secreted polypeptide overexpressed by tumors that cause phosphate wasting. *J Clin Endocrinol Metab* 86:497-500.
20. White, K.E., Carn, G., Lorenz-Depiereux, B., Benet-Pages, A., Strom, T.M., and Econs, M.J. 2001. Autosomal-dominant hypophosphatemic rickets (ADHR) mutations stabilize FGF-23. *Kidney Int* 60:2079-2086.
21. Shimada, T., Mizutani, S., Muto, T., Yoneya, T., Hino, R., Takeda, S., Takeuchi, Y., Fujita, T., Fukumoto, S., and Yamashita, T. 2001. Cloning and characterization of FGF23 as a causative factor of tumor-induced osteomalacia. *Proc Natl Acad Sci U S A* 98:6500-6505.
22. Yamashita, T., Konishi, M., Miyake, A., Inui, K., and Itoh, N. 2002. Fibroblast growth factor (FGF)-23 inhibits renal phosphate reabsorption by activation of the mitogen-activated protein kinase pathway. *J Biol Chem* 277:28265-28270.
23. Shimada, T., Kakitani, M., Yamazaki, Y., Hasegawa, H., Takeuchi, Y., Fujita, T., Fukumoto, S., Tomizuka, K., and Yamashita, T. 2004. Targeted ablation of Fgf23 demonstrates an essential physiological role of FGF23 in phosphate and vitamin D metabolism. *J Clin Invest* 113:561-568.
24. Shimada, T., Hasegawa, H., Yamazaki, Y., Muto, T., Hino, R., Takeuchi, Y., Fujita, T., Nakahara, K., Fukumoto, S., and Yamashita, T. 2004. FGF-23 is a potent regulator of vitamin D metabolism and phosphate homeostasis. *J Bone Miner Res* 19:429-435.
25. Murakami, M., and Simons, M. 2008. Fibroblast growth factor regulation of neovascularization. *Curr Opin Hematol* 15:215-220.
26. Miraoui, H., and Marie, P.J. 2010. Fibroblast growth factor receptor signaling crosstalk in skeletogenesis. *Sci Signal* 3:re9.
27. Dode, C., Levilliers, J., Dupont, J.M., De Paepe, A., Le Du, N., Soussi-Yanicostas, N., Coimbra, R.S., Delmaghani, S., Compain-Nouaille, S., Baverel, F., et al. 2003. Loss-of-function mutations in FGFR1 cause autosomal dominant Kallmann syndrome. *Nat Genet* 33:463-465.
28. DiMeglio, L.A., and Econs, M.J. 2001. Hypophosphatemic rickets. *Rev Endocr Metab Disord* 2:165-173.
29. Econs, M.J. 1999. New insights into the pathogenesis of inherited phosphate wasting disorders. *Bone* 25:131-135.
30. Dickson, C., Spencer-Dene, B., Dillon, C., and Fantl, V. 2000. Tyrosine kinase signalling in breast cancer: fibroblast growth factors and their receptors. *Breast Cancer Res* 2:191-196.
31. Moroni, E., Dell'Era, P., Rusnati, M., and Presta, M. 2002. Fibroblast growth factors and their receptors in hematopoiesis and hematological tumors. *J Hematother Stem Cell Res* 11:19-32.
32. Cronauer, M.V., Schulz, W.A., Seifert, H.H., Ackermann, R., and Burchardt, M. 2003. Fibroblast growth factors and their receptors in urological cancers: basic research and clinical implications. *Eur Urol* 43:309-319.
33. Hunter, T. 2000. Signaling--2000 and beyond. *Cell* 100:113-127.

## References

34. Schlessinger, J. 2000. Cell signaling by receptor tyrosine kinases. *Cell* 103:211-225.
35. Schlessinger, J., Plotnikov, A.N., Ibrahimi, O.A., Eliseenkova, A.V., Yeh, B.K., Yayon, A., Linhardt, R.J., and Mohammadi, M. 2000. Crystal structure of a ternary FGF-FGFR-heparin complex reveals a dual role for heparin in FGFR binding and dimerization. *Mol Cell* 6:743-750.
36. Ong, S.H., Guy, G.R., Hadari, Y.R., Laks, S., Gotoh, N., Schlessinger, J., and Lax, I. 2000. FRS2 proteins recruit intracellular signaling pathways by binding to diverse targets on fibroblast growth factor and nerve growth factor receptors. *Mol Cell Biol* 20:979-989.
37. Dhalluin, C., Yan, K.S., Plotnikova, O., Lee, K.W., Zeng, L., Kutu, M., Mujtaba, S., Goldfarb, M.P., and Zhou, M.M. 2000. Structural basis of SNT PTB domain interactions with distinct neurotrophic receptors. *Mol Cell* 6:921-929.
38. Mohammadi, M., Dikic, I., Sorokin, A., Burgess, W.H., Jaye, M., and Schlessinger, J. 1996. Identification of six novel autophosphorylation sites on fibroblast growth factor receptor 1 and elucidation of their importance in receptor activation and signal transduction. *Mol Cell Biol* 16:977-989.
39. Mohammadi, M., Honegger, A.M., Rotin, D., Fischer, R., Bellot, F., Li, W., Dionne, C.A., Jaye, M., Rubinstein, M., and Schlessinger, J. 1991. A tyrosine-phosphorylated carboxy-terminal peptide of the fibroblast growth factor receptor (Flg) is a binding site for the SH2 domain of phospholipase C-gamma 1. *Mol Cell Biol* 11:5068-5078.
40. Deng, C.X., Wynshaw-Boris, A., Shen, M.M., Daugherty, C., Ornitz, D.M., and Leder, P. 1994. Murine FGFR-1 is required for early postimplantation growth and axial organization. *Genes Dev* 8:3045-3057.
41. Yamaguchi, T.P., Harpal, K., Henkemeyer, M., and Rossant, J. 1994. fgfr-1 is required for embryonic growth and mesodermal patterning during mouse gastrulation. *Genes Dev* 8:3032-3044.
42. Arman, E., Haffner-Krausz, R., Chen, Y., Heath, J.K., and Lonai, P. 1998. Targeted disruption of fibroblast growth factor (FGF) receptor 2 suggests a role for FGF signaling in pregastrulation mammalian development. *Proc Natl Acad Sci U S A* 95:5082-5087.
43. Colvin, J.S., Bohne, B.A., Harding, G.W., McEwen, D.G., and Ornitz, D.M. 1996. Skeletal overgrowth and deafness in mice lacking fibroblast growth factor receptor 3. *Nat Genet* 12:390-397.
44. Deng, C., Wynshaw-Boris, A., Zhou, F., Kuo, A., and Leder, P. 1996. Fibroblast growth factor receptor 3 is a negative regulator of bone growth. *Cell* 84:911-921.
45. Weinstein, M., Xu, X., Ohyama, K., and Deng, C.X. 1998. FGFR-3 and FGFR-4 function cooperatively to direct alveogenesis in the murine lung. *Development* 125:3615-3623.
46. Yu, K., Herr, A.B., Waksman, G., and Ornitz, D.M. 2000. Loss of fibroblast growth factor receptor 2 ligand-binding specificity in Apert syndrome. *Proc Natl Acad Sci U S A* 97:14536-14541.
47. Ornitz, D.M., and Itoh, N. 2001. Fibroblast growth factors. *Genome Biol* 2:REVIEWS3005.
48. Mohammadi, M., Olsen, S.K., and Ibrahimi, O.A. 2005. Structural basis for fibroblast growth factor receptor activation. *Cytokine Growth Factor Rev* 16:107-137.
49. Goetz, R., Beenken, A., Ibrahimi, O.A., Kalinina, J., Olsen, S.K., Eliseenkova, A.V., Xu, C., Neubert, T.A., Zhang, F., Linhardt, R.J., et al. 2007. Molecular insights into the klotho-dependent, endocrine mode of action of fibroblast growth factor 19 subfamily members. *Mol Cell Biol* 27:3417-3428.
50. Cuevas, P., Carceller, F., Ortega, S., Zazo, M., Nieto, I., and Gimenez-Gallego, G. 1991.

## References

- Hypotensive activity of fibroblast growth factor. *Science* 254:1208-1210.
51. Cuevas, P., Garcia-Calvo, M., Carceller, F., Reimers, D., Zazo, M., Cuevas, B., Munoz-Willery, I., Martinez-Coso, V., Lamas, S., and Gimenez-Gallego, G. 1996. Correction of hypertension by normalization of endothelial levels of fibroblast growth factor and nitric oxide synthase in spontaneously hypertensive rats. *Proc Natl Acad Sci U S A* 93:11996-12001.
  52. Ware, J.A., and Simons, M. 1997. Angiogenesis in ischemic heart disease. *Nat Med* 3:158-164.
  53. Yanagisawa-Miwa, A., Uchida, Y., Nakamura, F., Tomaru, T., Kido, H., Kamijo, T., Sugimoto, T., Kaji, K., Utsuyama, M., Kurashima, C., et al. 1992. Salvage of infarcted myocardium by angiogenic action of basic fibroblast growth factor. *Science* 257:1401-1403.
  54. Scholz, D., Cai, W.J., and Schaper, W. 2001. Arteriogenesis, a new concept of vascular adaptation in occlusive disease. *Angiogenesis* 4:247-257.
  55. Khurana, R., and Simons, M. 2003. Insights from angiogenesis trials using fibroblast growth factor for advanced arteriosclerotic disease. *Trends Cardiovasc Med* 13:116-122.
  56. Sugi, Y., Ito, N., Szebenyi, G., Myers, K., Fallon, J.F., Mikawa, T., and Markwald, R.R. 2003. Fibroblast growth factor (FGF)-4 can induce proliferation of cardiac cushion mesenchymal cells during early valve leaflet formation. *Dev Biol* 258:252-263.
  57. Sun, X., Mariani, F.V., and Martin, G.R. 2002. Functions of FGF signalling from the apical ectodermal ridge in limb development. *Nature* 418:501-508.
  58. Feldman, B., Poueymirou, W., Papaioannou, V.E., DeChiara, T.M., and Goldfarb, M. 1995. Requirement of FGF-4 for postimplantation mouse development. *Science* 267:246-249.
  59. Hebert, J.M., Rosenquist, T., Gotz, J., and Martin, G.R. 1994. FGF5 as a regulator of the hair growth cycle: evidence from targeted and spontaneous mutations. *Cell* 78:1017-1025.
  60. Armand, A.S., Laziz, I., and Chanoine, C. 2006. FGF6 in myogenesis. *Biochim Biophys Acta* 1763:773-778.
  61. Werner, S., Peters, K.G., Longaker, M.T., Fuller-Pace, F., Banda, M.J., and Williams, L.T. 1992. Large induction of keratinocyte growth factor expression in the dermis during wound healing. *Proc Natl Acad Sci U S A* 89:6896-6900.
  62. Baskin, L.S., Sutherland, R.S., Thomson, A.A., Nguyen, H.T., Morgan, D.M., Hayward, S.W., Hom, Y.K., DiSandro, M., and Cunha, G.R. 1997. Growth factors in bladder wound healing. *J Urol* 157:2388-2395.
  63. Ichimura, T., Finch, P.W., Zhang, G., Kan, M., and Stevens, J.L. 1996. Induction of FGF-7 after kidney damage: a possible paracrine mechanism for tubule repair. *Am J Physiol* 271:F967-976.
  64. Tekin, M., Hismi, B.O., Fitoz, S., Ozdag, H., Cengiz, F.B., Sirmaci, A., Aslan, I., Inceoglu, B., Yuksel-Konuk, E.B., Yilmaz, S.T., et al. 2007. Homozygous mutations in fibroblast growth factor 3 are associated with a new form of syndromic deafness characterized by inner ear agenesis, microtia, and microdontia. *Am J Hum Genet* 80:338-344.
  65. Min, H., Danilenko, D.M., Scully, S.A., Bolon, B., Ring, B.D., Tarpley, J.E., DeRose, M., and Simonet, W.S. 1998. Fgf-10 is required for both limb and lung development and exhibits striking functional similarity to Drosophila branchless. *Genes Dev* 12:3156-3161.
  66. Umemori, H., Linhoff, M.W., Ornitz, D.M., and Sanes, J.R. 2004. FGF22 and its close relatives are presynaptic organizing molecules in the mammalian brain. *Cell* 118:257-270.
  67. Liu, X.H., Aigner, A., Wellstein, A., and Ray, P.E. 2001. Up-regulation of a fibroblast growth factor binding protein in children with renal diseases. *Kidney Int* 59:1717-1728.
  68. O'Leary, D.D., Chou, S.J., and Sahara, S. 2007. Area patterning of the mammalian cortex. *Neuron* 56:252-269.

## References

69. Meyers, E.N., Lewandoski, M., and Martin, G.R. 1998. An Fgf8 mutant allelic series generated by Cre- and Flp-mediated recombination. *Nat Genet* 18:136-141.
70. Xu, J., Liu, Z., and Ornitz, D.M. 2000. Temporal and spatial gradients of Fgf8 and Fgf17 regulate proliferation and differentiation of midline cerebellar structures. *Development* 127:1833-1843.
71. Liu, Z., Xu, J., Colvin, J.S., and Ornitz, D.M. 2002. Coordination of chondrogenesis and osteogenesis by fibroblast growth factor 18. *Genes Dev* 16:859-869.
72. Ohbayashi, N., Shibayama, M., Kurotaki, Y., Imanishi, M., Fujimori, T., Itoh, N., and Takada, S. 2002. FGF18 is required for normal cell proliferation and differentiation during osteogenesis and chondrogenesis. *Genes Dev* 16:870-879.
73. Colvin, J.S., Green, R.P., Schmahl, J., Capel, B., and Ornitz, D.M. 2001. Male-to-female sex reversal in mice lacking fibroblast growth factor 9. *Cell* 104:875-889.
74. Colvin, J.S., White, A.C., Pratt, S.J., and Ornitz, D.M. 2001. Lung hypoplasia and neonatal death in Fgf9-null mice identify this gene as an essential regulator of lung mesenchyme. *Development* 128:2095-2106.
75. Lu, S.Y., Sheikh, F., Sheppard, P.C., Fresnoza, A., Duckworth, M.L., Detillieux, K.A., and Cattini, P.A. 2008. FGF-16 is required for embryonic heart development. *Biochem Biophys Res Commun* 373:270-274.
76. Grose, R., and Dickson, C. 2005. Fibroblast growth factor signaling in tumorigenesis. *Cytokine Growth Factor Rev* 16:179-186.
77. Aigner, A., Butscheid, M., Kunkel, P., Krause, E., Lamszus, K., Wellstein, A., and Czubayko, F. 2001. An FGF-binding protein (FGF-BP) exerts its biological function by parallel paracrine stimulation of tumor cell and endothelial cell proliferation through FGF-2 release. *Int J Cancer* 92:510-517.
78. Bottcher, R.T., Pollet, N., Delius, H., and Niehrs, C. 2004. The transmembrane protein XFLRT3 forms a complex with FGF receptors and promotes FGF signalling. *Nat Cell Biol* 6:38-44.
79. Casu, B. 1985. Structure and biological activity of heparin. *Adv Carbohydr Chem Biochem* 43:51-134.
80. Plotnikov, A.N., Schlessinger, J., Hubbard, S.R., and Mohammadi, M. 1999. Structural basis for FGF receptor dimerization and activation. *Cell* 98:641-650.
81. Kjellen, L., and Lindahl, U. 1991. Proteoglycans: structures and interactions. *Annu Rev Biochem* 60:443-475.
82. Rapraeger, A.C. 1993. The coordinated regulation of heparan sulfate, syndecans and cell behavior. *Curr Opin Cell Biol* 5:844-853.
83. Gospodarowicz, D., and Cheng, J. 1986. Heparin protects basic and acidic FGF from inactivation. *J Cell Physiol* 128:475-484.
84. Saksela, O., Moscatelli, D., Sommer, A., and Rifkin, D.B. 1988. Endothelial cell-derived heparan sulfate binds basic fibroblast growth factor and protects it from proteolytic degradation. *J Cell Biol* 107:743-751.
85. Vlodavsky, I., Folkman, J., Sullivan, R., Fridman, R., Ishai-Michaeli, R., Sasse, J., and Klagsbrun, M. 1987. Endothelial cell-derived basic fibroblast growth factor: synthesis and deposition into subendothelial extracellular matrix. *Proc Natl Acad Sci U S A* 84:2292-2296.
86. Baird, A., and Ling, N. 1987. Fibroblast growth factors are present in the extracellular matrix produced by endothelial cells in vitro: implications for a role of heparinase-like enzymes in the neovascular response. *Biochem Biophys Res Commun* 142:428-435.

## References

87. Folkman, J., Klagsbrun, M., Sasse, J., Wadzinski, M., Ingber, D., and Vlodavsky, I. 1988. A heparin-binding angiogenic protein--basic fibroblast growth factor--is stored within basement membrane. *Am J Pathol* 130:393-400.
88. Bashkin, P., Doctrow, S., Klagsbrun, M., Svahn, C.M., Folkman, J., and Vlodavsky, I. 1989. Basic fibroblast growth factor binds to subendothelial extracellular matrix and is released by heparitinase and heparin-like molecules. *Biochemistry* 28:1737-1743.
89. Flaumenhaft, R., Moscatelli, D., Saksela, O., and Rifkin, D.B. 1989. Role of extracellular matrix in the action of basic fibroblast growth factor: matrix as a source of growth factor for long-term stimulation of plasminogen activator production and DNA synthesis. *J Cell Physiol* 140:75-81.
90. Schlessinger, J., Lax, I., and Lemmon, M. 1995. Regulation of growth factor activation by proteoglycans: what is the role of the low affinity receptors? *Cell* 83:357-360.
91. Jacobs, A.L., Julian, J., Sahin, A.A., and Carson, D.D. 1997. Heparin/heparan sulfate interacting protein expression and functions in human breast cancer cells and normal breast epithelia. *Cancer Res* 57:5148-5154.
92. Kuro-o, M., Matsumura, Y., Aizawa, H., Kawaguchi, H., Suga, T., Utsugi, T., Ohyama, Y., Kurabayashi, M., Kaname, T., Kume, E., et al. 1997. Mutation of the mouse klotho gene leads to a syndrome resembling ageing. *Nature* 390:45-51.
93. Ito, S., Kinoshita, S., Shiraishi, N., Nakagawa, S., Sekine, S., Fujimori, T., and Nabeshima, Y.I. 2000. Molecular cloning and expression analyses of mouse betaklotho, which encodes a novel Klotho family protein. *Mech Dev* 98:115-119.
94. Davies, G., and Henrissat, B. 1995. Structures and mechanisms of glycosyl hydrolases. *Structure* 3:853-859.
95. Wang, Q., Trimbur, D., Graham, R., Warren, R.A., and Withers, S.G. 1995. Identification of the acid/base catalyst in *Agrobacterium faecalis* beta-glucosidase by kinetic analysis of mutants. *Biochemistry* 34:14554-14562.
96. Kurosu, H., Ogawa, Y., Miyoshi, M., Yamamoto, M., Nandi, A., Rosenblatt, K.P., Baum, M.G., Schiavi, S., Hu, M.C., Moe, O.W., et al. 2006. Regulation of fibroblast growth factor-23 signaling by klotho. *J Biol Chem* 281:6120-6123.
97. Urakawa, I., Yamazaki, Y., Shimada, T., Iijima, K., Hasegawa, H., Okawa, K., Fujita, T., Fukumoto, S., and Yamashita, T. 2006. Klotho converts canonical FGF receptor into a specific receptor for FGF23. *Nature* 444:770-774.
98. Gotoh, N., Laks, S., Nakashima, M., Lax, I., and Schlessinger, J. 2004. FRS2 family docking proteins with overlapping roles in activation of MAP kinase have distinct spatial-temporal patterns of expression of their transcripts. *FEBS Lett* 564:14-18.
99. Kodama, Y., Asai, N., Kawai, K., Jijiwa, M., Murakumo, Y., Ichihara, M., and Takahashi, M. 2005. The RET proto-oncogene: a molecular therapeutic target in thyroid cancer. *Cancer Sci* 96:143-148.
100. Kurokawa, K., Iwashita, T., Murakami, H., Hayashi, H., Kawai, K., and Takahashi, M. 2001. Identification of SNT/FRS2 docking site on RET receptor tyrosine kinase and its role for signal transduction. *Oncogene* 20:1929-1938.
101. Melillo, R.M., Santoro, M., Ong, S.H., Billaud, M., Fusco, A., Hadari, Y.R., Schlessinger, J., and Lax, I. 2001. Docking protein FRS2 links the protein tyrosine kinase RET and its oncogenic forms with the mitogen-activated protein kinase signaling cascade. *Mol Cell Biol* 21:4177-4187.
102. Degoutin, J., Vigny, M., and Gouzi, J.Y. 2007. ALK activation induces Shc and FRS2

## References

- recruitment: Signaling and phenotypic outcomes in PC12 cells differentiation. *FEBS Lett* 581:727-734.
103. Kouhara, H., Hadari, Y.R., Spivak-Kroizman, T., Schilling, J., Bar-Sagi, D., Lax, I., and Schlessinger, J. 1997. A lipid-anchored Grb2-binding protein that links FGF-receptor activation to the Ras/MAPK signaling pathway. *Cell* 89:693-702.
  104. Hadari, Y.R., Kouhara, H., Lax, I., and Schlessinger, J. 1998. Binding of Shp2 tyrosine phosphatase to FRS2 is essential for fibroblast growth factor-induced PC12 cell differentiation. *Mol Cell Biol* 18:3966-3973.
  105. Eswarakumar, V.P., Lax, I., and Schlessinger, J. 2005. Cellular signaling by fibroblast growth factor receptors. *Cytokine Growth Factor Rev* 16:139-149.
  106. Altomare, D.A., and Testa, J.R. 2005. Perturbations of the AKT signaling pathway in human cancer. *Oncogene* 24:7455-7464.
  107. Lax, I., Wong, A., Lamothe, B., Lee, A., Frost, A., Hawes, J., and Schlessinger, J. 2002. The docking protein FRS2alpha controls a MAP kinase-mediated negative feedback mechanism for signaling by FGF receptors. *Mol Cell* 10:709-719.
  108. Gotoh, N. 2008. Regulation of growth factor signaling by FRS2 family docking/scaffold adaptor proteins. *Cancer Sci* 99:1319-1325.
  109. Klint, P., and Claesson-Welsh, L. 1999. Signal transduction by fibroblast growth factor receptors. *Front Biosci* 4:D165-177.
  110. Falasca, M., Logan, S.K., Lehto, V.P., Baccante, G., Lemmon, M.A., and Schlessinger, J. 1998. Activation of phospholipase C gamma by PI 3-kinase-induced PH domain-mediated membrane targeting. *EMBO J* 17:414-422.
  111. Hart, K.C., Robertson, S.C., Kanemitsu, M.Y., Meyer, A.N., Tynan, J.A., and Donoghue, D.J. 2000. Transformation and Stat activation by derivatives of FGFR1, FGFR3, and FGFR4. *Oncogene* 19:3309-3320.
  112. Kang, S., Elf, S., Dong, S., Hitosugi, T., Lythgoe, K., Guo, A., Ruan, H., Lonial, S., Khoury, H.J., Williams, I.R., et al. 2009. Fibroblast growth factor receptor 3 associates with and tyrosine phosphorylates p90 RSK2, leading to RSK2 activation that mediates hematopoietic transformation. *Mol Cell Biol* 29:2105-2117.
  113. Thien, C.B., and Langdon, W.Y. 2001. Cbl: many adaptations to regulate protein tyrosine kinases. *Nat Rev Mol Cell Biol* 2:294-307.
  114. Wong, A., Lamothe, B., Lee, A., Schlessinger, J., and Lax, I. 2002. FRS2 alpha attenuates FGF receptor signaling by Grb2-mediated recruitment of the ubiquitin ligase Cbl. *Proc Natl Acad Sci U S A* 99:6684-6689.
  115. Zhao, Y., and Zhang, Z.Y. 2001. The mechanism of dephosphorylation of extracellular signal-regulated kinase 2 by mitogen-activated protein kinase phosphatase 3. *J Biol Chem* 276:32382-32391.
  116. Casci, T., Vinos, J., and Freeman, M. 1999. Sprouty, an intracellular inhibitor of Ras signaling. *Cell* 96:655-665.
  117. Hacohen, N., Kramer, S., Sutherland, D., Hiromi, Y., and Krasnow, M.A. 1998. sprouty encodes a novel antagonist of FGF signaling that patterns apical branching of the Drosophila airways. *Cell* 92:253-263.
  118. Furthauer, M., Lin, W., Ang, S.L., Thisse, B., and Thisse, C. 2002. Sef is a feedback-induced antagonist of Ras/MAPK-mediated FGF signalling. *Nat Cell Biol* 4:170-174.
  119. Tsang, M., Friesel, R., Kudoh, T., and Dawid, I.B. 2002. Identification of Sef, a novel

## References

- modulator of FGF signalling. *Nat Cell Biol* 4:165-169.
120. Thisse, B., and Thisse, C. 2005. Functions and regulations of fibroblast growth factor signaling during embryonic development. *Dev Biol* 287:390-402.
  121. Tsang, M., and Dawid, I.B. 2004. Promotion and attenuation of FGF signaling through the Ras-MAPK pathway. *Sci STKE* 2004:pe17.
  122. Francavilla, C., Cattaneo, P., Berezin, V., Bock, E., Ami, D., de Marco, A., Christofori, G., and Cavallaro, U. 2009. The binding of NCAM to FGFR1 induces a specific cellular response mediated by receptor trafficking. *J Cell Biol* 187:1101-1116.
  123. Chin, K., DeVries, S., Fridlyand, J., Spellman, P.T., Roydasgupta, R., Kuo, W.L., Lapuk, A., Neve, R.M., Qian, Z., Ryder, T., et al. 2006. Genomic and transcriptional aberrations linked to breast cancer pathophysiologies. *Cancer Cell* 10:529-541.
  124. Toyokawa, T., Yashiro, M., and Hirakawa, K. 2009. Co-expression of keratinocyte growth factor and K-sam is an independent prognostic factor in gastric carcinoma. *Oncol Rep* 21:875-880.
  125. Behrens, C., Lin, H.Y., Lee, J.J., Raso, M.G., Hong, W.K., Wistuba, II, and Lotan, R. 2008. Immunohistochemical expression of basic fibroblast growth factor and fibroblast growth factor receptors 1 and 2 in the pathogenesis of lung cancer. *Clin Cancer Res* 14:6014-6022.
  126. Kwabi-Addo, B., Ozen, M., and Ittmann, M. 2004. The role of fibroblast growth factors and their receptors in prostate cancer. *Endocr Relat Cancer* 11:709-724.
  127. Chang, H., Stewart, A.K., Qi, X.Y., Li, Z.H., Yi, Q.L., and Trudel, S. 2005. Immunohistochemistry accurately predicts FGFR3 aberrant expression and t(4;14) in multiple myeloma. *Blood* 106:353-355.
  128. Allerstorfer, S., Sonvilla, G., Fischer, H., Spiegl-Kreinecker, S., Gauglhofer, C., Setinek, U., Czech, T., Marosi, C., Buchroithner, J., Pichler, J., et al. 2008. FGF5 as an oncogenic factor in human glioblastoma multiforme: autocrine and paracrine activities. *Oncogene* 27:4180-4190.
  129. Freier, K., Schwaenen, C., Sticht, C., Flechtenmacher, C., Muhling, J., Hofele, C., Radlwimmer, B., Lichter, P., and Joos, S. 2007. Recurrent FGFR1 amplification and high FGFR1 protein expression in oral squamous cell carcinoma (OSCC). *Oral Oncol* 43:60-66.
  130. Baird, K., Davis, S., Antonescu, C.R., Harper, U.L., Walker, R.L., Chen, Y., Glatfelter, A.A., Duray, P.H., and Meltzer, P.S. 2005. Gene expression profiling of human sarcomas: insights into sarcoma biology. *Cancer Res* 65:9226-9235.
  131. Nord, H., Segersten, U., Sandgren, J., Wester, K., Busch, C., Menzel, U., Komorowski, J., Dumanski, J.P., Malmstrom, P.U., and Diaz de Stahl, T. 2010. Focal amplifications are associated with high grade and recurrences in stage Ta bladder carcinoma. *Int J Cancer* 126:1390-1402.
  132. Courjal, F., Cuny, M., Simony-Lafontaine, J., Louason, G., Speiser, P., Zeillinger, R., Rodriguez, C., and Theillet, C. 1997. Mapping of DNA amplifications at 15 chromosomal localizations in 1875 breast tumors: definition of phenotypic groups. *Cancer Res* 57:4360-4367.
  133. Jacquemier, J., Adelaide, J., Parc, P., Penault-Llorca, F., Planche, J., deLapeyriere, O., and Birnbaum, D. 1994. Expression of the FGFR1 gene in human breast-carcinoma cells. *Int J Cancer* 59:373-378.
  134. Reis-Filho, J.S., Simpson, P.T., Turner, N.C., Lambros, M.B., Jones, C., Mackay, A., Grigoriadis, A., Sarriso, D., Savage, K., Dexter, T., et al. 2006. FGFR1 emerges as a potential therapeutic target for lobular breast carcinomas. *Clin Cancer Res* 12:6652-6662.
  135. Gorringer, K.L., Jacobs, S., Thompson, E.R., Sridhar, A., Qiu, W., Choong, D.Y., and Campbell,



## References

- I.G. 2007. High-resolution single nucleotide polymorphism array analysis of epithelial ovarian cancer reveals numerous microdeletions and amplifications. *Clin Cancer Res* 13:4731-4739.
136. Simon, R., Richter, J., Wagner, U., Fijan, A., Bruderer, J., Schmid, U., Ackermann, D., Maurer, R., Alund, G., Knonagel, H., et al. 2001. High-throughput tissue microarray analysis of 3p25 (RAF1) and 8p12 (FGFR1) copy number alterations in urinary bladder cancer. *Cancer Res* 61:4514-4519.
137. Missiaglia, E., Selfe, J., Hamdi, M., Williamson, D., Schaaf, G., Fang, C., Koster, J., Summersgill, B., Messahel, B., Versteeg, R., et al. 2009. Genomic imbalances in rhabdomyosarcoma cell lines affect expression of genes frequently altered in primary tumors: an approach to identify candidate genes involved in tumor development. *Genes Chromosomes Cancer* 48:455-467.
138. Kunii, K., Davis, L., Gorenstein, J., Hatch, H., Yashiro, M., Di Bacco, A., Elbi, C., and Lutterbach, B. 2008. FGFR2-amplified gastric cancer cell lines require FGFR2 and Erbb3 signaling for growth and survival. *Cancer Res* 68:2340-2348.
139. Takeda, M., Arao, T., Yokote, H., Komatsu, T., Yanagihara, K., Sasaki, H., Yamada, Y., Tamura, T., Fukuoka, K., Kimura, H., et al. 2007. AZD2171 shows potent antitumor activity against gastric cancer over-expressing fibroblast growth factor receptor 2/keratinocyte growth factor receptor. *Clin Cancer Res* 13:3051-3057.
140. Rand, V., Huang, J., Stockwell, T., Ferriera, S., Buzko, O., Levy, S., Busam, D., Li, K., Edwards, J.B., Eberhart, C., et al. 2005. Sequence survey of receptor tyrosine kinases reveals mutations in glioblastomas. *Proc Natl Acad Sci U S A* 102:14344-14349.
141. Chou, A., Dekker, N., and Jordan, R.C. 2009. Identification of novel fibroblast growth factor receptor 3 gene mutations in actinic cheilitis and squamous cell carcinoma of the lip. *Oral Surg Oral Med Oral Pathol Oral Radiol Endod* 107:535-541.
142. Greenman, C., Stephens, P., Smith, R., Dalglish, G.L., Hunter, C., Bignell, G., Davies, H., Teague, J., Butler, A., Stevens, C., et al. 2007. Patterns of somatic mutation in human cancer genomes. *Nature* 446:153-158.
143. Davies, H., Hunter, C., Smith, R., Stephens, P., Greenman, C., Bignell, G., Teague, J., Butler, A., Edkins, S., Stevens, C., et al. 2005. Somatic mutations of the protein kinase gene family in human lung cancer. *Cancer Res* 65:7591-7595.
144. Ruhe, J.E., Streit, S., Hart, S., Wong, C.H., Specht, K., Knyazev, P., Knyazeva, T., Tay, L.S., Loo, H.L., Foo, P., et al. 2007. Genetic alterations in the tyrosine kinase transcriptome of human cancer cell lines. *Cancer Res* 67:11368-11376.
145. Tomlinson, D.C., Hurst, C.D., and Knowles, M.A. 2007. Knockdown by shRNA identifies S249C mutant FGFR3 as a potential therapeutic target in bladder cancer. *Oncogene* 26:5889-5899.
146. van Rhijn, B.W., van Tilborg, A.A., Lurkin, I., Bonaventure, J., de Vries, A., Thiery, J.P., van der Kwast, T.H., Zwarthoff, E.C., and Radvanyi, F. 2002. Novel fibroblast growth factor receptor 3 (FGFR3) mutations in bladder cancer previously identified in non-lethal skeletal disorders. *Eur J Hum Genet* 10:819-824.
147. van Rhijn, B.W., Montironi, R., Zwarthoff, E.C., Jobsis, A.C., and van der Kwast, T.H. 2002. Frequent FGFR3 mutations in urothelial papilloma. *J Pathol* 198:245-251.
148. Stephens, P., Edkins, S., Davies, H., Greenman, C., Cox, C., Hunter, C., Bignell, G., Teague, J., Smith, R., Stevens, C., et al. 2005. A screen of the complete protein kinase gene family identifies diverse patterns of somatic mutations in human breast cancer. *Nat Genet* 37:590-592.

## References

149. Jang, J.H., Shin, K.H., and Park, J.G. 2001. Mutations in fibroblast growth factor receptor 2 and fibroblast growth factor receptor 3 genes associated with human gastric and colorectal cancers. *Cancer Res* 61:3541-3543.
150. Hernandez, S., de Muga, S., Agell, L., Juanpere, N., Esgueva, R., Lorente, J.A., Mojal, S., Serrano, S., and Lloreta, J. 2009. FGFR3 mutations in prostate cancer: association with low-grade tumors. *Mod Pathol* 22:848-856.
151. Dutt, A., Salvesen, H.B., Chen, T.H., Ramos, A.H., Onofrio, R.C., Hatton, C., Nicoletti, R., Winckler, W., Grewal, R., Hanna, M., et al. 2008. Drug-sensitive FGFR2 mutations in endometrial carcinoma. *Proc Natl Acad Sci U S A* 105:8713-8717.
152. Ding, L., Getz, G., Wheeler, D.A., Mardis, E.R., McLellan, M.D., Cibulskis, K., Sougnez, C., Greulich, H., Muzny, D.M., Morgan, M.B., et al. 2008. Somatic mutations affect key pathways in lung adenocarcinoma. *Nature* 455:1069-1075.
153. Pollock, P.M., Gartside, M.G., Dejeza, L.C., Powell, M.A., Mallon, M.A., Davies, H., Mohammadi, M., Futreal, P.A., Stratton, M.R., Trent, J.M., et al. 2007. Frequent activating FGFR2 mutations in endometrial carcinomas parallel germline mutations associated with craniosynostosis and skeletal dysplasia syndromes. *Oncogene* 26:7158-7162.
154. Chesi, M., Brents, L.A., Ely, S.A., Bais, C., Robbiani, D.F., Mesri, E.A., Kuehl, W.M., and Bergsagel, P.L. 2001. Activated fibroblast growth factor receptor 3 is an oncogene that contributes to tumor progression in multiple myeloma. *Blood* 97:729-736.
155. Ornitz, D.M., and Marie, P.J. 2002. FGF signaling pathways in endochondral and intramembranous bone development and human genetic disease. *Genes Dev* 16:1446-1465.
156. Cappellen, D., De Oliveira, C., Ricol, D., de Medina, S., Bourdin, J., Sastre-Garau, X., Chopin, D., Thiery, J.P., and Radvanyi, F. 1999. Frequent activating mutations of FGFR3 in human bladder and cervix carcinomas. *Nat Genet* 23:18-20.
157. Rosty, C., Aubriot, M.H., Cappellen, D., Bourdin, J., Cartier, I., Thiery, J.P., Sastre-Garau, X., and Radvanyi, F. 2005. Clinical and biological characteristics of cervical neoplasias with FGFR3 mutation. *Mol Cancer* 4:15.
158. Goriely, A., Hansen, R.M., Taylor, I.B., Olesen, I.A., Jacobsen, G.K., McGowan, S.J., Pfeifer, S.P., McVean, G.A., Meyts, E.R., and Wilkie, A.O. 2009. Activating mutations in FGFR3 and HRAS reveal a shared genetic origin for congenital disorders and testicular tumors. *Nat Genet* 41:1247-1252.
159. Naski, M.C., Wang, Q., Xu, J., and Ornitz, D.M. 1996. Graded activation of fibroblast growth factor receptor 3 by mutations causing achondroplasia and thanatophoric dysplasia. *Nat Genet* 13:233-237.
160. di Martino, E., L'Hote, C.G., Kennedy, W., Tomlinson, D.C., and Knowles, M.A. 2009. Mutant fibroblast growth factor receptor 3 induces intracellular signaling and cellular transformation in a cell type- and mutation-specific manner. *Oncogene* 28:4306-4316.
161. Taylor, J.G.t., Cheuk, A.T., Tsang, P.S., Chung, J.Y., Song, Y.K., Desai, K., Yu, Y., Chen, Q.R., Shah, K., Youngblood, V., et al. 2009. Identification of FGFR4-activating mutations in human rhabdomyosarcomas that promote metastasis in xenotransplanted models. *J Clin Invest* 119:3395-3407.
162. Jackson, C.C., Medeiros, L.J., and Miranda, R.N. 2010. 8p11 myeloproliferative syndrome: a review. *Hum Pathol* 41:461-476.
163. Patnaik, M.M., and Tefferi, A. 2009. Molecular diagnosis of myeloproliferative neoplasms. *Expert Rev Mol Diagn* 9:481-492.

## References

164. Avet-Loiseau, H., Facon, T., Daviet, A., Godon, C., Rapp, M.J., Harousseau, J.L., Grosbois, B., and Bataille, R. 1999. 14q32 translocations and monosomy 13 observed in monoclonal gammopathy of undetermined significance delineate a multistep process for the oncogenesis of multiple myeloma. Intergroupe Francophone du Myelome. *Cancer Res* 59:4546-4550.
165. Marsh, S.K., Bansal, G.S., Zammit, C., Barnard, R., Coope, R., Roberts-Clarke, D., Gomm, J.J., Coombes, R.C., and Johnston, C.L. 1999. Increased expression of fibroblast growth factor 8 in human breast cancer. *Oncogene* 18:1053-1060.
166. Mattila, M.M., and Harkonen, P.L. 2007. Role of fibroblast growth factor 8 in growth and progression of hormonal cancer. *Cytokine Growth Factor Rev* 18:257-266.
167. Murphy, T., Darby, S., Mathers, M.E., and Gnanapragasam, V.J. 2010. Evidence for distinct alterations in the FGF axis in prostate cancer progression to an aggressive clinical phenotype. *J Pathol* 220:452-460.
168. Theodorou, V., Kimm, M.A., Boer, M., Wessels, L., Theelen, W., Jonkers, J., and Hilkens, J. 2007. MMTV insertional mutagenesis identifies genes, gene families and pathways involved in mammary cancer. *Nat Genet* 39:759-769.
169. Daphna-Iken, D., Shankar, D.B., Lawshe, A., Ornitz, D.M., Shackelford, G.M., and MacArthur, C.A. 1998. MMTV-Fgf8 transgenic mice develop mammary and salivary gland neoplasia and ovarian stromal hyperplasia. *Oncogene* 17:2711-2717.
170. MacArthur, C.A., Shankar, D.B., and Shackelford, G.M. 1995. Fgf-8, activated by proviral insertion, cooperates with the Wnt-1 transgene in murine mammary tumorigenesis. *J Virol* 69:2501-2507.
171. Giri, D., Ropiquet, F., and Ittmann, M. 1999. Alterations in expression of basic fibroblast growth factor (FGF) 2 and its receptor FGFR-1 in human prostate cancer. *Clin Cancer Res* 5:1063-1071.
172. Ropiquet, F., Giri, D., Kwabi-Addo, B., Mansukhani, A., and Ittmann, M. 2000. Increased expression of fibroblast growth factor 6 in human prostatic intraepithelial neoplasia and prostate cancer. *Cancer Res* 60:4245-4250.
173. Finak, G., Bertos, N., Pepin, F., Sadekova, S., Souleimanova, M., Zhao, H., Chen, H., Omeroglu, G., Meterissian, S., Omeroglu, A., et al. 2008. Stromal gene expression predicts clinical outcome in breast cancer. *Nat Med* 14:518-527.
174. Relf, M., LeJeune, S., Scott, P.A., Fox, S., Smith, K., Leek, R., Moghaddam, A., Whitehouse, R., Bicknell, R., and Harris, A.L. 1997. Expression of the angiogenic factors vascular endothelial cell growth factor, acidic and basic fibroblast growth factor, tumor growth factor beta-1, platelet-derived endothelial cell growth factor, placenta growth factor, and pleiotrophin in human primary breast cancer and its relation to angiogenesis. *Cancer Res* 57:963-969.
175. Nicholes, K., Guillet, S., Tomlinson, E., Hillan, K., Wright, B., Frantz, G.D., Pham, T.A., Dillard-Telm, L., Tsai, S.P., Stephan, J.P., et al. 2002. A mouse model of hepatocellular carcinoma: ectopic expression of fibroblast growth factor 19 in skeletal muscle of transgenic mice. *Am J Pathol* 160:2295-2307.
176. Wang, Y., and Becker, D. 1997. Antisense targeting of basic fibroblast growth factor and fibroblast growth factor receptor-1 in human melanomas blocks intratumoral angiogenesis and tumor growth. *Nat Med* 3:887-893.
177. Abdel-Rahman, W.M., Kalinina, J., Shoman, S., Eissa, S., Ollikainen, M., Elomaa, O., Eliseenkova, A.V., Butzow, R., Mohammadi, M., and Peltomaki, P. 2008. Somatic FGF9 mutations in colorectal and endometrial carcinomas associated with membranous beta-catenin.

## References

- Hum Mutat* 29:390-397.
178. Birrer, M.J., Johnson, M.E., Hao, K., Wong, K.K., Park, D.C., Bell, A., Welch, W.R., Berkowitz, R.S., and Mok, S.C. 2007. Whole genome oligonucleotide-based array comparative genomic hybridization analysis identified fibroblast growth factor 1 as a prognostic marker for advanced-stage serous ovarian adenocarcinomas. *J Clin Oncol* 25:2281-2287.
  179. Marek, L., Ware, K.E., Fritzsche, A., Hercule, P., Helton, W.R., Smith, J.E., McDermott, L.A., Coldren, C.D., Nemenoff, R.A., Merrick, D.T., et al. 2009. Fibroblast growth factor (FGF) and FGF receptor-mediated autocrine signaling in non-small-cell lung cancer cells. *Mol Pharmacol* 75:196-207.
  180. Cha, J.Y., Lambert, Q.T., Reuther, G.W., and Der, C.J. 2008. Involvement of fibroblast growth factor receptor 2 isoform switching in mammary oncogenesis. *Mol Cancer Res* 6:435-445.
  181. Ezzat, S., Zheng, L., Zhu, X.F., Wu, G.E., and Asa, S.L. 2002. Targeted expression of a human pituitary tumor-derived isoform of FGF receptor-4 recapitulates pituitary tumorigenesis. *J Clin Invest* 109:69-78.
  182. Itoh, H., Hattori, Y., Sakamoto, H., Ishii, H., Kishi, T., Sasaki, H., Yoshida, T., Kono, M., Sugimura, T., and Terada, M. 1994. Preferential alternative splicing in cancer generates a K-sam messenger RNA with higher transforming activity. *Cancer Res* 54:3237-3241.
  183. Cha, J.Y., Maddileti, S., Mitin, N., Harden, T.K., and Der, C.J. 2009. Aberrant receptor internalization and enhanced FRS2-dependent signaling contribute to the transforming activity of the fibroblast growth factor receptor 2 IIIb C3 isoform. *J Biol Chem* 284:6227-6240.
  184. Savagner, P., Valles, A.M., Jouanneau, J., Yamada, K.M., and Thiery, J.P. 1994. Alternative splicing in fibroblast growth factor receptor 2 is associated with induced epithelial-mesenchymal transition in rat bladder carcinoma cells. *Mol Biol Cell* 5:851-862.
  185. Yan, G., Fukabori, Y., McBride, G., Nikolaropolous, S., and McKeenan, W.L. 1993. Exon switching and activation of stromal and embryonic fibroblast growth factor (FGF)-FGF receptor genes in prostate epithelial cells accompany stromal independence and malignancy. *Mol Cell Biol* 13:4513-4522.
  186. Oltean, S., Sorg, B.S., Albrecht, T., Bonano, V.I., Brazas, R.M., Dewhirst, M.W., and Garcia-Blanco, M.A. 2006. Alternative inclusion of fibroblast growth factor receptor 2 exon IIIc in Dunning prostate tumors reveals unexpected epithelial mesenchymal plasticity. *Proc Natl Acad Sci U S A* 103:14116-14121.
  187. Easton, D.F., Pooley, K.A., Dunning, A.M., Pharoah, P.D., Thompson, D., Ballinger, D.G., Struwing, J.P., Morrison, J., Field, H., Luben, R., et al. 2007. Genome-wide association study identifies novel breast cancer susceptibility loci. *Nature* 447:1087-1093.
  188. Hunter, D.J., Kraft, P., Jacobs, K.B., Cox, D.G., Yeager, M., Hankinson, S.E., Wacholder, S., Wang, Z., Welch, R., Hutchinson, A., et al. 2007. A genome-wide association study identifies alleles in FGFR2 associated with risk of sporadic postmenopausal breast cancer. *Nat Genet* 39:870-874.
  189. Garcia-Closas, M., Hall, P., Nevanlinna, H., Pooley, K., Morrison, J., Richesson, D.A., Bojesen, S.E., Nordestgaard, B.G., Axelsson, C.K., Arias, J.I., et al. 2008. Heterogeneity of breast cancer associations with five susceptibility loci by clinical and pathological characteristics. *PLoS Genet* 4:e1000054.
  190. Bange, J., Prechtel, D., Cheburkin, Y., Specht, K., Harbeck, N., Schmitt, M., Knyazeva, T., Muller, S., Gartner, S., Sures, I., et al. 2002. Cancer progression and tumor cell motility are associated with the FGFR4 Arg(388) allele. *Cancer Res* 62:840-847.

## References

191. Spinola, M., Leoni, V.P., Tanuma, J., Pettinicchio, A., Frattini, M., Signoroni, S., Agresti, R., Giovanazzi, R., Pilotti, S., Bertario, L., et al. 2005. FGFR4 Gly388Arg polymorphism and prognosis of breast and colorectal cancer. *Oncol Rep* 14:415-419.
192. Fritzsche, S., Kenzelmann, M., Hoffmann, M.J., Muller, M., Engers, R., Grone, H.J., and Schulz, W.A. 2006. Concomitant down-regulation of SPRY1 and SPRY2 in prostate carcinoma. *Endocr Relat Cancer* 13:839-849.
193. Darby, S., Sahadevan, K., Khan, M.M., Robson, C.N., Leung, H.Y., and Gnanapragasam, V.J. 2006. Loss of Sef (similar expression to FGF) expression is associated with high grade and metastatic prostate cancer. *Oncogene* 25:4122-4127.
194. Zisman-Rozen, S., Fink, D., Ben-Izhak, O., Fuchs, Y., Brodski, A., Kraus, M.H., Bejar, J., and Ron, D. 2007. Downregulation of Sef, an inhibitor of receptor tyrosine kinase signaling, is common to a variety of human carcinomas. *Oncogene* 26:6093-6098.
195. Abate-Shen, C., and Shen, M.M. 2007. FGF signaling in prostate tumorigenesis--new insights into epithelial-stromal interactions. *Cancer Cell* 12:495-497.
196. Zhong, C., Saribekyan, G., Liao, C.P., Cohen, M.B., and Roy-Burman, P. 2006. Cooperation between FGF8b overexpression and PTEN deficiency in prostate tumorigenesis. *Cancer Res* 66:2188-2194.
197. Pardo, O.E., Arcaro, A., Salerno, G., Raguz, S., Downward, J., and Seckl, M.J. 2002. Fibroblast growth factor-2 induces translational regulation of Bcl-XL and Bcl-2 via a MEK-dependent pathway: correlation with resistance to etoposide-induced apoptosis. *J Biol Chem* 277:12040-12046.
198. Pardo, O.E., Lesay, A., Arcaro, A., Lopes, R., Ng, B.L., Warne, P.H., McNeish, I.A., Tetley, T.D., Lemoine, N.R., Mehmet, H., et al. 2003. Fibroblast growth factor 2-mediated translational control of IAPs blocks mitochondrial release of Smac/DIABLO and apoptosis in small cell lung cancer cells. *Mol Cell Biol* 23:7600-7610.
199. Pardo, O.E., Wellbrock, C., Khanzada, U.K., Aubert, M., Arozarena, I., Davidson, S., Bowen, F., Parker, P.J., Filonenko, V.V., Gout, I.T., et al. 2006. FGF-2 protects small cell lung cancer cells from apoptosis through a complex involving PKCepsilon, B-Raf and S6K2. *EMBO J* 25:3078-3088.
200. Nomura, S., Yoshitomi, H., Takano, S., Shida, T., Kobayashi, S., Ohtsuka, M., Kimura, F., Shimizu, H., Yoshidome, H., Kato, A., et al. 2008. FGF10/FGFR2 signal induces cell migration and invasion in pancreatic cancer. *Br J Cancer* 99:305-313.
201. Xian, W., Schwertfeger, K.L., Vargo-Gogola, T., and Rosen, J.M. 2005. Pleiotropic effects of FGFR1 on cell proliferation, survival, and migration in a 3D mammary epithelial cell model. *J Cell Biol* 171:663-673.
202. Acevedo, V.D., Gangula, R.D., Freeman, K.W., Li, R., Zhang, Y., Wang, F., Ayala, G.E., Peterson, L.E., Ittmann, M., and Spencer, D.M. 2007. Inducible FGFR-1 activation leads to irreversible prostate adenocarcinoma and an epithelial-to-mesenchymal transition. *Cancer Cell* 12:559-571.
203. Winter, S.F., Acevedo, V.D., Gangula, R.D., Freeman, K.W., Spencer, D.M., and Greenberg, N.M. 2007. Conditional activation of FGFR1 in the prostate epithelium induces angiogenesis with concomitant differential regulation of Ang-1 and Ang-2. *Oncogene* 26:4897-4907.
204. Carmeliet, P., and Jain, R.K. 2000. Angiogenesis in cancer and other diseases. *Nature* 407:249-257.
205. Javerzat, S., Auguste, P., and Bikfalvi, A. 2002. The role of fibroblast growth factors in vascular

## References

- development. *Trends Mol Med* 8:483-489.
206. Cross, M.J., and Claesson-Welsh, L. 2001. FGF and VEGF function in angiogenesis: signalling pathways, biological responses and therapeutic inhibition. *Trends Pharmacol Sci* 22:201-207.
207. Auguste, P., Gursel, D.B., Lemiere, S., Reimers, D., Cuevas, P., Carceller, F., Di Santo, J.P., and Bikfalvi, A. 2001. Inhibition of fibroblast growth factor/fibroblast growth factor receptor activity in glioma cells impedes tumor growth by both angiogenesis-dependent and -independent mechanisms. *Cancer Res* 61:1717-1726.
208. Seghezzi, G., Patel, S., Ren, C.J., Gualandris, A., Pintucci, G., Robbins, E.S., Shapiro, R.L., Galloway, A.C., Rifkin, D.B., and Mignatti, P. 1998. Fibroblast growth factor-2 (FGF-2) induces vascular endothelial growth factor (VEGF) expression in the endothelial cells of forming capillaries: an autocrine mechanism contributing to angiogenesis. *J Cell Biol* 141:1659-1673.
209. Liotta, L.A., Steeg, P.S., and Stetler-Stevenson, W.G. 1991. Cancer metastasis and angiogenesis: an imbalance of positive and negative regulation. *Cell* 64:327-336.
210. Terranova, V.P., DiFlorio, R., Lyall, R.M., Hic, S., Friesel, R., and Maciag, T. 1985. Human endothelial cells are chemotactic to endothelial cell growth factor and heparin. *J Cell Biol* 101:2330-2334.
211. Stokes, C.L., Rupnick, M.A., Williams, S.K., and Lauffenburger, D.A. 1990. Chemotaxis of human microvessel endothelial cells in response to acidic fibroblast growth factor. *Lab Invest* 63:657-668.
212. Mattila, M.M., Ruohola, J.K., Valve, E.M., Tasanen, M.J., Seppanen, J.A., and Harkonen, P.L. 2001. FGF-8b increases angiogenic capacity and tumor growth of androgen-regulated S115 breast cancer cells. *Oncogene* 20:2791-2804.
213. Gillis, P., Savla, U., Volpert, O.V., Jimenez, B., Waters, C.M., Panos, R.J., and Bouck, N.P. 1999. Keratinocyte growth factor induces angiogenesis and protects endothelial barrier function. *J Cell Sci* 112 ( Pt 12):2049-2057.
214. Underwood, P.A., Bean, P.A., and Gamble, J.R. 2002. Rate of endothelial expansion is controlled by cell:cell adhesion. *Int J Biochem Cell Biol* 34:55-69.
215. Ricol, D., Cappellen, D., El Marjou, A., Gil-Diez-de-Medina, S., Girault, J.M., Yoshida, T., Ferry, G., Tucker, G., Poupon, M.F., Chopin, D., et al. 1999. Tumour suppressive properties of fibroblast growth factor receptor 2-IIIb in human bladder cancer. *Oncogene* 18:7234-7243.
216. Amann, T., Bataille, F., Spruss, T., Dettmer, K., Wild, P., Liedtke, C., Muhlbauer, M., Kiefer, P., Oefner, P.J., Trautwein, C., et al. 2010. Reduced expression of fibroblast growth factor receptor 2IIIb in hepatocellular carcinoma induces a more aggressive growth. *Am J Pathol* 176:1433-1442.
217. Yasumoto, H., Matsubara, A., Mutaguchi, K., Usui, T., and McKeenan, W.L. 2004. Restoration of fibroblast growth factor receptor2 suppresses growth and tumorigenicity of malignant human prostate carcinoma PC-3 cells. *Prostate* 61:236-242.
218. Katoh, M. 2009. FGFR2 abnormalities underlie a spectrum of bone, skin, and cancer pathologies. *J Invest Dermatol* 129:1861-1867.
219. Yu, C.E., Oshima, J., Fu, Y.H., Wijsman, E.M., Hisama, F., Alisch, R., Matthews, S., Nakura, J., Miki, T., Ouais, S., et al. 1996. Positional cloning of the Werner's syndrome gene. *Science* 272:258-262.
220. Bachrati, C.Z., and Hickson, I.D. 2003. RecQ helicases: suppressors of tumorigenesis and premature aging. *Biochem J* 374:577-606.

## References

221. Opresko, P.L., Cheng, W.H., and Bohr, V.A. 2004. Junction of RecQ helicase biochemistry and human disease. *J Biol Chem* 279:18099-18102.
222. Huang, S., Lee, L., Hanson, N.B., Lenaerts, C., Hoehn, H., Poot, M., Rubin, C.D., Chen, D.F., Yang, C.C., Juch, H., et al. 2006. The spectrum of WRN mutations in Werner syndrome patients. *Hum Mutat* 27:558-567.
223. Uhrhammer, N.A., Lafarge, L., Dos Santos, L., Domaszewska, A., Lange, M., Yang, Y., Aractingi, S., Bessis, D., and Bignon, Y.J. 2006. Werner syndrome and mutations of the WRN and LMNA genes in France. *Hum Mutat* 27:718-719.
224. Goto, M., Yamabe, Y., Shiratori, M., Okada, M., Kawabe, T., Matsumoto, T., Sugimoto, M., and Furuichi, Y. 1999. Immunological diagnosis of Werner syndrome by down-regulated and truncated gene products. *Hum Genet* 105:301-307.
225. Moser, M.J., Kamath-Loeb, A.S., Jacob, J.E., Bennett, S.E., Oshima, J., and Monnat, R.J., Jr. 2000. WRN helicase expression in Werner syndrome cell lines. *Nucleic Acids Res* 28:648-654.
226. Opresko, P.L., Otterlei, M., Graakjaer, J., Bruheim, P., Dawut, L., Kolvraa, S., May, A., Seidman, M.M., and Bohr, V.A. 2004. The Werner syndrome helicase and exonuclease cooperate to resolve telomeric D loops in a manner regulated by TRF1 and TRF2. *Mol Cell* 14:763-774.
227. Chang, S., Multani, A.S., Cabrera, N.G., Naylor, M.L., Laud, P., Lombard, D., Pathak, S., Guarente, L., and DePinho, R.A. 2004. Essential role of limiting telomeres in the pathogenesis of Werner syndrome. *Nat Genet* 36:877-882.
228. Du, X., Shen, J., Kugan, N., Furth, E.E., Lombard, D.B., Cheung, C., Pak, S., Luo, G., Pignolo, R.J., DePinho, R.A., et al. 2004. Telomere shortening exposes functions for the mouse Werner and Bloom syndrome genes. *Mol Cell Biol* 24:8437-8446.
229. Crabbe, L., Verdun, R.E., Haggblom, C.I., and Karlseder, J. 2004. Defective telomere lagging strand synthesis in cells lacking WRN helicase activity. *Science* 306:1951-1953.
230. Laud, P.R., Multani, A.S., Bailey, S.M., Wu, L., Ma, J., Kingsley, C., Lebel, M., Pathak, S., DePinho, R.A., and Chang, S. 2005. Elevated telomere-telomere recombination in WRN-deficient, telomere dysfunctional cells promotes escape from senescence and engagement of the ALT pathway. *Genes Dev* 19:2560-2570.
231. Eller, M.S., Liao, X., Liu, S., Hanna, K., Backvall, H., Opresko, P.L., Bohr, V.A., and Gilchrest, B.A. 2006. A role for WRN in telomere-based DNA damage responses. *Proc Natl Acad Sci U S A* 103:15073-15078.
232. Lombard, D.B., Beard, C., Johnson, B., Marciniak, R.A., Dausman, J., Bronson, R., Buhlmann, J.E., Lipman, R., Curry, R., Sharpe, A., et al. 2000. Mutations in the WRN gene in mice accelerate mortality in a p53-null background. *Mol Cell Biol* 20:3286-3291.
233. Lebel, M., and Leder, P. 1998. A deletion within the murine Werner syndrome helicase induces sensitivity to inhibitors of topoisomerase and loss of cellular proliferative capacity. *Proc Natl Acad Sci U S A* 95:13097-13102.
234. Lebel, M., Cardiff, R.D., and Leder, P. 2001. Tumorigenic effect of nonfunctional p53 or p21 in mice mutant in the Werner syndrome helicase. *Cancer Res* 61:1816-1819.
235. Wang, L., Ogburn, C.E., Ware, C.B., Ladiges, W.C., Youssoufian, H., Martin, G.M., and Oshima, J. 2000. Cellular Werner phenotypes in mice expressing a putative dominant-negative human WRN gene. *Genetics* 154:357-362.
236. Smith, E.D., Kudlow, B.A., Frock, R.L., and Kennedy, B.K. 2005. A-type nuclear lamins, progerias and other degenerative disorders. *Mech Ageing Dev* 126:447-460.

## References

237. McKeon, F.D., Kirschner, M.W., and Caput, D. 1986. Homologies in both primary and secondary structure between nuclear envelope and intermediate filament proteins. *Nature* 319:463-468.
238. Stuurman, N., Heins, S., and Aebi, U. 1998. Nuclear lamins: their structure, assembly, and interactions. *J Struct Biol* 122:42-66.
239. Spann, T.P., Goldman, A.E., Wang, C., Huang, S., and Goldman, R.D. 2002. Alteration of nuclear lamin organization inhibits RNA polymerase II-dependent transcription. *J Cell Biol* 156:603-608.
240. Ivorra, C., Kubicek, M., Gonzalez, J.M., Sanz-Gonzalez, S.M., Alvarez-Barrientos, A., O'Connor, J.E., Burke, B., and Andres, V. 2006. A mechanism of AP-1 suppression through interaction of c-Fos with lamin A/C. *Genes Dev* 20:307-320.
241. Frock, R.L., Kudlow, B.A., Evans, A.M., Jameson, S.A., Hauschka, S.D., and Kennedy, B.K. 2006. Lamin A/C and emerin are critical for skeletal muscle satellite cell differentiation. *Genes Dev* 20:486-500.
242. Nitta, R.T., Jameson, S.A., Kudlow, B.A., Conlan, L.A., and Kennedy, B.K. 2006. Stabilization of the retinoblastoma protein by A-type nuclear lamins is required for INK4A-mediated cell cycle arrest. *Mol Cell Biol* 26:5360-5372.
243. Rusinol, A.E., and Sinensky, M.S. 2006. Farnesylated lamins, progeroid syndromes and farnesyl transferase inhibitors. *J Cell Sci* 119:3265-3272.
244. Hennekam, R.C. 2006. Hutchinson-Gilford progeria syndrome: review of the phenotype. *Am J Med Genet A* 140:2603-2624.
245. Hutchinson, J. 1886. Congenital Absence of Hair and Mammary Glands with Atrophic Condition of the Skin and its Appendages, in a Boy whose Mother had been almost wholly Bald from Alopecia Areata from the age of Six. *Med Chir Trans* 69:473-477.
246. Eriksson, M., Brown, W.T., Gordon, L.B., Glynn, M.W., Singer, J., Scott, L., Erdos, M.R., Robbins, C.M., Moses, T.Y., Berglund, P., et al. 2003. Recurrent de novo point mutations in lamin A cause Hutchinson-Gilford progeria syndrome. *Nature* 423:293-298.
247. De Sandre-Giovannoli, A., Bernard, R., Cau, P., Navarro, C., Amiel, J., Boccaccio, I., Lyonnet, S., Stewart, C.L., Munnich, A., Le Merrer, M., et al. 2003. Lamin a truncation in Hutchinson-Gilford progeria. *Science* 300:2055.
248. Cao, H., and Hegele, R.A. 2003. LMNA is mutated in Hutchinson-Gilford progeria (MIM 176670) but not in Wiedemann-Rautenstrauch progeroid syndrome (MIM 264090). *J Hum Genet* 48:271-274.
249. Pendas, A.M., Zhou, Z., Cadinanos, J., Freije, J.M., Wang, J., Hultenby, K., Astudillo, A., Wernerson, A., Rodriguez, F., Tryggvason, K., et al. 2002. Defective prelamin A processing and muscular and adipocyte alterations in Zmpste24 metalloproteinase-deficient mice. *Nat Genet* 31:94-99.
250. Kuro-o, M. 2010. A potential link between phosphate and aging--lessons from Klotho-deficient mice. *Mech Ageing Dev* 131:270-275.
251. Razzaque, M.S., Sitara, D., Taguchi, T., St-Arnaud, R., and Lanske, B. 2006. Premature aging-like phenotype in fibroblast growth factor 23 null mice is a vitamin D-mediated process. *FASEB J* 20:720-722.
252. Stubbs, J.R., Liu, S., Tang, W., Zhou, J., Wang, Y., Yao, X., and Quarles, L.D. 2007. Role of hyperphosphatemia and 1,25-dihydroxyvitamin D in vascular calcification and mortality in fibroblastic growth factor 23 null mice. *J Am Soc Nephrol* 18:2116-2124.



## References

253. Tsujikawa, H., Kurotaki, Y., Fujimori, T., Fukuda, K., and Nabeshima, Y. 2003. Klotho, a gene related to a syndrome resembling human premature aging, functions in a negative regulatory circuit of vitamin D endocrine system. *Mol Endocrinol* 17:2393-2403.
254. Ohnishi, M., Nakatani, T., Lanske, B., and Razzaque, M.S. 2009. Reversal of mineral ion homeostasis and soft-tissue calcification of klotho knockout mice by deletion of vitamin D 1alpha-hydroxylase. *Kidney Int* 75:1166-1172.
255. Hesse, M., Frohlich, L.F., Zeitz, U., Lanske, B., and Erben, R.G. 2007. Ablation of vitamin D signaling rescues bone, mineral, and glucose homeostasis in Fgf-23 deficient mice. *Matrix Biol* 26:75-84.
256. Morishita, K., Shirai, A., Kubota, M., Katakura, Y., Nabeshima, Y., Takeshige, K., and Kamiya, T. 2001. The progression of aging in klotho mutant mice can be modified by dietary phosphorus and zinc. *J Nutr* 131:3182-3188.
257. Ohnishi, M., and Razzaque, M.S. 2010. Dietary and genetic evidence for phosphate toxicity accelerating mammalian aging. *FASEB J* 24:3562-3571.
258. Boer, V.M., Amini, S., and Botstein, D. 2008. Influence of genotype and nutrition on survival and metabolism of starving yeast. *Proc Natl Acad Sci U S A* 105:6930-6935.
259. Brauer, M.J., Huttenhower, C., Airoidi, E.M., Rosenstein, R., Matese, J.C., Gresham, D., Boer, V.M., Troyanskaya, O.G., and Botstein, D. 2008. Coordination of growth rate, cell cycle, stress response, and metabolic activity in yeast. *Mol Biol Cell* 19:352-367.
260. DeRisi, J.L., Iyer, V.R., and Brown, P.O. 1997. Exploring the metabolic and genetic control of gene expression on a genomic scale. *Science* 278:680-686.
261. Cao, S.X., Dhahbi, J.M., Mote, P.L., and Spindler, S.R. 2001. Genomic profiling of short- and long-term caloric restriction effects in the liver of aging mice. *Proc Natl Acad Sci U S A* 98:10630-10635.
262. Kayo, T., Allison, D.B., Weindruch, R., and Prolla, T.A. 2001. Influences of aging and caloric restriction on the transcriptional profile of skeletal muscle from rhesus monkeys. *Proc Natl Acad Sci U S A* 98:5093-5098.
263. Lee, C.K., Klopp, R.G., Weindruch, R., and Prolla, T.A. 1999. Gene expression profile of aging and its retardation by caloric restriction. *Science* 285:1390-1393.
264. Masoro, E.J. 2006. Dietary restriction-induced life extension: a broadly based biological phenomenon. *Biogerontology* 7:153-155.
265. Wetter, T.J., Gazdag, A.C., Dean, D.J., and Cartee, G.D. 1999. Effect of calorie restriction on in vivo glucose metabolism by individual tissues in rats. *Am J Physiol* 276:E728-738.
266. Xie, W., Li, Y., Mechin, M.C., and Van De Werve, G. 1999. Up-regulation of liver glucose-6-phosphatase in rats fed with a P(i)-deficient diet. *Biochem J* 343 Pt 2:393-396.
267. Xie, W., Tran, T.L., Finegood, D.T., and van de Werve, G. 2000. Dietary P(i) deprivation in rats affects liver cAMP, glycogen, key steps of gluconeogenesis and glucose production. *Biochem J* 352 Pt 1:227-232.
268. Clancy, D.J., Gems, D., Harshman, L.G., Oldham, S., Stocker, H., Hafen, E., Leevers, S.J., and Partridge, L. 2001. Extension of life-span by loss of CHICO, a Drosophila insulin receptor substrate protein. *Science* 292:104-106.
269. Kenyon, C. 2005. The plasticity of aging: insights from long-lived mutants. *Cell* 120:449-460.
270. Kenyon, C., Chang, J., Gensch, E., Rudner, A., and Tabtiang, R. 1993. A C. elegans mutant that lives twice as long as wild type. *Nature* 366:461-464.
271. Morris, J.Z., Tissenbaum, H.A., and Ruvkun, G. 1996. A phosphatidylinositol-3-OH kinase

## References

- family member regulating longevity and diapause in *Caenorhabditis elegans*. *Nature* 382:536-539.
272. Tatar, M., Kopelman, A., Epstein, D., Tu, M.P., Yin, C.M., and Garofalo, R.S. 2001. A mutant *Drosophila* insulin receptor homolog that extends life-span and impairs neuroendocrine function. *Science* 292:107-110.
273. Nagai, T., Yamada, K., Kim, H.C., Kim, Y.S., Noda, Y., Imura, A., Nabeshima, Y., and Nabeshima, T. 2003. Cognition impairment in the genetic model of aging *klotho* gene mutant mice: a role of oxidative stress. *FASEB J* 17:50-52.
274. Di Marco, G.S., Hausberg, M., Hillebrand, U., Rustemeyer, P., Wittkowski, W., Lang, D., and Pavenstadt, H. 2008. Increased inorganic phosphate induces human endothelial cell apoptosis in vitro. *Am J Physiol Renal Physiol* 294:F1381-1387.
275. Bose, S., French, S., Evans, F.J., Joubert, F., and Balaban, R.S. 2003. Metabolic network control of oxidative phosphorylation: multiple roles of inorganic phosphate. *J Biol Chem* 278:39155-39165.
276. Papa, S., and Skulachev, V.P. 1997. Reactive oxygen species, mitochondria, apoptosis and aging. *Mol Cell Biochem* 174:305-319.
277. Utsugi, T., Ohno, T., Ohyama, Y., Uchiyama, T., Saito, Y., Matsumura, Y., Aizawa, H., Itoh, H., Kurabayashi, M., Kawazu, S., et al. 2000. Decreased insulin production and increased insulin sensitivity in the *klotho* mutant mouse, a novel animal model for human aging. *Metabolism* 49:1118-1123.
278. Nishimura, T., Utsunomiya, Y., Hoshikawa, M., Ohuchi, H., and Itoh, N. 1999. Structure and expression of a novel human FGF, FGF-19, expressed in the fetal brain. *Biochim Biophys Acta* 1444:148-151.
279. Choi, M., Moschetta, A., Bookout, A.L., Peng, L., Umetani, M., Holmstrom, S.R., Suino-Powell, K., Xu, H.E., Richardson, J.A., Gerard, R.D., et al. 2006. Identification of a hormonal basis for gallbladder filling. *Nat Med* 12:1253-1255.
280. Inagaki, T., Choi, M., Moschetta, A., Peng, L., Cummins, C.L., McDonald, J.G., Luo, G., Jones, S.A., Goodwin, B., Richardson, J.A., et al. 2005. Fibroblast growth factor 15 functions as an enterohepatic signal to regulate bile acid homeostasis. *Cell Metab* 2:217-225.
281. Ito, S., Fujimori, T., Furuya, A., Satoh, J., and Nabeshima, Y. 2005. Impaired negative feedback suppression of bile acid synthesis in mice lacking *betaKlotho*. *J Clin Invest* 115:2202-2208.
282. Nishimura, T., Nakatake, Y., Konishi, M., and Itoh, N. 2000. Identification of a novel FGF, FGF-21, preferentially expressed in the liver. *Biochim Biophys Acta* 1492:203-206.
283. Kharitonov, A., Shiyanova, T.L., Koester, A., Ford, A.M., Micanovic, R., Galbreath, E.J., Sandusky, G.E., Hammond, L.J., Moyers, J.S., Owens, R.A., et al. 2005. FGF-21 as a novel metabolic regulator. *J Clin Invest* 115:1627-1635.
284. Badman, M.K., Pissios, P., Kennedy, A.R., Koukos, G., Flier, J.S., and Maratos-Flier, E. 2007. Hepatic fibroblast growth factor 21 is regulated by PPARalpha and is a key mediator of hepatic lipid metabolism in ketotic states. *Cell Metab* 5:426-437.
285. Inagaki, T., Dutchak, P., Zhao, G., Ding, X., Gautron, L., Parameswara, V., Li, Y., Goetz, R., Mohammadi, M., Esser, V., et al. 2007. Endocrine regulation of the fasting response by PPARalpha-mediated induction of fibroblast growth factor 21. *Cell Metab* 5:415-425.
286. Kurosu, H., Choi, M., Ogawa, Y., Dickson, A.S., Goetz, R., Eliseenkova, A.V., Mohammadi, M., Rosenblatt, K.P., Kliwer, S.A., and Kuro-o, M. 2007. Tissue-specific expression of *betaKlotho* and fibroblast growth factor (FGF) receptor isoforms determines metabolic activity

## References

- of FGF19 and FGF21. *J Biol Chem* 282:26687-26695.
287. Ogawa, Y., Kurosu, H., Yamamoto, M., Nandi, A., Rosenblatt, K.P., Goetz, R., Eliseenkova, A.V., Mohammadi, M., and Kuro-o, M. 2007. BetaKlotho is required for metabolic activity of fibroblast growth factor 21. *Proc Natl Acad Sci U S A* 104:7432-7437.
288. Quarles, L.D. 2003. FGF23, PHEX, and MEPE regulation of phosphate homeostasis and skeletal mineralization. *Am J Physiol Endocrinol Metab* 285:E1-9.
289. Schiavi, S.C., and Kumar, R. 2004. The phosphatonin pathway: new insights in phosphate homeostasis. *Kidney Int* 65:1-14.
290. White, K.E., Koller, D.L., Takacs, I., Buckwalter, K.A., Foroud, T., and Econs, M.J. 1999. Locus heterogeneity of autosomal dominant osteopetrosis (ADO). *J Clin Endocrinol Metab* 84:1047-1051.
291. Yamashita, T., Yoshioka, M., and Itoh, N. 2000. Identification of a novel fibroblast growth factor, FGF-23, preferentially expressed in the ventrolateral thalamic nucleus of the brain. *Biochem Biophys Res Commun* 277:494-498.
292. Yamashita, T. 2005. Structural and biochemical properties of fibroblast growth factor 23. *Ther Apher Dial* 9:313-318.
293. Feng, J.Q., Ward, L.M., Liu, S., Lu, Y., Xie, Y., Yuan, B., Yu, X., Rauch, F., Davis, S.I., Zhang, S., et al. 2006. Loss of DMP1 causes rickets and osteomalacia and identifies a role for osteocytes in mineral metabolism. *Nat Genet* 38:1310-1315.
294. Lorenz-Depiereux, B., Bastepe, M., Benet-Pages, A., Amyere, M., Wagenstaller, J., Muller-Barth, U., Badenhoop, K., Kaiser, S.M., Rittmaster, R.S., Shlossberg, A.H., et al. 2006. DMP1 mutations in autosomal recessive hypophosphatemia implicate a bone matrix protein in the regulation of phosphate homeostasis. *Nat Genet* 38:1248-1250.
295. Topaz, O., Indelman, M., Chefetz, I., Geiger, D., Metzker, A., Altschuler, Y., Choder, M., Bercovich, D., Uitto, J., Bergman, R., et al. 2006. A deleterious mutation in SAMD9 causes normophosphatemic familial tumoral calcinosis. *Am J Hum Genet* 79:759-764.
296. Liu, S., Gupta, A., and Quarles, L.D. 2007. Emerging role of fibroblast growth factor 23 in a bone-kidney axis regulating systemic phosphate homeostasis and extracellular matrix mineralization. *Curr Opin Nephrol Hypertens* 16:329-335.
297. Miller, W.L., and Portale, A.A. 2000. Vitamin D 1 alpha-hydroxylase. *Trends Endocrinol Metab* 11:315-319.
298. Henry, H.L. 2001. The 25(OH)D(3)/1alpha,25(OH)(2)D(3)-24R-hydroxylase: a catabolic or biosynthetic enzyme? *Steroids* 66:391-398.
299. Yoshida, T., Fujimori, T., and Nabeshima, Y. 2002. Mediation of unusually high concentrations of 1,25-dihydroxyvitamin D in homozygous klotho mutant mice by increased expression of renal 1alpha-hydroxylase gene. *Endocrinology* 143:683-689.
300. Segawa, H., Yamanaka, S., Ohno, Y., Onitsuka, A., Shiozawa, K., Aranami, F., Furutani, J., Tomoe, Y., Ito, M., Kuwahata, M., et al. 2007. Correlation between hyperphosphatemia and type II Na-Pi cotransporter activity in klotho mice. *Am J Physiol Renal Physiol* 292:F769-779.
301. Hu, M.C., Shi, M., Zhang, J., Pastor, J., Nakatani, T., Lanske, B., Razzaque, M.S., Rosenblatt, K.P., Baum, M.G., Kuro-o, M., et al. 2010. Klotho: a novel phosphaturic substance acting as an autocrine enzyme in the renal proximal tubule. *FASEB J* 24:3438-3450.
302. Hurwitz, S. 1996. Homeostatic control of plasma calcium concentration. *Crit Rev Biochem Mol Biol* 31:41-100.
303. Muller, D., Hoenderop, J.G., Merckx, G.F., van Os, C.H., and Bindels, R.J. 2000. Gene structure

## References

- and chromosomal mapping of human epithelial calcium channel. *Biochem Biophys Res Commun* 275:47-52.
304. Weber, K., Erben, R.G., Rump, A., and Adamski, J. 2001. Gene structure and regulation of the murine epithelial calcium channels ECaC1 and 2. *Biochem Biophys Res Commun* 289:1287-1294.
305. Hoenderop, J.G., Dardenne, O., Van Abel, M., Van Der Kemp, A.W., Van Os, C.H., St -Arnaud, R., and Bindels, R.J. 2002. Modulation of renal Ca<sup>2+</sup> transport protein genes by dietary Ca<sup>2+</sup> and 1,25-dihydroxyvitamin D<sub>3</sub> in 25-hydroxyvitamin D<sub>3</sub>-1alpha-hydroxylase knockout mice. *FASEB J* 16:1398-1406.
306. Hoenderop, J.G., Muller, D., Van Der Kemp, A.W., Hartog, A., Suzuki, M., Ishibashi, K., Imai, M., Sweep, F., Willems, P.H., Van Os, C.H., et al. 2001. Calcitriol controls the epithelial calcium channel in kidney. *J Am Soc Nephrol* 12:1342-1349.
307. Inoue, Y., Segawa, H., Kaneko, I., Yamanaka, S., Kusano, K., Kawakami, E., Furutani, J., Ito, M., Kuwahata, M., Saito, H., et al. 2005. Role of the vitamin D receptor in FGF23 action on phosphate metabolism. *Biochem J* 390:325-331.
308. Shimada, T., Yamazaki, Y., Takahashi, M., Hasegawa, H., Urakawa, I., Oshima, T., Ono, K., Kakitani, M., Tomizuka, K., Fujita, T., et al. 2005. Vitamin D receptor-independent FGF23 actions in regulating phosphate and vitamin D metabolism. *Am J Physiol Renal Physiol* 289:F1088-1095.
309. 2000. Autosomal dominant hypophosphataemic rickets is associated with mutations in FGF23. *Nat Genet* 26:345-348.
310. Bianchine, J.W., Stambler, A.A., and Harrison, H.E. 1971. Familial hypophosphatemic rickets showing autosomal dominant inheritance. *Birth Defects Orig Artic Ser* 7:287-295.
311. Silve, C., and Beck, L. 2002. Is FGF23 the long sought after phosphaturic factor phosphatonin? *Nephrol Dial Transplant* 17:958-961.
312. Shimada, T., Muto, T., Urakawa, I., Yoneya, T., Yamazaki, Y., Okawa, K., Takeuchi, Y., Fujita, T., Fukumoto, S., and Yamashita, T. 2002. Mutant FGF-23 responsible for autosomal dominant hypophosphatemic rickets is resistant to proteolytic cleavage and causes hypophosphatemia in vivo. *Endocrinology* 143:3179-3182.
313. Jonsson, K.B., Zahradnik, R., Larsson, T., White, K.E., Sugimoto, T., Imanishi, Y., Yamamoto, T., Hampson, G., Koshiyama, H., Ljunggren, O., et al. 2003. Fibroblast growth factor 23 in oncogenic osteomalacia and X-linked hypophosphatemia. *N Engl J Med* 348:1656-1663.
314. Econs, M.J., and Drezner, M.K. 1994. Tumor-induced osteomalacia--unveiling a new hormone. *N Engl J Med* 330:1679-1681.
315. Cai, Q., Hodgson, S.F., Kao, P.C., Lennon, V.A., Klee, G.G., Zinsmeister, A.R., and Kumar, R. 1994. Brief report: inhibition of renal phosphate transport by a tumor product in a patient with oncogenic osteomalacia. *N Engl J Med* 330:1645-1649.
316. Rowe, P.S., de Zoysa, P.A., Dong, R., Wang, H.R., White, K.E., Econs, M.J., and Oudet, C.L. 2000. MEPE, a new gene expressed in bone marrow and tumors causing osteomalacia. *Genomics* 67:54-68.
317. Carpenter, T.O., Ellis, B.K., Insogna, K.L., Philbrick, W.M., Sterpka, J., and Shimkets, R. 2005. Fibroblast growth factor 7: an inhibitor of phosphate transport derived from oncogenic osteomalacia-causing tumors. *J Clin Endocrinol Metab* 90:1012-1020.
318. Berndt, T., Craig, T.A., Bowe, A.E., Vassiliadis, J., Reczek, D., Finnegan, R., Jan De Beur, S.M., Schiavi, S.C., and Kumar, R. 2003. Secreted frizzled-related protein 4 is a potent tumor-

## References

- derived phosphaturic agent. *J Clin Invest* 112:785-794.
319. Folpe, A.L., Fanburg-Smith, J.C., Billings, S.D., Bisceglia, M., Bertoni, F., Cho, J.Y., Econs, M.J., Inwards, C.Y., Jan de Beur, S.M., Mentzel, T., et al. 2004. Most osteomalacia-associated mesenchymal tumors are a single histopathologic entity: an analysis of 32 cases and a comprehensive review of the literature. *Am J Surg Pathol* 28:1-30.
320. Jan de Beur, S.M. 2005. Tumor-induced osteomalacia. *JAMA* 294:1260-1267.
321. Perry, W., and Stamp, T.C. 1978. Hereditary hypophosphataemic rickets with autosomal recessive inheritance and severe osteosclerosis. A report of two cases. *J Bone Joint Surg Br* 60-B:430-434.
322. Sriver, C.R., Reade, T., Halal, F., Costa, T., and Cole, D.E. 1981. Autosomal hypophosphataemic bone disease responds to 1,25-(OH)<sub>2</sub>D<sub>3</sub>. *Arch Dis Child* 56:203-207.
323. Sriver, C.R., Reade, T.M., DeLuca, H.F., and Hamstra, A.J. 1978. Serum 1,25-dihydroxyvitamin D levels in normal subjects and in patients with hereditary rickets or bone disease. *N Engl J Med* 299:976-979.
324. Drezner, M.K., Lyles, K.W., Haussler, M.R., and Harrelson, J.M. 1980. Evaluation of a role for 1,25-dihydroxyvitamin D<sub>3</sub> in the pathogenesis and treatment of X-linked hypophosphatemic rickets and osteomalacia. *J Clin Invest* 66:1020-1032.
325. Fukase, M., Avioli, L.V., Birge, S.J., and Chase, L.R. 1984. Abnormal regulation of 25-hydroxyvitamin D<sub>3</sub>-1 alpha-hydroxylase activity by calcium and calcitonin in renal cortex from hypophosphatemic (Hyp) mice. *Endocrinology* 114:1203-1207.
326. Tenenhouse, H.S., and Jones, G. 1990. Abnormal regulation of renal vitamin D catabolism by dietary phosphate in murine X-linked hypophosphatemic rickets. *J Clin Invest* 85:1450-1455.
327. Ichikawa, S., Imel, E.A., Kreiter, M.L., Yu, X., Mackenzie, D.S., Sorenson, A.H., Goetz, R., Mohammadi, M., White, K.E., and Econs, M.J. 2007. A homozygous missense mutation in human KLOTHO causes severe tumoral calcinosis. *J Clin Invest* 117:2684-2691.
328. Lyles, K.W., Burkes, E.J., Ellis, G.J., Lucas, K.J., Dolan, E.A., and Drezner, M.K. 1985. Genetic transmission of tumoral calcinosis: autosomal dominant with variable clinical expressivity. *J Clin Endocrinol Metab* 60:1093-1096.
329. Topaz, O., Shurman, D.L., Bergman, R., Indelman, M., Ratajczak, P., Mizrachi, M., Khamaysi, Z., Behar, D., Petronius, D., Friedman, V., et al. 2004. Mutations in GALNT3, encoding a protein involved in O-linked glycosylation, cause familial tumoral calcinosis. *Nat Genet* 36:579-581.
330. Fukagawa, M., and Kazama, J.J. 2005. With or without the kidney: the role of FGF23 in CKD. *Nephrol Dial Transplant* 20:1295-1298.
331. Ben-Dov, I.Z., Galitzer, H., Lavi-Moshayoff, V., Goetz, R., Kuro-o, M., Mohammadi, M., Sirkis, R., Naveh-Many, T., and Silver, J. 2007. The parathyroid is a target organ for FGF23 in rats. *J Clin Invest* 117:4003-4008.
332. Nakanishi, S., Kazama, J.J., Nii-Kono, T., Omori, K., Yamashita, T., Fukumoto, S., Gejyo, F., Shigematsu, T., and Fukagawa, M. 2005. Serum fibroblast growth factor-23 levels predict the future refractory hyperparathyroidism in dialysis patients. *Kidney Int* 67:1171-1178.
333. Kazama, J.J., Sato, F., Omori, K., Hama, H., Yamamoto, S., Maruyama, H., Narita, I., Gejyo, F., Yamashita, T., Fukumoto, S., et al. 2005. Pretreatment serum FGF-23 levels predict the efficacy of calcitriol therapy in dialysis patients. *Kidney Int* 67:1120-1125.
334. Matsumura, Y., Aizawa, H., Shiraki-Iida, T., Nagai, R., Kuro-o, M., and Nabeshima, Y. 1998. Identification of the human klotho gene and its two transcripts encoding membrane and secreted

## References

- klotho protein. *Biochem Biophys Res Commun* 242:626-630.
335. Ohyama, Y., Kurabayashi, M., Masuda, H., Nakamura, T., Aihara, Y., Kaname, T., Suga, T., Arai, M., Aizawa, H., Matsumura, Y., et al. 1998. Molecular cloning of rat klotho cDNA: markedly decreased expression of klotho by acute inflammatory stress. *Biochem Biophys Res Commun* 251:920-925.
  336. Shiraki-Iida, T., Aizawa, H., Matsumura, Y., Sekine, S., Iida, A., Anazawa, H., Nagai, R., Kuro-o, M., and Nabeshima, Y. 1998. Structure of the mouse klotho gene and its two transcripts encoding membrane and secreted protein. *FEBS Lett* 424:6-10.
  337. Imura, A., Iwano, A., Tohyama, O., Tsuji, Y., Nozaki, K., Hashimoto, N., Fujimori, T., and Nabeshima, Y. 2004. Secreted Klotho protein in sera and CSF: implication for post-translational cleavage in release of Klotho protein from cell membrane. *FEBS Lett* 565:143-147.
  338. Takeshita, K., Fujimori, T., Kurotaki, Y., Honjo, H., Tsujikawa, H., Yasui, K., Lee, J.K., Kamiya, K., Kitaichi, K., Yamamoto, K., et al. 2004. Sinoatrial node dysfunction and early unexpected death of mice with a defect of klotho gene expression. *Circulation* 109:1776-1782.
  339. Kumar, R., and Thompson, J.R. 2011. The regulation of parathyroid hormone secretion and synthesis. *J Am Soc Nephrol* 22:216-224.
  340. de Groot, T., Bindels, R.J., and Hoenderop, J.G. 2008. TRPV5: an ingeniously controlled calcium channel. *Kidney Int* 74:1241-1246.
  341. Cha, S.K., Ortega, B., Kurosu, H., Rosenblatt, K.P., Kuro, O.M., and Huang, C.L. 2008. Removal of sialic acid involving Klotho causes cell-surface retention of TRPV5 channel via binding to galectin-1. *Proc Natl Acad Sci U S A* 105:9805-9810.
  342. Imura, A., Tsuji, Y., Murata, M., Maeda, R., Kubota, K., Iwano, A., Obuse, C., Togashi, K., Tominaga, M., Kita, N., et al. 2007. alpha-Klotho as a regulator of calcium homeostasis. *Science* 316:1615-1618.
  343. Tohyama, O., Imura, A., Iwano, A., Freund, J.N., Henrissat, B., Fujimori, T., and Nabeshima, Y. 2004. Klotho is a novel beta-glucuronidase capable of hydrolyzing steroid beta-glucuronides. *J Biol Chem* 279:9777-9784.
  344. Hayes, G., Busch, A., Lotscher, M., Waldegger, S., Lang, F., Verrey, F., Biber, J., and Murer, H. 1994. Role of N-linked glycosylation in rat renal Na/Pi-cotransport. *J Biol Chem* 269:24143-24149.
  345. Virkki, L.V., Biber, J., Murer, H., and Forster, I.C. 2007. Phosphate transporters: a tale of two solute carrier families. *Am J Physiol Renal Physiol* 293:F643-654.
  346. Pfister, M.F., Ruf, I., Stange, G., Ziegler, U., Lederer, E., Biber, J., and Murer, H. 1998. Parathyroid hormone leads to the lysosomal degradation of the renal type II Na/Pi cotransporter. *Proc Natl Acad Sci U S A* 95:1909-1914.
  347. Kurosu, H., Yamamoto, M., Clark, J.D., Pastor, J.V., Nandi, A., Gurnani, P., McGuinness, O.P., Chikuda, H., Yamaguchi, M., Kawaguchi, H., et al. 2005. Suppression of aging in mice by the hormone Klotho. *Science* 309:1829-1833.
  348. Chateau, M.T., Araiz, C., Descamps, S., and Galas, S. 2010. Klotho interferes with a novel FGF-signalling pathway and insulin/Igf-like signalling to improve longevity and stress resistance in *Caenorhabditis elegans*. *Aging (Albany NY)* 2:567-581.
  349. Lorenzi, O., Veyrat-Durebex, C., Wollheim, C.B., Villemin, P., Rohner-Jeanrenaud, F., Zanchi, A., and Vischer, U.M. 2010. Evidence against a direct role of klotho in insulin resistance. *Pflugers Arch* 459:465-473.
  350. Wolf, I., Levanon-Cohen, S., Bose, S., Ligumsky, H., Sredni, B., Kanety, H., Kuro-o, M.,

## References

- Karlan, B., Kaufman, B., Koeffler, H.P., et al. 2008. Klotho: a tumor suppressor and a modulator of the IGF-1 and FGF pathways in human breast cancer. *Oncogene* 27:7094-7105.
351. Hsieh, C.C., Kuro-o, M., Rosenblatt, K.P., Brobey, R., and Papaconstantinou, J. 2010. The ASK1-Signalosome regulates p38 MAPK activity in response to levels of endogenous oxidative stress in the Klotho mouse models of aging. *Aging (Albany NY)* 2:597-611.
352. Saitoh, M., Nishitoh, H., Fujii, M., Takeda, K., Tobiume, K., Sawada, Y., Kawabata, M., Miyazono, K., and Ichijo, H. 1998. Mammalian thioredoxin is a direct inhibitor of apoptosis signal-regulating kinase (ASK) 1. *EMBO J* 17:2596-2606.
353. Liu, H., Nishitoh, H., Ichijo, H., and Kyriakis, J.M. 2000. Activation of apoptosis signal-regulating kinase 1 (ASK1) by tumor necrosis factor receptor-associated factor 2 requires prior dissociation of the ASK1 inhibitor thioredoxin. *Mol Cell Biol* 20:2198-2208.
354. Papaconstantinou, J., and Hsieh, C.C. 2010. Activation of senescence and aging characteristics by mitochondrially generated ROS: how are they linked? *Cell Cycle* 9:3831-3833.
355. Nishitoh, H., Saitoh, M., Mochida, Y., Takeda, K., Nakano, H., Rothe, M., Miyazono, K., and Ichijo, H. 1998. ASK1 is essential for JNK/SAPK activation by TRAF2. *Mol Cell* 2:389-395.
356. Matsuzawa, A., and Ichijo, H. 2005. Stress-responsive protein kinases in redox-regulated apoptosis signaling. *Antioxid Redox Signal* 7:472-481.
357. Sumbayev, V.V., and Yasinska, I.M. 2005. Regulation of MAP kinase-dependent apoptotic pathway: implication of reactive oxygen and nitrogen species. *Arch Biochem Biophys* 436:406-412.
358. Toyama, R., Fujimori, T., Nabeshima, Y., Itoh, Y., Tsuji, Y., and Osamura, R.Y. 2006. Impaired regulation of gonadotropins leads to the atrophy of the female reproductive system in klotho-deficient mice. *Endocrinology* 147:120-129.
359. Kamemori, M., Ohyama, Y., Kurabayashi, M., Takahashi, K., Nagai, R., and Furuya, N. 2002. Expression of Klotho protein in the inner ear. *Hear Res* 171:103-110.
360. Anamizu, Y., Kawaguchi, H., Seichi, A., Yamaguchi, S., Kawakami, E., Kanda, N., Matsubara, S., Kuro-o, M., Nabeshima, Y., Nakamura, K., et al. 2005. Klotho insufficiency causes decrease of ribosomal RNA gene transcription activity, cytoplasmic RNA and rough ER in the spinal anterior horn cells. *Acta Neuropathol* 109:457-466.
361. Min, D., Panoskaltsis-Mortari, A., Kuro, O.M., Hollander, G.A., Blazar, B.R., and Weinberg, K.I. 2007. Sustained thymopoiesis and improvement in functional immunity induced by exogenous KGF administration in murine models of aging. *Blood* 109:2529-2537.
362. Kawaguchi, H., Manabe, N., Miyaura, C., Chikuda, H., Nakamura, K., and Kuro-o, M. 1999. Independent impairment of osteoblast and osteoclast differentiation in klotho mouse exhibiting low-turnover osteopenia. *J Clin Invest* 104:229-237.
363. Ishii, M., Yamaguchi, Y., Yamamoto, H., Hanaoka, Y., and Ouchi, Y. 2008. Airspace enlargement with airway cell apoptosis in klotho mice: a model of aging lung. *J Gerontol A Biol Sci Med Sci* 63:1289-1298.
364. Sato, A., Hirai, T., Imura, A., Kita, N., Iwano, A., Muro, S., Nabeshima, Y., Suki, B., and Mishima, M. 2007. Morphological mechanism of the development of pulmonary emphysema in klotho mice. *Proc Natl Acad Sci U S A* 104:2361-2365.
365. Suga, T., Kurabayashi, M., Sando, Y., Ohyama, Y., Maeno, T., Maeno, Y., Aizawa, H., Matsumura, Y., Kuwaki, T., Kuro, O.M., et al. 2000. Disruption of the klotho gene causes pulmonary emphysema in mice. Defect in maintenance of pulmonary integrity during postnatal life. *Am J Respir Cell Mol Biol* 22:26-33.

## References

366. Gery, S., Tanosaki, S., Bose, S., Bose, N., Vadgama, J., and Koeffler, H.P. 2005. Down-regulation and growth inhibitory role of C/EBPalpha in breast cancer. *Clin Cancer Res* 11:3184-3190.
367. Gomis, R.R., Alarcon, C., Nadal, C., Van Poznak, C., and Massague, J. 2006. C/EBPbeta at the core of the TGFbeta cytostatic response and its evasion in metastatic breast cancer cells. *Cancer Cell* 10:203-214.
368. Wolf, I., O'Kelly, J., Rubinek, T., Tong, M., Nguyen, A., Lin, B.T., Tai, H.H., Karlan, B.Y., and Koeffler, H.P. 2006. 15-hydroxyprostaglandin dehydrogenase is a tumor suppressor of human breast cancer. *Cancer Res* 66:7818-7823.
369. Wolf, I., Laitman, Y., Rubinek, T., Abramovitz, L., Novikov, I., Beeri, R., Kuro, O.M., Koeffler, H.P., Catane, R., Freedman, L.S., et al. 2010. Functional variant of KLOTHO: a breast cancer risk modifier among BRCA1 mutation carriers of Ashkenazi origin. *Oncogene* 29:26-33.
370. Hudelist, G., Wagner, T., Rosner, M., Fink-Retter, A., Gschwantler-Kaulich, D., Czerwenka, K., Kroiss, R., Tea, M., Pischinger, K., Kostler, W.J., et al. 2007. Intratumoral IGF-I protein expression is selectively upregulated in breast cancer patients with BRCA1/2 mutations. *Endocr Relat Cancer* 14:1053-1062.
371. Maor, S., Yosepovich, A., Papa, M.Z., Yarden, R.I., Mayer, D., Friedman, E., and Werner, H. 2007. Elevated insulin-like growth factor-I receptor (IGF-IR) levels in primary breast tumors associated with BRCA1 mutations. *Cancer Lett* 257:236-243.
372. Gattineni, J., Bates, C., Twombly, K., Dwarakanath, V., Robinson, M.L., Goetz, R., Mohammadi, M., and Baum, M. 2009. FGF23 decreases renal NaPi-2a and NaPi-2c expression and induces hypophosphatemia in vivo predominantly via FGF receptor 1. *Am J Physiol Renal Physiol* 297:F282-291.
373. Ranch, D., Zhang, M.Y., Portale, A.A., and Perwad, F. 2011. Fibroblast growth factor 23 regulates renal 1,25-dihydroxyvitamin D and phosphate metabolism via the MAP kinase signaling pathway in Hyp mice. *J Bone Miner Res* 26:1883-1890.
374. Weisman, Y., Harell, A., Edelstein, S., David, M., Spirer, Z., and Golander, A. 1979. 1 alpha, 25-Dihydroxyvitamin D3 and 24,25-dihydroxyvitamin D3 in vitro synthesis by human decidua and placenta. *Nature* 281:317-319.
375. Gray, T.K., Lester, G.E., and Lorenc, R.S. 1979. Evidence for extra-renal 1 alpha-hydroxylation of 25-hydroxyvitamin D3 in pregnancy. *Science* 204:1311-1313.
376. Stoffels, K., Overbergh, L., Bouillon, R., and Mathieu, C. 2007. Immune regulation of 1alpha-hydroxylase in murine peritoneal macrophages: unravelling the IFNgamma pathway. *J Steroid Biochem Mol Biol* 103:567-571.
377. Esteban, L., Vidal, M., and Dusso, A. 2004. 1alpha-Hydroxylase transactivation by gamma-interferon in murine macrophages requires enhanced C/EBPbeta expression and activation. *J Steroid Biochem Mol Biol* 89-90:131-137.
378. Dusso, A.S., Brown, A.J., and Slatopolsky, E. 2005. Vitamin D. *Am J Physiol Renal Physiol* 289:F8-28.
379. Gorham, E.D., Garland, C.F., Garland, F.C., Grant, W.B., Mohr, S.B., Lipkin, M., Newmark, H.L., Giovannucci, E., Wei, M., and Holick, M.F. 2007. Optimal vitamin D status for colorectal cancer prevention: a quantitative meta analysis. *Am J Prev Med* 32:210-216.
380. Skinner, H.G., Michaud, D.S., Giovannucci, E., Willett, W.C., Colditz, G.A., and Fuchs, C.S. 2006. Vitamin D intake and the risk for pancreatic cancer in two cohort studies. *Cancer Epidemiol Biomarkers Prev* 15:1688-1695.



## References

381. Giovannucci, E., Liu, Y., Rimm, E.B., Hollis, B.W., Fuchs, C.S., Stampfer, M.J., and Willett, W.C. 2006. Prospective study of predictors of vitamin D status and cancer incidence and mortality in men. *J Natl Cancer Inst* 98:451-459.
382. Giovannucci, E. 2009. Vitamin D and cancer incidence in the Harvard cohorts. *Ann Epidemiol* 19:84-88.
383. Forster, R.E., Jurutka, P.W., Hsieh, J.C., Haussler, C.A., Lowmiller, C.L., Kaneko, I., Haussler, M.R., and Kerr Whitfield, G. 2011. Vitamin D receptor controls expression of the anti-aging klotho gene in mouse and human renal cells. *Biochem Biophys Res Commun* 414:557-562.
384. Forster, I.C., Hernando, N., Biber, J., and Murer, H. 2006. Proximal tubular handling of phosphate: A molecular perspective. *Kidney Int* 70:1548-1559.
385. Panda, D.K., Miao, D., Tremblay, M.L., Sirois, J., Farookhi, R., Hendy, G.N., and Goltzman, D. 2001. Targeted ablation of the 25-hydroxyvitamin D 1alpha -hydroxylase enzyme: evidence for skeletal, reproductive, and immune dysfunction. *Proc Natl Acad Sci U S A* 98:7498-7503.
386. Segawa, H., Onitsuka, A., Furutani, J., Kaneko, I., Aranami, F., Matsumoto, N., Tomoe, Y., Kuwahata, M., Ito, M., Matsumoto, M., et al. 2009. Npt2a and Npt2c in mice play distinct and synergistic roles in inorganic phosphate metabolism and skeletal development. *Am J Physiol Renal Physiol* 297:F671-678.
387. Wöhrle, S., Bonny, O., Beluch, N., Gaulis, S., Stamm, C., Scheibler, M., Müller, M., Kinzel, B., Thuery, A., Brueggen, J., et al. 2011. FGF receptors control vitamin D and phosphate homeostasis by mediating renal FGF-23 signaling and regulating FGF-23 expression in bone. *J Bone Miner Res* 26:2486-2497.
388. Keisala, T., Minasyan, A., Lou, Y.R., Zou, J., Kalueff, A.V., Pyykko, I., and Tuohimaa, P. 2009. Premature aging in vitamin D receptor mutant mice. *J Steroid Biochem Mol Biol* 115:91-97.
389. Kato, S., Takeyama, K., Kitanaka, S., Murayama, A., Sekine, K., and Yoshizawa, T. 1999. In vivo function of VDR in gene expression-VDR knock-out mice. *J Steroid Biochem Mol Biol* 69:247-251.
390. Eicher, E.M., Southard, J.L., Scriver, C.R., and Glorieux, F.H. 1976. Hypophosphatemia: mouse model for human familial hypophosphatemic (vitamin D-resistant) rickets. *Proc Natl Acad Sci U S A* 73:4667-4671.
391. Aono, Y., Yamazaki, Y., Yasutake, J., Kawata, T., Hasegawa, H., Urakawa, I., Fujita, T., Wada, M., Yamashita, T., Fukumoto, S., et al. 2009. Therapeutic effects of anti-FGF23 antibodies in hypophosphatemic rickets/osteomalacia. *J Bone Miner Res* 24:1879-1888.
392. Matsuda, Y., Schlange, T., Oakeley, E.J., Boulay, A., and Hynes, N.E. 2009. WNT signaling enhances breast cancer cell motility and blockade of the WNT pathway by sFRP1 suppresses MDA-MB-231 xenograft growth. *Breast Cancer Res* 11:R32.
393. Biber, J., Stieger, B., Stange, G., and Murer, H. 2007. Isolation of renal proximal tubular brush-border membranes. *Nat Protoc* 2:1356-1359.
394. Tallquist, M.D., and Soriano, P. 2000. Epiblast-restricted Cre expression in MORE mice: a tool to distinguish embryonic vs. extra-embryonic gene function. *Genesis* 26:113-115.
395. Guo, C., Yang, W., and Lobe, C.G. 2002. A Cre recombinase transgene with mosaic, widespread tamoxifen-inducible action. *Genesis* 32:8-18.
396. Traykova-Brauch, M., Schonig, K., Greiner, O., Miloud, T., Jauch, A., Bode, M., Felsher, D.W., Glick, A.B., Kwiatkowski, D.J., Bujard, H., et al. 2008. An efficient and versatile system for acute and chronic modulation of renal tubular function in transgenic mice. *Nat Med* 14:979-984.
397. Schonig, K., Schwenk, F., Rajewsky, K., and Bujard, H. 2002. Stringent doxycycline dependent

## References

- control of CRE recombinase in vivo. *Nucleic Acids Res* 30:e134.
398. Aslakson, C.J., and Miller, F.R. 1992. Selective events in the metastatic process defined by analysis of the sequential dissemination of subpopulations of a mouse mammary tumor. *Cancer Res* 52:1399-1405.
399. Dey, J.H., Bianchi, F., Voshol, J., Bonenfant, D., Oakeley, E.J., and Hynes, N.E. 2010. Targeting fibroblast growth factor receptors blocks PI3K/AKT signaling, induces apoptosis, and impairs mammary tumor outgrowth and metastasis. *Cancer Res* 70:4151-4162.
400. Tobiume, K., Matsuzawa, A., Takahashi, T., Nishitoh, H., Morita, K., Takeda, K., Minowa, O., Miyazono, K., Noda, T., and Ichijo, H. 2001. ASK1 is required for sustained activations of JNK/p38 MAP kinases and apoptosis. *EMBO Rep* 2:222-228.
401. Knaup, K.X., Jozefowski, K., Schmidt, R., Bernhardt, W.M., Weidemann, A., Juergensen, J.S., Warnecke, C., Eckardt, K.U., and Wiesener, M.S. 2009. Mutual regulation of hypoxia-inducible factor and mammalian target of rapamycin as a function of oxygen availability. *Mol Cancer Res* 7:88-98.
402. Ferrara, N. 1995. The role of vascular endothelial growth factor in pathological angiogenesis. *Breast Cancer Res Treat* 36:127-137.
403. Lambert, G., Traebert, M., Biber, J., and Murer, H. 2000. Cleavage of disulfide bonds leads to inactivation and degradation of the type IIa, but not type IIb sodium phosphate cotransporter expressed in *Xenopus laevis* oocytes. *J Membr Biol* 176:143-149.
404. Chang, Q., Hoefs, S., van der Kemp, A.W., Topala, C.N., Bindels, R.J., and Hoenderop, J.G. 2005. The beta-glucuronidase klotho hydrolyzes and activates the TRPV5 channel. *Science* 310:490-493.
405. Bryant, D.M., and Stow, J.L. 2005. Nuclear translocation of cell-surface receptors: lessons from fibroblast growth factor. *Traffic* 6:947-954.
406. Wu, Y., Chen, Z., and Ullrich, A. 2003. EGFR and FGFR signaling through FRS2 is subject to negative feedback control by ERK1/2. *Biol Chem* 384:1215-1226.
407. Murakami, M., Elfenbein, A., and Simons, M. 2008. Non-canonical fibroblast growth factor signalling in angiogenesis. *Cardiovasc Res* 78:223-231.
408. Thomas, G.V., Tran, C., Mellinghoff, I.K., Welsbie, D.S., Chan, E., Fueger, B., Czernin, J., and Sawyers, C.L. 2006. Hypoxia-inducible factor determines sensitivity to inhibitors of mTOR in kidney cancer. *Nat Med* 12:122-127.
409. Pende, M., Um, S.H., Mieulet, V., Sticker, M., Goss, V.L., Mestan, J., Mueller, M., Fumagalli, S., Kozma, S.C., and Thomas, G. 2004. S6K1(-)/S6K2(-) mice exhibit perinatal lethality and rapamycin-sensitive 5'-terminal oligopyrimidine mRNA translation and reveal a mitogen-activated protein kinase-dependent S6 kinase pathway. *Mol Cell Biol* 24:3112-3124.
410. Ruvinsky, I., Sharon, N., Lerer, T., Cohen, H., Stolovich-Rain, M., Nir, T., Dor, Y., Zisman, P., and Meyuhas, O. 2005. Ribosomal protein S6 phosphorylation is a determinant of cell size and glucose homeostasis. *Genes Dev* 19:2199-2211.
411. Razzaque, M.S., and Lanske, B. 2006. Hypervitaminosis D and premature aging: lessons learned from Fgf23 and Klotho mutant mice. *Trends Mol Med* 12:298-305.

## 10 Abbreviations

1,25(OH) <sub>2</sub> D	active vitamin D		(EGFR) family (avian
AC	adenylat cyclase		erythroblastosis oncogene B)
ADAM	a disintegrin and metalloproteinase domain	ERK1/2	extracellular signal-regulated kinase
ADHR	autosomal dominant hypophosphatemic rickets	ES	embryonic cells
ANG	angiopoietin	FAK	Focal adhesion kinase
AREG	epiregulin, amphiregulin	FD	Fibrous dysplasia
ARHR	autosomal recessive hypophosphatemic rickets	FEPO4	Fractional excretion of phosphate
BBM	brush border membrane	FGF/FGFR	fibroblast growth factor / receptor
BCL	b-cell lymphoma	FGFBP	FGF-binding protein
BCR	breakpoint cluster region	FLRT3	Fibronectin leucin-rich transmembrane protein 3
BLM	Bloom's syndrome (known as Bloom-Torre-Machacek syndrome)	FOP	FGFR1 oncogene partner
BTC	betacellulin	FRS2	FGF receptor substrate 2
BUN	blood urea nitrogen	GAPDH	Glycerinaldehyd-3-phosphat-Dehydrogenase
CaR	Calcium-sensing receptor	GAB1	GRB2-associated binding protein 1
CB28	Calbindin 1	GALNT3	UDP-N-acetyl-a-D-galactosamine/polypeptide N-acetylgalactosaminyl transferase-3
CBL	casitas B-lineage lymphoma	GFR	glomerular filtration rate
C/EBP	CCAAT/enhancer-binding protein	GRB2	growth factor receptor-bound 2
CKD	chronic kidney disease	HB-EGF	heparin binding EGF-like growth factor
cKO	conditional knock-out	HBS	heparan sulphate glycosaminoglycan binding site
CoCl <sub>2</sub>	cobalt chloride	HGF	hepatocyte growth factor
COFS	cerebro-oculo-facio-skeletal syndrome	HGPS	Hutchinson-Gilford progeria syndrome
Cyp7A1	cholesterol 7 $\alpha$ -hydroxylase	HIF1 $\alpha$	hypoxia inducible factor 1 $\alpha$
DAG	diacylglycerol	HR	homologous recombination
DMP1	Dentin Matrix Protein-1	HS	heparan sulphate
DSB	double-strand break	HSGAG	heparan sulphate glycosaminoglycan
ECM	extracellular matrix	HSS	hyperostosis-hyperphosphatemia
EGF/EGFR	epidermal growth factor/receptor		
EMT	epithelial-mesenchymal-transition		
ER	estrogen receptor		
ErbB1-4	epidermal growth factor receptor		

## Abbreviations

	syndrome		family
IAP1	Inhibitor of apoptosis	PKA	Protein kinase A
ICL	interstrand crosslinks	PKC	Protein kinase C
Ig	Immunoglobulin	PLC	Phospholipase C
IGH	Immunoglobulin heavy chain	PMCA	plasma membrane Ca <sup>2+</sup> ATPase
JNK	Jun N-terminal kinase	PTB	phosphotyrosine binding
KD	knock-down	PTEN	phosphatase and tensin homolog
kDa	kilo Dalton	PTH	parathyroid hormone
KGF	keratinocyte growth factor	PTHrP	parathyroid hormone receptor 1
KO	knock-out	PTHrP	PTH-related peptide
KsM	kidney specific Memo knock-out	PZHR1	PZH/PTHrP-receptor
LC-MSMS	Liquid Chromatography/Mass Spectrometry/Mass Spectrometry	QPCR	quantitative real time PCR
		RET	rearranged during transfection
LDL	low density lipoprotein	RMS	rhabdomyosarcoma
LMNA	the lamin A/C gene	RXR	retinoid receptor
MAPK	Mitogen activated protein kinase	S6K/RSK	S6 kinase/ribosomal S6 Kinase
MEF	mouse embryonic fibroblast	SCLL	stem cell leukemia/lymphoma syndrome
Memo	Mediator of ErbB-driven cell motility	SEF	similar expression to <i>fgf</i> genes
		Ser	serine
MEPE	a gene expressed in bone marrow and tumors causing osteomalacia	sFRP-4	secreted frizzled-related protein-4
		SH2	src homology 2
MKP3	MAPK phosphatase 3	SHP2	src homology phosphatase 2
MMP	matrix metalloproteinase	SIBLING	small integrin binding ligand n-linked glycoprotein
Na-Pi	sodium phosphate cotransporter		
NCAM	neural cell adhesion molecule	SNP	single nucleotide polymorphism
NGAL	Neutrophil gelatinase-associated lipocalin	SOS	son of sevenless
		STAT	transducer and activator of transcription proteins
NHERF1	Na/H-exchanger regulatory factors	TC-NER	transcription-coupled nucleotide excision repair
NRG	neuregulin	TGF	Transforming growth factor
NTRK1	neurotrophic tyrosine kinase receptor type 1	TIO	Tumor-induced rickets/osteomalacia
NCX1	sodium-calcium exchanger	TOP	5' terminal oligopyrimidine tract
PDZ	PSD-95, Discs-large and ZO-1	TOR	Target of rapamycin
PHEX	phosphate regulating gene with homologies to endopeptidases on the X chromosome	TrkA/TrkB	tropomyosine receptor kinase A/B
		TRP	Tubular reabsorption of phosphate
PI	phosphatidylinositol	TRPV5	transient receptor potential vanilloid 5
PI3K	Phosphatidylinositol-3 kinase		
PIP3	phosphatidylinositol-3,4,5-triphosphate	Tyr	tyrosine
Pit-2	a type III Na-Pi cotransporter, that belongs to the SLC20 gene	VDR	vitamin D receptor

## Abbreviations

VDRE	vitamin D response element	XFE	Epf-Errcc1 syndrome
VEGF	vascular endothelial growth factor	XIAP	X-linked inhibitor of apoptosis
WCE	whole cell extract	XLH	<u>X</u> -linked <u>h</u> ypophosphatemic rickets
Wrn/WS	Werner gene	ZNF	zinkfinger

## 11 Acknowledgments

I would like to thank Nancy for giving me the opportunity to work in her lab and on this amazing project.

I would also like to thank my Thesis Committee members; Lukas Sommer my co-referee and Denis Monard.

I thank Makoto Kuro-o for having me as a guest in his lab in Dallas, Tx, for three month. That was an amazing experience.

I thank Olivier Bonny for the fantastic collaboration and for having me several times as a guest in his lab in Lausanne. Thanks a lot for the many discussions.

I thank Régis Masson for kindly introducing me into the world of Memo and mice. I would like to thank Regis and Gwen MacDonald-Madeux for the stimulating discussions.

Thanks to Gwen and Jason Gillkenins for reading parts of my written thesis.

Many thanks to my friends Alessia, Anna, Constanze, Gwen, Ivan and Vanessa for their true friendship.

Thanks to all the former and current labmembers for the great atmosphere in the lab.

Last but certainly not least I would like to thank my family for their great support during my whole PhD thesis! Thank you!

## 12 Curriculum Vitae

### Barbara Hänzi

#### Personal data

Name	Hänzi	Phone (work)	+41 (0)61 697 20 69
First Name	Barbara	Phone (home)	+41 (0)52 366 52 64
Address	Trottenstrasse 9 8546 Islikon	Email	barbara.haenzi(at)fmi.ch
		Date of birth	19.6.1980

#### Academic experience

03.2006 - present      Doctoral Thesis  
Supervised by Nancy E. Hynes  
at the Friedrich Miescher Institute (FMI), University of Basel, Switzerland  
Title: The role of Memo in premature aging and downstream of the FGFR pathway  
During my PhD I showed that the protein Memo1 has an essential role in kidney physiology and that ablation of Memo in the whole body leads to a premature aging syndrome. I characterized two Memo knock-out mouse models, an inducible full body and an inducible kidney-specific. In addition, I showed *in vitro* that Memo1 is a novel downstream effector of the FGFR pathway and that Memo1 knock-out dampens and shortens the duration of FGFR signaling. I further characterized cell lines for their cell biological properties upon knock-out or knock-down of Memo.

06.2004-03.2005      Diploma thesis (equivalent to Master's degree)  
Supervised by Wilhelm Krek

## Curriculum Vitae

at the ETH Zurich, Switzerland, department of cell biology

I worked on the IGF-1/insulin signaling pathway in renal clear cell carcinoma cell lines and learned a lot about cell signaling and cancer biology.

### Technical expertise

- In vitro: Cell Culture, Western blot analysis, Immunoprecipitation, PCR, quantitative PCR, Immunohistochemistry and imaging, migration-, proliferation- and apoptosis assays, FACS
- In vivo: Handling of mice, developing complex breeding strategies, injections and oral gavage, blood sampling, studies in metabolic cages, dissection, isolation of specific segments of the nephron, isolation of brush border membranes of the nephron, tumour isolation, cryo- and paraffin sectioning

### Education

- 09.2001-09.2005 Biology studies with focus on chemistry in the first two years, ETH Zurich, Switzerland
- January 2000 Federal maturity, Zurich, Switzerland

### General Skills

- Design, planning and execution of *in vivo* and *in vitro* experiments.
- Oral presentations and discussions of data for laboratory and department meetings.
- Oral presentations and poster presentations of results during international conferences.
- Writing of a scientific paper.
- Teaching biology lectures for first year students in English: In the course of a tutorial at the University of Basel I was teaching basic biology to students. This included correcting their homework, discussion of it and offering advice for upcoming exams.



## Curriculum Vitae

- Employment as flight attendant at Swissair, the former national airline of Switzerland: I worked for Swissair for one and a half years to make use of the gap between the end of my federal maturity and the start of university. During this time I gained a lot of experience in dealing with people from different nations, working efficiently and quickly in minimal space and in working in teams, always keeping in mind that our team skills may dictate death or survival in an emergency.

### Languages

German	Mother tongue
English	Fluent spoken and written, working language
French	Spoken and written

### IT Knowledge

MS Office (Word, Power Point, Excel)  
Adobe (Photoshop and Illustrator)  
ImageAccess (Image database)

### Publication

Submitted

### Fellowships

10.2008-12.2008      EMBO Short-Term Fellowship for visiting Dr. Makoto Kuro-o's laboratory in Dallas, Tx, USA

## Selected Talks

- 03.2010 Gordon Research Conference – Fibroblast Growth Factors in Development and Disease, Ventura, CA, USA
- 09.2008 Cold Spring Harbor Meeting – Molecular Genetics of Aging, NY, USA
- 06.2008 CIG Symposium of the University of Lausanne, Switzerland
- 10.2007 Annual Conference of the German Society of Genetics – Genetics of Aging in Jena, Germany

## Posters

- 09.2011 Tor, PI3K, and AKT – 20 years on, Basel, Switzerland
- 03.2010 Gordon Research Conference – Fibroblast Growth Factors in Development and Disease, Ventura, CA, USA
- 09.2008 Cold Spring Harbor Meeting – Molecular Genetics of Aging, NY, USA
- 06.2008 CIG Symposium of the University of Lausanne, Switzerland
- 10.2007 Annual Conference of the German Society of Genetics – Genetics of Aging in Jena, Germany
- 03.2007 Transfog meeting in Innsbruck, Austria
- 12.2006 “Targeting the Kinome” meeting in Basel, Switzerland
- 11.2006 Steiner Foundation meeting in Brunnen, Switzerland

## Neurex Workshops

- 10.2011 What genetically modified rodents tell us about neurological and psychiatric disorders?
- 10.2011 Plasticity in the dopaminergic system and in Parkinson’s disease
- 05.2011 Translational approaches in Stress and Neurodegeneration
- 03.2011 Update on Depression: semiological characterization, neurobiological

## Curriculum Vitae

mechanisms, current treatment and therapeutic perspectives

11.2009

Multiple Sklerosis

## Referees

- Nancy E. Hynes      Growth Control Department, Friedrich Miescher Institute for Biomedical Research, Maulbeerstrasse 66, CH-4058 Basel, Switzerland. Phone: 41 61 6978107; FAX: 41 61 6973976; E-mail: [nancy.hynes@fmi.ch](mailto:nancy.hynes@fmi.ch)
- Olivier Bonny      University of Lausanne, Department of Pharmacology and Toxicology, Rue du Bugnon 27, CH-1005 Lausanne, Switzerland. Phone: 41 21 692 54 17; FAX: 41 21 692 53 55; E-mail: [Olivier.Bonny@unil.ch](mailto:Olivier.Bonny@unil.ch)
- Makoto Kuro-o      UT Southwestern Medical Center, 5323 Harry Hines Boulevard, Dallas, Texas 75390. Phone: 1-214-648-4088; FAX: 1-214-648-4070; E-mail: makoto.kuro-o@utsouthwestern.edu